The Effect of Prewetting on the Pressure Drop, Liquid Holdup and Gas-Liquid Mass Transfer in Trickle-Bed Reactors

Dylan Loudon

The Effect of Prewetting on the Pressure Drop, Liquid Holdup and Gas-Liquid Mass Transfer in Trickle-Bed Reactors

Dylan Loudon

Submitted in partial fulfilment of the requirements of the degree Master of Engineering (Chemical Engineering) in the Faculty of Engineering, Built Environment and Information Technology, University of Pretoria, Pretoria.

9 December 2005

The Effect of Prewetting on the Pressure Drop, Liquid Holdup and Gas-Liquid Mass Transfer in Trickle-Bed Reactors

by

Dylan Loudon

Professor Willie Nicol

Department of Chemical Engineering

Master of Engineering (Chemical Engineering)

The prewetting of a trickle-bed reactor has important implications in the design and operation of these reactors. This is because the prewetting changes the flow morphology (shape and texture) of the liquid flowing through the bed and leads to the existence of multiple hydrodynamic states. The extent of this change in flow morphology can be seen in the effect the prewetting of the reactor has on the pressure drop, liquid holdup and gas-liquid mass transfer. The following prewetting procedures were used:

- **Levec-wetted:** the bed is flooded and drained and after residual holdup stabilisation the gas and liquid flow is reintroduced
- **Kan-wetted:** the bed is operated in the pulse flow regime and liquid and gas flow rates are reduced to the desired set point
- **Super-wetted:** the bed is flooded and gas and liquid flow are introduced once draining commences

For the pressure drop:

- The different prewetting procedures resulted in two distinct regions (Upper region Kan and Super-wetted, Lower region Dry and Levec-wetted)
- There was no significant difference between the Dry and Levec-wetted beds
- The pressure drop in the Kan and Super-wetted beds can be as much as seven times greater than the pressure drop in the Dry and Levec-wetted beds

For the liquid holdup:

- The different prewetting procedures resulted in four distinct regions (Kan-wetted, Super-wetted, Levec-wetted, Dry bed)
- The liquid holdup in the Kan-wetted bed can be as much as four times greater than the liquid holdup in the Dry bed
- The liquid holdup in the Levec-wetted can be as much as thirty percent lower than the liquid holdup in the Kan-wetted bed

For the gas-liquid mass transfer:

- The different prewetting procedures resulted in three distinct regions (Kan and Super-wetted, Levec-wetted, Dry bed)
- The volumetric gas-liquid mass transfer coefficient in the Kan and Super-wetted beds can be as much as six times greater than the mass transfer coefficient in the Dry bed
- The volumetric gas-liquid mass transfer coefficient in the Kan and Super-wetted beds can be as much as two and a half times greater than the mass transfer coefficient in the Levec-wetted bed

While an increase in the liquid flow rate results in an increase in the pressure drop, liquid holdup and gas-liquid mass transfer for all of the experiments, the effect of increasing gas flow on the measured variables were more pronounced for the prewetted beds. In a prewetted bed (Kan, Super and Levec-wetted) an increase in the gas flow rate causes an increase in the volumetric gas-liquid mass transfer coefficient and a decrease in the liquid holdup. The decrease in the liquid holdup is due to the fact that the increased gas flow rate causes the films around the particles to thin and spread out. In the dry bed the flow is predominantly in the form of rivulets and the increase in gas flow rate does not affect the liquid holdup. In the case of the volumetric gas-liquid mass transfer coefficient the increased gas flow rate causes an increase in the mass transfer coefficient regardless of the prewetting procedure. This increase is due to the effect that the gas flow rate has on the liquid holdup as well as the increase in the gas-liquid interfacial area due to the increased gas-liquid interaction.

If the pulsing in the Kan-wetted bed is induced by increasing the gas flow rate and keeping the liquid flow rate constant the results are significantly different. The pressure drop in the gas-pulsing experiments was lower than the pressure drop in the recorded in the Kan and Super-wetted beds, but higher than the pressure drop in the dry and Levec-wetted beds. However, the liquid holdup in the gas-pulsing experiments was higher than the liquid holdup in any of the other beds. The volumetric gas-liquid mass transfer coefficient in the gas-pulsing experiments was lower than the mass transfer coefficients of the Kan and Super-wetted beds, but higher than the mass transfer coefficients in the dry and Levec-wetted beds.

The multiple operating points obtained from the different prewetting procedures are by no means the only possible operating points. By simply decreasing the draining time in the Levec-wetted bed steady state operating points can be found between those of the Super and Levec-wetted beds. This alludes to the fact that the operating conditions determined from the different prewetting modes are only boundaries and that the actual operating point can lie anywhere between these boundaries. The existence of these multiple hydrodynamic states complicates things further when a correlation is developed to determine the pressure drop, liquid holdup or the volumetric gas-liquid mass transfer coefficient. No correlation tested was able to accurately predict the pressure drop, liquid holdup or volumetric gas-liquid mass transfer coefficient in the dry or prewetted beds.

KEYWORDS: prewetting, gas-liquid mass transfer, pressure drop, liquid holdup, trickle flow

Acknowledgements

The financial assistance of the National Research Foundation (NRF) towards this research is hereby acknowledged. Opinions expressed and conclusions arrived at, are those of the author and are not necessarily to be attributed to the NRF.

The support of Sasol R&D, and in particular the efforts of Arno de Klerk, toward the Hydrodynamics Focus Group at the University of Pretoria, are hereby acknowledged.

Contents

Nomenclature

Symbols Used

A	Constant in equation 2.5	
A_1	Correlating variable in equation 2.13	
a_1	Constant in equation 2.60	
a_S	External surface area of particles and wall per unit volume	m^{-1}
a_V	Bed specific surface area (equation 2.33)	m^{-1}
B	Constant in equation 2.5	
b_1	Constant in equation 2.60	
c	Constant in equation 2.10	
C_1	Constant in equation 2.38	
c_1	Constant in equation 2.60	
$C_{L,O2}$	Concentration of dissolved oxygen in water	$kmol/m^3$
d	Constant in equation 2.10	
D	Molecular diffusivity of the gas in the liquid	m^2/s
d'	Modified particle diameter	m
D_1	Constant in equation 2.38	
d_1	Constant in equation 2.60	
D_C	Column diameter	m
d_h	Krischer-Kast hydraulic diameter (equation 2.7)	m
d_p	Particle diameter	m
E	Constant in equation 2.38	
E_1	Ergun constant (equations 2.24 and 2.25)	
e_1	Constant in equation 2.60	
E_2	Ergun constant (equations 2.24 and 2.25)	
E_L	Energy dissipation per unit volume (equation 2.71)	$ft.lb_f/ft^3s$
E_L^*	Liquid-phase energy loss	kg/m^2s
G	Gas mass flux	kg/m^2s
g	Gravitational acceleration	m^2/s
Ga_G^*	Modified Gas Galileo number (equation 2.27)	
Ga_L	Liquid Galileo number (equation 2.32)	

Ga_L^*	Modified Liquid Galileo number (equation 2.26)	
Ga_L^{**}	Modified Liquid Galileo number (equation 2.47)	
H*	Henry's constant	
H_{dr}	Free-draining liquid holdup	
H_G	Gas-phase holdup	
H_{stat}	Static or residual liquid holdup	
H_t	Total liquid holdup	
K	Correlating variable in equation 2.34	
K_0	Correlating variable in equation 2.6	
k_G	Relative permeability of gas phase	
k_ga	Volumetric gas-side mass transfer coefficient	s^{-1}
k_L	Relative permeability of liquid phase	
K_La	Overall volumetric liquid-phase mass transfer coefficient	s^{-1}
k_La	Volumetric liquid-side mass transfer coefficient	s^{-1}
L	Liquid mass flux	kg/m^2s
m	Constant in equation 2.10	
M	Wall correction factor (equation 2.23)	
m_1	Constant in equation 2.36	
n	Constant in equation 2.10	
N	Correlating variable in equation 2.55	
n_1	Constant in equation 2.36	
P	Pressure drop	Pa
p	Constant in equation 2.36	
P_1	Correlating variable in equation 2.44	
q	Constant in equation 2.36	
R	Constant in equation 2.36	
Re_G	Gas Reynolds number (equation 2.2)	
Re_G*	Modified Gas Reynolds number (equation 2.29)	
Re_G'	Modified Gas Reynolds number (equation 2.21)	
Re_L	Liquid Reynolds number (equation 2.3)	
Re_L^*	Modified Liquid Reynolds number (equation 2.28)	
$Re_{L'}$	Modified Liquid Reynolds number (equation 2.20)	

S	Constant in equation 2.36	
Sc_L	Liquid Schmidt number (equation 2.59)	
U_G	Superficial gas velocity	m/s
U_L	Superficial liquid velocity	m/s
We_G	Gas Weber number (equation 2.4)	
We_L	Liquid Weber number (equation 2.9)	
X_G	Modified Lockhart-Martenelli ratio (equation 2.8)	
X_L	Correlating variable in equation 2.55	
X_L	Modified Lockhart-Martenelli ratio (equation 2.37)	
Y_G	Correlating variable in equation 2.67	
Z	Correlating variable in equation 2.14	

Greek Symbols

δ_L	Reduced saturation of liquid phase	
χ	Correlating variable in equation 2.16	
ε_B	Bed porosity	
Γ	Correlating variable in equation 2.38	
μ_G	Dynamic gas viscosity	Pa.s
μ_L	Dynamic liquid viscosity	Pa.s
θ	Correlating variable in equation 2.60	
ρ_G	Gas density	kg/m^3
ρ_L	Liquid density	kg/m^3
σ_L	Liquid surface tension	N/m
ξ	Correlating variable in equation 2.35	
ξ_1	Correlating variable in equation 2.10	
Ω	Constant in equation 2.60	

Subscripts

e	Exit (equation 2.76)	e
e'	Exit of empty bed (equation 2.76)	e'
f	Feed (equation 2.76)	f
f'	Feed of empty bed (equation 2.76)	f'

G	Gas phase	G
L	Liquid phase	L

1. Introduction

The trickle-bed reactor (TBR) is the most widely used three-phase gas-liquid-solid reaction system encountered in industrial practice. They are used in the petroleum, petrochemical and chemical industries, in waste treatment, and in biochemical and electrochemical processing (Al-Dahhan *et al*, 1997).

In this study the trickle flow regime is defined to be gravity driven flow of a liquid over a stationary bed of packed particles in the presence of a co-current flowing gaseous species. A schematic representation is shown in figure 1-1.

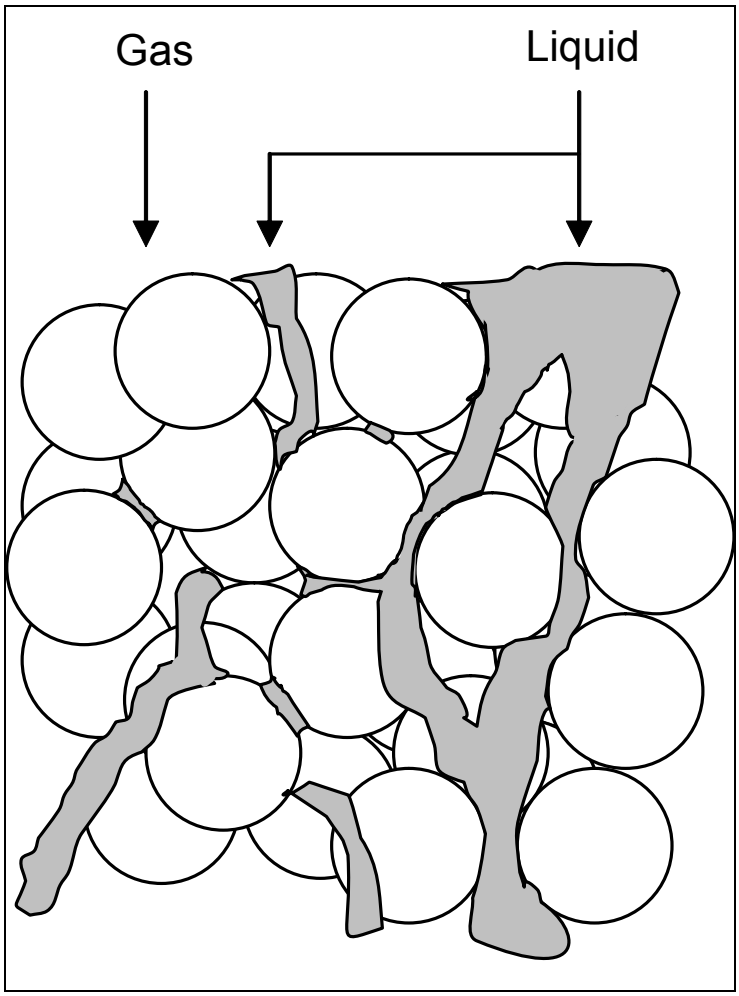

Figure 1-1: A schematic of trickle flow (Van der Merwe, 2004)

The prewetting of a trickle-bed involves the flooding of the bed with the liquid or operating at high liquid and/or gas flow rates (before setting the flow rates

to the operating specifications) to ensure that all of the catalyst is wet (covered in liquid) before the reaction takes place. Prewetting of the trickle-bed reactor can lead to the existence of multiple hydrodynamic states and this has important implications in the design and operation of these reactors.

Kan and Greenfield (1978, 1979) were the first to provide experimental evidence of the existence of these multiple hydrodynamic states. In this ground breaking research they found that the liquid holdup and the pressure drop exhibited hysteresis when the operating conditions were changed. In their experiments the packing was prewetted by increasing the liquid flow rate beyond the operating point for a specified time while the gas flow rate was kept at the desired operating point. The liquid flow rate was then decreased to the operating point and pressure drop and liquid holdup readings were taken. After these readings were taken the gas flow rate was increased and brought back to the desired operating point before the relevant measurements were taken. The result was two distinct curves of pressure drop versus gas flow rate and liquid holdup versus gas flow rate for the gas decreasing and gas increasing experiments.

Levec *et al* (1986, 1988) performed similar experiments but there were some fundamental differences in the operating procedures. Levec *et al* (1986, 1988) prewetted the bed by increasing the gas and liquid flow rates beyond the operating point until the pulsing regime was reached. Once the bed was completely wet the gas and liquid flow was shut off and the column was allowed to drain for twenty minutes before the experiments were performed. The gas flow rate was then set at the desired operating point and experiments were performed by varying the liquid flow rate. The result was two distinct curves of pressure drop versus liquid flow rate and liquid holdup versus liquid flow rate for the liquid decreasing and liquid increasing experiments.

The observation of these hysteresis loops was confirmed by many other researchers, including Christensen *et al* (1986) and Wang *et al* (1995). The reasons for the existence of these hysteresis loops has been attributed to the imperfect wetting of the catalyst particles and the difference between

advancing and receding contact angles at gas-liquid-solid contact lines (Levec *et al,* 1986 & 1988), the difference between film and rivulet flow (Christensen *et al,* 1986), the change in tortuosity of the gas flow channels (Kan and Greenfield, 1978 &1979) as well as the non-uniformity of the flow (Wang *et al* 1995).

While the bulk of research has been based on the hysteresis observed when one type of prewetting is used, prewetting and hysteresis are not mutually exclusive. Both prewetting and hysteresis are functions of the bed history and the effect of the history on the achieved steady state. If the history of the bed entails a liquid and/or gas flow increase up to the pulsing regime, Kan-prewetting is in essence achieved. In this regard specifically defined prewetting procedures can be seen as the boundary cases for all multiple steady states within hysteresis loops (although this has not been proven)

Multiple steady states in trickle-bed reactors are normally quantified by pressure drop and liquid holdup measurements. In this study the extent of pressure drop and liquid holdup variation for different prewetting methods were quantified and the additional variable of gas-liquid mass transfer was included to obtain additional information on the different flow morphologies.

2. Literature Study

2.1 Background

For a number of years chemical engineers' attention has been addressed to trickle-bed reactors, owing to the their suitability for many operations on chemical, oil refining, petrochemical and biochemical processes (Gianetto & Specchia, 1992). Researchers are always looking for ways to improve the performance of these reactors.

In an effort to improve the performance of these reactors the packing material is often prewetted as this is known to improve the liquid distribution. This is done by introducing the liquid reagent to the reactor before operation. Since the hydrodynamic performance of such a system is dependent on the history of the process, the prewetting procedure needs to be taken into account. Even the type of prewetting the bed has undergone is important since different types of prewetting result in different hydrodynamic measurements.

The prewetting procedure followed affects every hydrodynamic parameter of the bed. These parameters include the pressure drop, liquid holdup, gas-liquid mass transfer, liquid-solid mass transfer and catalyst wetting to name but a few. These parameters are not only functions of the operating conditions but also of the operating modes, due to the imperfect wetting conditions that exist in these beds (Levec, Saez & Carbonell, 1986).

For the sake of clarity the prewetting modes can be divided into three broad categories:

- **Non-prewetted** (Dry)
- **Levec-type prewetting** (Levec) (Levec *et al*, 1988)
- **Kan-type prewetting** (Kan) (Kan & Greenfield, 1979)

A non-prewetted bed is a bed packed with completely dry particles. The liquid and gas are introduced into the system at the desired flow rate. For a Levec-

wetted bed the bed is prewetted by flooding the packed bed or by operating in the pulsing regime for a specified time. Once the bed has been prewetted the liquid flow to the bed is shut off and the liquid is allowed to drain from the bed until only the residual holdup remains. Once the liquid has been given sufficient time to drain the liquid can be re-introduced into the system. For a Kan-wetted bed the column is prewetted by either flooding or by once again operating the column in the pulsing flow regime (By increasing either the liquid or gas flow rate or both). The bed is then allowed to drain but while draining the liquid and gas flow rates are kept at their specific setpoints, thus the draining takes place under irrigation (Van der Merwe, 2004).

Table 2-1 lists references of some of the studies that have used the different prewetting procedures. These studies were conducted with bench scale apparatus with uniform distributors at low pressure:

Table 2-1: Studies grouped by prewetting procedure(s) used

Dry	**Levec**	**Kan**
Sicardi *et. al.* (1980)	Levec *et. al.* (1988)	Kan & Greenfield (1978)
Kushalkar & Pangarkar (1990)	Levec *et. al.* (1986)	Kan & Greenfield (1979)
Lazzaroni, Keselman & Figoli (1988)	Christensen, McGovern & Sundaresan (1986)	Lazzaroni, Keselman & Figoli (1988)
Lazzaroni, Keselman & Figoli (1989)	Lutran *et. al.* (1991)	Lazzaroni, Keselman & Figoli (1989)
Kantzas (1994)	Stegeman *et. al.* (1996)	Lutran *et. al.* (1991)
Van der Merwe, 2004	Sederman & Gladden (2001)	Ravindra *et. al.* (1997)
	De Klerk (2003)	Sederman & Gladden (2001)
	Van der Merwe, 2004	Van der Merwe, 2004

NOTE: For the experiments undertaken in this investigation the Levec-wetted bed is prewetted by flooding the column and the draining takes place under conditions of zero gas flow and normal gas flow operating conditions. Both types of Kan wetting are also tested and for the sake of clarity the prewetting

procedure by flooding the column is known as Super wetting and the prewetting by operating in the pulsing regime (by increasing the liquid flow rate) is known as Kan wetting.

2.2 Flow Characteristics

2.2.1 Flow Regimes (Al-Dahhan et al, 1997)

There are two broad categories into which the different number of flow regimes in trickle-bed reactors can be divided: a low interaction regime (LIR which consists of the trickle flow regime) and a high interaction regime (HIR which consists of the pulse, spray, bubble and dispersed bubble flow regimes). A schematic representation of the flow regimes encountered in trickle-bed reactors is shown in figure 2-1.

The LIR is observed at low gas and liquid flow rates and can be characterized by a weak gas-liquid interfacial activity and gravity driven liquid flow. For a trickle-bed operating at atmospheric conditions, as is the case for this investigation, the gas-liquid interaction increases at high gas and liquid flow rates. The liquid trickles down the packing in the form of droplets, films and rivulets, while the continuous gas phase occupies the remaining porous space and flows separately.

The HIR is characterized by a moderate to intense gas-liquid shear due to moderate to high flow rate of either the gas, or the liquid, or both. At low gas flow rates, and sufficiently high liquid flow rates, the bubble flow regime is encountered. This is characterised by a continuous liquid phase that contains small spherical bubbles. The dispersed bubble flow regime is characterised by a continuous liquid phase but the bubbles coalesce, due to the increase in the gas flow, causing the gas to flow in the form of elongated bubbles. This flow regime is encountered at high liquid flow rates and medium gas flow rates. The pulsing flow regime may be approached from either the gas-continuous

trickle flow (as done when prewetting the bed) or from the liquid-continuous coalesced bubble flow regime. This flow regime is observed for moderate liquid flow rates and moderate to high gas flow rates. The pulse flow regime can be seen as a macroscopic combination of dispersed bubbles in a liquid rich slug and trickle flow in a gas rich slug moving down the bed. If the gas flow rate is increased a mist or spray flow is eventually observed for which the gas becomes the continuous phase and the liquid is entrained as droplets

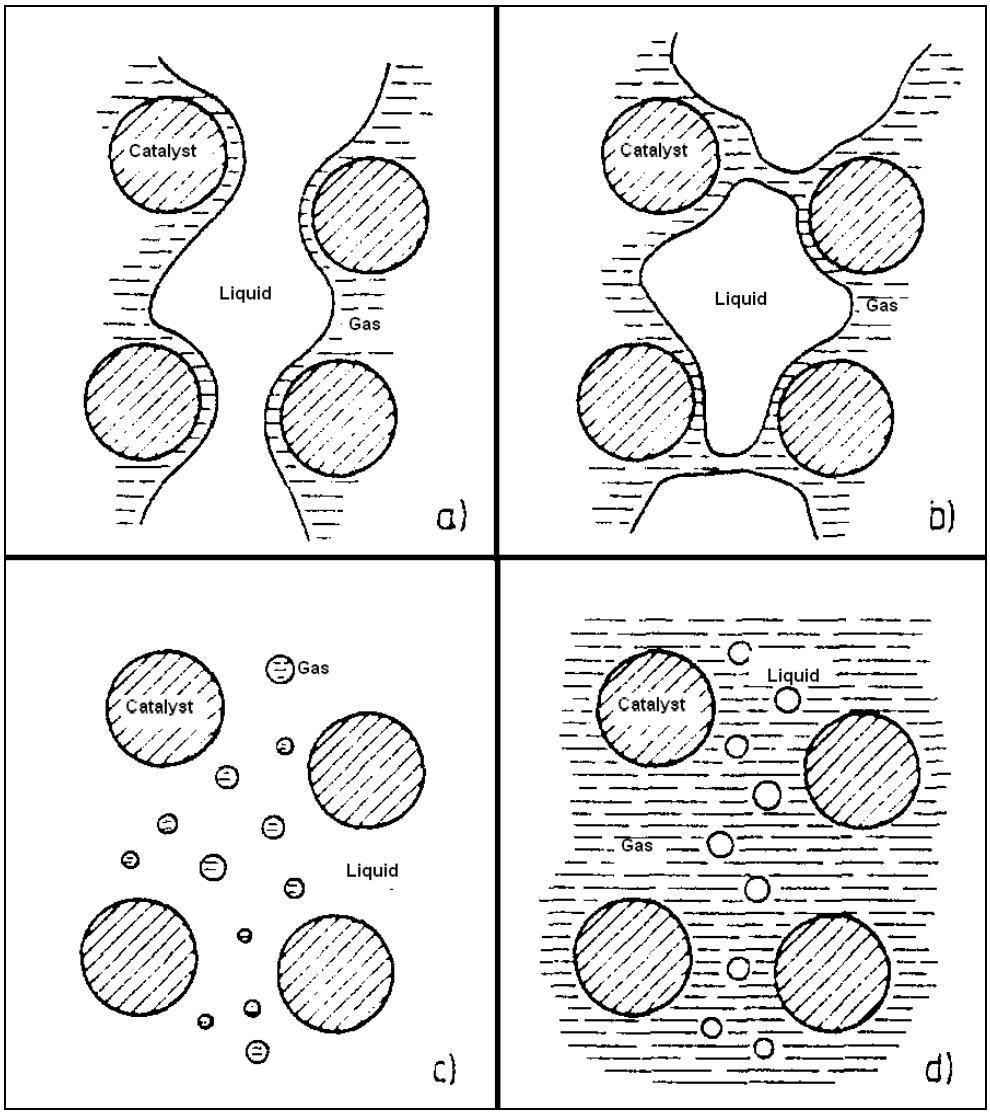

Figure 2-1: A schematic representation of the flow regimes encountered in trickle-bed reactors: a) trickle flow, b) pulse flow, c) spray flow and d) bubble flow (Reinecke & Mewes, 1996)

2.2.2 Flow Types

According to Sederman and Gladden (2001), the vast majority of the previous research on trickle-beds has concentrated on bed-scale properties of the reactor in which the packing is often treated as a homogeneous system and only the bulk characteristics of the flow are considered. The major drawback of this approach is that it ignores the complexities of the flow within the interparticle space of the packing reducing the description of the problem to macroscopic average quantities, i.e. liquid holdup. They felt that the details of local properties, such as wetting efficiency, may be the most important factors influencing the behaviour of a given process occurring within the system and are crucial to understanding the macroscopic behaviour of the reactor.

In order to understand these local properties, one first has to understand the different possibilities in flow types experienced in trickle-bed reactors. In the trickle flow regime the liquid is in the form of films or rivulets. A brief definition of these different types of flow is given below, as well as a schematic representation in figure 2-2. (Zimmerman & Ng, 1986; Lutran, Ng & Delikat, 1991; Sederman & Gladden, 2001; Ravindra, Rao & Rao, 1997; Moller *et al*, 1996)

Films – A thin, laminar liquid stream that partially covers a particle (figure 2-2a)
Rivulets – A continuous stream of liquid over the surface of a particle (figure 2-2b)
Filaments – A liquid stream that flows down the bed in the form of film (figure 2-2c) or rivulet flow (figure 2-2d) connecting liquid pockets

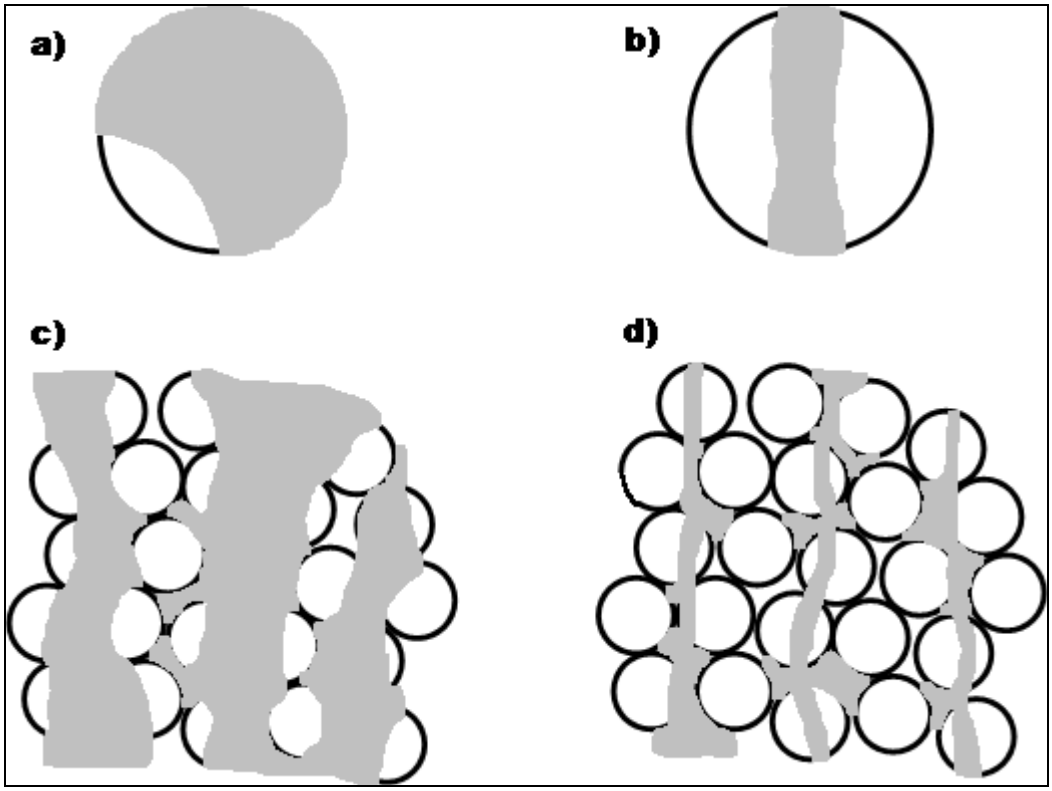

Figure 2-2: Schematics of flow textures: a) Particle-scale film flow b) Particle-scale rivulet flow c) Bed-scale film flow d) Bed-scale rivulet flow

Although film flow would offer the best covering of the catalyst particle it is not necessarily the most stable configuration, since surface tension will tend to reduce the total film area. Observations in trickle-bed reactors during reaction indicate that even with excellent initial distribution, the liquid may gather in rivulets, which tend to maintain their position with time (Satterfield, 1975)

The prewetting history of the bed once again plays an important role in the type of flow in the bed. Christensen *et al* (1986) concluded that in a non-prewetted bed the flow is dominated by filament flow in the form of rivulets. However, in a prewetted bed, the dominant flow pattern is film flow.

Although film flow is prominent in prewetted beds, Ravindra *et al* (1997) did state that if after prewetting the liquid was allowed to drain, Levec wetting, the films over the particles could be broken and the bed may behave similar to a non-prewetted bed.

2.3 Pressure Drop

2.3.1 Background

In trickle-bed reactors the pressure drop over the reactor governs the energy required to move the fluids through the system. This makes pressure drop an extremely important variable in the design, scale-up and operation of reactors (Ellman *et al*, 1988).

In this section the following aspects of pressure drop will be dealt with:

- Pressure Drop Hysteresis
- Pressure Drop Correlations

2.3.2 Pressure Drop Hysteresis

The existence of various hydrodynamic states has important implications in the design and operation of trickle-beds. Kan and Greenfield (1978) stated that the pressure drop in one hydrodynamic state could differ from that of another by as much as 50%. This would not only affect the operating costs but also pose problems in the scale-up from small reactors.

The pressure drop hysteresis trends for the Kan, Levec and Dry beds are shown in figure 2-3 and are based on the work of many different researchers (Van der Merwe, 2004).

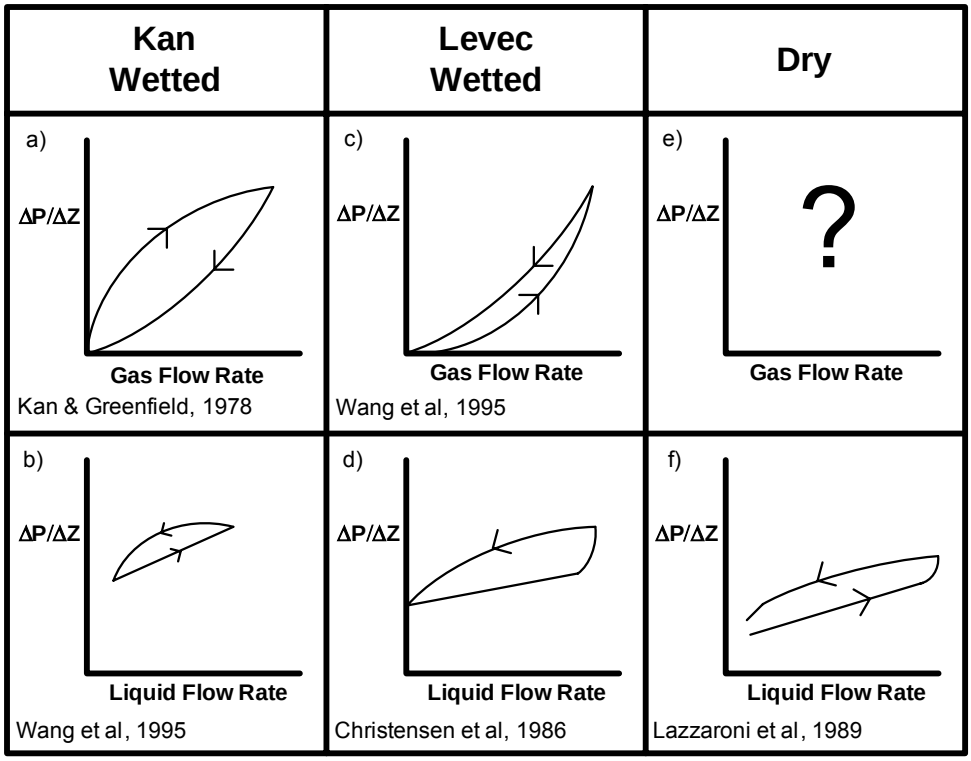

Figure 2-3: Pressure drop hysteresis for the different wetting modes

Figure 2-3a) corresponds to the Reduced Gas Flowrate condition of Kan and Greenfield (1978). They found that for a given gas flow rate, the pressure drop is lower if the flow has been reduced from a higher value. The steady-state value attained for a given gas flow rate is dependent on the maximum gas flow rate that the bed was subjected to.

The reason for the difference in pressure drop, according to Kan and Greenfield, is that in a prewetted bed, in the absence of gas flow, the liquid bridges are orientated randomly. As the gas flow rate is increased the liquid bridges transverse to the general flow of the gas tend to be broken down, thereby decreasing the gas flow path density and tortuosity. Due to the high surface tension, even when the gas flow rate is reduced, this flow pattern is retained and results in a lower pressure drop.

Figure 2-3b) shows the experimental findings of Wang *et al* (1995). For a given liquid flow rate, the pressure drop is higher if the liquid flow rate has been reduced from a higher value. The reason for this can be attributed to the research of Ravindra *et al* (1997), who found that the liquid distribution in the

Kan mode was more uniformly distributed when the liquid flow rate was decreased from a higher value. This means that more of the bed is filled with liquid and the cross-sectional area available for gas flow is decreased and a higher pressure drop is recorded.

Figure 2-3c) is also based on the experimental findings of Wang *et al* (1995). The results show the opposite trend to what was seen in the Kan-wetted bed. They found that for a Levec wetted bed, the pressure drop for a given gas flow rate that has been reached by decreasing the gas flow rate from a maximum value, was higher than the pressure drop recorded for the run where the gas flow rate was always increasing. It is important to note that if the gas flow rate was increased to the point of pulsing (as was the case here), the return leg is actually the same as the Kan-wetted leg where pulsing is induced by increasing the gas flow rate.

Figure 2-3d) is based on the work done by Christensen *et al* (1986). They found that the pressure gradients for the upper curve (decreasing the liquid flow rate from a previously attained maximum) could be as much as 100% for those for the lower curve (increasing the liquid flow rate from zero). They also found that the fractional difference in pressure gradient between the upper and lower curves became smaller as the gas flow rate was increased.

Figure 2-3f) is based on the work done by Lazzaroni *et al* (1989). They found in their experiments, on a dry bed, that when the liquid was taken to a maximum value and then decreased that the pressure drop of the system would be higher than the pressure drop obtained through increasing the liquid flow rate from 0. They justified this by the fact that the increasing liquid flow rate resulted in the liquid spreading to new parts of the bed and when decreased, the flow remained in these sections. This resulted in a decreased cross-sectional area of the bed for the gas to flow through, thus resulting in a higher pressure drop.

2.3.3 Pressure Drop Correlations

The proof of pressure drop hysteresis is undeniable. However, most of the proposed correlations do not even take it into account. Wang *et al* (1995) stated that the ignorance of the phenomenon of hysteresis in the trickle flow regime makes the proposed pressure drop correlations valid for merely estimating the average pressure drop in certain modes. They also stated that the theoretical models have not been developed into quantitative predictive tools.

The following correlations were tested:

- Clements & Schmidt, 1980
- Larachi *et al*, 1991
- Ellman *et al*, 1988
- Turpin & Huntington, 1967 (as given in Kan & Greenfield, 1979)
- Sato *et al*, 1973
- Holub, Dudukovic & Ramachandran, 1992
- Westerterp and Wammes (1992)

The results from the Trickle-bed Reactor Simulator of Larachi *et al* (1999) were also used.

Clements and Schmidt (1980) developed their model based on experimental results obtained with Dow-Corning DC200 series silicone fluids as the liquid phase and air as the gas phase. The reactor had an internal diameter of 55mm and was 1.5mm long. Three different types of packing were used, namely 1.6 and 2.9mm spheres and 0.8mm extrudates. No prewetting procedure is followed so the correlation is based on experiments done on a dry bed. The proposed model is:

$$\left(\frac{\Delta P}{\Delta G}\right)_{LG} = 190 d_p \mu_L \left(\frac{\Delta P}{\Delta Z}\right)_G \left(\frac{\varepsilon_B}{1-\varepsilon_B}\right)^3 \left(\frac{\mathrm{Re}_G We_G}{\mathrm{Re}_L}\right)^{-1/3} \tag{2.1}$$

$$\mathrm{Re}_G = \frac{G d_p}{\mu_G} \tag{2.2}$$

$$\mathrm{Re}_L = \frac{Ld_p}{\mu_L} \tag{2.3}$$

$$We_G = \frac{Gd_p}{\rho_G \sigma_L} \tag{2.4}$$

The constant, 190, is for D_p in ft and μ_L in lb_m/ft.hr.

The correlation proposed by Larachi *et al* (1991) is based on some 1500 experimental results. 12 different gas-liquid-solid systems and a wide range of operating pressures (0.2 – 8.1MPa) were taken into account. No mention is made of the prewetting procedures followed by the different investigators so the correlation can be assumed to be valid for the dry bed operations. The proposed correlation is:

$$\left(\frac{\Delta P}{\Delta Z}\right)_{LG} = \frac{2G^2}{d_h \rho_G}\left[\frac{1}{K_O^{1.5}}\left(A + \frac{B}{K_O^{0.5}}\right)\right] \tag{2.5}$$

$$K_O = X_G\left(\mathrm{Re}_L We_L\right)^{0.25} \tag{2.6}$$

$$d_h = d_p\left\{\frac{16\varepsilon_B^3}{9\pi(1-\varepsilon_B)^2}\right\}^{1/3} \tag{2.7}$$

$$X_G = \frac{G}{L}\sqrt{\frac{\rho_L}{\rho_G}} \tag{2.8}$$

$$We_L = \frac{Ld_p}{\rho_L \sigma_L} \tag{2.9}$$

$A = 31.3 \pm 3.9$

$B = 17.3 \pm 0.6$

The correlation of Ellman *et al* (1988) is based on a database of some 4600 experimental results. This incorporated a wide range of liquid and gas flow rates as well as various pressures. They also tested 12 different packing geometries. No mention is made of the prewetting procedures followed by the different investigators so the correlation can be assumed to be valid for the dry bed operations. The proposed correlation is:

$$\left(\frac{\Delta P}{\Delta Z}\right)_{LG} = \frac{2G^2}{d_h \rho_G}\left[c\left(X_G \xi_2\right)^m + d\left(X_G \xi_2\right)^n\right] \tag{2.10}$$

$$\xi_2 = \frac{\mathrm{Re}_L^2}{0.01 + \mathrm{Re}_L^{1.5}} \tag{2.11}$$

$$X_G = \left[\frac{We_G}{We_L}\right]^{0.5} \tag{2.12}$$

$c = 200$

$d = 85$

$m = -1.2$

$n = -0.5$

The correlation of Turpin and Huntington (1967) (as given in Kan & Greenfield, 1979) was determined from experiments performed on 7.5 to 8.1mm tabular alumina particles. The system was an air-water system tested in all of the hydrodynamic regimes (Gianetto *et al*, 1978). No mention is made of the prewetting procedure followed so it is assumed that the correlation is based on work done on a dry bed. The proposed correlation is:

$$\left(\frac{\Delta P}{\Delta Z}\right)_{LG} = \frac{3\rho_G U_G^2 (1-\varepsilon_B)}{d_p \varepsilon_B} e^{A_1} \tag{2.13}$$

$$A_1 = 7.96 - 1.34 \ln Z + 0.0021(\ln Z)^2 - 0.00078(\ln Z)^3 \tag{2.14}$$

$$Z = \frac{\mathrm{Re}_G^{1.167}}{\mathrm{Re}_L^{0.767}} \tag{2.15}$$

The correlation proposed by Sato *et al* (1973) was based on their experimental results. The experiments were performed on a water and air system and 6 different sizes of glass spheres were used (2.52 – 24.27mm). Two columns were used, with internal diameters of 65.8 and 122mm, respectively. No prewetting procedure was followed so the correlation is based on experiments performed on a dry bed. The proposed correlation is:

$$\left(\frac{\Delta P}{\Delta Z}\right)_{LG} = \left(\frac{\Delta P}{\Delta Z}\right)_L \left(1.3 + 1.85 \chi^{-0.85}\right) \tag{2.16}$$

$$\chi = \sqrt{\left(\frac{\Delta P}{\Delta Z}\right)_L \Big/ \left(\frac{\Delta P}{\Delta Z}\right)_G} \tag{2.17}$$

ΔP_L and ΔP_G are the pressure loss that would exist if the liquid and gas were assumed to flow alone in single phase flow with the same flow rates as those in the two phase flow and can be calculated as (Sato *et al*, 1973):

$$\left(\frac{\Delta P}{\Delta L}\right)_L = \frac{\mu_L U_L (1-\varepsilon_B)^2}{d'^2\,\varepsilon_B^3}\left[150 + 4.2\,\mathrm{Re}'^{5/6}_L\right] \tag{2.18}$$

$$\left(\frac{\Delta P}{\Delta L}\right)_G = \frac{\mu_G U_G (1-\varepsilon_B)^2}{d'^2\,\varepsilon_B^3}\left[150 + 4.2\,\mathrm{Re}'^{5/6}_G\right] \tag{2.19}$$

$$\mathrm{Re}'_L = \frac{Ld'}{\mu_L(1-\varepsilon_B)} \tag{2.20}$$

$$\mathrm{Re}'_G = \frac{Gd'}{\mu_G(1-\varepsilon_B)} \tag{2.21}$$

$$d' = \frac{d_p}{M} \tag{2.22}$$

$$M = 1 + \frac{4d_P}{6D_C(1-\varepsilon_B)} \tag{2.23}$$

The five correlations above have all got one major thing in common, there is no parameter in either of them that will allow for even an estimation of multiple pressure drop predictions. These correlations will therefore, at best, only predict an average value.

The correlation proposed by Holub *et al* (1992) is a phenomenological pore-scale, hydrodynamic model based on experimental results obtained for a wide range of gas-liquid-solid systems. The pressure drop can be calculated directly if the holdup is known (Al-Dahhan *et al*, 1998). The proposed correlations are:

$$\left(\frac{\Delta P}{\Delta Z}\right)_{LG} = \rho_G g\left\{\left(\frac{\varepsilon_B}{\varepsilon_B - H_t}\right)^3\left[\frac{E_1\,\mathrm{Re}^*_G}{Ga^*_G} + \frac{E_2\,\mathrm{Re}^{*\,2}_G}{Ga^*_G}\right] - 1\right\} \tag{2.24}$$

$$\left(\frac{\Delta P}{\Delta Z}\right)_{LG} = \rho_L g\left\{\left(\frac{\varepsilon_B}{H_t}\right)^3\left[\frac{E_1\,\mathrm{Re}^*_L}{Ga^*_L} + \frac{E_2\,\mathrm{Re}^{*\,2}_L}{Ga^*_L}\right] - 1\right\} \tag{2.25}$$

$$Ga^*_L = \frac{g d_p^3 \varepsilon_B^3 \rho_L^2}{\mu_L^2 (1-\varepsilon_B)^3} \tag{2.26}$$

$$Ga_G^* = \frac{g d_p^3 \varepsilon_B^3 \rho_G^2}{\mu_G^2 (1-\varepsilon_B)^3} \tag{2.27}$$

$$\mathrm{Re}_L^* = \frac{L d_p}{\mu_L (1-\varepsilon_B)} \tag{2.28}$$

$$\mathrm{Re}_G^* = \frac{G d_p}{\mu_G (1-\varepsilon_B)} \tag{2.29}$$

The correlation proposed by Westerterp and Wammes (1992) was based on experiments performed on a reactor with an internal diameter of 51mm. The packing was 3mm glass spheres. The liquids tested were water, 40% Ethyleneglycol and ethanol. Two different gases were tested, namely nitrogen and helium. The proposed correlation is:

$$\left(\frac{\Delta P}{\Delta Z}\right)_{LG} = \frac{155}{2 d_p \rho_G U_G^2} \left[\frac{\rho_G U_G d_p \varepsilon_B}{\mu_G (1-\varepsilon_B)}\right]^{-0.37} \left[\frac{1-\varepsilon_B}{\varepsilon_B \left(1 - H_t / \varepsilon_B\right)}\right] \tag{2.30}$$

The correlations proposed by Holub *et al* (1992) and Westerterp and Wammes (1992) both incorporate the liquid holdup in their respective pressure drop correlations. Although no specific mention is made of the prewetting procedure followed, the fact that liquid holdup is a function of the prewetting procedure may result in multiple pressure drop predictions for the different prewetting modes.

2.4 Liquid Holdup

2.4.1 Background

In the design and modelling of trickle-bed reactors a hydrodynamic parameter of primary importance is the liquid holdup (Satterfield, 1975). The liquid holdup has an effect on each of the following parameters (Ellman *et al*, 1990):

- Pressure drop

- The degree of wetting of the catalyst particles
- The thickness of the liquid film around a particle
- The transfer of heat from the catalyst
- The capacity of the reactor to take up heat generated in highly exothermic reactions without thermal runaways occurring
- Gas-liquid mass transfer

Due to the fact that liquid holdup is such an important aspect in trickle-bed reactors it is understandable that there are also many different definitions. For the work presented in this report all holdups are expressed as volumetric fractions of the total bed volume, and not as saturation values, which are fractions of the void space. The following definitions are also required:

- Total or Operating Holdup (H_t) – the total amount of liquid inside the bed at steady-state conditions during operation
- Residual Liquid Holdup (H_{res}) – the amount of liquid that remains in the bed after the liquid feed was stopped and the bed was allowed to drain freely
- Free-draining Liquid Holdup (H_{dr}) – the part of the operating holdup that drains from the bed when the liquid feed is stopped
- Static Liquid Holdup – the part of the operating holdup that is stagnant during operation
- Dynamic Liquid Holdup – the part of the operating holdup that is not stagnant during operation

It is important to note that the total liquid holdup is the sum of either the static and dynamic liquid holdups, or the residual and free-draining liquid holdup.

The remainder of this section will deal with liquid holdup hysteresis, some of the available correlations for liquid holdup and methods used to measure liquid holdup.

2.4.2 Liquid Holdup Hysteresis

The liquid holdup in a reactor is an integral part of current design procedures. This is due to the fact that the liquid holdup determines the residence time of the liquid phase reactants in the reactor. Thus, the existence of various hydrodynamic states has important implications in the design and operation of these reactors. Since holdup varies as a function of the particular hydrodynamic state, so must the performance of the reactor (Kan & Greenfield, 1978)

The holdup hysteresis trends for the Kan, Levec and Dry beds are shown in figure 2-4 (Van der Merwe, 2004).

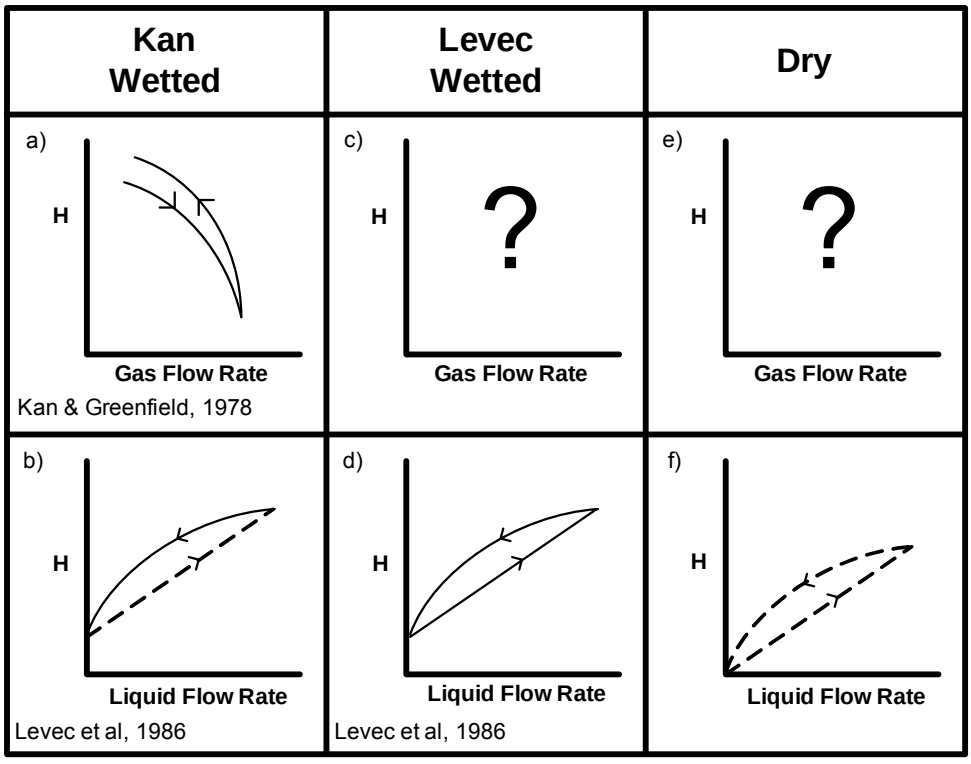

Figure 2-4: Holdup hysteresis for the different prewetting modes

Figure 2-4a) is based on the work done by Kan and Greenfield (1978). The results are based on the Reduced Gas Flowrate condition. They found that for a given gas flow rate the liquid holdup is higher if the flow has been reduced from a higher value. Thus, the holdup is a function of the highest gas flow rate

previously attained. Their reason is in essence exactly the same as that proposed for the pressure drop hysteresis in section 2.3.2. The decrease in the gas flow path density and tortuosity results in a higher liquid holdup due to the fact that the liquid holdup is directly affected by the gas velocity acting on the liquid surface (Kan & Greenfield, 1979).

Figure 2-4b) is based on the work done by Levec *et al* (1986). The dashed line in the figure was not directly observed, but was included by implication due to the pressure drop hysteresis for the same conditions, and the relationship that Kan and Greenfield (1978) have reported between pressure drop and holdup (Van der Merwe, 2004). This implies that for a given liquid flow rate the liquid holdup is higher if the flow has been reduced from a higher value.

Figure 2-4d) is based on the work done by Levec *et al* (1986) and Wang *et al* (1995). In both cases the lower branch is for the liquid-increasing path. In the experiments of Levec *et al* (1986), the liquid flow rate was actually increased to the flooding point. This implies that the return loop is actually the lower loop of the Kan-wetted bed (figure 2-4b). The lower loop could be explained by the fact that during the draining process some of the films over the particles are broken, and parts of the bed behave similarly to a dry bed (Ravindra *et al*, 1997). As the liquid flow increases, the liquid distribution is improved, and upon reaching the flooding point the entire bed is once again wet and draining now takes place under irrigation, and the films which could have broken now are now re-established.

In their experiments Levec *et al* (1986) also found that if the operating mode was changed at an intermediate liquid flow rate, the decreasing liquid flow rate would take values within the loop. From this they proposed that the curves actually represented an envelope of the possible hydrodynamic states.

Figure 2-5f) is once again shown with dashed lines because the relationship was inferred based on the relationship of the pressure drop for the work done by Lazzaroni *et al* (1989). The trend shows that as the liquid flow rate

increases, and is brought back down, the resulting holdup will be higher than that which was achieved by merely increasing the liquid flow from zero. This is due to the fact that increasing the liquid flow rate will increase the liquid distribution. When the liquid flow rate is decreased once again, some of the liquid pockets formed at the high liquid flow rate will stay in the bed, and this will result in a higher liquid holdup (Moller *et al*, 1996)

2.4.3 Liquid Holdup Correlations

Levec *et al* (1986) stated that the extensive studies of hydrodynamics in trickle-bed reactors in the recent years have concentrated primarily on the development of empirical correlations as a way to predict the hydrodynamic performance of these systems. Due to the uncertainties associated with the prediction of the liquid holdup, the resulting correlations are only valid over a limited range of experimental conditions.

The following correlations were tested:

- Kohler & Richarz, 1985
- Ellman *et al*, 1990
- Larachi *et al*, 1991
- Clements & Schmidt, 1980
- Colombo *et al*, 1976
- Otake & Okada, 1953 (as given in Goto & Smith, 1975)
- Sato *et al*, 1973
- Holub *et al*, 1992
- Specchia & Baldi, 1977
- Stegeman *et al*, 1996
- Nemec & Levec, 2005
- Lakota, Levec & Carbonell, 2002

The results from the Trickle-bed Reactor Simulator of Larachi *et al* (1999) were also used.

The correlation proposed by Kohler and Richarz (1985) was based on their experimental results. The experiments were performed in a steel column with a 30mm inner diameter. The column was filled with different packings of height 0.2m, 0.4m, 0.6m and 0.8m, respectively. The packings were 1.5mm glass beads, 3mm alox pellets and 1.5mm alox beads. The liquid phase was either water or an organic mixture and two gases were used, namely, nitrogen and hydrogen. The liquid holdup was obtained from the measured mean residence time by the tracer method. There is no mention of any prewetting procedure followed during any of the experiments. The proposed correlation is:

$$\frac{H_{dr}}{\varepsilon_B} = 0.71 Ga_L^{-0.42}\,\mathrm{Re}_L^{0.53}\,\mathrm{Re}_G^{-0.31}\left(\frac{a_V d_p}{\varepsilon_B}\right)^{0.65} \tag{2.31}$$

$$Ga_L = \frac{\rho_L^2 g d_p^3}{\mu_L^2} \tag{2.32}$$

$$a_V = \frac{6(1-\varepsilon_B)}{d_p} \tag{2.33}$$

The correlation of Ellman *et al* (1988) is based on a database of some 5000 experimental results. This incorporated a wide range of liquid and gas flow rates as well as various pressures. They also tested 12 different packing geometries. No mention is made of the prewetting procedures followed by the different investigators so the correlation can be assumed to be valid for the dry bed operations. The proposed correlation is:

$$\frac{H_{dr}}{\varepsilon_B} = 10^K \tag{2.34}$$

$$K = 0.001 - \frac{R}{\xi^S} \tag{2.35}$$

$$\xi = X_L^{m_1}\,\mathrm{Re}_L^{n_1}\,We_L^p\left(\frac{a_V d_h}{1-\varepsilon_B}\right)^q \tag{2.36}$$

$$X_L = \left(\frac{We_L}{We_G}\right)^{0.5} \tag{2.37}$$

$R = 0.42$

$S = 0.48$

$m_1 = 0.5$

$n_1 = -0.3$

$p = 0$

$q = 0.3$

The correlation proposed by Larachi *et al* (1991) is based on some 1500 experimental results. 12 different gas-liquid-solid systems and a wide range of operating pressures (0.2 – 8.1MPa) were taken into account. No mention is made of the prewetting procedures followed by the different investigators so the correlation can be assumed to be valid for the dry bed operations. The proposed correlation is:

$$\frac{H_t}{\varepsilon_B} = 1 - 10^{-\Gamma} \tag{2.38}$$

$$\Gamma = \frac{1.22 We_L^{C_1}}{\mathrm{Re}_L^E \, X_G^{D_1}} \tag{2.39}$$

$C_1 = 0.15 \pm 0.016$

$D_1 = 0.15 \pm 0.008$

$E = 0.20 \pm 0.013$

Clements and Schmidt (1980) developed their model based on experimental results obtained with Dow-Corning DC200 series silicone fluids as the liquid phase and air as the gas phase, although R12 (dichlorofluoromethane) was also used. The reactor had an internal diameter of 55mm and was 1.5mm long. Three different sizes of extrudate were used, namely 1.04mm, 1.39mm and 3.35mm. The liquid holdup measurements were taken by weighing the liquid that drained out after the feed was shut off. There is no mention of any prewetting procedure followed during any of the experiments. The proposed model is:

$$\frac{H_{dr}}{\varepsilon_B} = 0.84 \left(\frac{\mathrm{Re}_G \, We_G}{\mathrm{Re}_L} \right)^{-0.034} \tag{2.40}$$

Colombo *et al* (1976) developed their model based on experimental results obtained in a column with a 30mm internal diameter. The liquid was deionised water and two types of packing were used, namely, 1mm crushed particles of carbon and 3.8x4.8mm cylindrical carbon pellets. The liquid holdup measurements were taken by weighing the liquid that drained out after the feed was shut off. There is no mention of any prewetting procedure followed during any of the experiments. The proposed model is:

$$\frac{H_{dr}}{\varepsilon_B} = 3.86\,\mathrm{Re}_L^{0.565}\,Ga_L^{-0.42}\left(\frac{a_V d_p}{\varepsilon_B}\right)^{0.65} \tag{2.41}$$

The correlation of Otake and Okada (1953) (as given in Goto & Smith, 1975) was based on their experimental data. The experiments were performed with various different packing materials (Spheres, Raschig rings and Berl saddles) and various sizes (6.4 – 25.4mm) (Gianetto *et al*, 1978). There is no mention of any prewetting procedure followed during any of the experiments. The proposed correlation is:

$$\frac{H_{dr}}{\varepsilon_B} = 1.25\,\mathrm{Re}_L^{0.676}\,Ga_L^{-0.44}\,a_V d_p \varepsilon_B \tag{2.42}$$

The correlation proposed by Sato *et al* (1973) was based on their experimental results. The experiments were performed on a water and air system and 6 different sizes of glass spheres were used (2.52 – 24.27mm). Two columns were used, with internal diameters of 65.8 and 122mm, respectively. The liquid holdup was determined by the weighing method. No prewetting procedure was followed so the correlation is based on experiments performed on a dry bed. The proposed correlation is:

$$\frac{H_{dr}}{\varepsilon_B} = 0.4 a_V^{1/3} \chi^{0.22} \tag{2.43}$$

The constant 0.4 is valid when a_V is calculated in mm, and χ (and the corresponding gas and liquid pressure drops) can be solved for using the equations 2.17 to 2.23.

The seven correlations above have all got one major thing in common, there is no term in either of them that will allow for even an estimation of multiple liquid holdup predictions. These correlations will therefore, at best, only predict an average value.

The pressure drop correlation proposed by Holub *et al* (1992), given in equation 2.25, can be manipulated to predict the total holdup. For this correlation by using the pressure drop measured for the different prewetting modes, the holdup in these modes may be predicted. The correlation is:

$$\frac{H_t}{\varepsilon_B} = \left(E_1 \frac{\mathrm{Re}_L^*}{P_1 Ga_L^*} + E_2 \frac{\mathrm{Re}_L^{*2}}{P_1 Ga_L^*} \right)^{1/3} \tag{2.44}$$

$$P_1 = 1 + \frac{\left(\frac{\Delta P}{\Delta Z}\right)_{LG}}{\rho_L g} \tag{2.45}$$

The correlation proposed by Specchia and Baldi (1977) was based on their experimental results. Thee different gas-liquid systems were used, namely, air-water, air-glycerol aqueous solutions and air-water with surfactants. The packing was 6mm glass spheres and 2.7 and 5.4mm glass cylinders. The column had an internal diameter of 80mm and the liquid holdup was measured by weighing the liquid that drained from the column when the liquid flow rate was suddenly shut off. The proposed correlation is:

$$\frac{H_{dr}}{\varepsilon_B} = 3.86\,\mathrm{Re}_L^{0.545}\, Ga_L^{**-0.42} \left(\frac{a_V d_p}{\varepsilon_B} \right)^{0.65} \tag{2.46}$$

$$Ga_L^{**} = \frac{d_p^3 \rho_L \left(\rho_L g + \left(\frac{\Delta P}{\Delta Z}\right)_{LG} \right)}{\mu_L^2} \tag{2.47}$$

The proposed correlation incorporates the pressure drop in the modified Galileo number. Due to this correction, the correlation may be able to predict the different holdups for the different prewetted beds.

The correlation of Stegeman *et al* (1996) can be seen as an adjustment of the Holub correlation. In their experiments the turbulent region was never reached, and since only the laminar term is then of any importance the

turbulent term can be set equal to zero. The experiments were carried out in a 54mm inner diameter column and 3mm glass beads were packed to a height of 0.98m. The gas phase was nitrogen and the liquid phase was deionised water for one experiment, and a mixture of deionised water and 13.5-mol% ethylene glycol for the other. The bed was Levec-wetted before any experiments were carried out. The proposed correlation is:

$$\frac{H_{dr}}{\varepsilon_B} = \left(140 \frac{\mathrm{Re}_L^*}{P_1 Ga_L^*} \right)^{1/3} \tag{2.48}$$

The constant 140 only differs slightly from the original Ergun constant of 150.

The correlations proposed by Nemec and Levec (2005) and Lakota, Levec and Carbonell (2002) for the liquid holdup is based on the relative permeability concept. The correlation proposed by Nemec and Levec (2005) is based 1300 newly measured data pairs of pressure drop and liquid holdup obtained for a wide range of commercially relevant operating conditions as well as different types of packing. The correlation has been adapted to predict the liquid holdup in a Kan-wetted bed (based on the experimental results of Nemec & Levec, 2005) and the Levec-wetted bed (based on the experimental results of Levec *et al*, 1986). The liquid holdup is solved iteratively with the following steps:

Guess the total liquid holdup - H_t

$$H_G = 1 - H_t \tag{2.49}$$

$$\delta_L = \frac{H_t - H_{stat}}{\varepsilon_B - H_{stat}} \tag{2.50}$$

For the Levec-wetted bed:

$$k_L = \delta_L^2 \tag{2.51}$$

For the Kan-wetted bed:

$$k_L = \delta_L^{2.9} \tag{2.52}$$

$$k_G = 0.4 \left(\frac{H_G}{\varepsilon_B} \right) \tag{2.53}$$

Solve for H_t till the following equation is true:

$$\frac{1}{k_L}\left[E_1\frac{\mathrm{Re}_L^*}{Ga_L^*}+E_2\frac{\mathrm{Re}_L^{*2}}{Ga_L^*}\right]\frac{\rho_L}{\rho_L-\rho_G}-\frac{1}{k_G}\left[E_1\frac{\mathrm{Re}_G^*}{Ga_G^*}+E_2\frac{\mathrm{Re}_G^{*2}}{Ga_G^*}\right]\frac{\rho_G}{\rho_L-\rho_G}=1 \qquad (2.54)$$

For the correlation proposed by Lakota *et al* (2002) the experiments were performed in a air-water system and various types of packing were used. The packing was prewetted using the Levec-wetting procedure. The liquid holdup is solved iteratively with the following steps:

Guess the total liquid holdup - H_t

$$\delta_L=\frac{H_t-H_{stat}}{\varepsilon_B-H_{stat}} \qquad (2.50)$$

$$N=4.37+0.0478\,\mathrm{Re}_G^{*\,0.774} \qquad (2.55)$$

Solve for H_t till the following equation is true:

$$\left(\frac{1}{\delta_L}\right)^{2.92}\left[150\frac{\mathrm{Re}_L^*}{Ga_L^*}+1.7\frac{\mathrm{Re}_L^{*2}}{Ga_L^*}\right]-\left(\frac{\varepsilon_B}{\varepsilon_B-H_t}\right)^N\left[150\frac{\mathrm{Re}_G^*}{Ga_G^*}+1.7\frac{\mathrm{Re}_G^{*2}}{Ga_G^*}\right]\frac{\rho_G}{\rho_L}=1 \qquad (2.56)$$

2.4.4 Measuring Liquid Holdup

Ellman *et al* (1990) stated that holdup could be measured as follows:

- By weighing the dry reactor and subtracting this result from the weight of the reactor when the liquid flows through it to obtain the total liquid holdup
- By simultaneously shutting off the inlet and outlet streams and then draining the reactor to obtain the dynamic or draining holdup
- By tracer techniques, to obtain the total holdup. The tail of the RTD is due to the stagnant liquid and may be used to derive the static liquid holdup and hence also the dynamic liquid holdup
- By exposing the liquid to a beam of electromagnetic radiation and measuring the attenuation of the beam due to the presence of the liquid, the total liquid holdup may be determined

- By measuring the apparent electrical conductivity across the bed in the presence of a conducting liquid. This conductivity is a function of the amount of liquid held between the two electrodes
- By measuring the volume of the liquid outside the bed when a known quantity of liquid circulates in a closed circuit through the reactor

2.5 Gas-Liquid Mass Transfer

2.5.1 Background

In a trickle-bed reactor the rate-controlling step can be one or a combination of the following (Dharwadkar & Sylvester, 1977):

- The rate of mass transfer of reactant between the bulk gas phase and the gas-liquid interface
- The rate of mass transfer between the gas-liquid interface and the bulk liquid
- The rate of mass transfer between the bulk liquid and the catalyst surface
- The rate of diffusion and simultaneous reaction within the catalyst pores

In the most commonly encountered situation the mass transfer limiting reagent is the gaseous species. The gaseous reactant is usually present in substantial stoichiometric excess and in relatively high fractional concentration in the vapour phase as well as being relatively insoluble in the liquid, especially in the case of hydrogen and oxygen. (Satterfield, 1975)

Gas-liquid mass transfer is one of the most fundamental steps in determining the absorption rate or the overall reaction rate. This is because in any absorption process, whether followed by a chemical reaction or not, the gas must first be dissolved in the liquid (Charpentier, 1976).

The overall gas-liquid mass transfer coefficient may be expressed, according to the two-film concept, in terms of the liquid side and the gas side mass transfer coefficients (Herskowitz & Smith, 1983):

$$\frac{1}{K_L a} = \frac{1}{H * k_g a} + \frac{1}{k_L a} \qquad (2.57)$$

In the case of a highly insoluble gas it is valid to assume that vapour-liquid equilibrium is established between the gas and the gas-liquid interface. This implies that there is no significant mass transfer resistance in the gas phase (Satterfield, 1975). This can be seen from the equation above. For a slightly soluble gas, like hydrogen or oxygen, the value of the Henry's constant is larger than unity. This results in the tern, $H*k_g a$ being at least one order of magnitude larger than $k_L a$ over the range of liquid and gas flow rates commonly encountered in trickle-beds. Thus, $K_L a$ can be approximated as $k_L a$ (Herskowitz & Smith, 1975)

However, if the gas is very soluble in the liquid, as is the case of carbon dioxide in water, it can be assumed that there is no significant mass transfer resistance in the liquid film of the gas-liquid mass transfer resistance in the liquid film of the gas-liquid interface and the experimental study is concentrated on the investigation of mass transfer in the gas film. (Iliuta, Iliuta & Thyrion, 1997)

2.5.2 Gas-Liquid Mass Transfer Hysteresis

Gas-liquid mass transfer hysteresis has not received as much attention in the literature as the liquid holdup and pressure drop. The hysteresis is actually not for the gas-liquid mass transfer but for the gas-liquid interfacial area, which is an integral part of the gas-liquid mass transfer coefficient. This hysteresis is shown in figure 2-5.

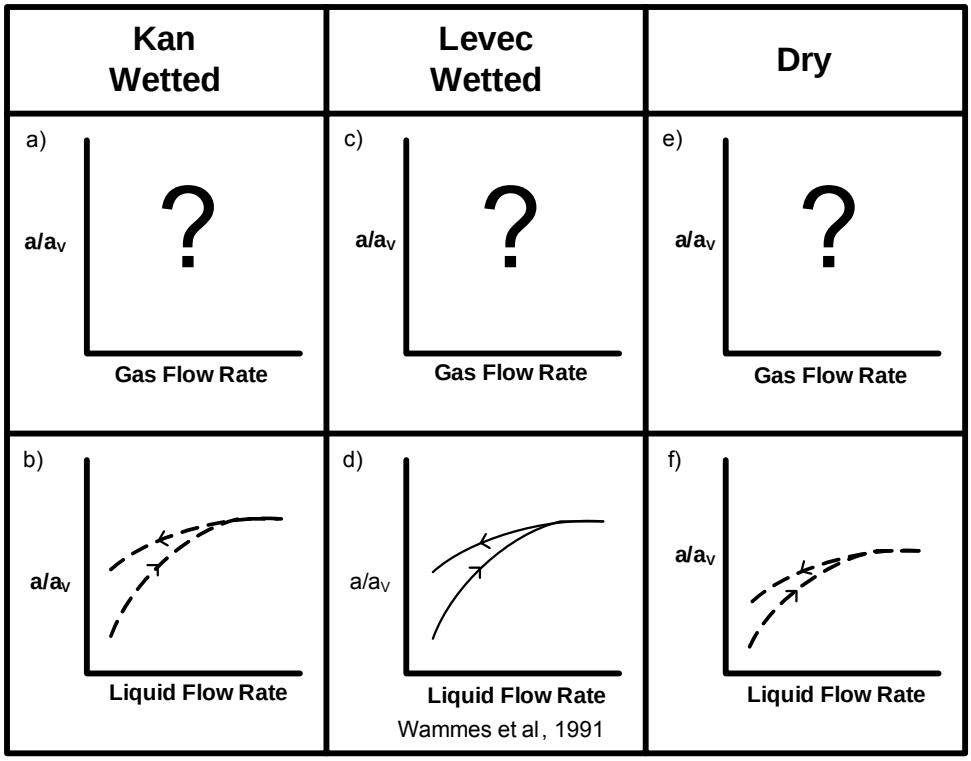

Figure 2-5: Gas-liquid interfacial area hysteresis for the Kan, Levec and Dry beds

Figure 2-5d) shows the only actual hysteresis results that could be found in literature. The results are based on the experimental work of Wammes *et al* (1991). They found that the interfacial area is larger when the liquid flow rate is decreased from a higher value, than the value obtained when the liquid flow rate is only increased. It is important to note that if the liquid flow rate is increased to the point of flooding and then decreased, the return leg is actually as a result of operating the bed in the Kan-wetted mode. The reason for the higher interfacial area is that as the liquid flow rate is increased there is a transition from rivulet flow to film flow. As the liquid flow rate is once again decreased the film flow pattern remains stable till a much lower liquid flow rate before the films break up into rivulets (Christensen *et al*, 1986). In the case of rivulet flow, less gas-liquid contact area is created in comparison to film flow at equal flow rates (Wammes *et al*, 1991).

Figure 2-5b) is represented by dashed lines as it was not directly observed but inferred. Ravindra *et al* (1997) found that the liquid distribution in the Kan mode was more uniformly distributed when the liquid was decreased from a

higher value. If we take into account the trend observed by Wammes *et al* (1991) observed in the Levec wetted bed, this would imply that better distribution results in a greater gas-liquid contact area. This implies that in a bed operated in the Kan-prewetted mode the gas-liquid interfacial area will be greater when the liquid flow rate is decreased from a higher value.

Figure 2-5f) is also represented by dashed lines due to the fact that it has not been observed. In a dry bed it has been observed that increasing the liquid flow rate will increase the liquid distribution. When the liquid flow rate is once again decreased, the distribution does not return to its previous state for a given liquid flow rate (Moller *et al*, 1996). Following from the observations made above, this will result in a larger gas-liquid interfacial area for the decreasing mode.

2.5.3 Gas-liquid Mass Transfer Correlations

In a trickle-bed reactor the gas-liquid mass transfer coefficient can have a detrimental effect on the overall performance of the reactor. This means that an accurate estimation of the gas-liquid mass transfer parameter is important for achieving successful reactor design or scale-up (Al-Dahhan *et al*, 1997)

The following correlations were tested:

- Mahajani & Sharma, 1979 (as given in Herskowitz & Smith, 1983)
- Ellman, 1988 (as given in Gianetto & Specchia, 1992)
- Hirose, Toda & Sato, 1974
- Wild *et al*, 1992 (as given in Iliuta *et al*, 1999b)
- Ermakova *et al*, 1977 (as given in Turek & Lange, 1981)
- Turek & Lange, 1981
- Reiss, 1967
- Fukushima & Kusaka, 1977

The results from the Trickle-bed Reactor Simulator of Larachi *et al* (1999) were also used.

Mahajani and Sharma (1979) proposed a correlation for the gas-continuous flow regime on the assumption that in this flow regime the interfacial area is a weak function of the gas and liquid flow rates. They measured the absorption of CO_2 in aqueous solutions of NaOH, MEA in n-butanol and CHA in p-xylene containing 10% isopropanol. The particles used were 4mm in diameter (Herskowitz & Smith, 1983). No mention was of any prewetting procedure. The proposed correlation is:

$$k_L a = 8.08 D \left(\frac{L}{\mu_L} \right)^{0.41} Sc_L^{0.5} \tag{2.58}$$

$$Sc_L = \frac{\mu_L}{\rho_L D} \tag{2.59}$$

The correlation proposed by Ellman (1988) is based on a large amount of data obtained with different gas-liquid systems for a wide range of operating conditions (Gianetto & Specchia, 1992). No mention is made of the prewetting procedures followed by the different investigators so the correlation can be assumed to be valid for the dry bed operations. The proposed correlation is:

$$k_L a = \left(\frac{D}{d_h^2} \right) \Omega X_G^{a_1} . \mathrm{Re}_L^{b_1} . We_L^{c_1} . Sc_L^{d_1} . \theta^{e_1} \tag{2.60}$$

$$\theta = \frac{a_V d_h}{1 - \varepsilon_B} \tag{2.61}$$

The constants for the correlation proposed by Ellman are given in table 2-2.

Table 2-2: Constants for equation 2.60

	Ω	a_1	b_1	c_1	d_1	e_1
$X_G < 0.8$	0.45	0.65	1.04	0.26	0.65	0.325
$0.8 < X_G < 1.2$	0.091	0.95	0.76	0.76	1.14	0.95
$X_G > 1.2$	0.00028	0.85	0.68	0.68	1.70	0.85

Hirose et al (1974) performed their reactions in a 65.8mm column (internal diameter) that was 0.25m long. The mass transfer coefficient was determined through the desorption of oxygen from presaturated water into a nitrogen stream. The experiment was repeated with four different sizes of glass beads, namely, 2.59, 5.61, 8.01 and 12.2mm. No prewetting procedure was used in their experiments. The proposed correlation is:

$$k_L a = 1 d_p^{-0.5} U_L^{0.8} U_G^{0.8} \tag{2.62}$$

Wild et al (1992) proposed the following correlation (as given in Iliuta *et al*, 1999b):

$$k_L a = 2.8\times10^{-4} \frac{D}{d_h^2} \left[X_G^{0.5}\, \mathrm{Re}_L^{0.8}\, We_L^{0.2}\, Sc_L^{0.5} \left(\frac{a_S d_h}{1-\varepsilon_B} \right)^{0.25} \right]^{3.4} \tag{2.63}$$

$$a_S = \frac{6(1-\varepsilon_B)}{d_p} + \frac{4}{D_C} \tag{2.64}$$

The correlation proposed by Ermakova *et al* (1997) as given in Turek and Lange (1981) is as follows:

$$k_L a = 0.02 D\, \mathrm{Re}_L^{0.95}\, Sc_L^{0.5} U_G^{-0.43} \tag{2.65}$$

Turek and Lange (1981) based their correlations on the experimental results obtained from the model reaction, the hydrogenation of α-methylstyrene. The reactor was 72cm long and had an internal diameter of 3.4cm. The liquid flow rate was varied between 0 and 1.5l/h and the gas flow rate from 0 – 100l/h. The reactor was operated at pressures of 0.15, 0.2 and 0.4MPa, respectively. No prewetting procedure was used in their experiments

The first correlation proposed by Turek and Lange (1981) was:

$$k_L a = 2\times10^2\, D H_d^{0.75} Sc_L^{0.5} \tag{2.66}$$

The dynamic holdup (H_d) can be obtained from experimental results or by substituting the correlation proposed by Turek and Lange (1981):

$$H_d = 2.13 Ga_L^{-0.24}\, \mathrm{Re}_L^{0.36}\, Y_G \tag{2.67}$$

For $Re_G < 1$:

$$Y_G = 1 - 0.32\,\mathrm{Re}_G^{0.25} \tag{2.68}$$

For $Re_G >= 1$

$$Y_G = 0.68 \tag{2.69}$$

However, Turek and Lange (1981) stated that the proposed correlation did not clearly represent the influence of particle size on the mass transfer. The correlation that produced the best fit for their experimental data was:

$$k_L a = 16.8 DGa_L^{-0.22}\,\mathrm{Re}_L^{0.25}\,Sc_L^{0.5} \tag{2.70}$$

As in the case of the pressure drop and liquid holdup correlations, the above mentioned correlations have no possible means of determining the gas-liquid mass transfer coefficient for different types of prewetting. The only exception is the first correlation proposed by Turek and Lange (1981) and that is only if you ignore their correlation for holdup and use the holdup values that have been determined from actual experiments for the different prewetting modes.

Reiss (1967) measured oxygen absorption into water from air. The packing was predominantly thin-walled polyethylene Raschig rings ranging from ½ to 3 inches. The correlation for the mass transfer coefficient is based on the concept of energy dissipation per unit volume. The proposed correlation is:

$$k_L a = 0.12 E_L^{1/2} \tag{2.71}$$

$$E_L = \left(\frac{\Delta P}{\Delta L}\right)_{LG} . V_L \tag{2.72}$$

The constant 0.12 is valid for the energy dissipation term for liquid flow being in the units $ft.lb_f/ft^3s$.

By incorporating the energy dissipation term the correlation may be able to predict the gas-liquid mass transfer for the different prewetting modes.

The correlation proposed by Fukushima and Kusaka (1977) is based on their experimental results. The experiments were based on the absorption of

oxygen from air into a sulphite solution. Cobaltous chloride was used as a homogeneous catalyst. The proposed correlation is:

$$k_L a = 2\frac{D\left(1-{H_t}/{\varepsilon_B}\right)}{d_p^2}\mathrm{Re}_L^{0.73}\,\mathrm{Re}_G^{0.2}\,Sc_L^{0.5}\left({d_p}/{D_C}\right)^{0.2} \tag{2.73}$$

By incorporating the liquid holdup in the correlation the gas-liquid mass transfer coefficient may be predicted for the different prewetting modes.

According to Hirose *et al* (1974) when the gas flows at a high velocity in a packed bed a considerable amount of energy dissipation occurs in the gas phase as well as in the liquid phase. When the liquid phase resistance to mass transfer is controlling the energy dissipation in the liquid phase is of primary importance. They did not propose a correlation for the trickle flow regime, but incorporate the liquid holdup and the pressure drop in their correlation. By incorporating the liquid holdup and the pressure drop, the correlation may be able to predict the gas-liquid mass transfer coefficient for the different prewetting modes. The proposed correlation is:

$$k_L a = 0.135\varepsilon_B\left(\frac{U_G}{\varepsilon_B}\right)^{0.6} E_L^{*0.31} \tag{2.74}$$

$$E_L^* = \left(\frac{\Delta P}{\Delta Z}\right)_{LG}\left(\frac{U_L}{H_t}\right) \tag{2.75}$$

When E^*_L and U_G/ε_B are chosen as the two correlating parameters the correlation can be seen as being explicitly independent of the packing size, however the packing diameter does affect k_La by changing E^*_L.

2.5.4 Measuring the Gas-Liquid Mass Transfer Coefficient

(Lara-Marquez, Wild & Midoux, 1994b):

Two types of techniques have been proposed in literature for the determination of the gas-liquid mass transfer coefficient, k_La, and they are:

- Physical absorption or desorption
- Chemical absorption

Physical absorption or desorption techniques are by far the most frequently used. In these techniques, oxygen is transferred either from air (eventually enriched with oxygen) to water (which has been stripped of oxygen) or from water (previously saturated with air) to nitrogen. The driving force for the desorption into nitrogen is easier to measure accurately due to its driving concentration difference $C_A \rightarrow 0$. The driving concentration difference for the absorption from air, on the other hand, is $C_A^* \rightarrow C_A$, and is more difficult to measure accurately (Lara-Marquez *et al*, 1994a).

For the chemical absorption techniques, the most frequently used is a fast pseudo m^{th} order reaction used to determine the interfacial area. However, there are a number of chemical techniques devoted to the determination of the volumetric mass transfer coefficient. These techniques are based on the measurement of the absorption rate of a gas reacting with a dissolved chemical species in a reaction where the absorption rate is proportional to $k_L a C_A^*$ (where A is the absorbed gas). Two reaction regimes have been proposed:

- Absorption with instantaneous reaction
- Absorption with a reaction that is slow in the mass transfer film but sufficiently fast in the bulk of the liquid that the concentration of A dissolved in the latter may be assumed negligible

2.5.5 Quantifying the Gas-Liquid Mass Transfer Coefficient

The equation used to calculate the volumetric mass transfer coefficient is based on the correlation proposed by Goto and Smith (1975). The equation takes into account the mass transfer in the end regions and the derivation can be seen in Appendix 1.

The expression derived from a simple mass balance for the calculation of the volumetric gas-liquid mass transfer coefficient is:

$$k_L a = \frac{U_L}{Z_B} \ln \left[\frac{\left(C_{L,O_2}\right)_{e'} \left(C_{L,O_2}\right)_f}{\left(C_{L,O_2}\right)_e \left(C_{L,O_2}\right)_{f'}} \right] \tag{2.76}$$

The definitions of the concentrations used in this equation can be seen in figure 2-6.

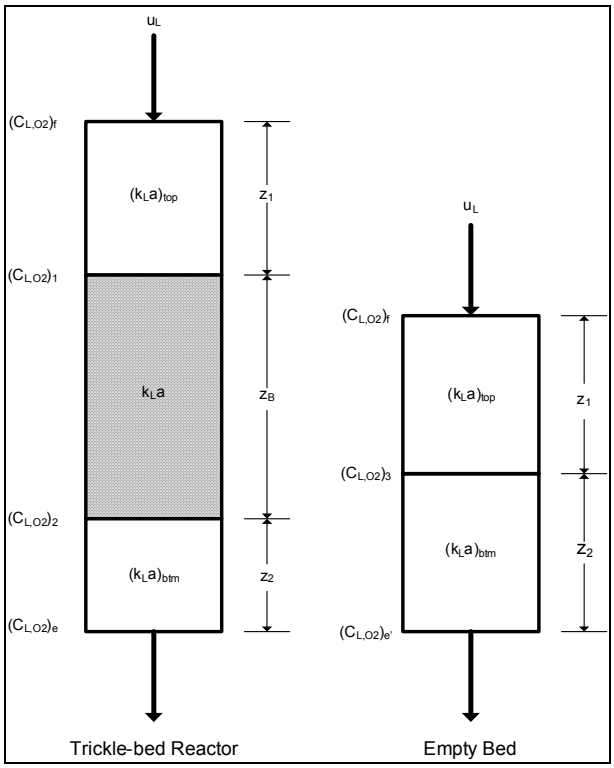

Figure 2-6: The modelling of end effects as shown by Goto and Smith (1975)

3. Experimental

3.1 Experimental Apparatus

A schematic drawing of the experimental apparatus is shown in figure 3-1. The setup has been designed to simultaneously measure the total liquid holdup, the pressure drop over a section of the bed and the dissolved oxygen in the inlet tank and the outlet stream.

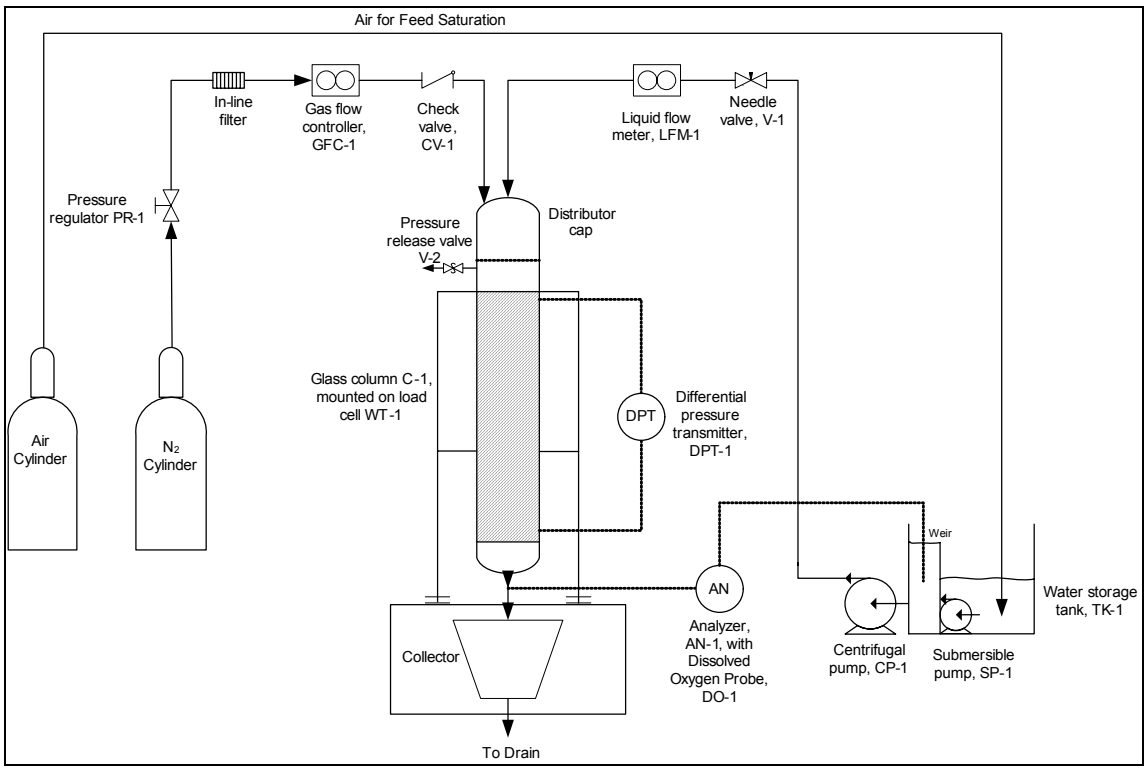

Figure 3-1: Experimental Setup

The reactor is a Perspex column with an internal diameter of 67mm and is 85cm long. The Perspex column was designed with a pressure release valve (V-6). The valve is opened when the column is being flooded to allow the gas to escape. The column is operated with an atmospheric outlet. The primary reason for this is to compare the results found in these experiments with those discussed in the literature. The majority of the research done on hydrodynamic hysteresis is done at low pressures and according to Dudukovic, Larachi and Mills (1999) may not be as prevalent at high

pressures. However, even at low pressures some investigators do not observe hysteresis with the pressure drop and the liquid holdup (Wammes *et al*, 1991).

The gas and liquid are fed concurrently into the bed. One distributor was used for all of the experiments. It is shown schematically in figure 3-2. The holes in the distributor plates for liquid distribution were 0.5mm in diameter and spaced in a square pitch arrangement 8mm apart. This resulted in a drip-point density of 16000 points/m^2. It was decided that this density was sufficient based on experiments by Burghardt *et al* (1995) who found that distributors with drip-point densities greater than 5000 points/m^2 were independent of the liquid distributor. The gas was fed into the column via three ¼" stainless steel tubes. The gas was distributed in this manner so as to ensure that even at high gas flow rates the distribution of the liquid stream was as uniform as possible.

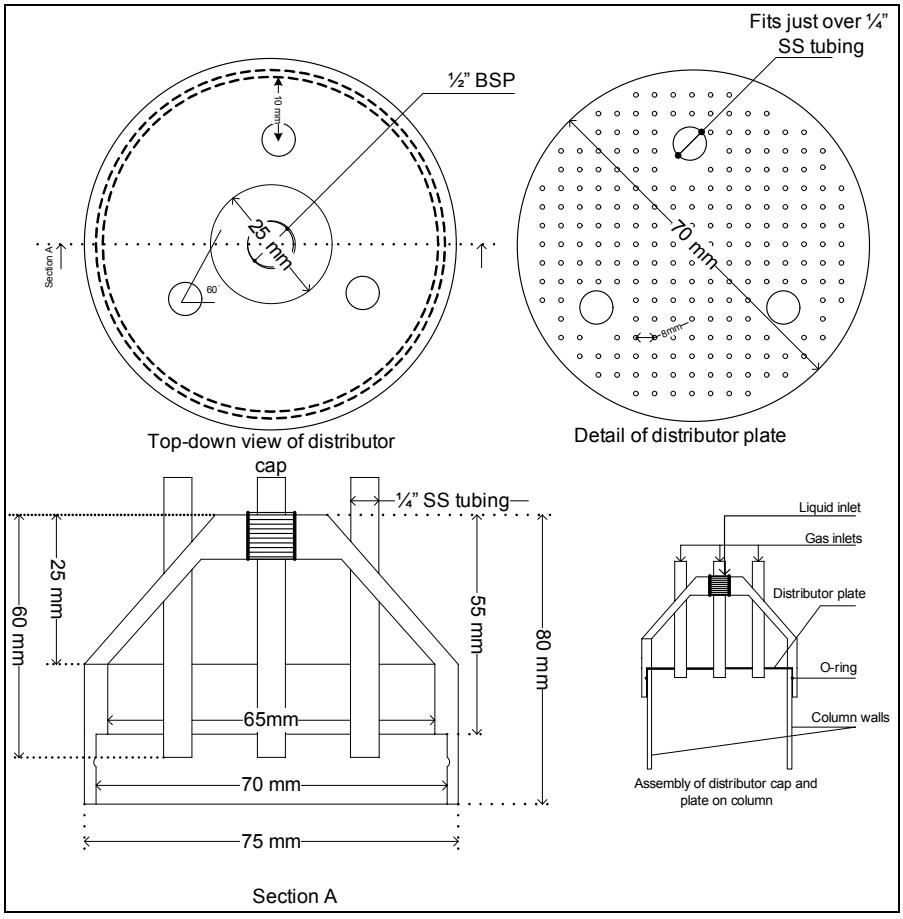

Figure 3-2: The gas and liquid distributor

The liquid used in all of the experiments is water and is measured by an Electromagnetic Flow Measuring System, the PROline promag 10H from Endress + Hauser. The flow meter has an accuracy of 0.5% of the rate when the flow is above 1l/min and an accuracy of 1.5% of the rate when the flow is between 0.2 and 1l/min. The gas phase is Nitrogen and is measured with a Brooks Smart Mass Flow Model 5851S. The range of the flow meter is 0 – 100l/min, and is calibrated for Nitrogen and has an accuracy of 0.7% of the range.

The water – nitrogen system is chosen because it is one of the most widely used systems in the study of gas-liquid mass transfer. In these experiments the nitrogen is used to strip dissolved oxygen from the water that has been pre-saturated with air. (Goto and Smith, 1975) (Reiss, 1967) (Hirose *et al*, 1974) (Lara Marquez *et al*, 1994b)

The size and shape of the packing is an important factor to take into account. 3mm glass beads are chosen due to the fact that they result in more uniform distribution than other types of packing (Tsochatzidis *et al*, 2002) and according to Gianetto *et al* (1978) in the trickle-flow regime the flow is more uniform if the particle diameter is less than 6mm.

The pressure drop over a section of the bed was measured by a Rosemount Model 3051CD Pressure Transmitter. The accuracy of the transmitter was 0.1% of the range and under normal operating conditions translates to an accuracy of approximately 6Pa. The pressure taps are placed 65cm apart along the length of the bed.

The total holdup was determined by a weighing method by mounting the column on a high accuracy load cell type 642C3 from Revere Transducers Europe. The accuracy of the load cell is 0.02% of the span, which relates to an accuracy of approximately 4g.

The dissolved oxygen in the feed tank and outlet stream was measured with the Dissolved Oxygen Sensor 499ADO from Rosemount Analytical. The range of the probe was 0 – 20 ppm and has a reported accuracy of 0.2ppm and a repeatability of 0.05ppm at 25°C. The analyser used was the SOLU COMP II analyser from Rosemount Analytical. The oxygen sensor needed to be calibrated for a zero standard (no dissolved oxygen) and air calibration. The apparatus for the analysis of the outlet stream is shown in figure 3-3.

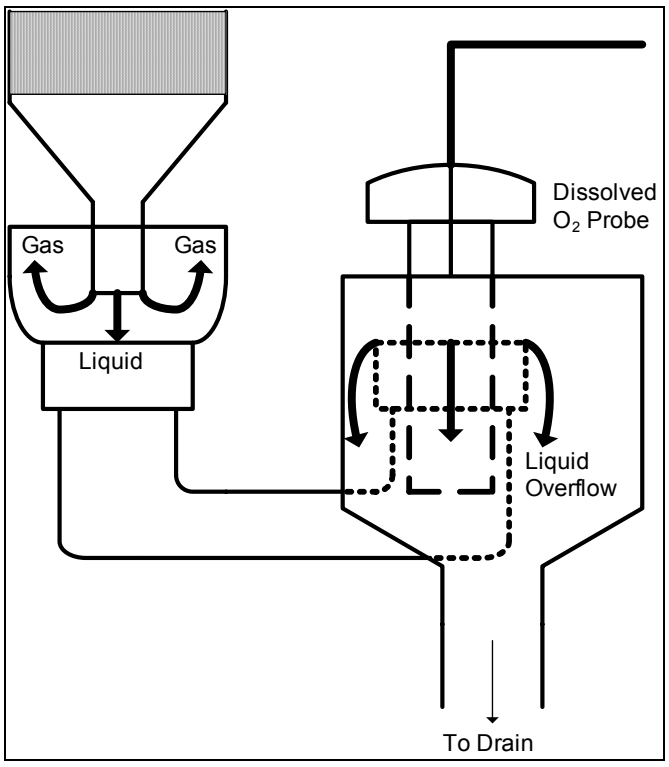

Figure 3-3: A schematic representation of the apparatus used in the analysis of the outlet concentration

The zero standard is obtained by placing the probe in a solution of 5% sodium sulphite in water. This method was preferred to oxygen-free nitrogen bubbling through the water. Air calibration is done by placing the probe 1cm above a glass beaker filled with water and waiting for the reading to stabilise.

The electrolyte solution in the probe was also regularly replaced to ensure the accuracy of the probe.

All readings and control of the equipment was done using the DeltaV® operating system and a continual historian ensured that all data was recorded during the experiments.

3.2 Operating Procedure

The column is packed with the 3mm glass beads to a height of 69cm. A metal sieve supports the glass beads at the bottom of the bed. The holes in the sieve are 2.5mm. This ensures that the 3mm beads are adequately supported but does not result in the build up of a liquid head (based on visual inspection) which may affect the liquid holdup and pressure drop readings. The mass of the beads placed in the column is recorded and from this the porosity can be calculated, as shown in equation 3.1. The average porosity of the bed was 0.375 for all of the experimental runs.

$$\varepsilon_B = 1 - \frac{Mass\ of\ beads}{Density\ of\ glass\ beads \times Bed\ volume} \tag{3.1}$$

The packed bed is then mounted on the load cell stand and the load cell is re-zeroed. By re-zeroing the load cell the total liquid holdup can be determined directly and not by subtracting the mass of the bed from the total mass of the bed and the liquid flowing through it during operation.

Before any liquid is introduced into the reactor the Ergun constants are determined by allowing only the nitrogen to flow through the dry bed. During these runs the air supply is opened and the feed tank is saturated with oxygen. The dissolved oxygen probe is left in the tank and no liquid is introduced to the reactor until the dissolved oxygen content of the feed tank has reached a steady-state value.

In order to investigate the effect that prewetting has on the liquid holdup, pressure drop and gas-liquid mass transfer the experiments are performed on the same bed. The general procedure followed is:

- Dry bed operation
- Prewetting by pulsing with liquid (Kan prewetting)
- Super prewetting
- Levec prewetting
- Prewetting by pulsing with liquid (Kan prewetting)

The liquid flow rates tested were 1, 3, 5, 7 and 9 mm/s and the gas superficial velocities tested were 10, 20, 40, 70 and 90 mm/s, respectively. The gas and liquid flow rates and their corresponding mass fluxes and Reynolds numbers (based on equations 2.2 and 2.3) are shown in tables 3-1 and 3-3, respectively. Figure 3-4 shows the plot of the experimental points with respect to the trickle and pulse boundary based on the Trickle-bed Simulator of Larachi *et al* (1999).

Table 3-1: Gas Flow Rates

U_G (mm/s)	G (kg/m^{2}s)	Re_G
10	0.013	2.1
20	0.026	4.1
40	0.052	8.2
70	0.091	14.4
90	0.117	18.5

Table 3-2: Liquid Flow Rates

U_L (mm/s)	L (kg/m^{2}s)	Re_L
1	1	3
3	3	9
5	5	15
7	7	21
9	9	27

The lower gas superficial velocities, 10 and 20 mm/s, encompass the operating range where the trickle-bed reactors fluid dynamics are seen to be

gravity driven and gas phase independent. For the higher gas superficial velocities, 70 and 90 mm/s, the hydrodynamic parameters such as liquid holdup and catalyst wetting, are affected by the gas phase. These two distinct operating ranges are the most common operating ranges for experiments in the trickle-flow regime (Al-Dahhan *et al*, 1997).

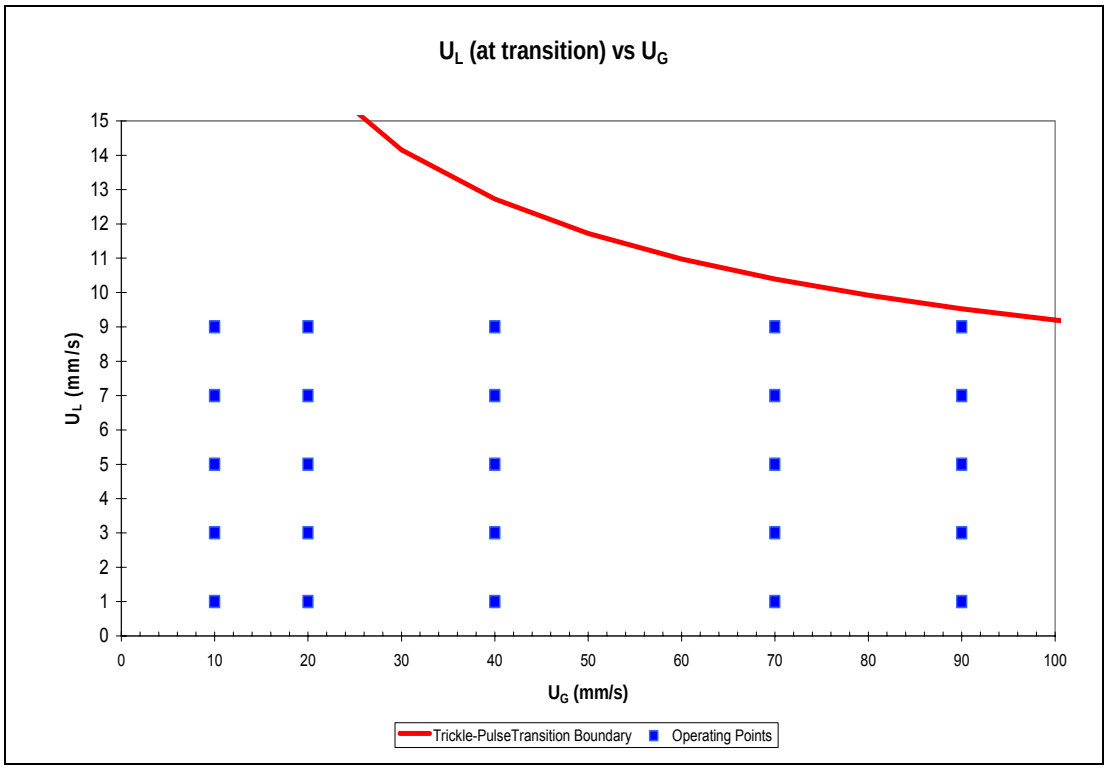

Figure 3-4: The experimental data points with respect to the trickle-pulse transition boundary

From the figure above it is clear that the flow rates chosen for the experiment represent a reasonably good distribution in the trickle-flow regime.

3.2.1 Dry Bed Operation

At the start of the dry bed operation the gas flow rate is set at the lowest gas flow rate (U_G = 10 mm/s). Once this desired set point has been reached the liquid flow rate is increased from zero to the desired setpoint. Care is taken to ensure that the liquid flow rate is not taken to a higher value than the setpoint.

Steady-state is assumed to be reached when the pressure drop, liquid holdup (as determined by the load cell) and dissolved oxygen in the exit stream no longer vary. Once steady-state has been reached (approximately 5 to 10 minutes) and the readings recorded, the gas flow rate is increased to the next setpoint. This procedure is repeated for all of the necessary gas flow rates at the specific liquid flow rate. For the dry bed runs the gas flow rate is always increased and never decreased. The reason for this is that the higher gas flow rate may have an effect on the distribution of the liquid and the results obtained could differ significantly. Any results obtained following this procedure have been labelled DRY.

3.2.2 Prewetting by Pulsing with Liquid (Kan prewetting)

Prewetting the bed by pulsing with liquid is a technique that has been used by many investigators in the past. In Kan prewetting the bed is prewetted by increasing the liquid flow rate, while the gas flow rate is kept at the desired setpoint, until the pulsing regime is reached. The limitations of the equipment used in the experiments are that pulsing could not be induced at the lowest gas flow rate investigated (U_G = 10 mm/s) because this liquid flow rate could not be attained. This means that the Kan prewetted beds were only operated at gas flow rates of 20 mm/s and higher.

After the experiments on the dry bed the gas flow rate is set at 20 mm/s and allowed time to stabilise. Once the gas flow rate has stabilised the liquid flow rate is increased to the point where pulsing is induced. Once pulsing has been induced in a part of the bed the liquid flow rate is increased further to the point where the pulsing is taking place over the entire length of the bed. The bed is left in the pulsing mode for approximately 15 seconds to ensure that the entire bed is wet. Once the bed is completely wet (based on a visual inspection) the flow rate is then decreased to the desired setpoint. Once again, steady state readings are taken for the pressure drop, liquid holdup and dissolved oxygen in the exit stream.

This procedure is repeated at all of the remaining gas flow rates. The Kan prewetting procedure was done twice during the experimental procedure for a specific liquid flow rate, once straight after the dry bed experiments, as explained above, and once right at the end, after the bed has been used for Super and Levec pre-wetting. By comparing the results from the experiments following the dry bed (denoted by KAN (Dry) in the results) and the experiments following the Levec prewetted experiments (denoted by KAN (Wet) in the results) you will be able to see if the prewetting history of the bed has any effect on the bed that is prewetted by inducing pulsing in the liquid phase.

3.2.3 Super Prewetting

For the first super prewetting experiment the gas flow rate is set at 10 mm/s after the Kan wetted experiments. Once the liquid has been set at the desired setpoint the pressure release valve (V-2) is opened and the bottom of the column is sealed. This starts flooding the column from the bottom and avoids the entrainment of bubbles. Instead of the gas building up in the column it can escape through the open valve. Once the column has been completely flooded the seal at the bottom of the column is removed and the liquid is allowed to drain out. The flow rate of the liquid into the column is never switched off or adjusted, and the irrigation continues throughout the flooding and draining period. Once steady-state has been achieved the pressure drop, liquid holdup and dissolved oxygen in the exit stream can once again be recorded.

The gas flow rate can then be raised to the next setpoint and the procedure is repeated for each of the desired gas flow rates. The results obtained for this operating procedure have been labelled SUPER in the results.

3.2.4 Levec Prewetting

The Levec prewetting procedure is similar to the Super prewetting procedure. The main difference is that once the bed is fully flooded the liquid flow into the column is shut off. The liquid is then allowed to drain and no liquid enters the column at this point in time. Liquid is only introduced once the mass in the column has remained constant for approximately five minutes. This liquid that remains in the bed is the residual liquid holdup.

Once the residual liquid holdup has been determined the liquid is re-introduced to the column. Once steady state has been reached the pressure drop, liquid holdup and dissolved oxygen in the exit stream are recorded.

Two different types of draining procedure were followed for each experiment. Firstly the gas supply was shut off and the liquid was allowed to drain under conditions with zero gas flow, these results are referred to as LEVEC (No Gas) in the results section. The second draining condition was draining under gas flow. In this draining procedure the gas supply was never switched off during draining. These results are referred to as LEVEC (Gas) in the results section.

3.2.5 Prewetting by Pulsing with Gas (Kan prewetting)

The Kan-prewetting mode described in section 3.2.2 involves the gas flow rate being kept at the desired operating point and the liquid flow rate being increased till pulsing is induced. However, increasing the gas flow rate and keeping the liquid flow rate at the desired operating point can also induce pulsing.

The limitations of the equipment used in the experiments resulted in the fact that pulsing by increasing the gas flow rate could only be induced at the highest liquid flow rate investigated (L = 9 mm/s).

For the gas pulsing experiment the liquid flow rate is set at 90 mm/s and the gas flow rate is set at 10 mm/s. The liquid flow rate is allowed time to stabilise and once it has stabilised the gas flow rate is increased to the point where pulsing is induced. Once pulsing has been induced in a part of the bed the gas flow rate is increased further to the point where the pulsing is taking place over the entire bed. The bed is left in the pulsing mode for approximately 10 seconds to ensure that the entire bed is wet. Once the bed is completely wet (based on a visual inspection) the flow rate is then decreased to 10 mm/s again. Once again, steady state readings are taken for the pressure drop, liquid holdup and dissolved oxygen in the exit stream.

The experiment is then repeated for each of the gas flow rates while the liquid flow rate remains at 90 mm/s. The results are shown in section 4 and are identified by the points labelled KAN (Gas).

3.3 Liquid Holdup and Gas-Liquid Mass Transfer

The liquid holdup is determined by a weighing method. Although similar to the methods described by Wammes *et al* (1991) and Ellman *et al* (1990), there are a few key differences. Instead of weighing the packed column before the experiment, and subtracting the value from the total weight of the column and liquid during operation, the packed column is placed on the load cell and the load cell is re-zeroed before any fluid enters it. This means that during operation the load cell is simply reporting the mass of the fluid in the column at that specific time. Since the glass beads are non-porous, and thus internal holdup is zero, the measured value is the total holdup (the sum of the dynamic and residual holdup).

The technique used to determine the gas-liquid mass transfer is similar to the desorption technique used by Goto and Smith (1975). The water in the feed tank is presaturated with oxygen by bubbling air through it continuously. The

saturated feed line is then sent to the reactor where the water is fed concurrently downwards with nitrogen gas, and the oxygen is transferred from the water to the nitrogen. Since oxygen has a relatively low solubility in water, the desorption method is favoured to the absorption method (from air to water which has been stripped of oxygen) due to the driving concentration difference being greater for the desorption method (Lara Marquez *et al*, 1994a).

In order to correctly quantify the volumetric gas-liquid mass transfer coefficient the end effects need to be taken into account. These end effects are taken into account by performing the experiment in a smaller bed that has no packing whatsoever. The column has the same internal diameter as the column used in the actual experiments but is only 10 cm in height.

Before the experiment commences the feed tank is saturated with oxygen. Once the water in the tank is saturated with oxygen the liquid flow rate is set at 1 mm/s and the gas flow rate is set at 10mm/s. The outlet streams dissolved oxygen concentration is measured and recorded. Once this reading has been taken the gas flow rate is increased and repeated until all of the gas flow rates have been tested.

Once the experiment has been repeated for all of the gas flow rates the gas flow rate is set at the lowest experimental setpoint and the liquid flow rate is increased to 3 mm/s. The experiment is then repeated for all of the required gas flow rates. This procedure is followed for all of the gas and liquid flow rates that are tested.

The concentrations of the outlet stream are then used in equation 2.68 and the volumetric gas-liquid mass transfer coefficient in the bed can be determined for a given flow rate. According to Goto and Smith (1975) these outlet concentrations can be as much as 36% lower than the feed concentration indicating that there is considerable mass transfer occurring in the end regions of the bed.

4. Results

4.1 Pressure Drop

The effect of the prewetting on the pressure drop, at constant gas flow rates, can be seen in figures 4-1 and 4-2. In these figures the average data point is shown and the accompanying bars represent the maximum and minimum values obtained in repeat experiments.

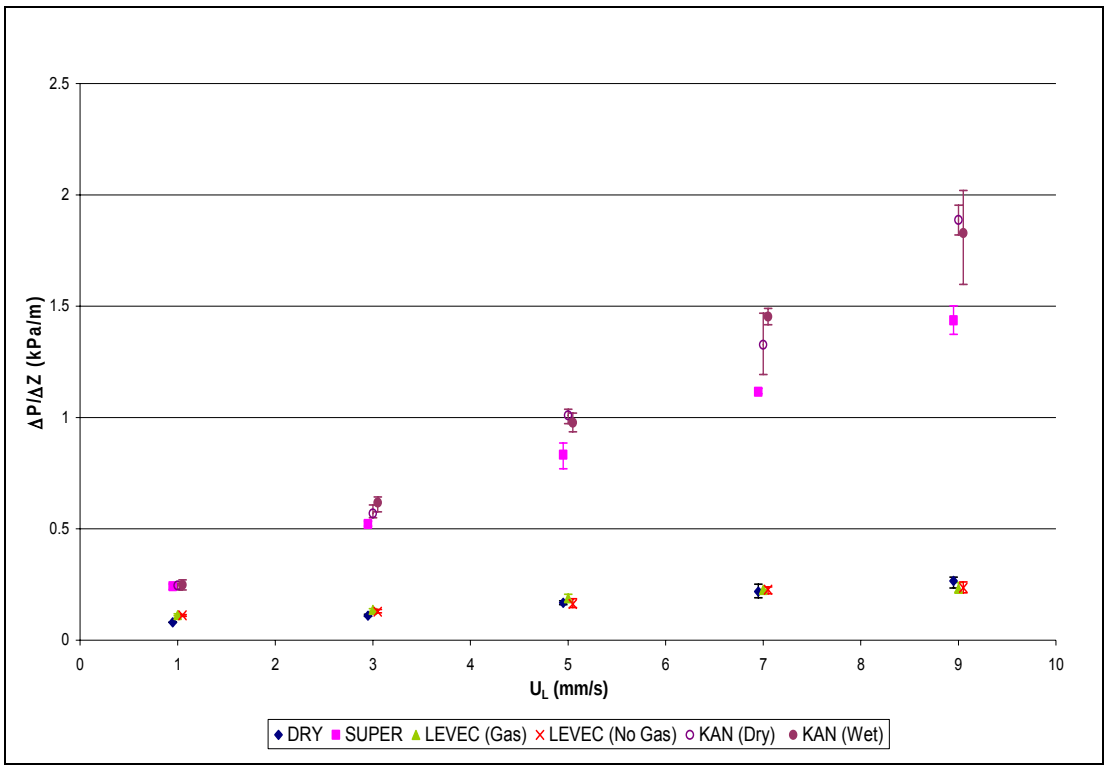

Figure 4-1: The effect of prewetting on the pressure drop at U_G = 20mm/s

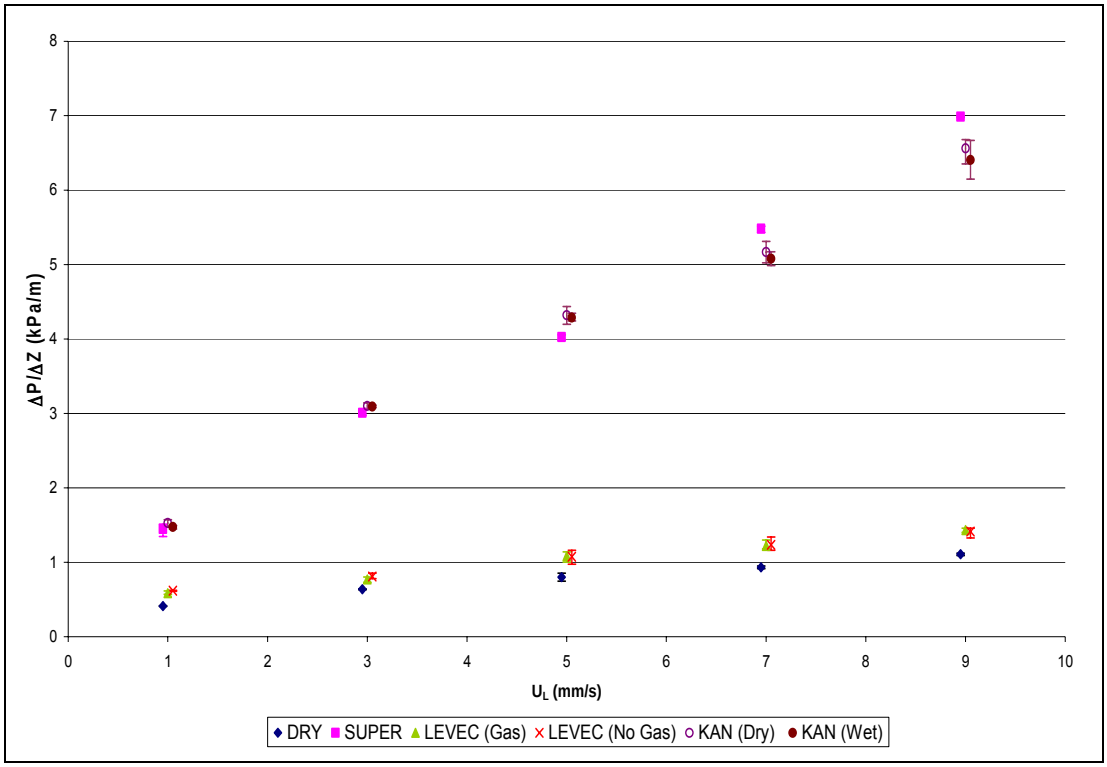

Figure 4-2: The effect of prewetting on the pressure drop at U_G = 90mm/s

From figures 4-1 and 4-2 the following trends are observed:

- The different prewetting procedures result in two distinct regions
- The pressure drop in the Levec-wetted bed is comparable to the pressure drop in the dry bed
- The difference between the two regions is substantial and the pressure drop in the Kan and Super-wetted bed are approximately seven times greater than the pressure drop in the dry and Levec-wetted beds at the highest liquid flow rate
- The pressure drop is a function of the liquid flow rate, and regardless of the prewetting procedure, the pressure drop will increase as the liquid flow rate increases
- There is no significant difference between the LEVEC (Gas) and LEVEC (No Gas) results
- There is no significant difference between the KAN (Dry) and KAN (Wet) results

The results for the intermediate gas flow rates are shown in appendix 2.

A 3-dimensional plot of the pressure drop for all of the gas and liquid flow rates tested is shown in figure 4-3.

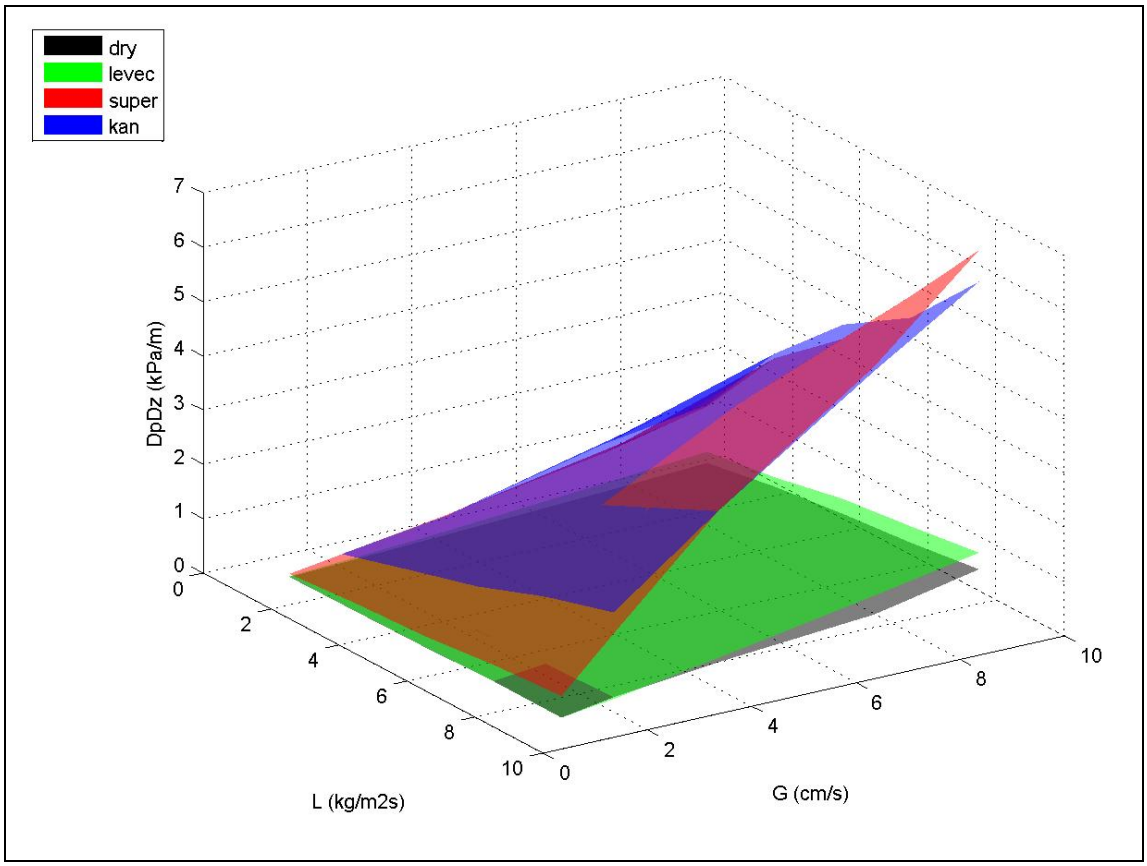

Figure 4-3: A 3-dimensional plot showing the effect of the gas and liquid flow rates on the pressure drop for the different prewetting modes.

Figure 4-3 shows clearly the two distinct regions that result from the different prewetting modes. As the gas and liquid flow rates are increased the gap between the different modes becomes larger with the Kan and Super-wetted beds recording substantially higher pressure drops than those of the dry and Levec-wetted beds.

4.2 Liquid Holdup

4.2.1 The Effect of Prewetting on the Liquid Holdup

The effect of the prewetting on the total liquid holdup, at constant gas flow rates, can be seen in figures 4-4 and 4-5. In these figures the average data point is shown and the accompanying bars represent the maximum and minimum values obtained in repeat experiments. The total liquid holdup is divided by the bed porosity to give the total liquid saturation.

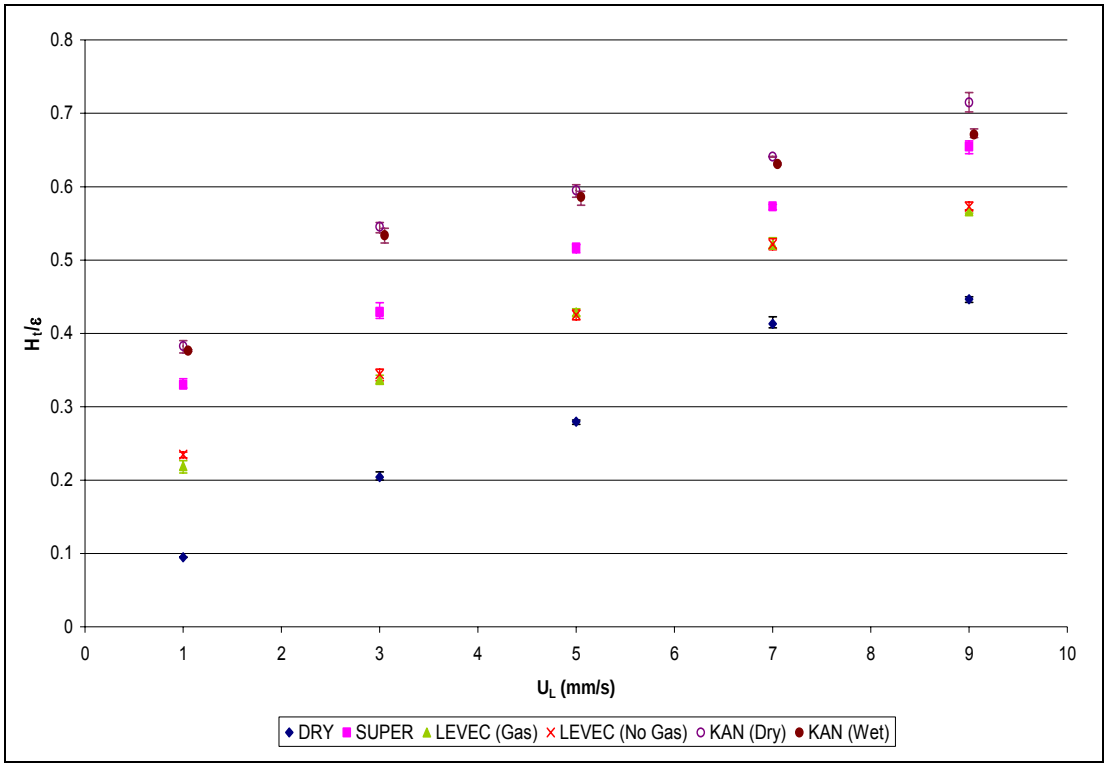

Figure 4-4: The effect of prewetting on the total liquid holdup at U_G = 20mm/s

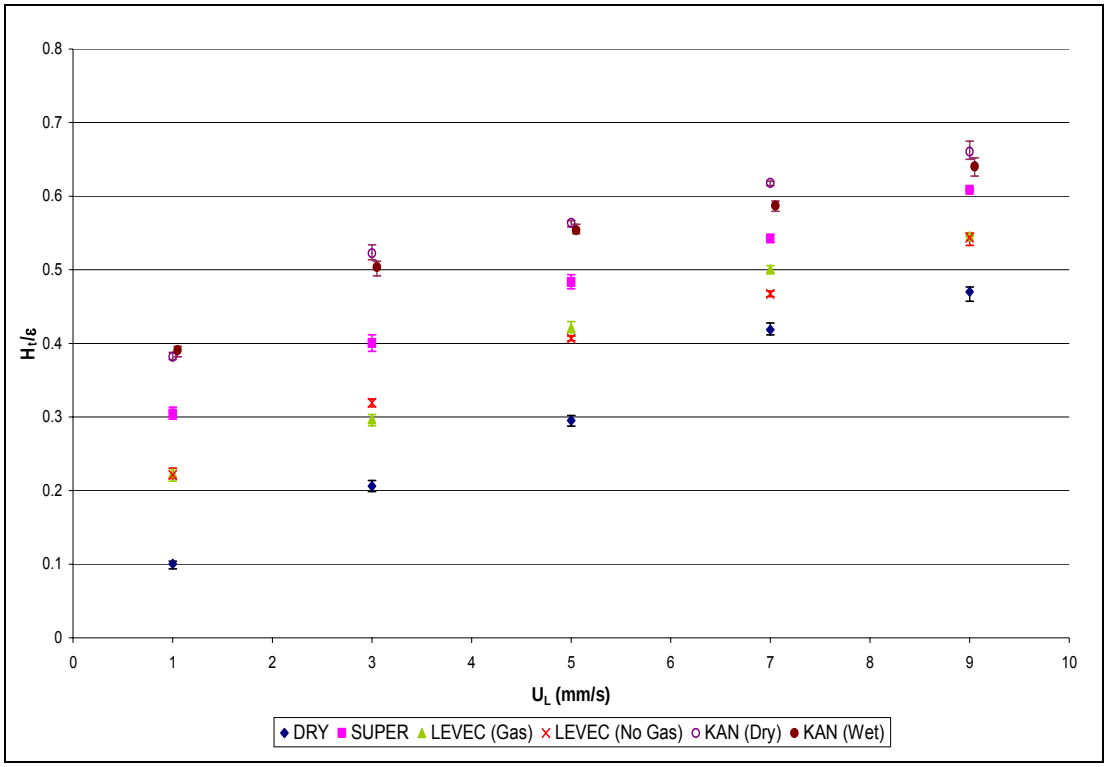

Figure 4-5: The effect of prewetting on the total liquid holdup at U_G = 90mm/s

From figures 4-4 and 4-5 the following trends are observed:

- The different prewetting procedures result in four distinct regions
- The difference between the regions is substantial and the total liquid holdup in the Kan-wetted bed is approximately four times larger than the total liquid holdup in the dry bed at the lowest liquid flow rate
- The liquid holdup in the Levec-wetted can be as much as thirty percent lower than the liquid holdup in the Kan-wetted bed
- Regardless of the prewetting procedure the liquid holdup increases with the liquid flow rate. This has been confirmed by many investigators (Burghardt *et al*, 1995) (Stegeman *et al*, 1996) (Levec *et al*, 1986) (Lazzaroni *et al*, 1989) (Dudukovic *et al*, 1999)
- There is no significant difference between the LEVEC (Gas) and LEVEC (No Gas) results
- There is no significant difference between the KAN (Dry) and KAN (Wet) results

The results for the intermediate gas flow rates are shown in appendix 3.

4.2.2 The Effect of Gas Flow rate on the Liquid Holdup

The effect of the gas flow rate for the different prewetting modes on the total liquid holdup can be seen in figures 4-6 and 4-7.

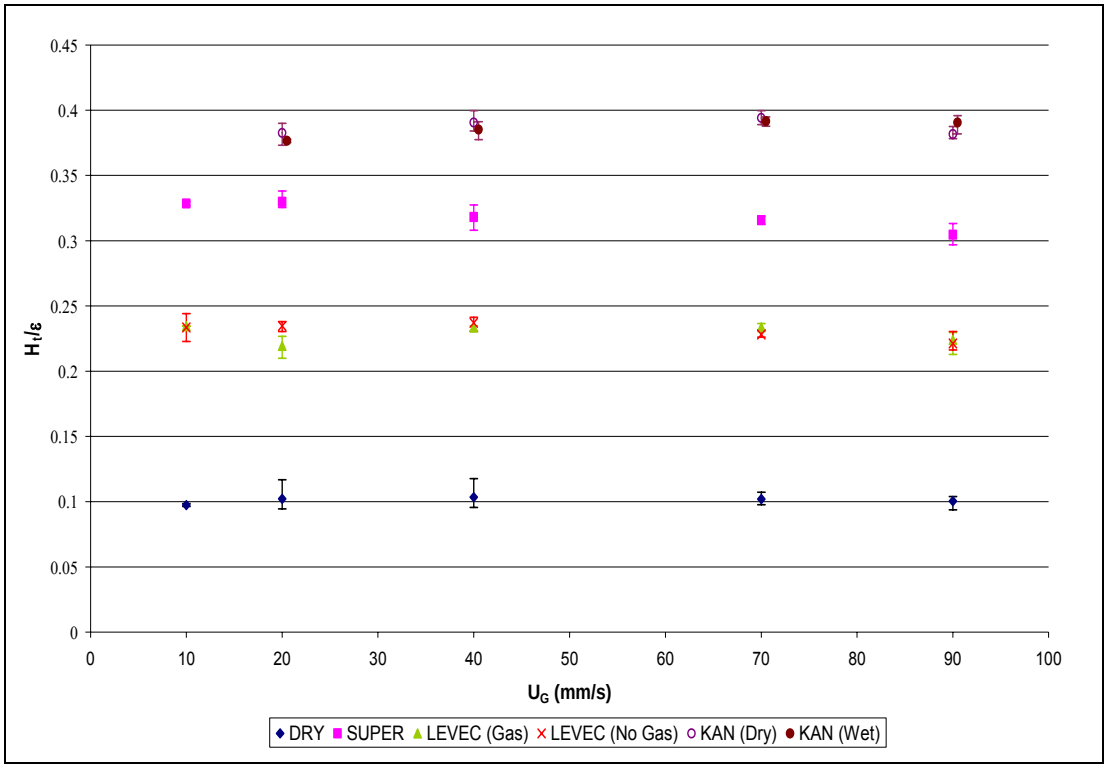

Figure 4-6: The effect of the gas flow rate on the total liquid holdup for the different prewetting modes at U_L = 1mm/s

From the figure above it is clear that the effect of the gas flow rate on the liquid holdup is not as noticeable as the effect of the liquid flow rate on the holdup. For the Dry bed there appears to be no effect on the liquid holdup when the gas flow rate is increased. For the Levec-wetted bed, when one takes into account the spread of the data, there also appears to be no recognizable increase or decrease in the liquid holdup with an increase in the gas flow rate. The Super-wetted bed appears to show a trend. At low gas flow rates (10 and 20mm/s) the liquid holdup does not appear to be affected by the gas flow rate at all. However, as the gas flow rate is increased from 40mm/s a slight decrease in the liquid holdup can be seen with the increased gas flow

rate. For the Kan-wetted bed the holdup does not appear to change with the gas flow rate.

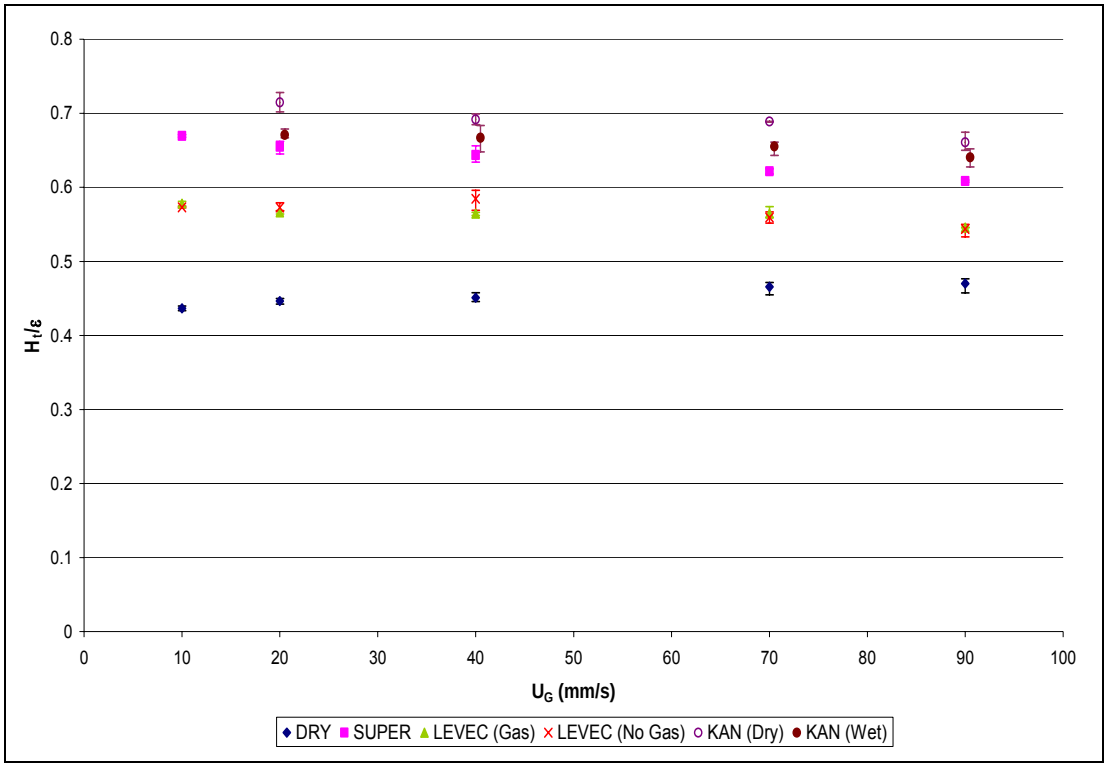

Figure 4-7: The effect of the gas flow rate on the total liquid holdup for the different prewetting modes at U_L = 9mm/s

Figure 4-7 shows the effect of the gas flow rate on the liquid holdup at the highest liquid flow rate tested. From this figure it is clear that as the gas flow rate is increased, the liquid holdup decreases slightly for the Kan, Super and Levec-prewetted beds. However, the dry bed does not appear to be affected by the gas flow rate at all.

The results for the intermediate liquid flow rates are shown in appendix 4.

A 3-dimensional plot of the liquid holdup at all of the gas and liquid flow rates tested is shown in figure 4-8.

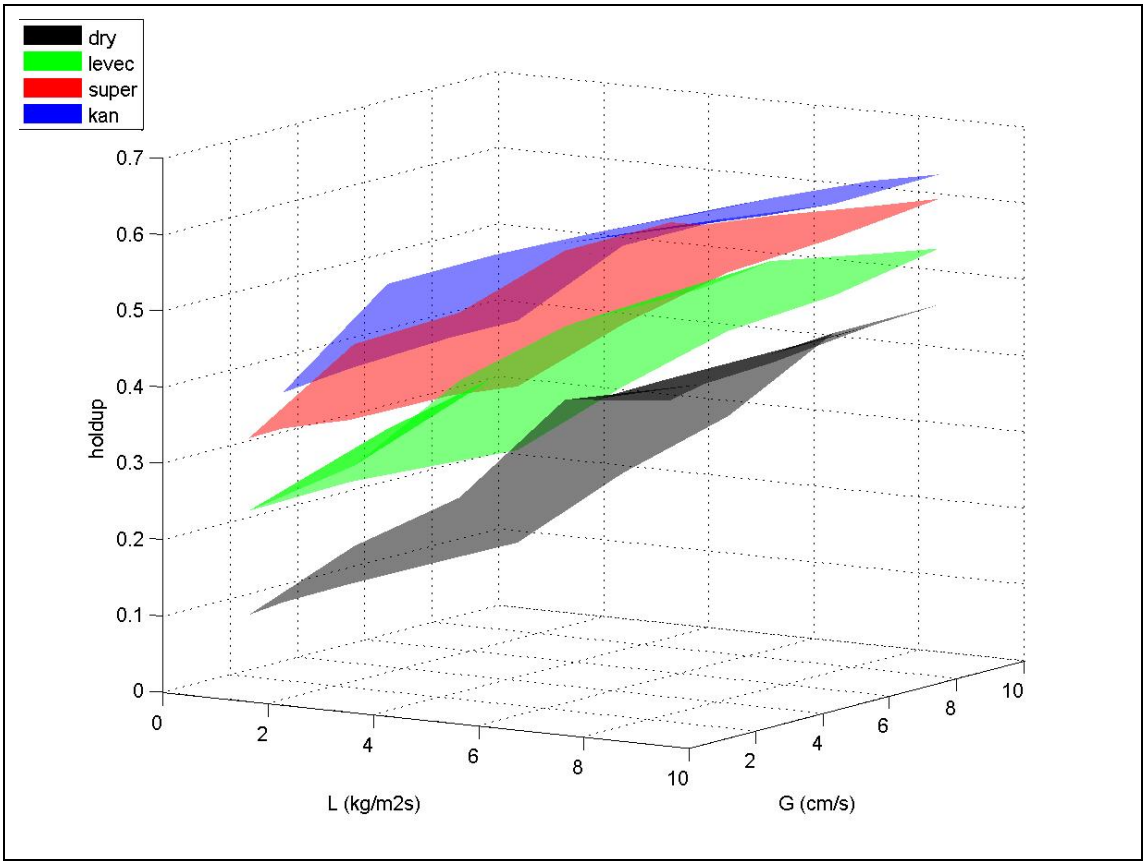

Figure 4-8: A 3-dimensional plot showing the effect of the gas and liquid flow rates on the liquid holdup for the different prewetting modes

Figure 4-8 clearly shows the four distinct regions of liquid holdup that result from the different prewetting modes.

4.3 Gas-Liquid Mass Transfer

4.3.1 The Effect of Prewetting on the Volumetric Gas-Liquid Mass Transfer Coefficient

The volumetric gas-liquid mass transfer coefficient was calculated using equation 2.68 (Goto & Smith, 1975):

$$k_L a = \frac{U_L}{Z_B} \ln\left[\frac{\left(C_{L,O_2}\right)_{e'}\left(C_{L,O_2}\right)_f}{\left(C_{L,O_2}\right)_e\left(C_{L,O_2}\right)_{f'}}\right] \qquad (2.76)$$

The effect of the prewetting on the volumetric gas-liquid mass transfer coefficient at constant gas flow rates can be seen in figures 4-9 and 4-10. In these figures the average data point is shown and the accompanying bars represent the maximum and minimum values obtained in repeat experiments.

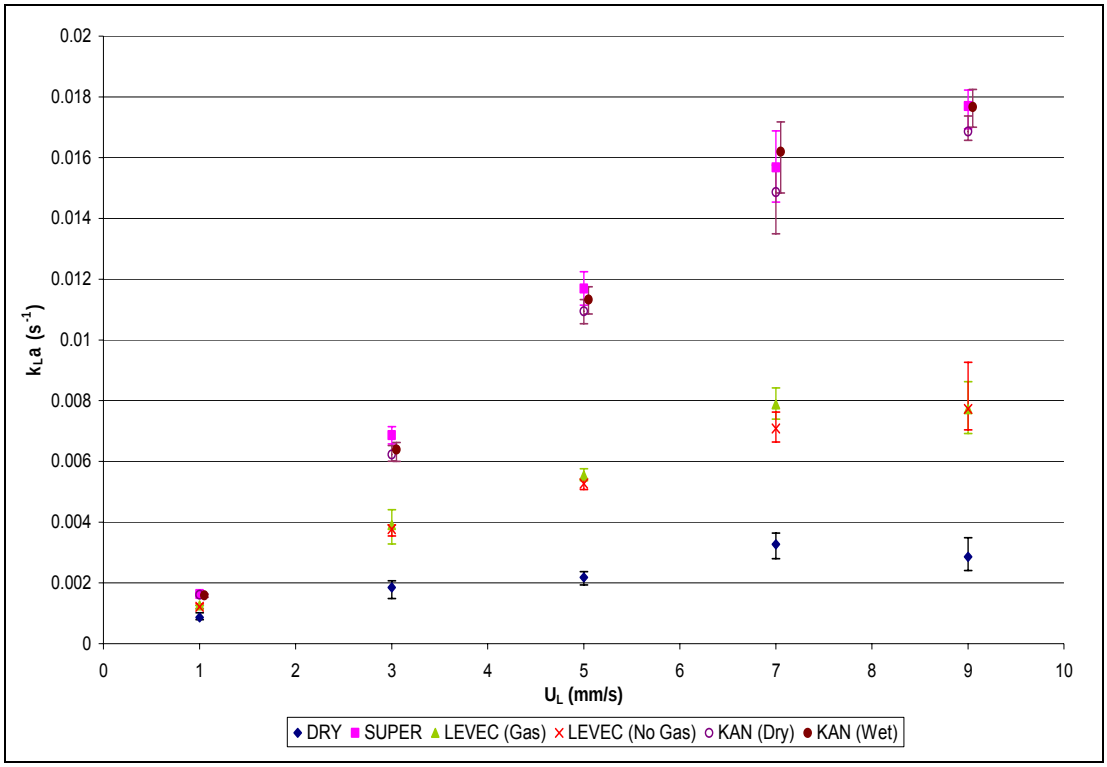

Figure 4-9: The effect of prewetting on the volumetric gas-liquid mass transfer coefficient at U_G = 20mm/s

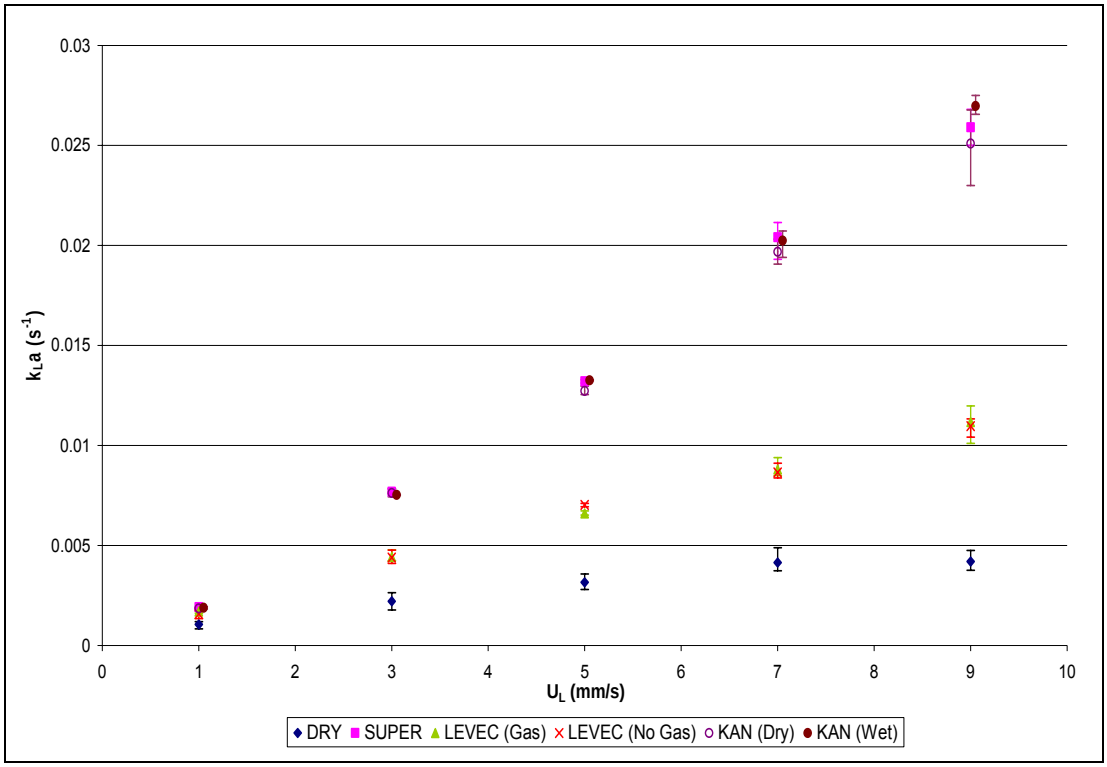

Figure 4-10: The effect of prewetting on the volumetric gas-liquid mass transfer coefficient at U_G = 90mm/s

From figures 4-9 and 4-10 the following trends are observed:

- The different prewetting procedures result in three distinct regions
- The difference between these regions is substantial and the volumetric gas-liquid mass transfer coefficient in the Kan and Super-wetted bed are approximately six times larger than in the dry bed at the highest liquid flow rate
- The volumetric gas-liquid mass transfer coefficient in the Kan and Super-wetted beds can be as much as two and a half times greater than the mass transfer coefficient in the Levec-wetted bed
- The volumetric gas-liquid mass transfer coefficient is a function of the liquid flow rate and increases with liquid flow regardless of the prewetting procedure
- There is no significant difference between the LEVEC (Gas) and LEVEC (No Gas) results
- There is no significant difference between the KAN (Dry) and KAN (Wet) results

The results for the intermediate gas flow rates are shown in appendix 5.

4.3.2 The Effect of Gas Flow rate on the Volumetric Gas-Liquid Mass Transfer Coefficient

The effect of the gas flow rate for the different prewetting modes on the gas-liquid mass transfer coefficient can be seen in figures 4-11 and 4-12.

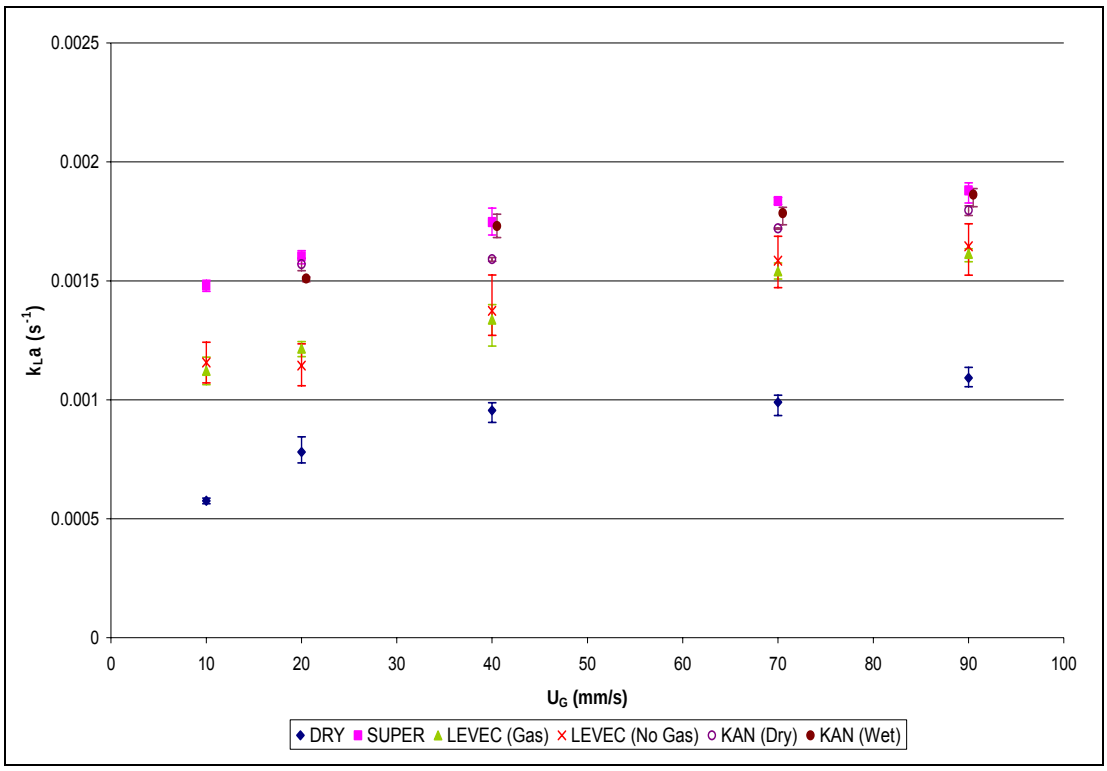

Figure 4-11: The effect of the gas flow rate on the gas-liquid mass transfer coefficient for the different prewetting modes at U_L = 1mm/s

From figure 4-11 it would appear that the gas flow rate does have an influence on the volumetric gas-liquid mass transfer coefficient. In general, an increase in the gas flow rate appears to cause an increase in the mass transfer coefficient, regardless of the prewetting procedure. These results confirm the findings of Geonaga, Smith and McCoy (1989) and Iliuta, Iliuta and Thyrion (1997).

In the dry and Levec-wetted bed there is a sharp increase in the volumetric mass transfer coefficient for the low gas flow rates and only a slight increase at the higher gas flow rates.

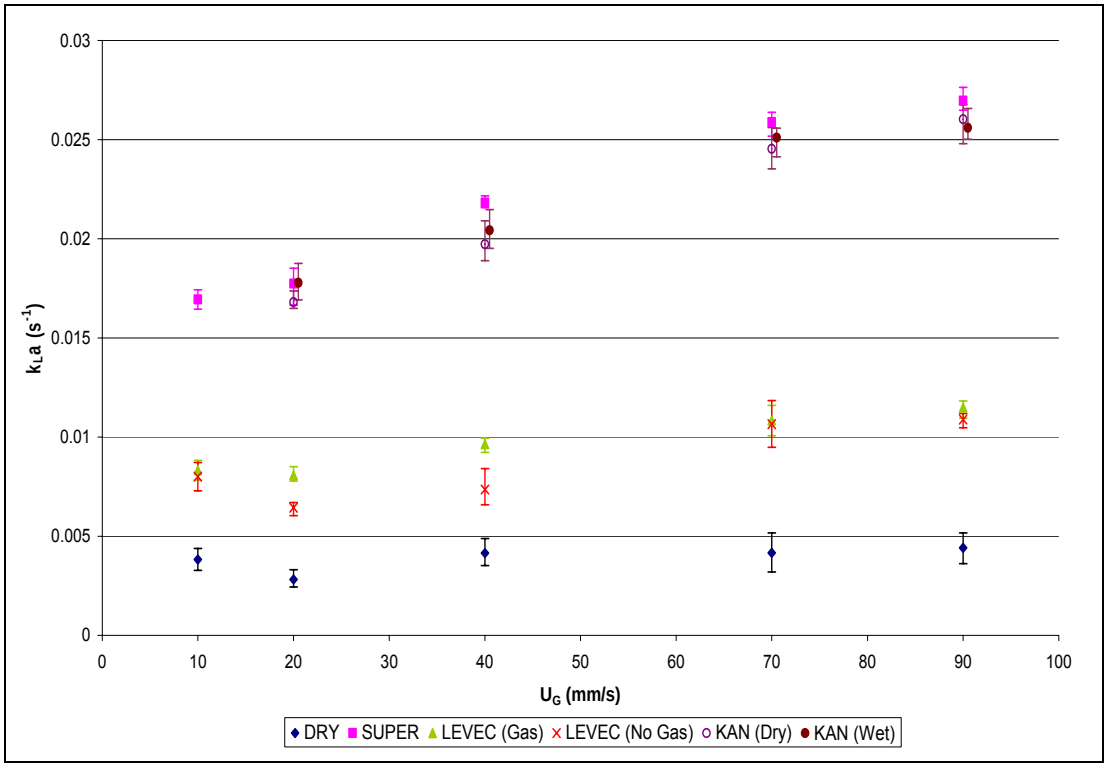

Figure 4-12: The effect of the gas flow rate on the gas-liquid mass transfer coefficient for the different prewetting modes at U_L = 9mm/s

In figure 4-12 it can once again be seen that the volumetric gas-liquid mass transfer coefficient increases with an increase in the gas flow rate. The increase observed in the Kan and Super-wetted beds are greater than the increase shown for the same beds at the lower liquid flow rate (figure 4-11).

The results for the intermediate liquid flow rates are shown in appendix 6

A 3-dimensional plot of the liquid holdup at all of the gas and liquid flow rates tested is shown in figure 4-13.

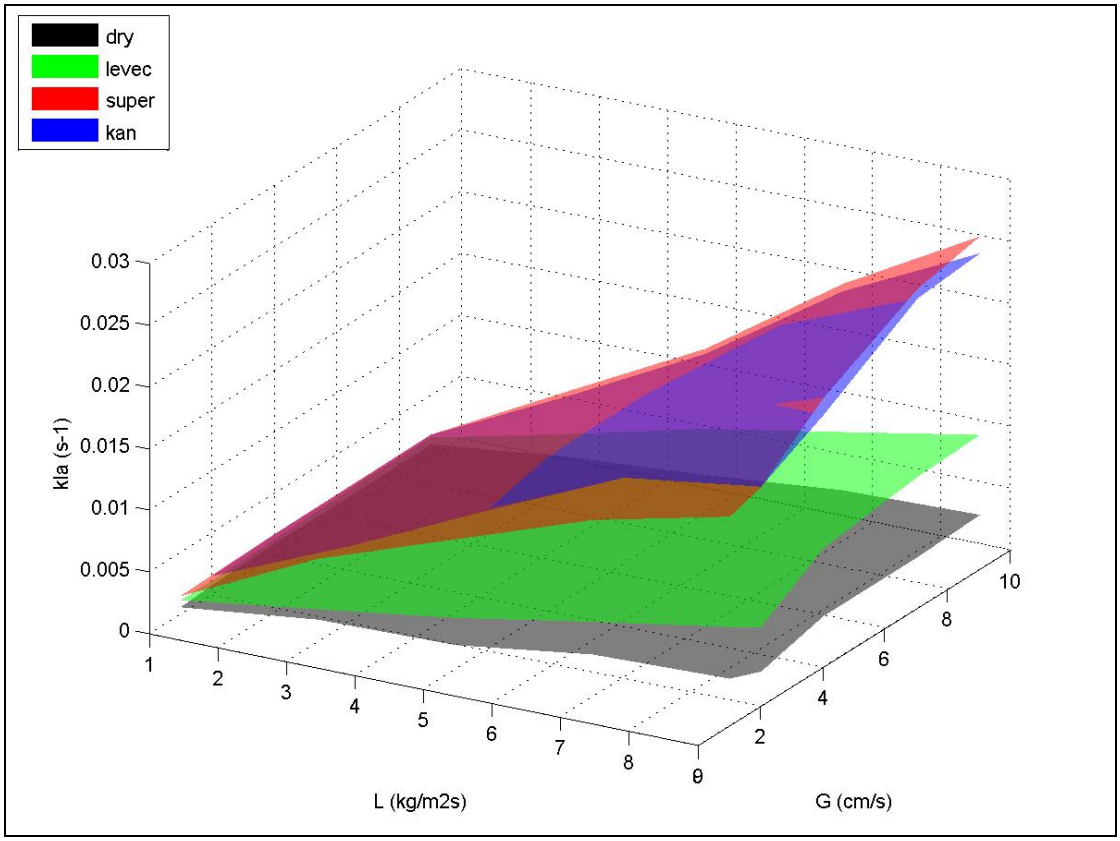

Figure 4-13: A 3-dimensional plot showing the effect of the gas and liquid flow rates on the volumetric gas-liquid mass transfer coefficient for the different prewetting modes

Figure 4-13 clearly shows the three distinct regions for the mass transfer coefficients as a result of the different prewetting modes.

4.4 Pulsing with Gas

Up until this point all of the experiments have been performed by prewetting the bed by flooding the bed with liquid or by operating the bed in the pulsing regime by increasing the liquid flow rate for a certain time before gas and liquid were set at the specified rates. The results in this section have all been obtained by inducing pulsing by increasing the gas flow rate and then decreasing the gas flow rate to the desired setpoint. The experiments were all performed at the highest liquid flow rate (L= 9mm/s).

The effect of prewetting the bed, by pulsing with gas, on the pressure drop, liquid holdup, and the volumetric gas-liquid mass transfer coefficient can be seen in figures 4-14, 4-15 and 4-16, respectively

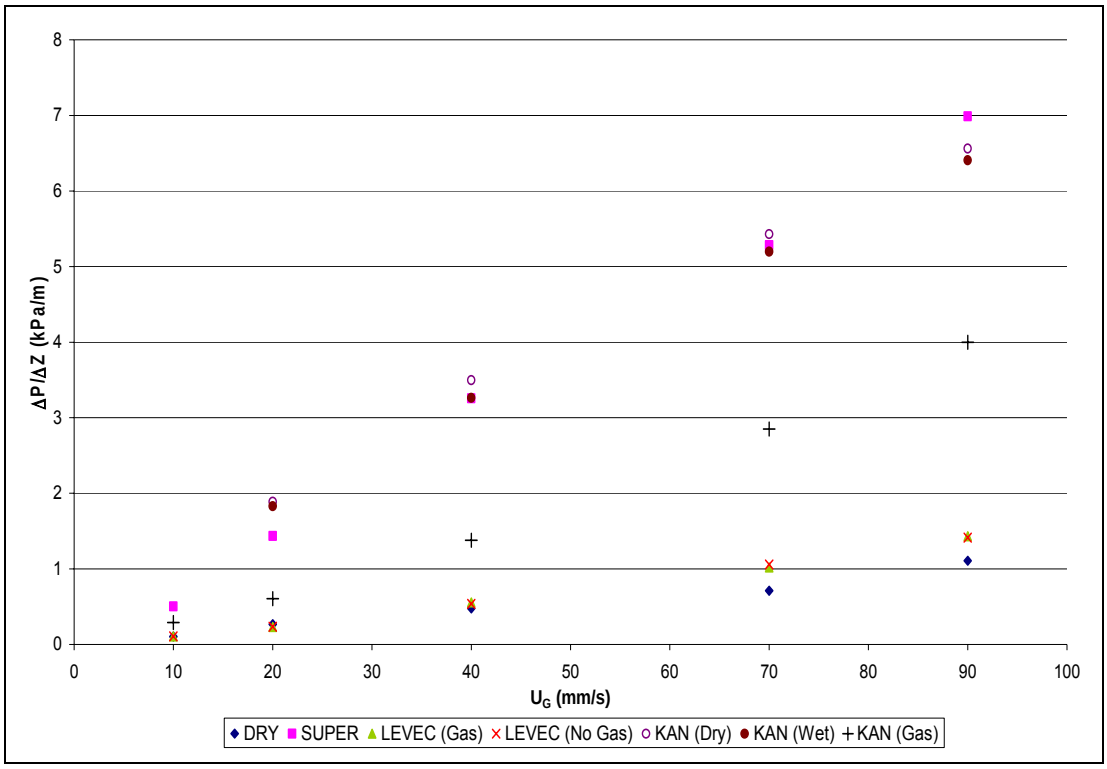

Figure 4-14: The effect of prewetting by pulsing with gas on the pressure drop at U_L = 9mm/s

Figure 4-14 corresponds to what Kan and Greenfield (1978) referred to as the Maximum Gas Flowrate Condition. It can be seen from the figure that inducing pulsing in the bed by increasing the gas flow rate results in a lower pressure drop than in the case of the pulsing being induced by increasing the liquid flow rate (where the gas flow rate would have been kept constant).

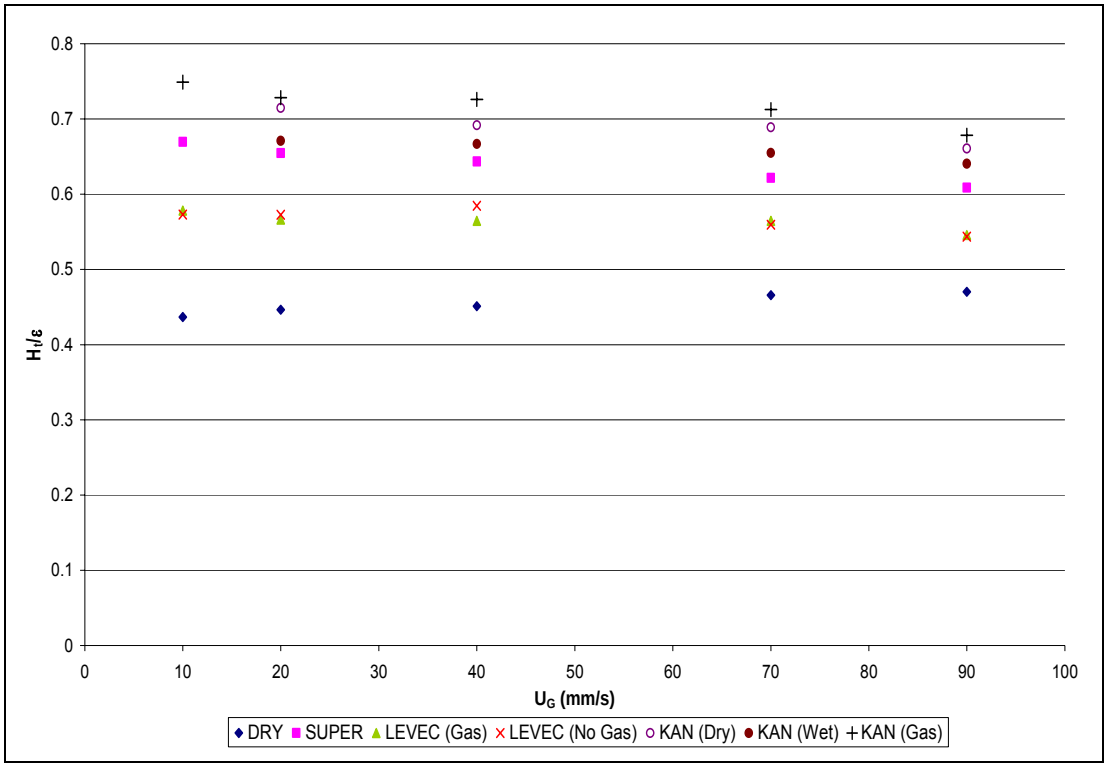

Figure 4-15: The effect of prewetting by pulsing with gas on the total liquid holdup at U_L = 9mm/s

Figure 4-15 also confirms the findings of Kan and Greenfield (1978) for the Maximum Gas Flowrate Condition. For this condition, the liquid holdup is higher if the gas flow rate has been reduced from a higher value. In the figure above it can be seen that the pulsing with gas resulted in higher liquid holdups than the pulsing with liquid.

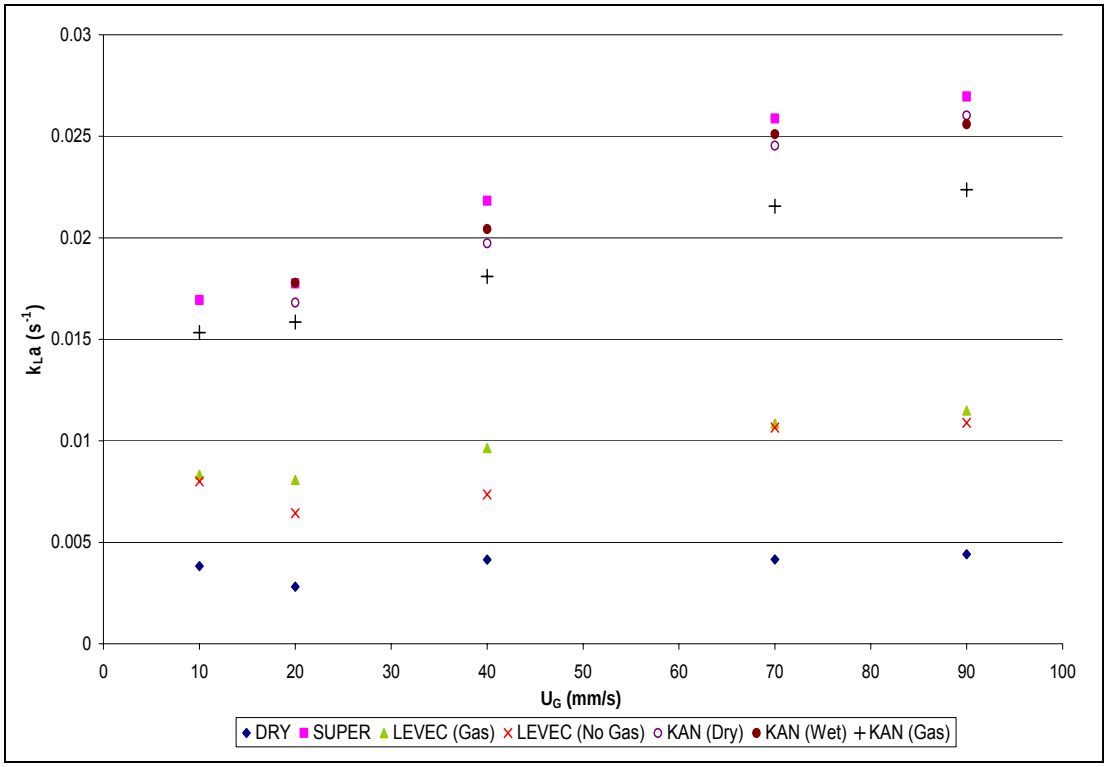

Figure 4-16: The effect of prewetting by pulsing with gas on the volumetric gas-liquid mass transfer coefficient at U_L = 9mm/s

In figure 4-16 it can be seen that pulsing with gas results in lower mass transfer coefficients than pulsing with liquid.

Thus, pulsing with gas results in a lower pressure drop and volumetric gas-liquid mass transfer coefficient but a higher liquid holdup than pulsing with liquid.

4.5 Operating Between the Modes

Levec *et al* (1986) proposed that the hysteresis curves actually represented an envelope of all the possible hydrodynamic states (as discussed in section 2.4.2). This implies that the operating point can lie anywhere on or between theses curves.

We have seen that the pressure drop, liquid holdup and gas-liquid mass transfer coefficient have a wide range of possible steady state operating points based on the mode of prewetting, but is it possible to operate between these modes?

In order to test this out the bed was flooded once again and drained (Levec wetting). However, this time instead of allowing the liquid to drain until the residual holdup was all that remained the liquid flow rate was reintroduced after 60 seconds. The results are represented as LEVEC (60s).

4.5.1 Pressure Drop

The results of the decreased draining time for the Levec wetted bed on the pressure drop are shown in figures 4-17 and 4-18.

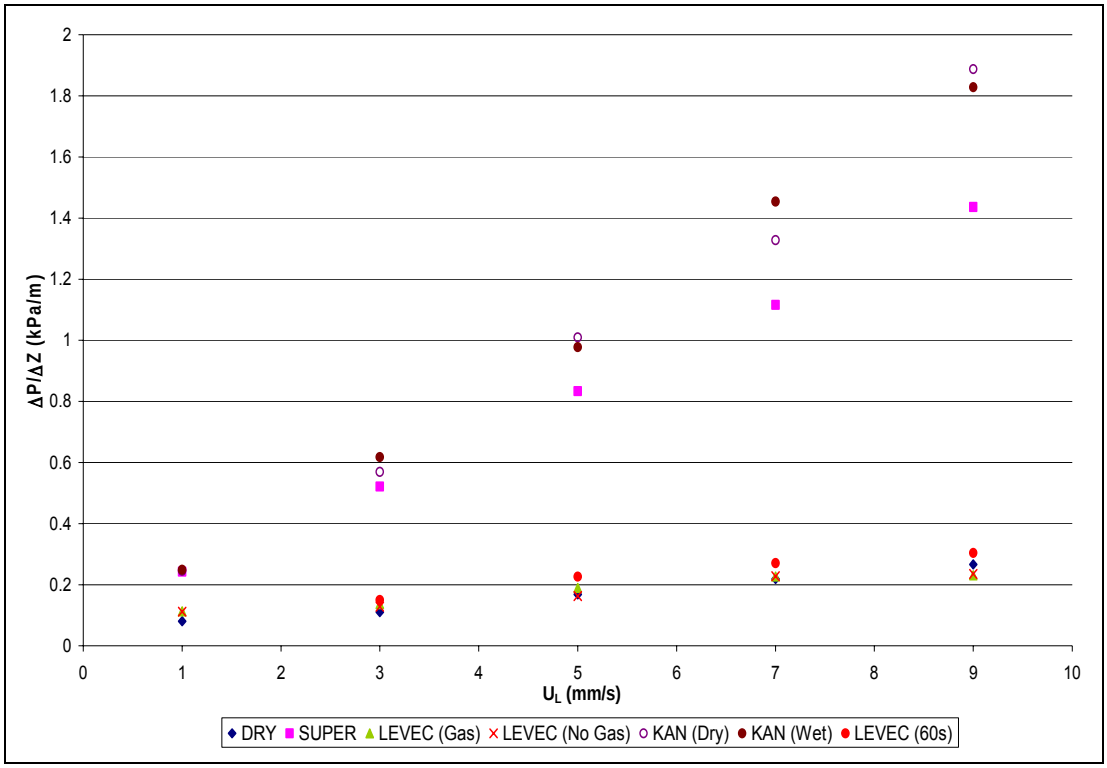

Figure 4-17: The effects of the decreased draining time for a Levec-wetted bed on the pressure drop at U_G = 20mm/s

From figure 4-17 it is clear that the decreased draining time for the Levec-wetted bed did not result in a pressure drop that was significantly higher than the ordinary Levec-wetted bed.

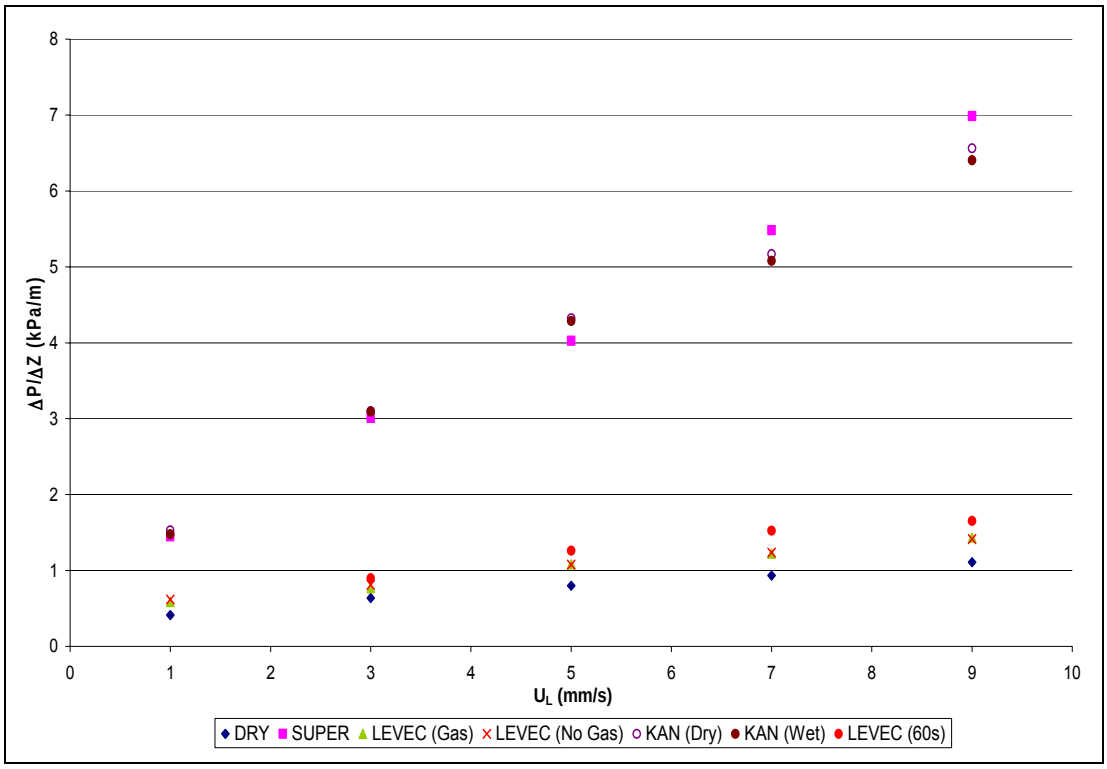

Figure 4-18: The effects of the decreased draining time for a Levec-wetted bed on the pressure drop at U_G = 90mm/s

In figure 4-18 it can again be seen that for the highest gas flow rate tested, a decrease in the draining time for the Levec-wetted bed did not result in pressure drop that was significantly higher that that obtained in the ordinary Levec-wetted bed. This trend was also observed for the intermediate gas flow rates and these results are shown in appendix 7.1.

4.5.2 Liquid Holdup

The results of the decreased draining time for the Levec wetted bed on the liquid holdup are shown in figures 4-19 and 4-20.

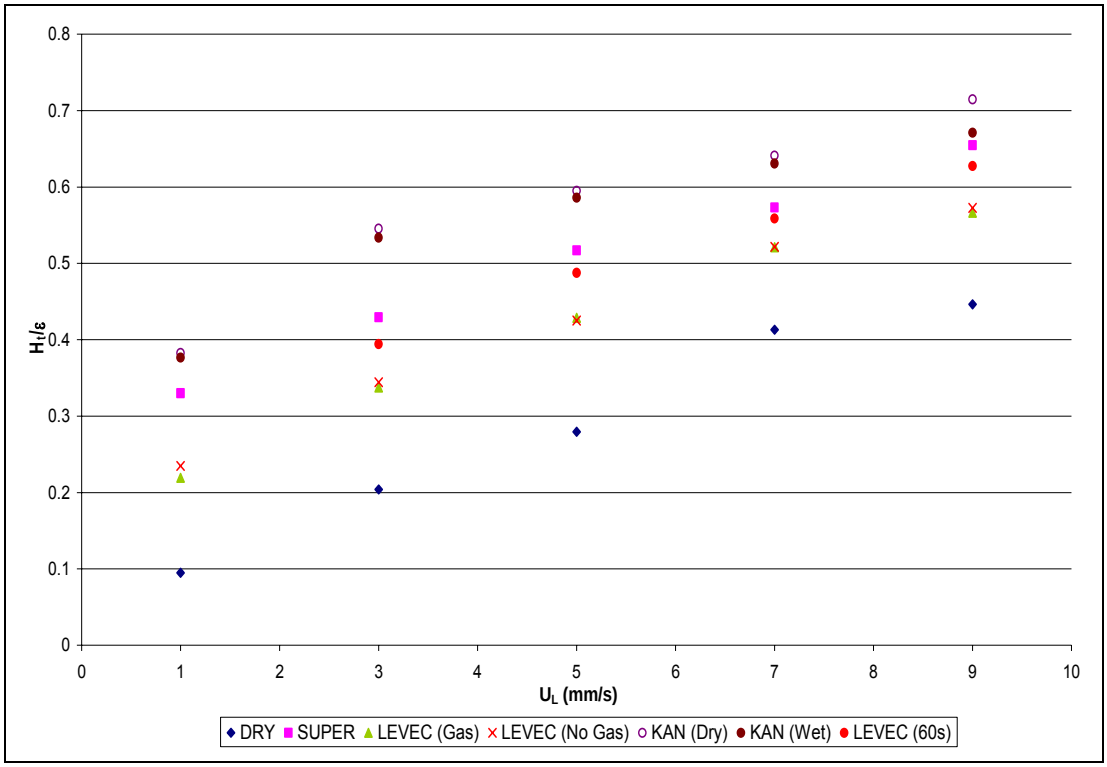

Figure 4-19: The effects of the decreased draining time for a Levec-wetted bed on the total liquid holdup at U_G = 20mm/s

In figure 4-18 it can be seen that the decreased draining time for the Levec-wetted bed resulted in a liquid holdup that was between the holdup of the Super-wetted and the ordinary Levec-wetted bed at all of the liquid flow rates.

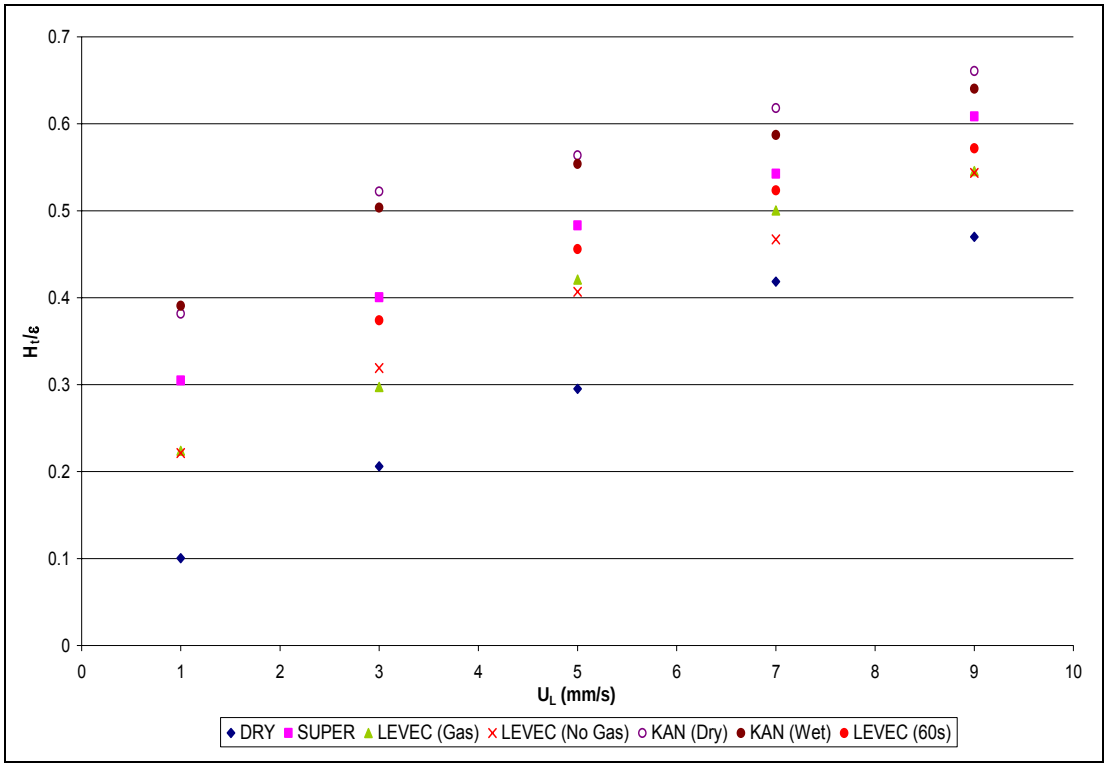

Figure 4-20: The effects of the decreased draining time for a Levec-wetted bed on the total liquid holdup at U_G = 90mm/s

Figure 4-20 shows that at the highest gas flow rate tested, the decreased draining time for the Levec-wetted bed also resulted in a liquid holdup that was between the holdup of the Super-wetted and the ordinary Levec-wetted bed at all of the liquid flow rates.

This trend can also be seen for the intermediate gas flow rates, the results of which are given in appendix 7.2.

4.5.3 Gas-Liquid Mass Transfer

The results of the decreased draining time for the Levec wetted bed on the gas-liquid mass transfer coefficient are shown in figures 4-21 and 4-22.

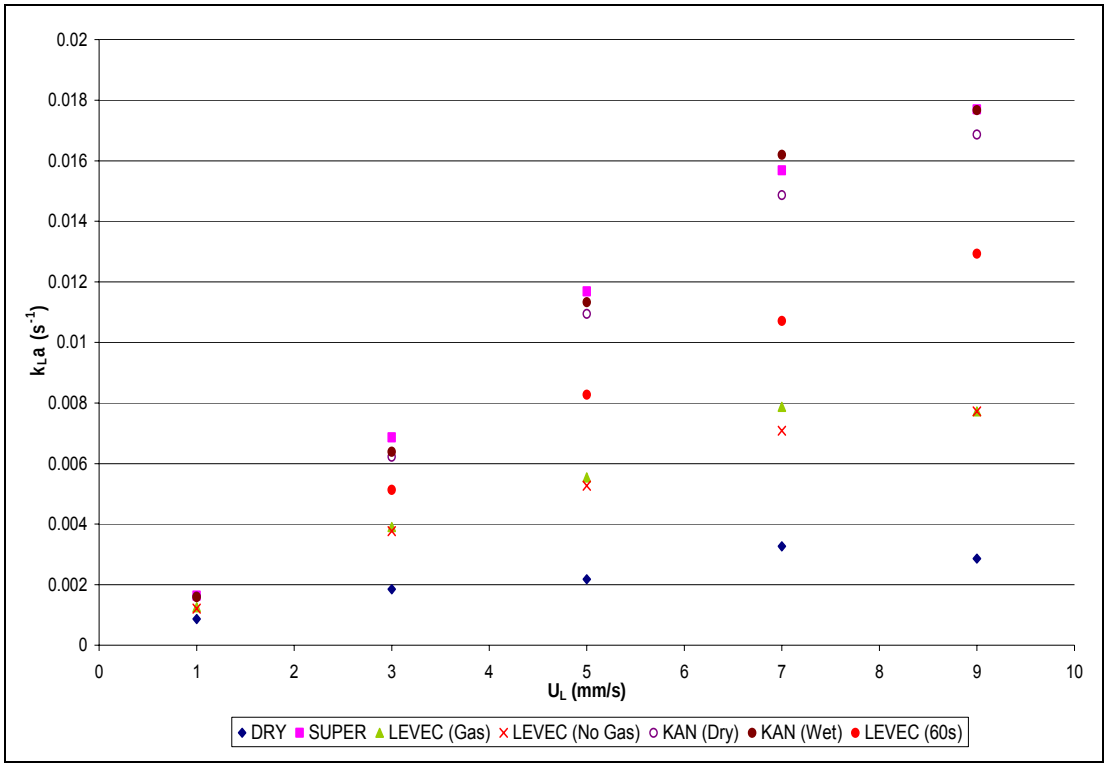

Figure 4-21: The effects of the decreased draining time for a Levec-wetted bed on the gas-liquid mass transfer coefficient at U_G = 20mm/s

From figure 4-21it can be seen that the decreased draining time for the Levec-wetted bed also affects the gas-liquid mass transfer coefficient. As in the case of the liquid holdup, the decreased draining time results in a volumetric gas-liquid mass transfer coefficient that lies between that of the Super-wetted bed and the ordinary Levec-wetted bed.

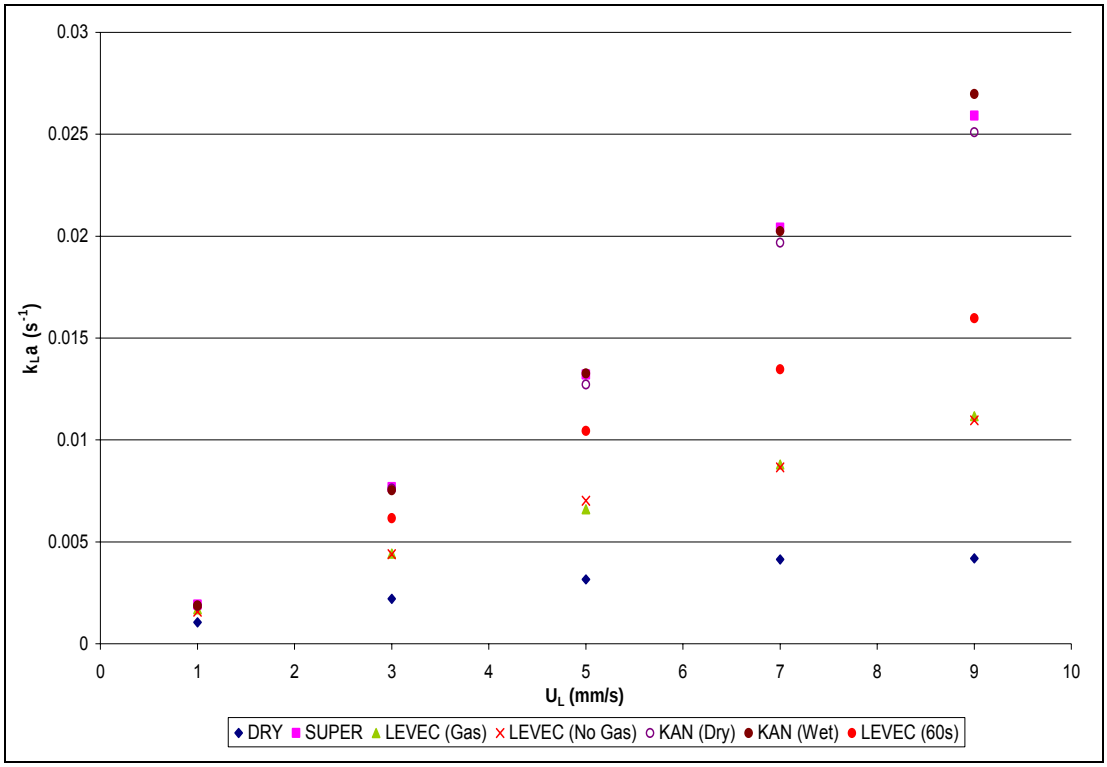

Figure 4-22: The effects of the decreased draining time for a Levec-wetted bed on the gas-liquid mass transfer coefficient at U_G = 90mm/s

At the highest gas flow rate tested, figure 4-22, the decrease in the draining time for the Levec-wetted bed results in a volumetric gas-liquid mass transfer coefficient that is between that of the Super-wetted bed and the ordinary Levec-wetted bed.

This trend was observed at the intermediate gas flow rates as well and the results are shown in appendix 7.3.

5. Correlations

The correlations for the pressure drop, liquid holdup and gas-liquid mass transfer coefficient have been divided into 2 main groups. The first group is for the correlations that do not have any parameters in them that could result in the prediction of multiple steady states. The second group all incorporate at least one parameter that may allow for the prediction of multiple steady states due to the prewetting procedure.

Due to there being no substantial difference between the KAN (Dry) and KAN (Wet) results, the two results are combined and represented as KAN on the accompanying figures. The same applies for the LEVEC (Gas) and LEVEC (No Gas) that are also combined and referred to as LEVEC in the accompanying figures. Only the average values for the different prewetting modes are shown in the figures.

5.1 Pressure Drop Correlations

5.1.1 Single Pressure Drop Correlations

The results of the single pressure drop correlations are shown for constant gas flow rates in figures 5-1 and 5-2.

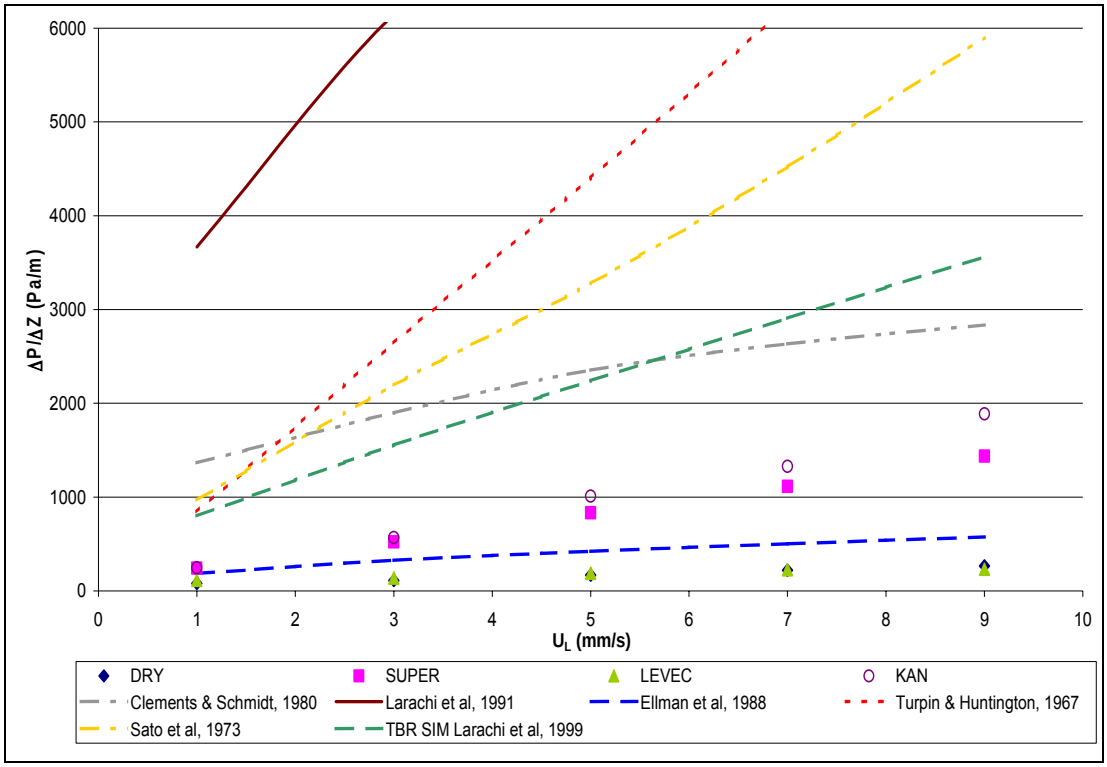

Figure 5-1: The performance of the pressure drop correlations at U_G = 20mm/s

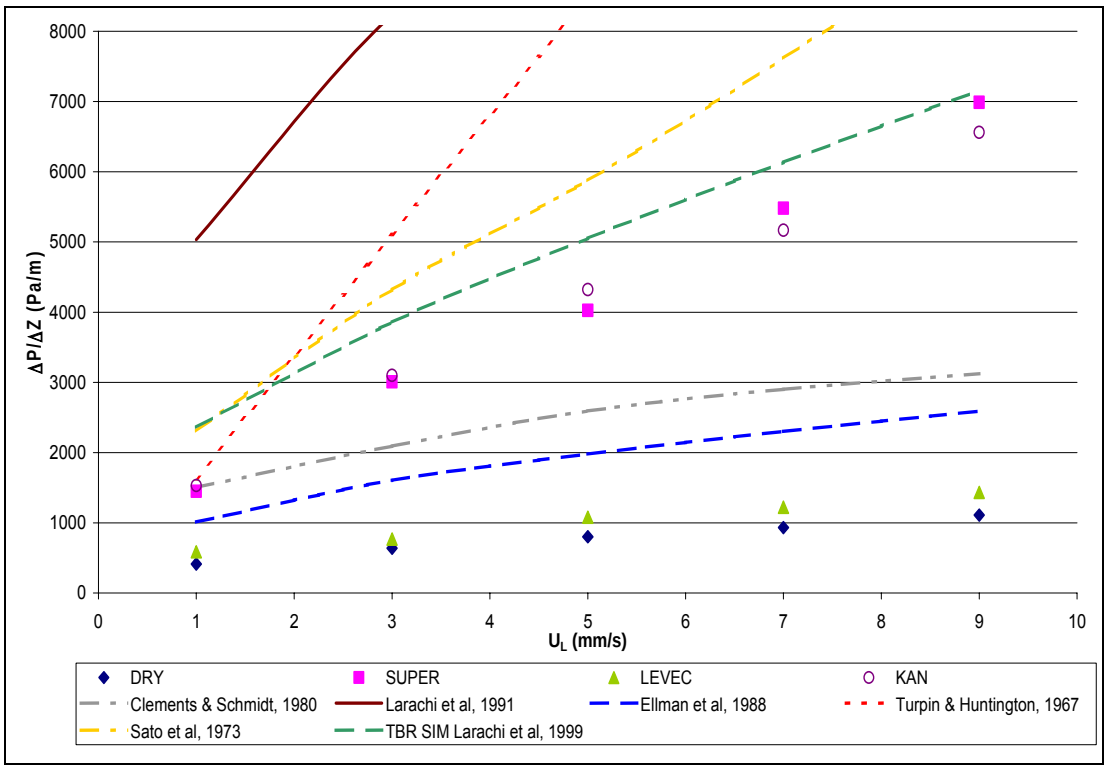

Figure 5-2: The performance of the pressure drop correlations at U_G = 90mm/s

From figures 5-1 and 5-2 it is obvious that the correlation is the correlation that best describes the data is the correlation proposed by Ellman *et al* (1988). The correlation predicts a pressure drop that lies between the upper and lower regions. The correlation proposed by Clements and Schmidt (1980) also predicts a pressure drop that lies between the upper and lower regions, but only at the highest gas flow rate. The other correlations result in pressure drop predictions that are substantially higher than those obtained for any of the prewetting modes.

The results of the predicted pressure drops for the intermediate gas flow rates can be seen in appendix 8.

5.1.2 Multiple Pressure Drop Correlations

The correlations proposed by Holub *et al* (1992) and Westerterp and Wammes (1992) both incorporate the liquid holdup in their correlations. By using the holdup obtained from the experimental work, the pressure drop correlations may prove more adaptable than the correlations shown above simply because they may be able to predict multiple steady state values for the pressure drop for the different prewetting modes. The results of the correlation proposed by Holub *et al* (1992) can be seen in figures 5-3 and 5-4, and the results of the Westerterp and Wammes (1992) correlation can be seen in figure 5-5.

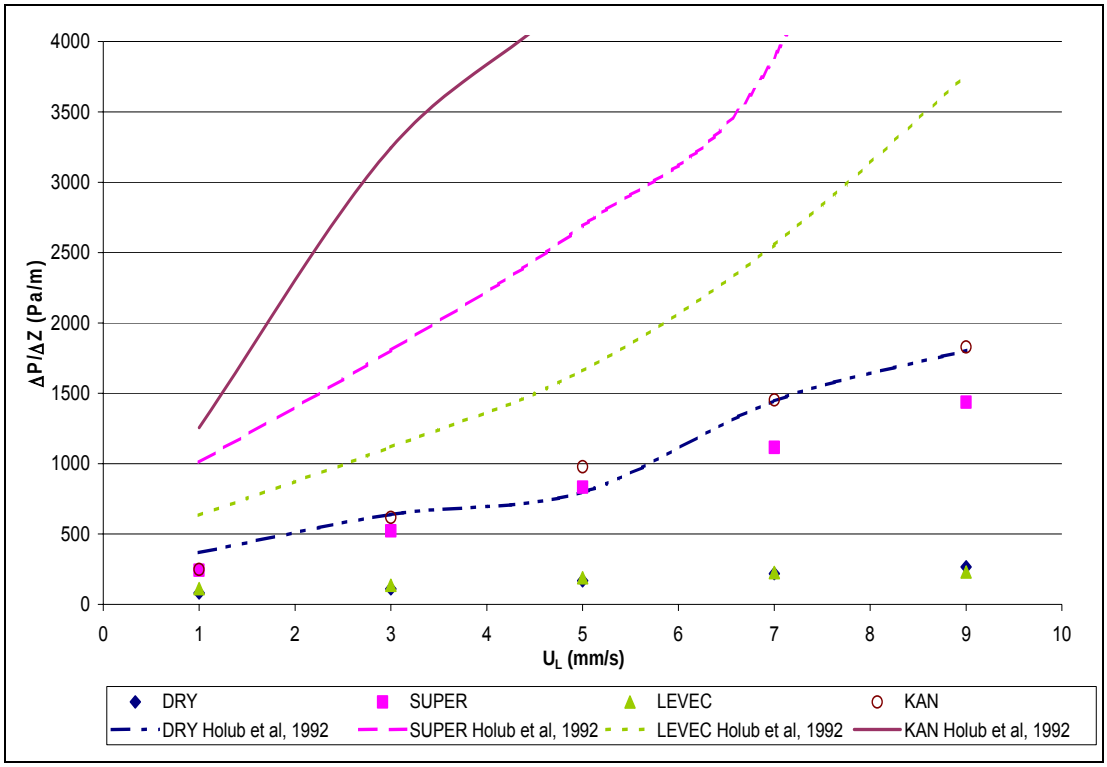

Figure 5-3: The performance of the pressure drop correlation proposed by Holub et al (1992) at U_G = 20mm/s

In figure 5-3 it is clear that the correlation proposed by Holub *et al* (1992) can result in the prediction of multiple pressure drops for the different prewetting modes if the liquid holdup for these modes is known.

However, even though the model has the ability to predict the multiple steady-state values for the pressure drop, it does not do so very accurately. This is evident in the fact that at this low gas flow rate, the Holub model predicts pressure drops for the dry bed that are actually comparable to the results obtained in the Kan-wetted bed.

The resulting pressure drops predicted by the Holub model also show four distinct regions, Kan, Super, Levec and Dry, as opposed to the two regions evident from the experimental results. This could be due to the strong dependence on the liquid holdup where it was seen that the different prewetting modes resulted in four distinct regions.

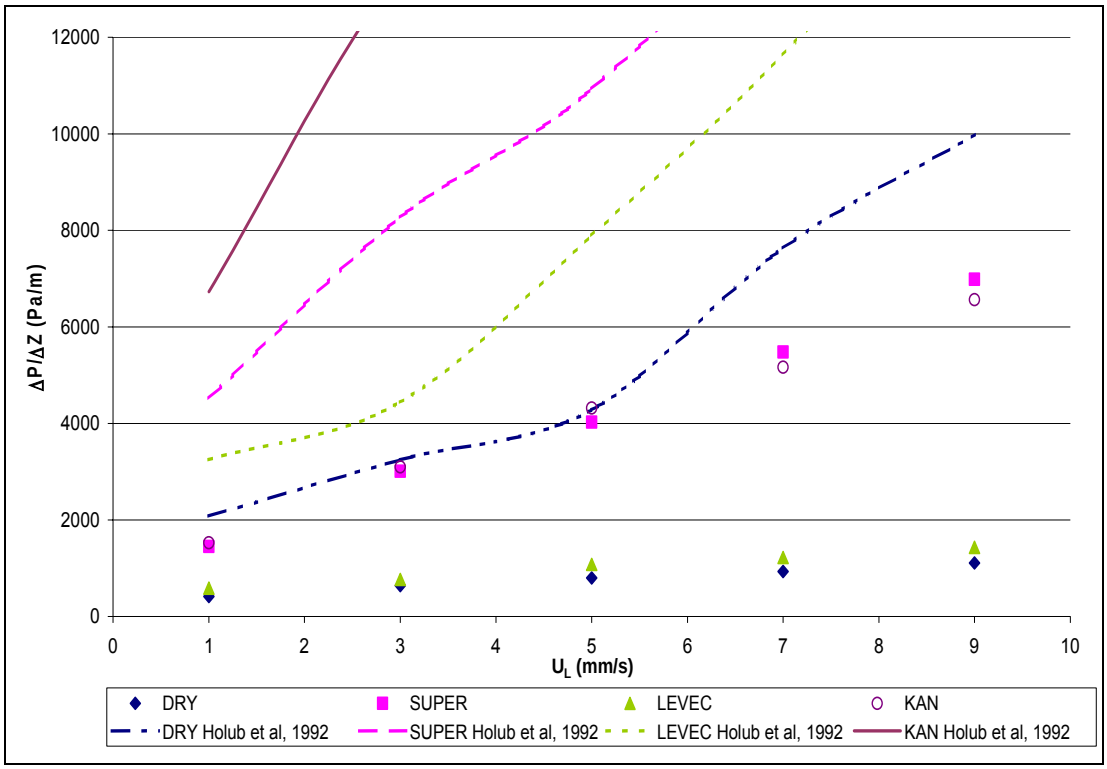

Figure 5-4: The performance of the pressure drop correlation proposed by Holub et al (1992) at U_G = 90mm/s

At the highest gas flow rate, figure 5-4, the predicted pressure drops from the Holub model do not get any better. In fact, as the liquid flow rate increases the model becomes more inaccurate. The Ergun constants used in the correlation (E_1 = 134 E_2 = 0.67) were calculated from experimental results obtained in the same bed with only the gas phase present before any liquid had been introduced into the system. Increasing the constants to the original Ergun constants did not improve the results of the model.

The pressure drop predictions from the Holub model for the intermediate gas flow rates can be seen in appendix 9.

The correlation proposed by Westerterp and Wammes (1992) incorporated the liquid holdup in the pressure drop correlation as well. By using the liquid holdup obtained by experimental results for the different prewetting modes,

the correlation should be able to predict different pressure drops for the different prewetting modes.

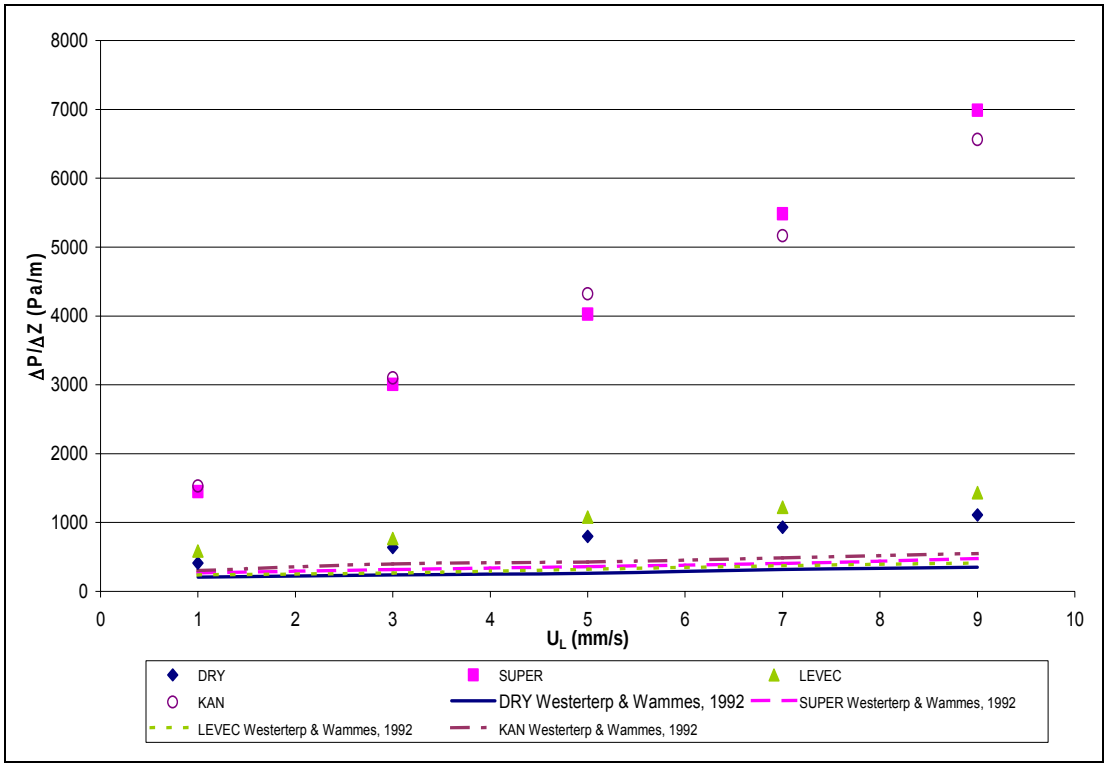

Figure 5-5: The performance of the pressure drop correlation proposed by Westerterp and Wammes (1992) at U_G = 90mm/s

From figure 5-5 it is clear that the correlation proposed by Westerterp and Wammes (1992) predicted pressure drops for the different modes that were substantially lower than those actually measured. This correlation did not perform any better at the lower gas flow rates and these results can be seen in appendix 10.

5.2 Liquid Holdup Correlations

5.2.1 Single Holdup Correlations

The results of the single liquid holdup correlations are shown for constant gas flow rates in figures 5-6 and 5-7. The liquid holdup is in the form of the draining saturation in these figures.

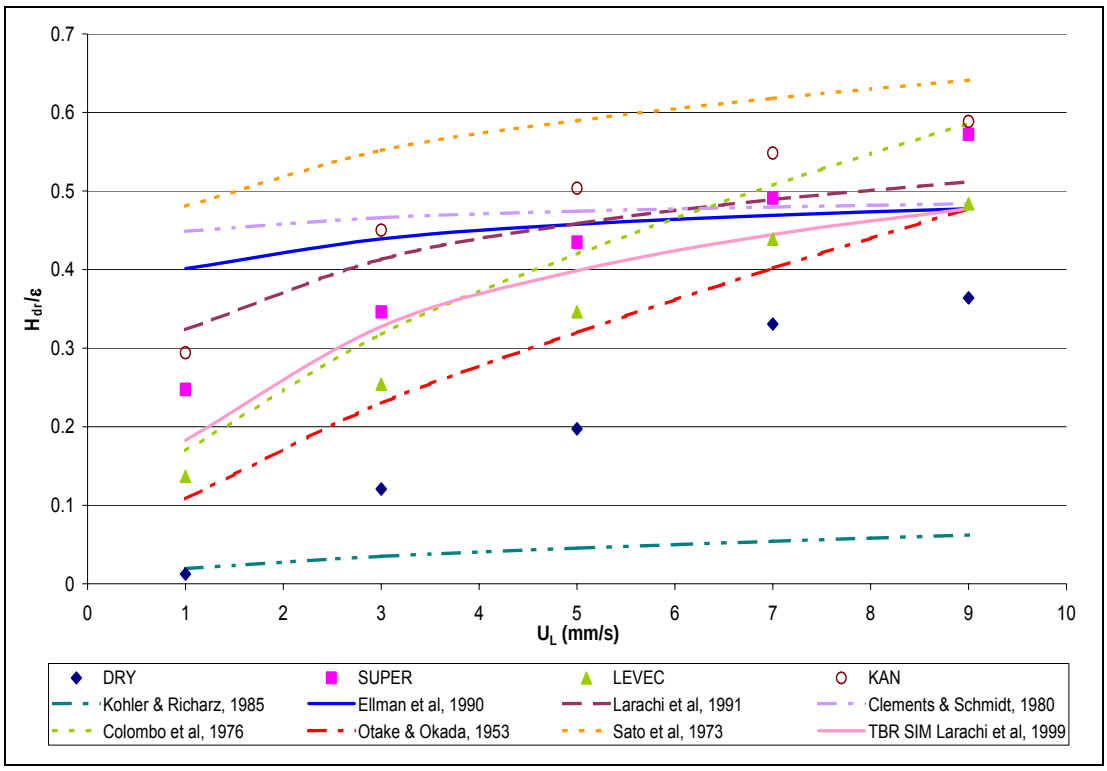

Figure 5-6: The performance of the liquid holdup correlations at U_G = 20mm/s

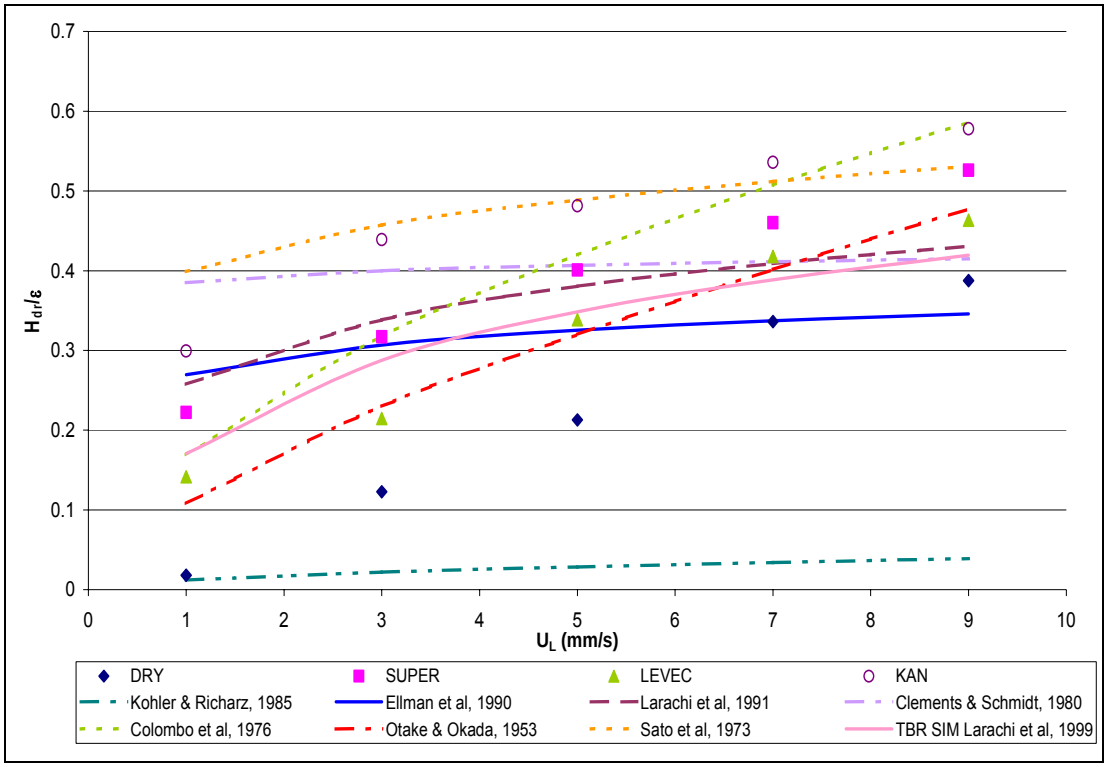

Figure 5-7: The performance of the liquid holdup correlations at U_G = 90mm/s

From figures 5-6 and 5-7 it can be seen that none of the correlations tested could predict the liquid holdup for the dry bed. The experiments performed by Kohler and Richarz (1985), Clements and Schmidt (1980), Colombo *et al* (1976) and Sato *et al* (1973) give no indication of any prewetting procedure and fail to predict the liquid holdup in the dry bed. The correlation proposed by Otake and Okada (1953) is based upon data obtained in absorption columns and predicts liquid holdups that are similar to those obtained in the Levec-wetted beds.

The correlations proposed by Ellman *et al* (1990), Larachi *et al* (1991) as well as the simulator (Larachi *et al*, 1999) are based on a database of various researchers experimental work and once again no specific mention is made to different prewetting methods. These correlations all predict liquid holdup values that vary between those obtained in the Kan-wetted bed at low liquid flow rates and the Levec-wetted bed at high liquid flow rates.

The performance of these correlations at the intermediate gas flow rates are shown in appendix 11.

5.2.2 Multiple Holdup Correlations

The correlations proposed by Holub *et al* (1992), Stegeman *et al* (1996) and Specchia and Baldi (1977) all incorporate the pressure drop in their correlations. By using the pressure drop obtained from the experimental runs, the holdup correlations may prove more adaptable than the correlations shown above simply because they may be able to predict multiple steady state values for the holdup for the different prewetting modes. The results of the correlation proposed by Holub *et al* (1992) can be seen in figures 5-8 and 5-9, the results of the Stegeman *et al* (1996) correlation in figure 5-10 and the results of the Specchia and Baldi (1977) correlation can be seen in figures 5-11 and 5-12. The results of the correlations based on the relative permeability concept are shown in figures 5-13 and 5-14.

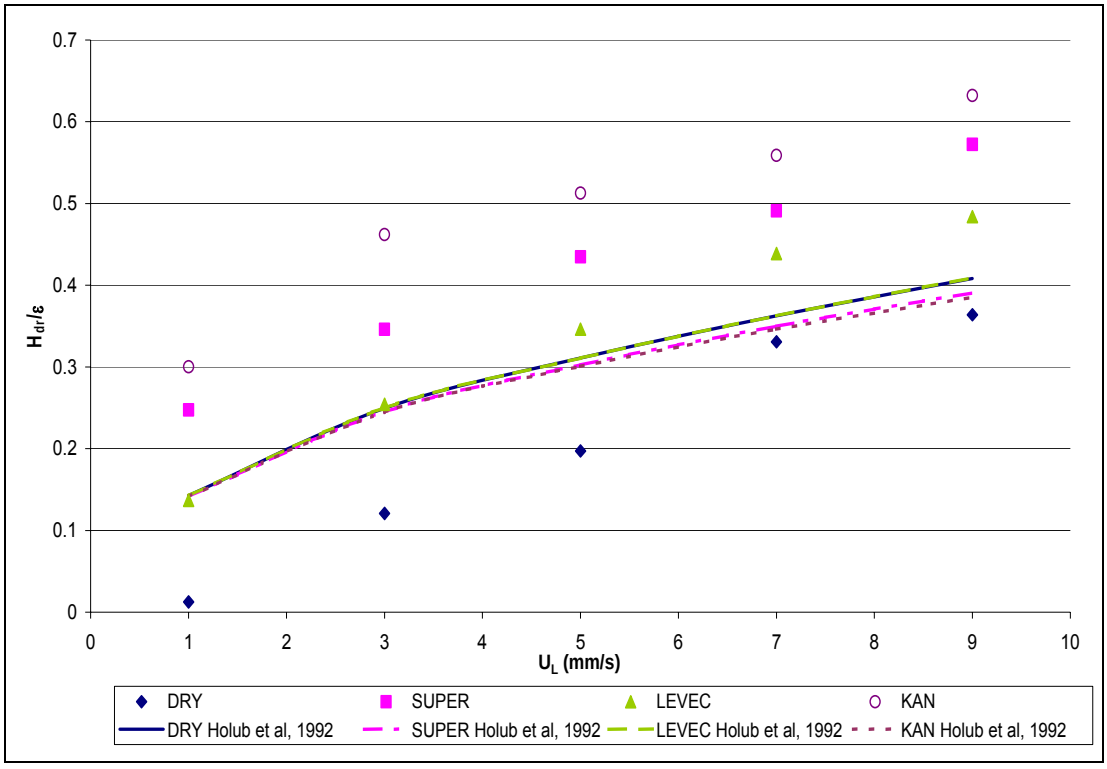

Figure 5-8: The performance of the liquid holdup correlation proposed by Holub et al (1992) at U_G = 20mm/s

From figure 5-8 it is clear that the model proposed by Holub *et al* (1992) is incapable of accurately predicting the liquid holdup for the different prewetting modes. However, it can be seen that the effect of the pressure drop is minimal and that the holdups predicted show no significant difference.

From the figure above it also appears as though the holdups predicted in the dry and Levec-wetted beds are higher than those of the Kan and Super-wetted beds at a given liquid flow rate.

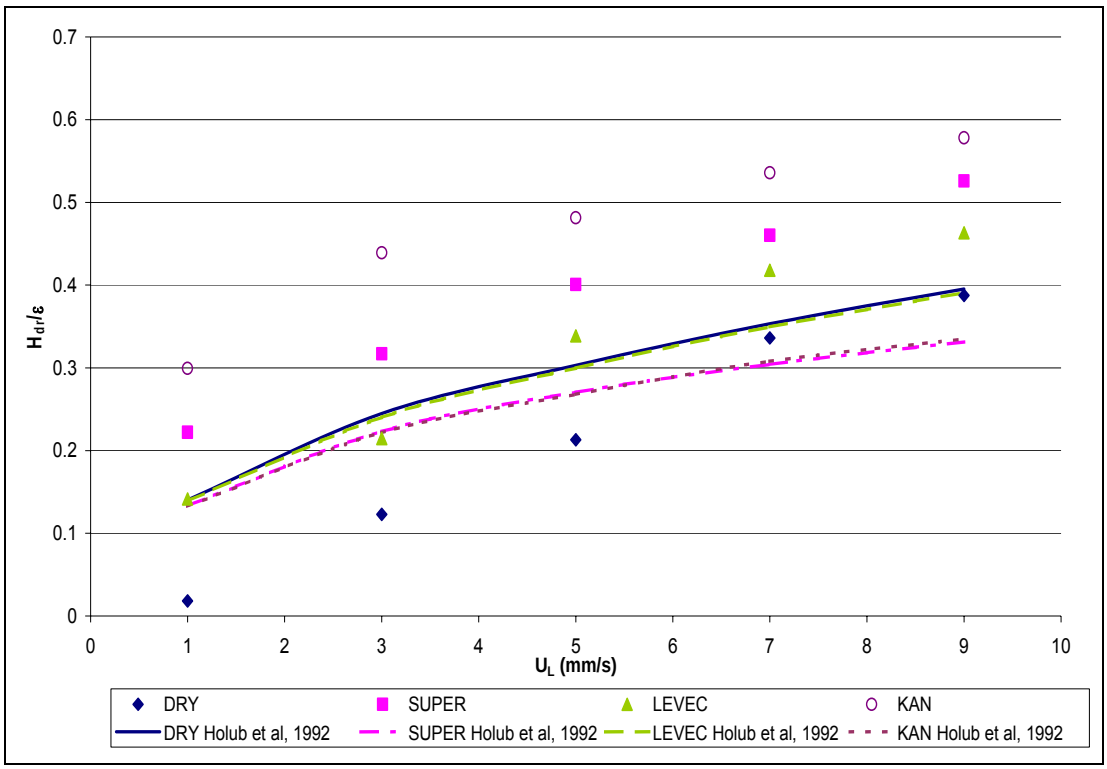

Figure 5-9: The performance of the liquid holdup correlation proposed by Holub et al (1992) at U_G = 90mm/s

The same trend is observed in figure 5-9 where the results from the model are shown for the highest gas flow rate. Although there is a more significant difference between the liquid holdups of the different modes, substituting the pressure drop for the different modes into the model results in a higher prediction of the liquid holdup in the dry and Levec-wetted beds.

The predicted pressure drops did not improve for the intermediate gas flow rates and these results can be seen in appendix 12.

The model proposed by Stegeman *et al* (1996) was actually based on the correlation proposed by Holub *et al* (1992). The only major difference is that Stegeman *et al* (1996) ignored the turbulent term of the model due to the fact that they never reached the turbulent regime.

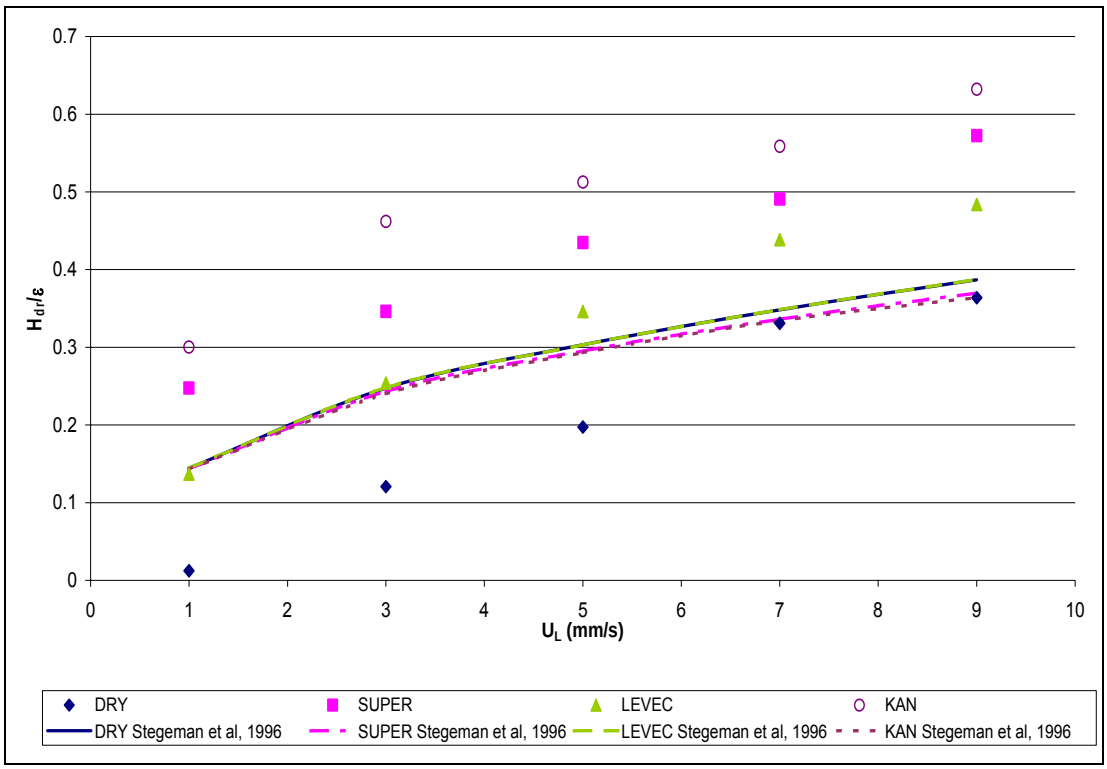

Figure 5-10: The performance of the liquid holdup correlation proposed by Stegeman et al (1996) at U_G = 20mm/s

From figure 5-10 it is apparent that there is no significant difference between their model and the original Holub model. However, Stegeman *et al* (1996) claimed that this model predicted their data quite well. The reason for this is that Stegeman *et al* (1996) operated their bed under Levec-wetted conditions, and at low liquid flow rates this model does predict the Levec-wetted bed quite accurately.

The results of the model proposed by Stegeman *et al* (1996) for the remaining gas flow rates are shown in appendix 13.

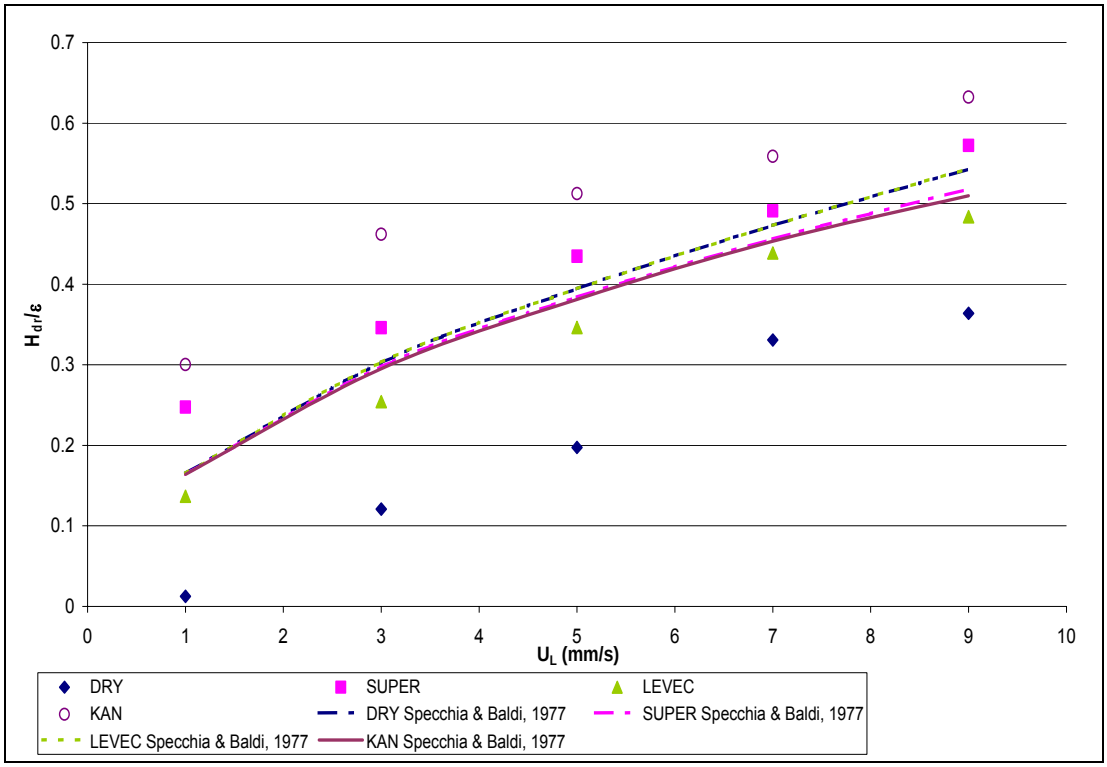

Figure 5-11: The performance of the liquid holdup correlation proposed by Specchia and Baldi (1977) at U_G = 20mm/s

From figure 5-11 it is clear that the model proposed by Specchia and Baldi (1977) is unable to predict the holdup for the different prewetting modes. As with the Holub model, the small effect that the pressure drop seems to have actually results in the correlation predicting higher holdup values for the dry and Levec-wetted beds than for the Kan and Super-wetted beds.

However, at atmospheric conditions the pressure drop term in the correlation cannot have any significant effect due to the fact that it is added to the product of the liquid density and the gravitational constant of acceleration ($\rho_L g \approx 10\,000$) in the modified Galileo number. This means the pressure drop needs to be quite high before it can have any real effect.

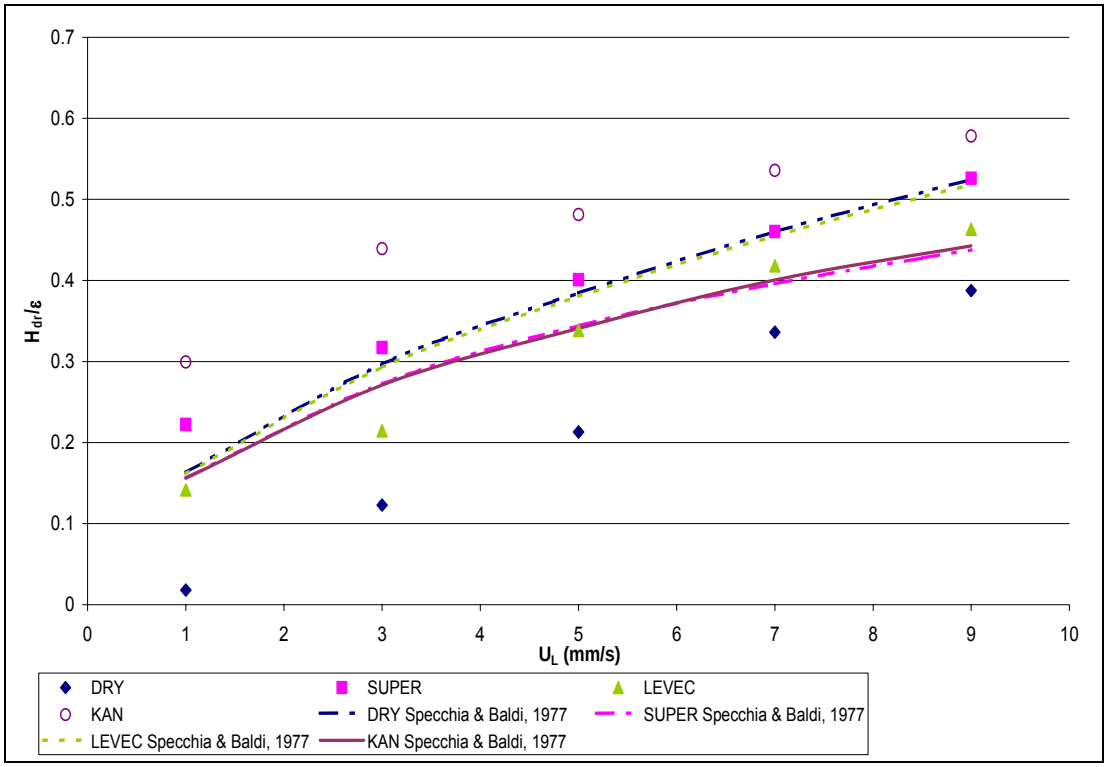

Figure 5-12: The performance of the liquid holdup correlation proposed by Specchia and Baldi (1977) at U_G = 90mm/s

For the highest gas flow rate tested, figure 5-12, the pressure drop does have a slightly more significant effect in the predictions of the correlation. However, the correlation still predicts higher holdups for the dry and Levec-wetted beds than for the Kan and Super-wetted beds.

For the intermediate gas flow rates the model did not perform any better and these results are shown in appendix 14.

The correlations based on the relative permeability concept all involve experimental work performed with some form of prewetting procedure. The correlation proposed by Lakota et al (2002) is based on the Levec-wetting procedure, whereas the correlation proposed by Nemec and Levec (2005) has been adapted to predict the liquid holdup in a Levec- and Kan-wetted bed.

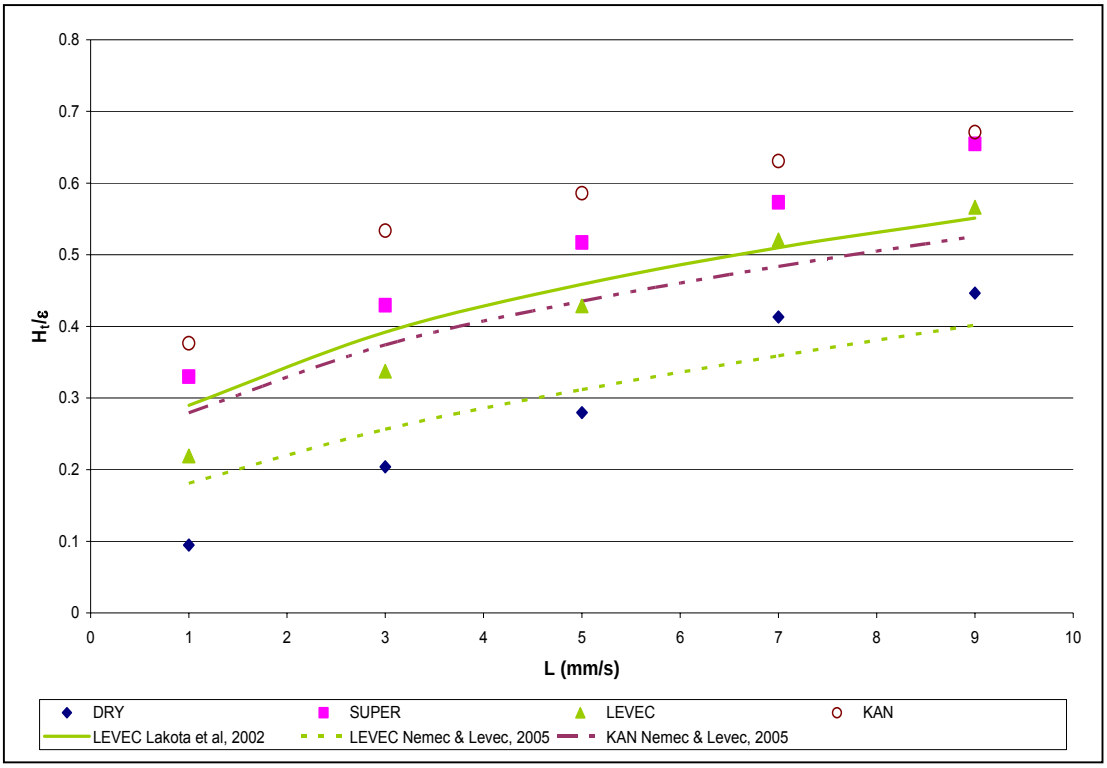

Figure 5-13: The performance of the liquid holdup correlations based on the relative permeability concept at U_G = 20mm/s

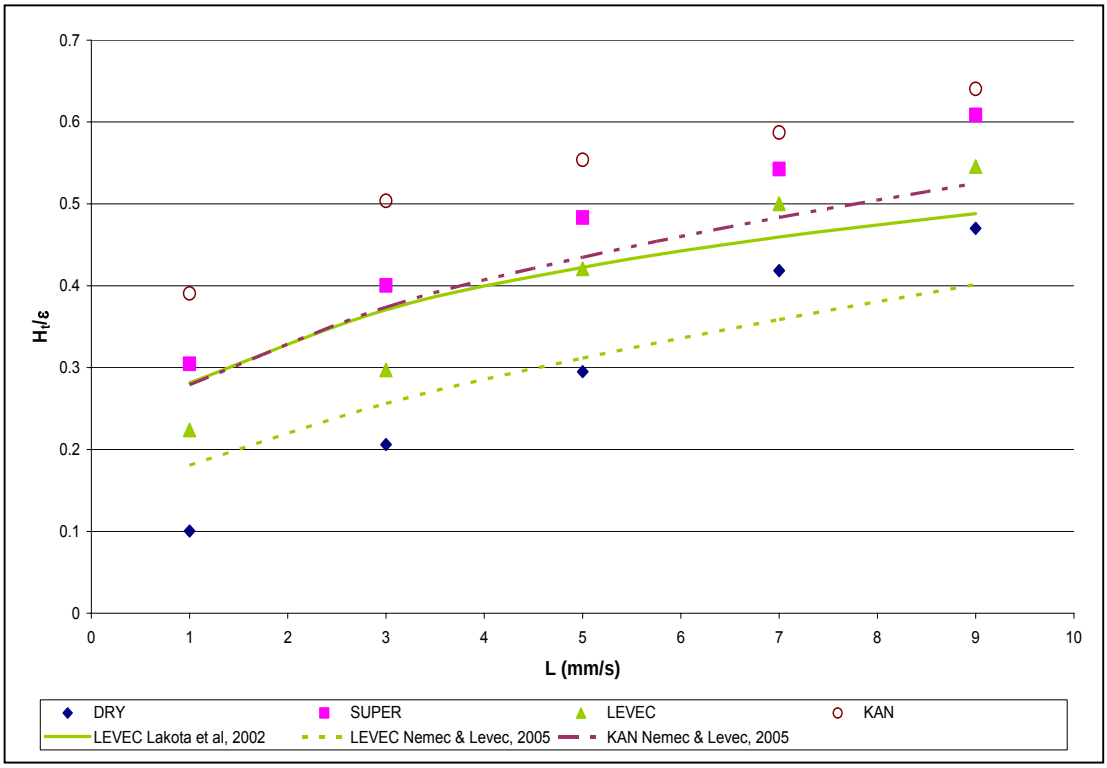

Figure 5-14: The performance of the liquid holdup correlations based on the relative permeability concept at U_G = 90mm/s

From the figures above it can be clearly seen that the correlations based on the relative permeability model cannot accurately predict the liquid holdup. In figure 5-13 it can be seen that the correlation proposed by Lakota *et al* (2002) performed the best and accurately predicts the liquid holdup for the higher liquid flow rates, however, at the lower liquid flow rates the correlation does predict significantly higher liquid holdups than those measured. On the other hand the correlations proposed by Nemec and Levec (2005) for the Kan-wetted and Levec-wetted beds continually under predicts the liquid holdup for all of the liquid flow rates tested.

At the highest gas flow rate tested, figure 5-14, the correlations proposed by Nemec and Levec (2005) continue the trend observed for the lowest gas flow rate and under predict the liquid holdup for the relevant prewetting procedure. The correlation proposed by Lakota *et al* (2002) for the Levec-wetted bed only predicts accurate liquid holdup results at the intermediate liquid flow rates. For the lower liquid flow rates the correlation results in higher liquid holdups than those found experimentally and at higher liquid flow rates the correlation results in lower liquid holdups than those found experimentally.

In general the models all seem to have a lower dependence on the liquid flow rate than the experimental results would suggest. This implies that even if the models accurately predict the liquid holdup at the low liquid flow rates they will be inaccurate at the higher liquid flow rates and vice versa. The performance of these correlations did not improve at the intermediate gas flow rates and the results can be seen in appendix 15.

5.3 Gas-Liquid Mass Transfer Correlations

5.3.1 Single Gas-Liquid Mass Transfer Correlations

The results of the single gas-liquid mass transfer correlations are shown for constant gas flow rates in figures 5-15 and 5-16.

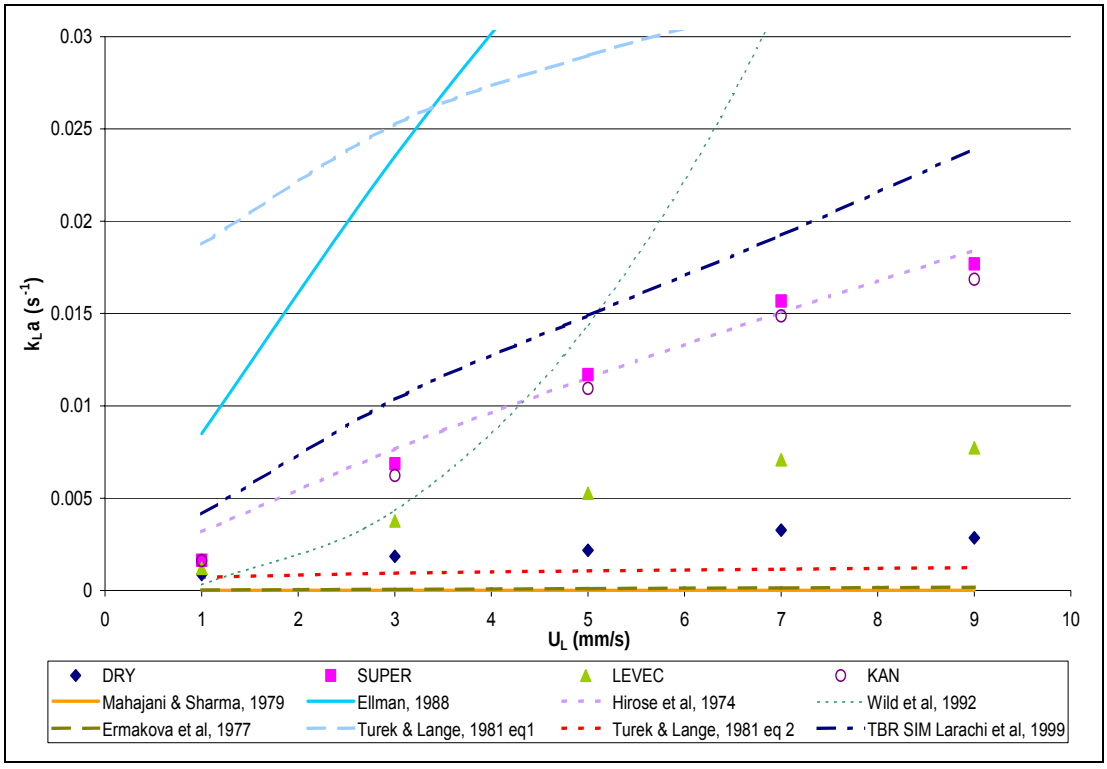

Figure 5-15: The performance of the gas-liquid mass transfer correlations at U_G = 20mm/s

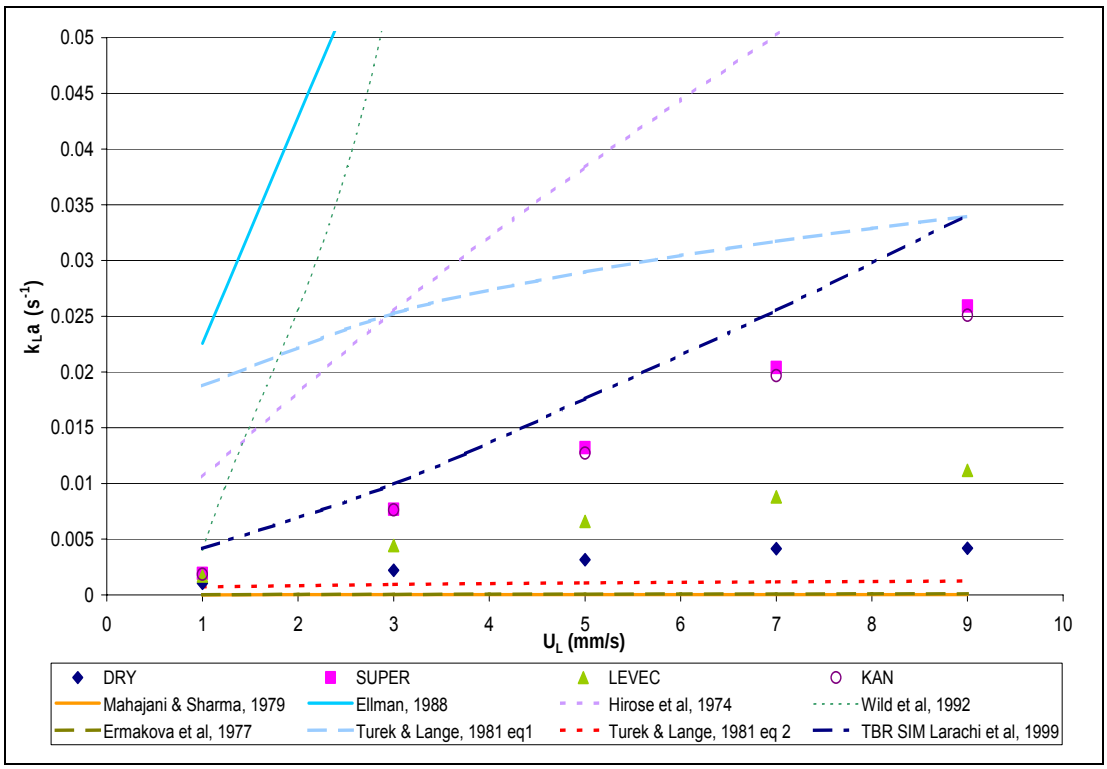

Figure 5-16: The performance of the gas-liquid mass transfer correlations at U_G = 90mm/s

None of the correlations shown in figures 5-15 and 5-16 can accurately predict the volumetric gas-liquid mass transfer coefficient for a dry bed. The correlations proposed by Ermakova *et al* (1977) and Mahajani and Sharma (1979) not only show almost no increase with the liquid flow rate but also predict mass transfer coefficients way below those of the dry bed. The correlation proposed by Hirose *et al* (1974) predicted values that were very similar to those obtained in the Kan and Super-wetted beds for the lowest gas flow rate but were substantially higher at the higher gas flow rates. However, the correlation is meant to predict the mass transfer coefficients for a dry bed since no prewetting procedure was followed.

Of the two correlations proposed by Turek and Lange (1981) the second correlation is the most accurate. This correlation predicts values that are the closer to those of the dry bed than any other correlation, but become more inaccurate as the liquid flow rate is increased. The first correlation proposed by them predicts mass transfer coefficients that are substantially higher than those obtained in any of the prewetted beds. The experiments performed by Turek and Lange (1981) were performed on a dry bed and the results should thus be compared to those of the dry bed.

The results of the Trickle-bed Reactor Simulator (Larachi *et al*, 1999) resulted in mass transfer coefficients that were higher than those obtained in the Kan and Super-wetted beds. This trend was the same for the correlation proposed by Ellman (1988) except that this correlation resulted in significant over predictions. The correlation proposed by Wild *et al* (1992) was reasonably accurate at the low liquid flow rates but showed a much stronger dependence on the liquid flow rate that resulted in a significant over prediction of the mass transfer coefficient at medium to high liquid flow rates. These correlations are all based on the work of various investigators and no indication was given to the prewetting procedure followed.

The performance of these correlations did not improve at the intermediate gas flow rates and the results can be seen in appendix 16.

5.3.2 Multiple Gas-Liquid Mass Transfer Correlations

The correlations proposed by Reiss (1967), Fukushima and Kusaka (1977), Turek and Lange (1981) and Hirose *et al* (1974) all incorporate either the pressure drop or the liquid holdup, or both, in their correlations. By using the results obtained from the experimental runs the correlations may prove more adaptable than the correlations shown above simply because they may be able to predict multiple steady state values for the mass transfer coefficient for the different prewetting modes. The correlation proposed by Reiss (1967) incorporates the pressure drop and the results can be seen in figures 5-17 and 5-18. On the other hand, the correlations of Fukushima and Kusaka (1977) and Turek and Lange (1981) use the liquid holdup and the results can be seen in figure 5-19 and figure 5-20, respectively. The correlation proposed by Hirose *et al* (1974) for the pulsing regime uses both the holdup and the pressure drop. The results of the correlation can be seen in figure 5-21.

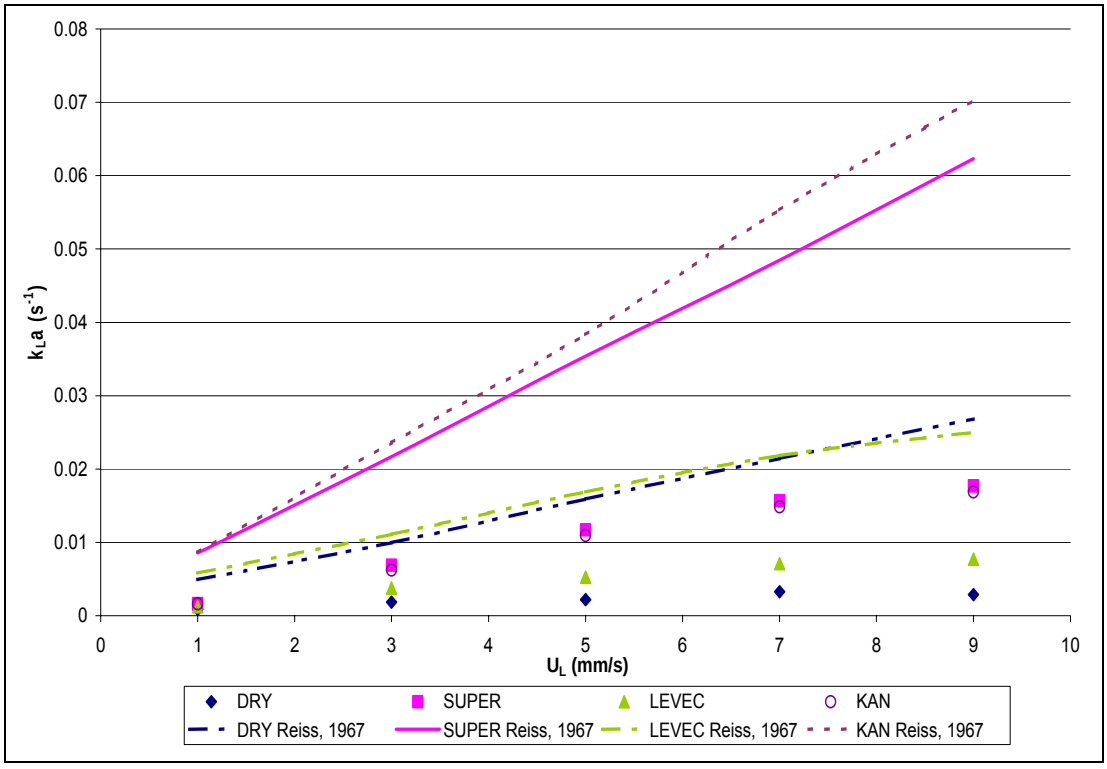

Figure 5-17: The performance of the gas-liquid mass transfer correlation proposed by Reiss (1967) at U_G = 20mm/s

From figure 5-17 it is clear that the Reiss (1967) correlation is unable to accurately predict the volumetric gas-liquid mass transfer coefficients for the different modes of prewetting. When the pressure drop from the different modes is used in the correlation the resulting mass transfer coefficient is substantially higher than the actual mass transfer measured.

At this gas flow rate it can be seen that the correlation predicts three distinct regions and that there is no significant difference between the predicted values of the dry and Levec-wetted beds. This is contrary to the results shown in chapter 4.

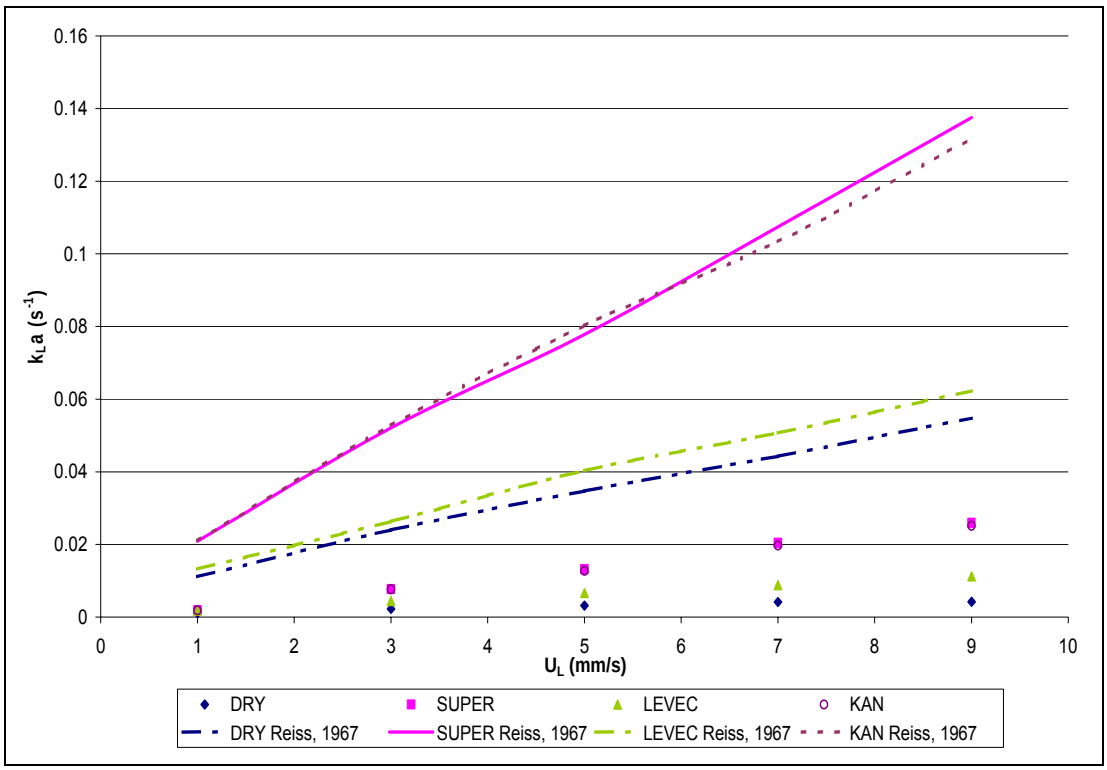

Figure 5-18: The performance of the gas-liquid mass transfer correlation proposed by Reiss (1967) at U_G = 90mm/s

From figure 5-18 it is clear that the correlation proposed by Reiss (1967) does not improve at higher gas flow rates. However, at this increased gas flow rate there is a distinction between the dry and Levec-wetted beds that was not seen at the lower gas flow rate.

The correlation did not perform any better at the intermediate gas flow rates and these results can be seen in appendix 17.

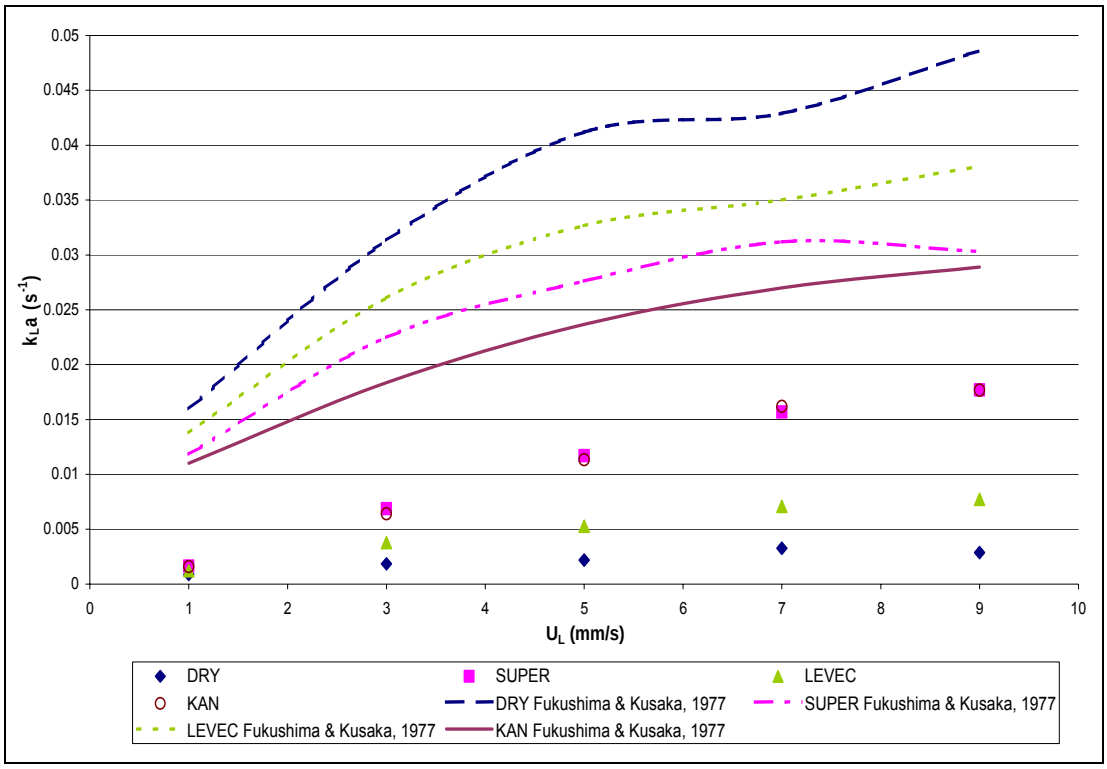

Figure 5-19: The performance of the gas-liquid mass transfer correlation proposed by Fukushima and Kusaka (1977) at U_G = 20mm/s

From figure 5-19 it is clear that the correlation proposed by Fukushima and Kusaka (1977) cannot accurately predict the volumetric gas-liquid mass transfer coefficient for the different modes. By using the holdup data from the different prewetting modes, different mass transfer coefficients were predicted. However, this correlation resulted in higher mass transfer coefficients for the dry bed than for any of the prewetted beds.

The correlation did not perform any better at the higher gas flow rates and these results can be seen in appendix 18.

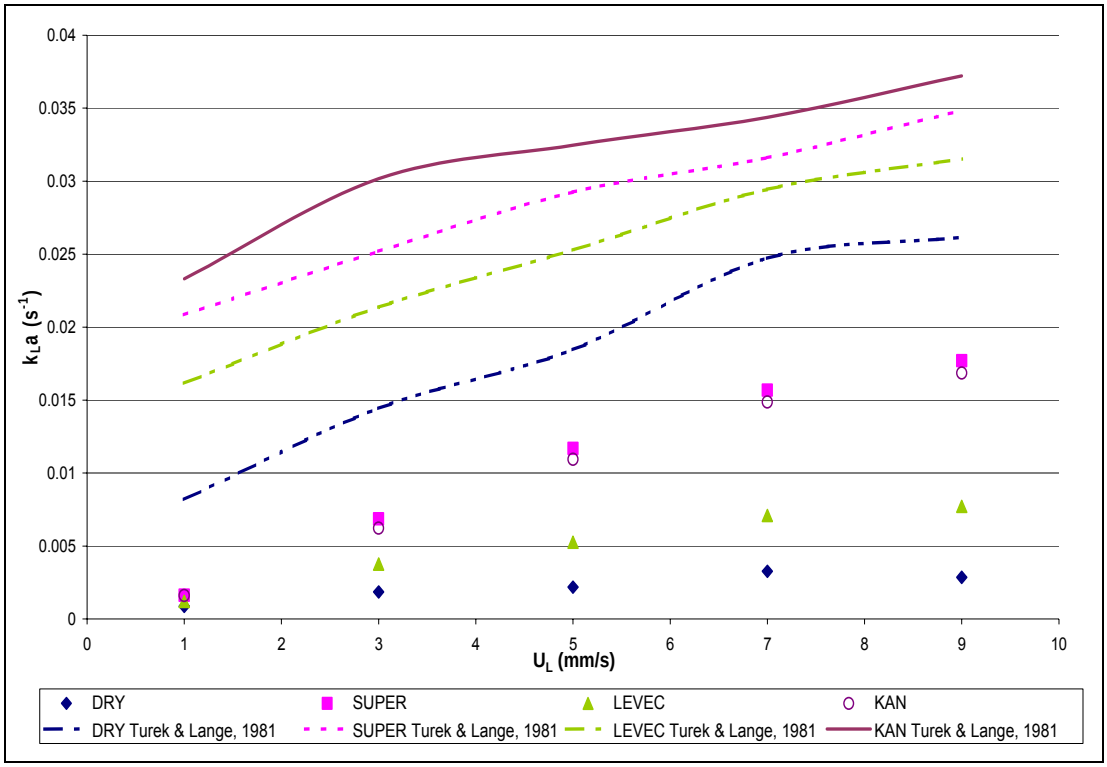

Figure 5-20: The performance of the gas-liquid mass transfer correlation proposed by Turek and Lange (1981) at U_G = 20mm/s

The correlation by Turek and Lange (1981) also uses the liquid holdup to predict the volumetric gas-liquid mass transfer coefficient. By using the liquid holdup the correlation predicts four distinct regions of mass transfer coefficients based on the different prewetting modes, as can be seen in figure 5-20. Although the correlation results in an over estimation in the holdup, unlike the correlation by Fukushima and Kusaka (1977) this correlation does result in higher mass transfer coefficients for the prewetted beds than those of the dry bed.

The correlation did not perform any better at the higher gas flow rates and these results can be seen in appendix 19.

The correlation proposed by Hirose *et al* (1974) incorporates the liquid holdup and the pressure drop but was actually derived for the pulsing regime. Although the experiments have all been in the trickle-flow regime the fact that this correlation is the only one to incorporate the pressure drop and the liquid

holdup may result in it being more adaptable to predicting the mass transfer coefficients obtained from the different prewetting modes.

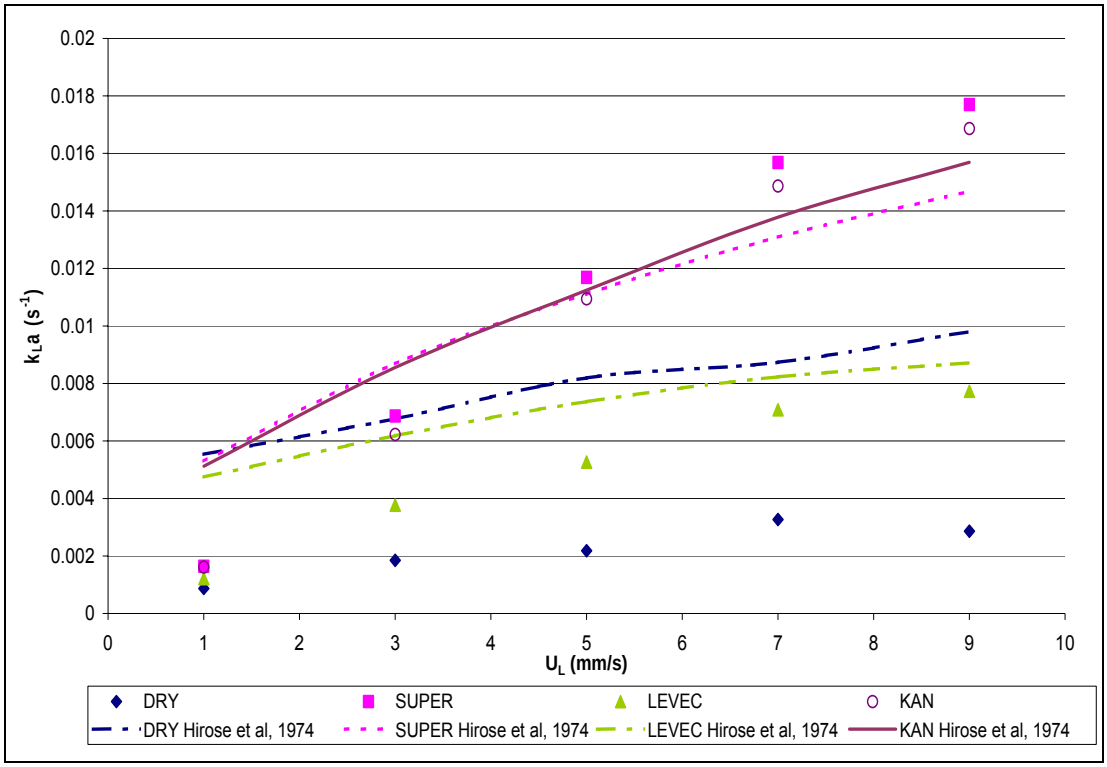

Figure 5-21: The performance of the gas-liquid mass transfer correlation proposed by Hirose et al (1974) at U_G = 20mm/s

In figure 5-21 it can be seen that by incorporating the liquid holdup and the pressure drop in the correlation for the mass transfer coefficient the result is three distinct regions. However, for this specific correlation it can be seen that the resulting mass transfer coefficient is actually higher for the dry bed than for the Levec-wetted bed.

The correlation did not perform any better at the higher gas flow rates and these results are shown in appendix 20. However, a correlation based on experiments in the pulsing regime cannot realistically be expected to predict accurate volumetric gas-liquid mass transfer coefficients in the trickle flow regime.

6. Discussion

6.1 The Effect of Prewetting on the Pressure Drop, Liquid Holdup and Gas-Liquid Mass Transfer

6.1.1 Liquid Flow Morphology

The effect of prewetting on the pressure drop, liquid holdup and gas-liquid mass transfer is substantial. From the results given in section 4 it can be seen that prewetting the bed can result in pressure drops that are up to seven times higher than those obtained in a dry bed, liquid holdups that are up to four times higher than those obtained in a dry bed and volumetric gas-liquid mass transfer coefficients that are up to six times higher than those obtained in a dry bed. Similarly the difference between the Kan and Levec-wetted beds is also substantial. In the Kan-wetted bed the pressure drop can be up to seven times greater, the liquid holdup can be up to thirty percent higher and the volumetric gas-liquid mass transfer coefficient can be as much as two and a half times greater than those obtained in the Levec-wetted bed.

These differences can be attributed to the flow morphologies in these beds. According to Christensen *et al* (1986) the dry bed is dominated by flow in the form of rivulets, whereas the dominant flow type is film flow in a prewetted bed.

The Kan, Super and Levec-wetted beds all exhibit much larger liquid holdups and mass transfer coefficients than those in the dry bed for the same operating conditions. This is mainly due to the liquid flow distribution in the bed. In a dry bed, which is dominated by rivulet flow, the catalyst in the bed is only partially wet and some of the areas of the bed remain totally dry. When the bed is prewetted (by flooding or pulsing), these areas that were initially dry are filled with water and the partially wet catalyst particles become totally wet. When the liquid flow rate is brought back to its normal operating point these

areas of the bed, that were initially dry but now contain liquid, retain this liquid and decreasing the liquid flow rate merely results in the liquid film around these particles decreasing in size.

This improvement in the liquid holdup is due to the fact that the liquid has now been spread to parts of the bed that were previously unused, and once the flow rate has been decreased some liquid remains in these newly wetted areas. The improvement in the gas-liquid mass transfer coefficient is mainly due to the fact that the flow in the bed is predominantly in the form of films and film flow offers a greater area for gas-liquid interaction.

A slightly different trend is observed in the pressure drop results. In the pressure drop results the recorded pressure drops in the Kan and Super-wetted were substantially greater than those recorded in the dry and Levec-wetted beds. In the Kan and Super-wetted beds the increase in liquid distribution decreases the cross-sectional area available for the gas to flow through, which results in higher pressure drops.

Unlike in the case of the liquid holdup and gas-liquid mass transfer results there was no substantial difference between the pressure drops of the dry and Levec-wetted beds. According to Ravindra *et al* (1997) during the draining process the films over the particles can rupture. This will result in the Levec-wetted bed behaving the same as a dry bed. However, if this were the case the areas of the bed where the film was ruptured could be dominated by rivulet flow and this would cause a drastic decrease in the gas-liquid mass transfer coefficient, and the mass transfer coefficients of the dry and Levec-wetted beds would be similar.

From these results it appears as though the Kan and Super-wetted beds are dominated by film flow and the dry bed is dominated by rivulet flow. However, the Levec-wetted bed appears to be a mixture of the two flow types and cannot be classified as being dominated by rivulet flow or film flow.

For the pressure drop, liquid holdup and gas-liquid mass transfer results the difference between the different prewetting modes is not as substantial at the lowest liquid flow rate (U_L = 1mm/s). According to Wammes *et al* (1991) at sufficiently low liquid flow rates the film thickness around a particle gets so thin that the film is broken up and once again rivulet flow is the dominant flow type regardless of the prewetting mode. This is more prominent in the results of the pressure drop and gas-liquid mass transfer.

6.1.2 The Effect of the Gas Flow Rate

The gas flow rate plays a significant role in a trickle bed reactor and the effect it has on the pressure drop, liquid holdup and gas-liquid mass transfer cannot be ignored. The effect of the gas flow rate on the gas-liquid mass transfer coefficient will be discussed in the section 6.2.

The effect of the gas flow rate on the liquid holdup is substantially greater in the prewetted beds For the liquid holdup an increase in the gas flow rate causes a decrease in the liquid holdup in the prewetted beds at all of the liquid flow rates except the lowest one tested. This decrease is due to the fact that in the prewetted beds the increase in gas flow rate results in the thinning and spreading out of the liquid films around the particles. The thinning out of the films results in a lower liquid holdup.

The dry bed, which is dominated by rivulet flow, does not show the same trend because the gas flow rate does not have the same effect on rivulets as it does on the films. This could be due to the fact that there is less gas-liquid interaction in the bed if the dominant flow formation is rivulets. The same reasoning could apply to the prewetted beds at the lowest liquid flow rate tested, where due to the fact that the liquid flow rate has been decreased, the films around the particles break down and the resultant flow formation is rivulet flow.

6.1.3 Pulsing with Gas

The results obtained when the pulsing regime was reached by increasing the gas flow rate and keeping the liquid flow rate constant proved to be very interesting. When comparing these results with those obtained when pulsing by increasing the liquid flow rate it was found that pulsing with gas resulted in lower pressure drops and gas-liquid mass transfer coefficients but higher liquid holdups.

The reason for the difference in pressure drop, according to Kan and Greenfield (1978 & 1979), is that in a prewetted bed, in the absence of gas flow, the liquid bridges are orientated randomly. As the gas flow rate is increased the liquid bridges transverse to the general flow of the gas tend to be broken down, thereby decreasing the gas flowpath density and tortuosity. Due to the high surface tension, even when the gas flow rate is reduced, this flow pattern is retained and results in a lower pressure drop. The decrease in the gas flowpath density and tortuosity results in a higher liquid holdup due to the fact that the liquid holdup is directly affected by the gas velocity acting on the liquid surface. However, Herskowitz and Smith (1978) found that this effect was not due to surface tension because when they lowered the surface tension of the water from 72 to 38×10^{-3} N/m the multiple steady states were still observed.

This phenomenon may be due to the fact that the liquid is forced into channels, or large rivulets. The resulting paths for gas flow rate will be relatively straight and the gas flow will not be hindered, which will result in a lower pressure drop. However, this will also reduce the available area for gas-liquid mass transfer and may explain the decrease observed in the volumetric gas-liquid mass transfer coefficient.

6.1.4 An Overview of the Effect of Prewetting

The effect of the different prewetting modes in trickle bed reactor operations cannot be under emphasised. If one were to look at just one of the results from one of the gas-liquid mass transfer experiments, figure 6-1, a number of key points could be raised.

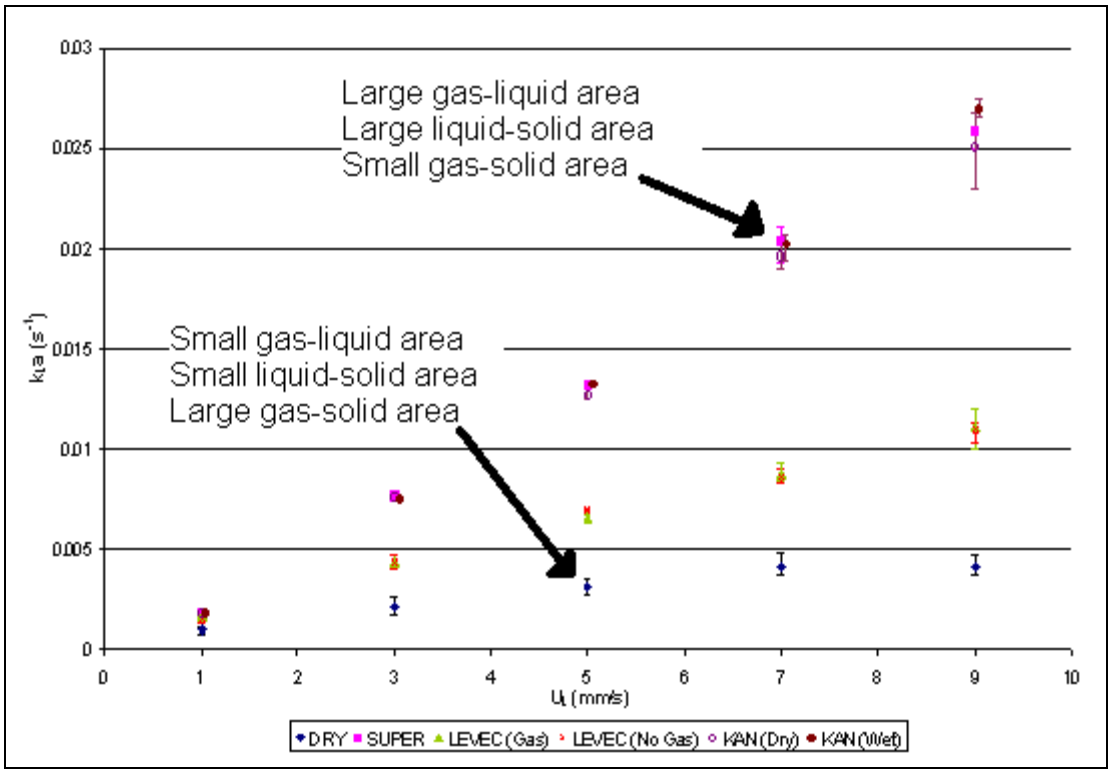

Figure 6-1: The effect of prewetting on the volumetric gas-liquid mass transfer coefficient at U_G = 90mm/s

Figure 6-1 shows the effect of the prewetting on the volumetric gas-liquid mass transfer coefficient. A similar trend is seen in the liquid holdup with the only major difference being the distinction between the Kan and Super-wetted beds. However, for this discussion the one graph will suffice.

By taking into account the two extremes, Kan-wetted and the dry bed, a number of significant differences can be seen which would greatly affect the operation of a trickle bed reactor. Firstly, since these results are based on the volumetric gas-liquid mass transfer coefficient it can clearly be seen from the large difference between the two modes that the Kan-wetted bed will have a

greater gas-liquid interfacial area than the dry bed. Following on from this, due to the fact that the liquid distribution is better in the Kan-wetted bed and the flow formation is predominantly film flow, it can be implied that the Kan-wetted bed will also have a greater liquid-solid interfacial area than the dry bed. However, if the Kan-wetted bed has a greater gas-liquid interfacial area as well as a greater liquid-solid interfacial area it must have a smaller gas-solid interfacial area than the dry bed.

These three interfacial areas could play an important role in determining the reaction rate in a trickle bed reactor. For instance, if the reaction was liquid limited it would require a larger liquid-solid interfacial area for the reaction to take place, thus making the Kan-wetted bed the better operating mode. However, if the reaction was gas limited, then the larger liquid-solid interfacial area will actually hinder the reaction and a larger gas-solid interfacial area would be more beneficial. In this case the dry bed operation would be preferred.

However, it is not that simple. By decreasing the draining time of the Levec-wetted bed it was shown that the values initially obtained from the different prewetting modes were merely boundaries and that an operating point could in fact lie any where between these boundaries. Levec *et al* (1986) actually referred to these hysteresis curves as an envelope of all the possible hydrodynamic states.

Thus for each specific reaction a play-off will exist in terms of the optimum gas-liquid, liquid-solid and gas-solid area. The shown continuum of possible flow morphologies will make it possible to select the ideal operating point for the reactor by taking these interfacial areas into account and this operating point can be attained by merely varying the prewetting or operating procedure.

6.2 Analysing the Effect of the Gas-Velocity on the Volumetric Gas-Liquid Mass Transfer Coefficient

The results shown in section 4 show that the gas flow rate does have an effect on the volumetric gas-liquid mass transfer coefficient k_La. However, whether this effect is due to the liquid holdup varying with gas flow rate or the gas-liquid interfacial area varying with gas flow rate is yet to be determined. There are arguments for both cases.

Rao and Drinkenburg (1985) state that at a given liquid velocity, the interstitial liquid velocity increases with increasing gas velocity due to a decrease in the liquid holdup. This increase in liquid velocity will result in an increase in the mass transfer coefficient due to its dependence on the liquid flow rate.

The gas-liquid interfacial area, a, also increases with gas flow rate (Dudukovic *et al*, 1999) (Iliuta *et al*, 1999) (Midoux *et al*, 1984) (Iliuta *et al*, 1997). According to Iliuta *et al* (1997) this increase may be attributed to the gradual thinning and spreading of the liquid over the catalyst surface as a result of the increased gas flow rate.

In order to remove the effect of the gas flow rate on the liquid holdup the superficial velocity can be divided by the liquid holdup. According to Gianetto, Specchia and Baldi (1973) the mass transfer coefficient is then directly proportional to the liquid velocity. The equations governing this are:

$$k_L \propto V_L^{*1.5} \tag{6.1}$$

where:

$$V_L^* = \frac{U_L}{H_t} \tag{6.2}$$

The equation is based on the relationship that exists between the modified liquid velocity and the gas-liquid mass transfer coefficient, k_L, and not the volumetric gas-liquid mass transfer coefficient k_La. If the volumetric mass transfer coefficient, k_La, does not deviate from this relationship it will prove

that the gas flow rate only affects the liquid holdup, however, if there is a deviation from this relationship it will prove that that gas flow rate affects the gas-liquid interfacial area, a.

The result of the dry bed is shown in figure 6-2, the result of the Levec-wetted bed is shown in figure 6-3, the result of the Super-wetted bed is shown in figure 6-4 and finally the result of the Kan-wetted bed is shown in figure 6-5. The trend line shown in each of the figures represents the relationship shown in equation 6.1.

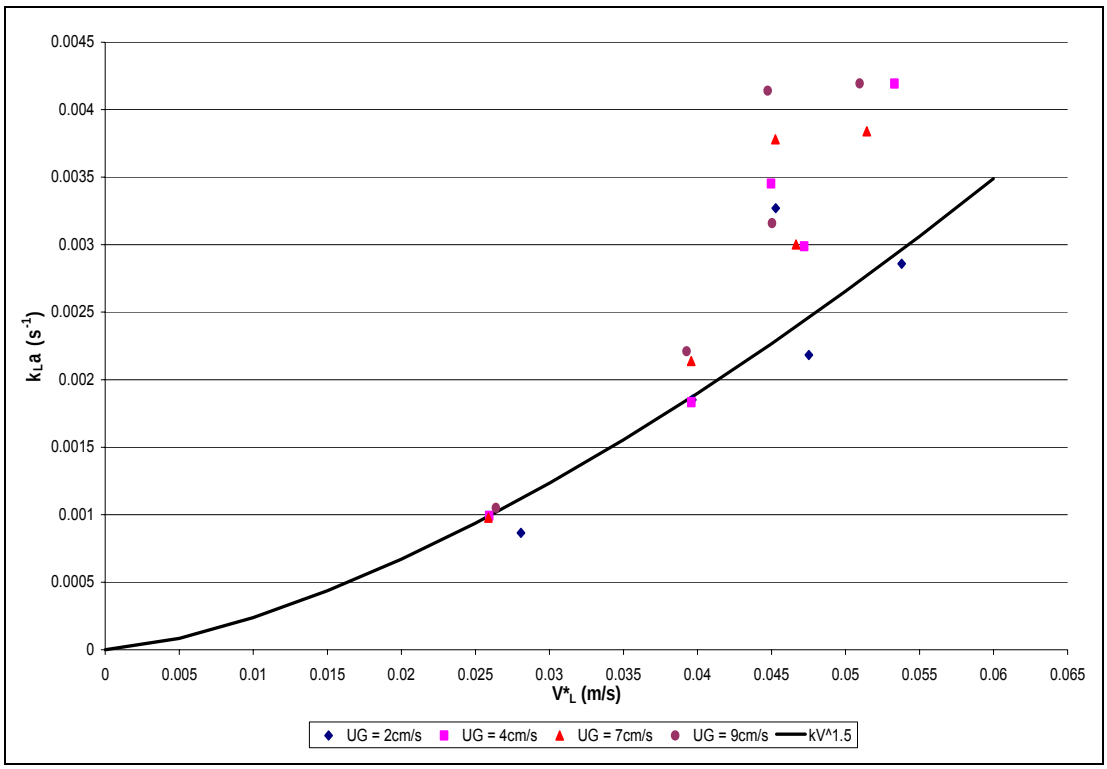

Figure 6-2: The effect of the gas flow rate on the volumetric gas-liquid mass transfer coefficient in the dry bed

From figure 6-2 it is clear that the effect of the gas flow rate is as a result of the liquid holdup and the gas-liquid interfacial area. At low liquid flow rates it can be seen that the relationship that exists between the mass transfer coefficient, k_L, and the modified liquid velocity holds for all of the gas flow rates except the lowest. This would imply that the only effect of the gas flow rate is the effect that it has on the liquid holdup.

As the liquid flow rate is increased there is a significant deviation from this relationship for all of the gas flow rates. This is due to the fact that the increase in the gas flow rate at these higher liquid velocities results in an improvement of the liquid distribution. Although the dry bed is dominated by rivulet flow, the increase in the gas flow rate can still cause these rivulets to spread out more. This spreading out will result in a greater area for gas-liquid interaction and will thus increase the volumetric gas-liquid mass transfer coefficient k_La.

The spread of the data for the dry bed is due to the fact that it is more difficult to obtain repeatable data in a dry bed than it is in a prewetted bed. This is partly due to the fact that in a dry bed the initial flow distribution is random and it is almost impossible to obtain exactly the same flow condition in a repeat run.

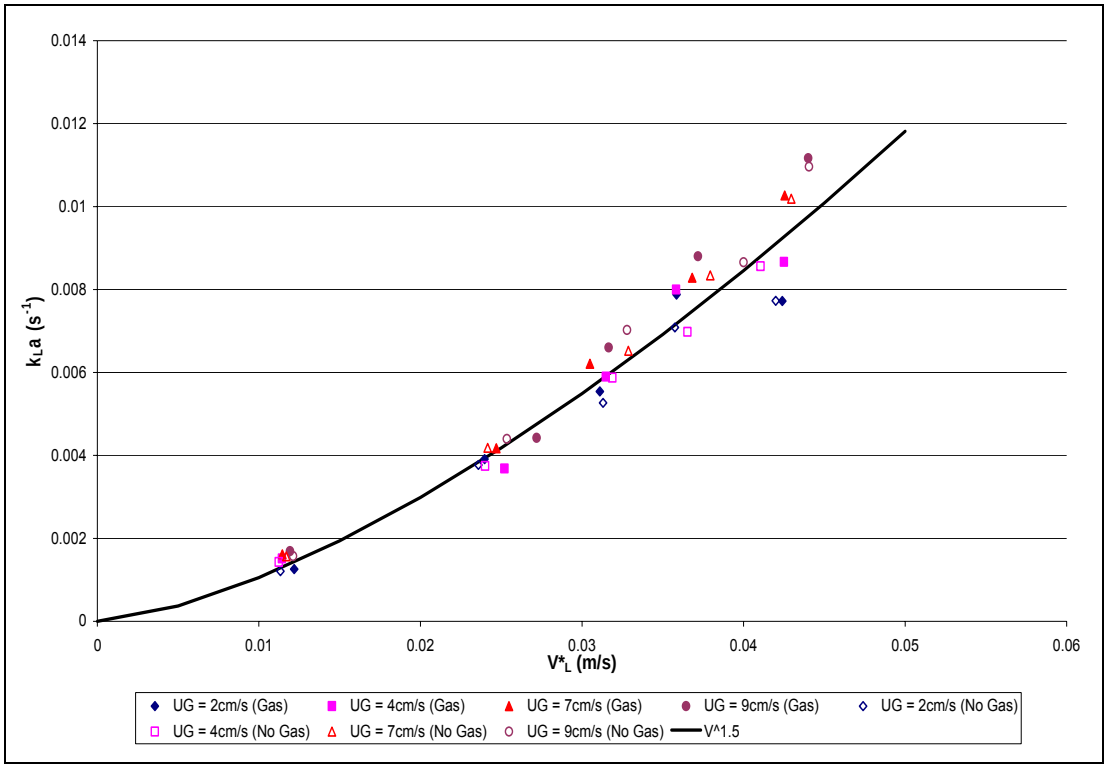

Figure 6-3: The effect of the gas flow rate on the volumetric gas-liquid mass transfer coefficient in the Levec-wetted bed

In figure 6-3 it can be seen that the same trend exists for the Levec-wetted bed. For the lower liquid flow rates the relationship that exists between the mass transfer coefficient, k_L, and the modified liquid velocity holds for all of the gas flow rates. This would imply that at the lower liquid flow rates the effect of the gas flow rate on the volumetric mass transfer coefficient is due to the effect that it has on the liquid holdup and that the gas-liquid interfacial area is not affected.

At higher liquid flow rates it can be seen that there is a definite deviation from this region. This deviation is due to the fact that an increase in the gas flow rate results in the films around the particles getting thinner and spreading out more. This increase in gas flow rate causes an increase in the gas-liquid interaction, which results in an increase in the gas-liquid interfacial area. An increase in the gas-liquid interfacial area results in an increase in the volumetric gas-liquid mass transfer coefficient. This effect is more prevalent at the highest liquid flow rate.

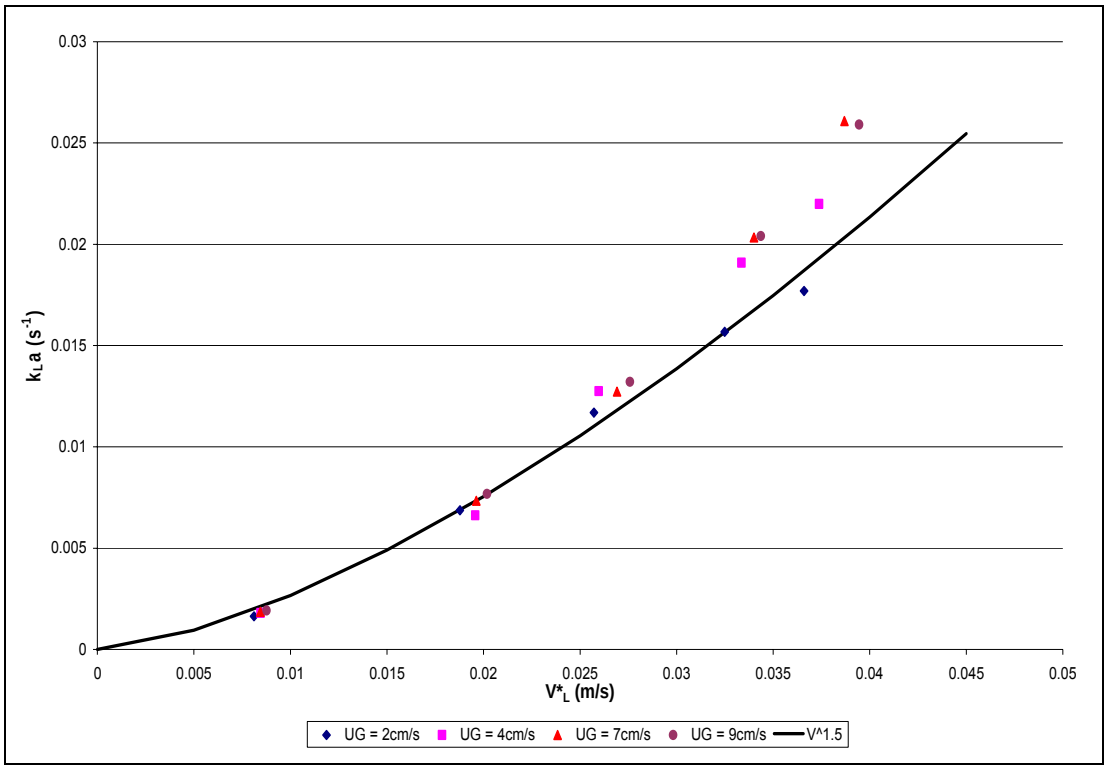

Figure 6-4: The effect of the gas flow rate on the volumetric gas-liquid mass transfer coefficient in the Super-wetted bed

In figure 6-4 it can be seen that the effect of the gas flow rate is mainly due its effect on the liquid holdup for low to medium liquid flow rates. For these liquid flow rates the relationship that exists between the mass transfer coefficient, k_L, and the modified liquid velocity holds for all of the gas flow rates and the gas-liquid interfacial area is not affected.

At the higher liquid flow rates it can be seen that the effect of the gas flow rate is not only due to its effect on the liquid holdup but also due to its effect on the gas-liquid interfacial area. The Super-wetted bed is dominated by film flow and an increase in the gas flow rate results in these films thinning out and spreading further across the catalyst surface. This causes an increase in the gas-liquid interaction and as a result an increase in the gas-liquid interfacial area.

The effect of the gas flow rate on the liquid distribution at higher liquid flow rates has been confirmed by Al-Dahhan *et al* (1999). For the low gas flow rates (10 and 20 mm/s) the fluid dynamics in the trickle-bed reactor are seen as being gravity driven and gas phase independent. However, at higher gas flow rates (70 and 90 mm/s) the increase in gas flow rate results in an increase in the liquid spreading across the reactor section and over the external catalyst surface.

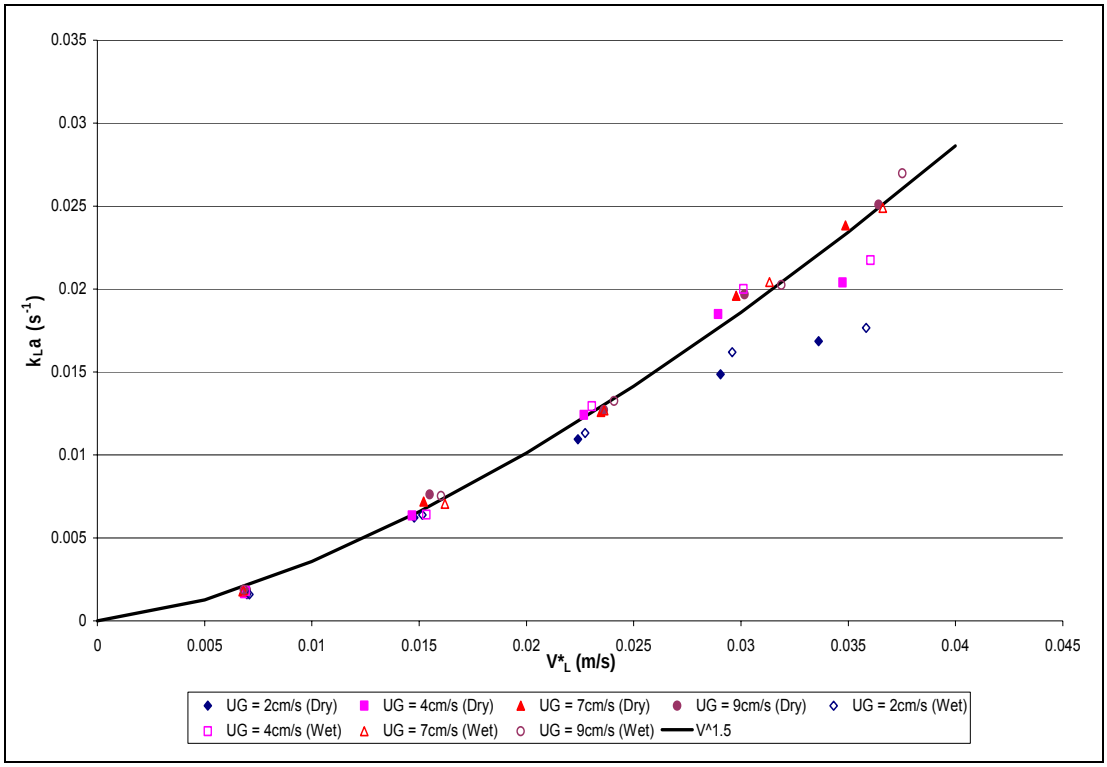

Figure 6-5: The effect of the gas flow rate on the volumetric gas-liquid mass transfer coefficient in the Kan-wetted bed

In figure 6-5 it can be seen that the trend is exactly the same as for the other prewetting modes. The effect of the gas flow rate can be seen as being due to the liquid holdup at low to medium liquid flow rates. For these liquid flow rates the relationship that exists between the mass transfer coefficient, k_L, and the modified liquid velocity holds for all of the gas flow rates.

Once again at high liquid flow rates there is a deviation from this trend. As described above this deviation is due to the effect that the higher gas flow rates have on the liquid distribution. This means that at the higher liquid flow rates the effect of the gas flow rate on the volumetric gas-liquid mass transfer is due to the effect of the gas on the interfacial area and the liquid holdup.

6.3 Correlations

A number of pressure drop, liquid holdup and gas-liquid mass transfer correlations were tested throughout the duration of this study. However, none of these correlations could accurately predict the values obtained in the dry and prewetted beds.

The fact that none of the correlations could accurately predict the pressure drop, liquid holdup or gas-liquid mass transfer coefficient is by no means a poor reflection on the investigators. However, it does point out the fact that the prewetting procedure has largely been ignored.

When one considers the fact that the pressure drop can be seven times larger, the liquid holdup four times larger and the gas-liquid mass transfer six times larger in a prewetted bed than those values obtained in a dry bed, the need for a review of these correlations becomes obvious. The prewetting procedure cannot be ignored or else all the correlation will be able to do is predict an arbitrary average, at best.

A classic example is that of the pressure drop correlation proposed by Ellman *et al* (1988). This correlation is based on over 4000 different experimental results and incorporates the work of many different researchers. However, no mention is made of the prewetting procedures that were followed and this results in a correlation that predicts pressure drops between those of a dry and prewetted bed.

The existence of pressure drop, liquid holdup and mass transfer hysteresis during operation only add to this dilemma. Even if the process is started on a dry bed any fluctuations in gas or liquid flow rates from the desired operating points could result in the process steadying itself out at a new operating condition.

Most of the correlations are only functions of the bed packing characteristics and the liquid and gas flow rates. In these correlations there is no parameter that would result in the prediction of multiple steady states. Although some correlations do incorporate these parameters, for example using the pressure drop to determine the liquid holdup, none of them were able to accurately predict the pressure drop, liquid holdup or gas-liquid mass transfer coefficients for the different prewetting modes.

Whether one would ever be able to develop a realistic correlation for either of these parameters is highly unlikely due to the fact that the different prewetting procedures do not have the same affect on the different parameters. In the case of the pressure drop the different prewetting procedures result in two distinct regions, with no clear distinction between the dry and Levec-wetted beds, as well as no clear distinction between the Kan and Super-wetted beds. In the case of the liquid holdup the prewetting procedures result in four distinct regions, with a clear distinction between the holdups of the dry, Levec, Super and Kan-wetted beds. For the volumetric gas-liquid mass transfer coefficient the different prewetting procedures resulted in three distinct regions, with a clear distinction between the dry, Levec and Kan, Super-wetted beds, but no clear distinction between the Kan and Super-wetted beds.

This implies that if only the pressure drop was used to determine the volumetric gas-liquid mass transfer coefficient the resulting correlation would predict similar mass transfer coefficients for the dry and Levec-wetted beds, which is incorrect. Similarly, if the liquid holdup were used to determine the volumetric gas-liquid mass transfer coefficient the resulting correlation would predict different mass transfer coefficient for the Kan and Super-wetted beds. The same trends would be seen if the holdup or mass transfer coefficients were used to determine the pressure drop, or the pressure drop or mass transfer coefficient were used to used determine the liquid holdup.

7. Conclusions and Recommendations

From this study it can be concluded that the pressure drop, liquid holdup and volumetric gas-liquid mass transfer coefficient are all functions of the prewetting procedure. The different prewetting procedures resulted in two distinct regions for the pressure drop, four distinct regions for the liquid holdup and three distinct regions for the gas-liquid mass transfer. The primary reason for the dependency of these hydrodynamic parameters on the prewetting procedure is the liquid flow morphology, in other words the form of the liquid flowing over the particles. The results confirm the notion that the predominant flow formation in a dry bed is in the form of rivulets and the predominant flow formation in the Kan- and Super-wetted beds is in the form of films. The flow formation in the Levec-wetted bed can be seen as being a mixture of rivulets and films and does not appear to be dominated by either flow formation.

Film flow offers greater liquid spreading and a greater area for gas-liquid interaction. This results in increased pressure drops, increased liquid holdups and increased gas-liquid mass transfer coefficients. In fact in a prewetted bed the pressure drop can be as much as seven times higher, the liquid holdup as much as four times higher and the volumetric gas-liquid mass transfer coefficient as much as six times higher than the values recorded in a dry bed for the same flow conditions. This trend can also be seen when one compares the Kan-wetted bed and the Levec-wetted bed, in a Kan-wetted bed the pressure drop can be as much as seven times higher, the liquid holdup as much as thirty percent higher and the volumetric gas-liquid mass transfer coefficient as much as two and a half times higher than the values recorded in a Levec-wetted bed for the same flow conditions

The effect of the gas flow rate on these hydrodynamic parameters is also more pronounced if the flow is in the form of films. This is especially true in the case of the liquid holdup. An increase in the gas flow rate causes a decrease in the liquid holdup in the prewetted beds (Kan, Super and Levec-wetted beds). However, the same increase in gas flow rate appears to have

no effect on the liquid holdup in a dry bed. This is due to the fact that when the flow is in the form of films the increased gas flow rate causes these films to spread out across the catalyst surface and this results in a lower liquid holdup. In the case of the dry bed, which is dominated by rivulet flow, this increase in gas flow rate did not cause the rivulets to spread out.

For the volumetric gas-liquid mass transfer coefficient the increase in the gas flow rate caused an increase in the mass transfer coefficient. This was due to a combination of the effect of the gas flow rate on the liquid holdup and the effect of the gas flow rate on the gas-liquid interfacial area. At low liquid flow rates the effect of the gas flow rate was primarily due to the decrease in the liquid holdup caused by the increase in the gas flow rate. As the holdup decreases the interstitial liquid velocity is increased and this results in the mass transfer coefficient increasing due to its dependence on the liquid flow rate. At higher liquid flow rates the decrease in the liquid holdup, caused by the increasing gas flow rate, still results in an increase in the mass transfer coefficient but there is also a contribution from the effect that the increased gas flow rate has on the gas-liquid interfacial area. At these higher liquid flow rates there is less open space for the gas to move through and this results in higher pressure drops and more gas-liquid interaction. The increased gas flow rate causes a gradual thinning and spreading of the liquid over the catalyst surface which results in a greater gas-liquid interfacial area and a greater volumetric gas-liquid mass transfer coefficient.

The multiple operating points obtained from the different prewetting procedures are by no means the only possible operating points. By simply decreasing the draining time in the Levec-wetted bed it was found that steady state operating points could be found between those of the Super and Levec-wetted beds. This alludes to the fact that the operating conditions determined from the different prewetting modes are only boundaries and that the actual operating point can lie anywhere between these boundaries.

This could have important implications in the design and operation of trickle-bed reactors. If the predominant flow formation in the reactor were in the form

of rivulets there would be less liquid-solid interaction and less gas-liquid interaction but more gas-solid interaction than the reactor that is dominated by film flow. The continuum of possible flow morphologies will make it possible to select the ideal operating point for the reactor by taking these interfacial areas into account and this operating point can be attained by merely varying the prewetting or operating procedure.

A number of pressure drop, liquid holdup and gas-liquid mass transfer correlations were tested but none could accurately predict these parameters in the dry or prewetted beds. The most surprising aspect of the results obtained from the correlations was that little to no attention had been paid to the prewetting procedure followed.

It is recommended that these experiments be repeated with different catalysts, including porous catalysts, as well as at high pressure due to speculation that hydrodynamic hysteresis may not be as prevelant at higher pressures (Dudukovic *et al* 1999).

8. References

Al-Dahhan, M. H., Larachi, F., Dudukovic, M. P. and Laurent, A. (1997) "High-Pressure Trickle-Bed Reactors: A Review" *Ind. Eng. Chem. Res., 36,* 3292-3314.

Al-Dahhan, M.H., Khadilkar, M.R., Wu, Y. and Dudukovic, M.P. (1998) "Prediction of Pressure Drop and Liquid Holdup in High-Pressure Trickle-Bed Reactors" *Ind. Eng. Chem. Res., 37*, 793 – 798

Burghardt, A., Bartelmus, G., Jaroszynski, M. and Kolodziej, A. (1995) "Hydrodynamics and Mass Transfer in a Three-Phase Fixed-Bed Reactor with Cocurrent Gas-Liquid Downflow" *Chem. Eng. J.*, 58, 83 – 99

Charpentier, J.C. (1976) "Recent Progress in Two Phase Gas-Liquid Mass Transfer in Packed Beds" *Chem. Eng. J.,* 11, 161 – 181

Christensen, G., McGovern, S. J. and Sundaresan, S. (1986) "Cocurrent Downflow of Air and Water in a Two-Dimensional Packed Column" *A.I.Ch.E. J., 32, (10),* 1677-1689.

Clements, L.D. and Schmidt, P.C. (1980) "Two-Phase Pressure Drop in Cocurrent Downflow in Packed Beds: Air-Silicone Oil Systems" *A.I.Ch.E. J., 26*, (2), 314 – 319

Colombo, A. J., Baldi, G. and Sicardi, S. (1976) "Solid-Liquid Contacting Effectiveness in Trickle Bed Reactors" *Chem. Eng. Sci., 31,* 1101-1108.

De Klerk, A. (2003) "Liquid Holdup in Packed Beds at Low Mass Flux" *A.I.Ch.E. J., 49, (6),* 1597-1600.

Dharwadkar, A. and Sylvester, N.D. (1977) “Liquid-Solid Mass Transfer in Trickle Beds” *A.I.Ch.E. J.,* 23, (3), 376 – 378

Dudukovic, M. P., Larachi, F. and Mills, P. L. (1999) “Multiphase Reactors – Revisited” *Chem. Eng. Sci., 54,* 1975-1995.

Ellman, M. J., Midoux, N., Laurent, A. and Charpentier, J. C. (1988) “A New, Improved Pressure Drop Correlation for Trickle-Bed Reactors” *Chem. Eng. Sci., 43,* 2201-2210.

Ellman, M. J., Midoux, N., Wild, G., Laurent, A. and Charpentier, J. C. (1990) “A New, Improved Liquid Holdup Correlation for Trickle-Bed Reactors” *Chem. Eng. Sci., 45,* 1677 - 1684.

Fukushima, S. and Kusaka, K. (1977) “Liquid-Phase Volumetric and Mass-Transfer Coefficient, and Boundary of Hydrodynamic Flow Region in Packed Column With Cocurrent Downward Flow” *J. Chem. Eng. Japan*, 10, (6), 468 – 474

Geonaga, A., Smith, J.M. and McCoy, B.J. (1989) “Study of Gas-to-Liquid Mass Transfer by Dynamic Methods in Trickle Beds” *A.I.Ch.E. J.,* 35, (1), 159 – 163

Gianetto, A. and Specchia, V. (1992) “Trickle-bed Reactors: State of Art and Perspectives” *Chem. Eng. Sci.*, 27, (13), 3197 – 3213

Gianetto, A., Baldi, G., Specchia, V and Sicardi, S. (1978) “Hydrodynamics and Solid-Liquid Contacting Effectiveness in Trickle-Bed Reactors” *A.I.Ch.E. J.*, 24, (6), 1087 – 1104

Gianetto, A., Specchia, V. and Baldi, G. (1973) “Absorption in Packed Towers with Concurrent Downward High-Velocity Flows – II: Mass Transfer” *A.I.Ch.E. J., 19, (5),* 916 – 922

Goto, S. and Smith, J.M. (1975) “Trickle-Bed Reactor Performance – Part 1. Holdup and Mass Transfer” *A.I.Ch.E. J., 21*, 706 – 713

Herskowitz, M. and Smith, J.M. (1983) “Trickle-bed Reactors: A Review” *A.I.Ch.E. J.,* 29, (1), 1-18

Hirose, T., Toda, M. and Sato, Y. (1974) “Liquid Phase Mass Transfer in Packed Bed Reactor with Cocurrent Gas-Liquid Downflow” *J. Chem. Eng. Japan*, 7, (3), 187 – 192

Holub, R. A., Dudukovic, M. P. and Ramachandran, P. A. (1992) “A Phenomenological Model for Pressure Drop, Liquid Hold-up and Flow Regime Transition in Gas-Liquid Trickle Flow” *Chem. Eng. Sci., 47,* 2343-2348.

Iliuta, I., Iliuta, M.C. and Thyrion, F.C. (1997) “Gas-Liquid Mass Transfer in Trickle-Bed Reactors: Gas-Side Mass Transfer” *Chem. Eng.Tech.* 20, 589 – 595

Iliuta, I., Larachi, F., Grandjean, B. P. A. and Wild, G. (1999) “Gas-Liquid Interfacial Mass Transfer in Trickle-Bed Reactors: State-of-the-art Correlations” *Chem*. *Eng. Sci*., 54, 5633 – 5645

Iliuta, I., Ortiz-Arroyo, A., Larachi, F., Grandjean, B.P.A. and Wild, G. (1999) “Hydrodynamics and Mass Transfer in Trickle-Bed Reactors: An Overview” *Chem. Eng. Sci.,* 54, 5329 – 5337

Kan, K. M. and Greenfield, P. F. (1978) “Multiple Hydrodynamic States in Cocurrent Two-Phase Down-Flow through Packed Beds” *Ind. Eng. Chem. Process Des. Dev., 17,* 482 - 485.

Kan, K. M. and Greenfield, P. F. (1979) “Pressure Drop and Holdup in Two-Phase Cocurrent Trickle Flows through Packed Beds” *Ind. Eng. Chem. Process Des. Dev., 18,* 740-745.

Kantzas, A. (1994) Computation of Holdups in Fluidized and Trickle Beds by Computer-Assisted Tomography" *A.I.Ch.E. J., 40, (7),* 1254-1261.

Kohler, M. and Richarz, W. (1985) "Investigation of Liquid Holdup in Trickle Bed Reactors" *German Chem. Eng., 8*, 295 – 300

Kushalkar, K. B. and Pangarkar, V. G. (1990) "Liquid Holdup and Dispersion in Packed Columns" *Chem. Eng. Sci. 45, (3),* 759 - 763.

Lakota, A., Levec, J. and Carbonell, R.G. (2002) "Hydrodynamics of Trickling Flow in Packed Beds: Relative Permeability Concept" *A.I.Ch.E. J., 48,* 731 - 738.

Larachi, F., Grandjean, B., Iliuta, I., Bensetiti, Z., Andre, A., Wild, G., and Chen, M. (1999) Excel Worksheet Simulators for Packed Bed Reactors, http://www.gch.ulaval.ca/bgrandjean/pbrsimul/pbrsimul.html, [2005, November 8]

Larachi, F., Laurent, A., Midoux, N. and Wild, G. (1991) "Experimental Study of a Trickle-Bed Reactor Operating at High Pressure: Two-Phase Pressure Drop and Liquid Saturation" *Chem. Eng. Sci.*, 46, 1233 – 1246

Lara-Marquez, A., Nguyen, C., Poncin, S., Wild, G. and Midoux, N. (1994a) "A Novel Hydrazine Oxidation Technique for the Determination of k_La in Gas-Liquid and Liquid-Solid Reactors" *Chem. Eng. Sci., 49,* 5667 - 5679.

Lara-Marquez, A., Wild, G. and Midoux, N. (1994b) "A Review of Recent Techniques for the Determination of the Volumetric Mass-Transfer Coefficient k_La in Gas-LIquid Reactors" *Chem. Eng Proc.,* 33, 247 – 260

Lazzaroni, C. L., Keselman, H. R. and Figoli, N. S. (1988) "Colorimetric Evaluation of the Efficiency of Liquid-Solid Contacting in Trickle Flow" *Ind. Eng. Chem. Res., 27,* 1132-1135

Lazzaroni, C. L., Keselman, H. R. and Figoli, N. S. (1989) "Trickle Bed Reactors. Multiplicity of Hydrodynamic States. Relation between the Pressure Drop and the Liquid Holdup" *Ind. Eng. Chem. Res., 28,* 119-121.

Levec, J., Grosser, K. and Carbonell, R. G. (1988) "The Hysteretic Behaviour of Pressure Drop and Liquid Holdup in Trickle Beds" *A.I.Ch.E. J., 34,* 1027-1030.

Levec, J., Saez, A. E. and Carbonell, R. G. (1986) "The Hydrodynamics of Trickling Flow in Packed Beds, Part I: Conduit Models" *A.I.Ch.E. J., 32,* 515-523.

Lutran, P. G., Ng, K. M. and Delikat, E. P. (1991) "Liquid Distribution in Trickle Beds. An Experimental Study using Computer-Assisted Tomography" *Ind. Eng. Chem. Res., 30,* 1270-1280.

Midoux, N., Morsi, M., Purwasasmita, M., Laurent, A. and Charpentier, J.C. (1984) "Interfacial Area and Liquid Side Mass Transfer Coefficient in Trickle Bed Reactors Operating with Organic Liquids" *Chem. Eng. Sci.,* 39, (5), 781 – 794

Moller, L. B., Halken, C., Hansen, J. A. and Bartholdy, J. (1996) "Liquid and Gas Distribution in Trickle-Bed Reactors" *Ind. Eng. Chem. Res., 35*, 926 – 930

Nemec, D. and Levec, J. (2005) "Flow through Packed Bed Reactors: 2. Two-phase Concurrent Downflow" *Chem. Eng. Sci., 60,* 6958 – 6970

Rao, V.G. and Drinkenburg, A.A.H. (1985) "Solid-Liquid Mass Transfer in Packed Beds with Cocurrent Gas-Liquid Downflow" *A.I.Ch.E. J.,* 31, (7), 1059 – 1068

Ravindra, P. V., Rao, D. P. and Rao, M. S. (1997) “Liquid Flow Texture in Trickle-Bed Reactors: An Experimental Study” *Ind. Eng. Chem. Res., 36,* 5133-5145.

Reinecke, N. and Mewes, D. (1997) “Investigation of the Two-Phase Flow in Trickle-Bed Reactors using Capacitance Tomography” *Chem. Eng. Sci., 52, (13),* 2111-2127.

Reiss, L.P. (1967) “Cocurrent Gas-Liquid Contacting in Packed Columns” *Ind. Eng. Chem. Process Des. Dev.*, 6, (4), 486 – 499

Sato, Y., Hirose, T., Takahashi, F. and Toda, M. (1973) “Pressure Loss and Liquid Holdup in Packed Bed Reactor with Cocurrent Gas-Liquid Downflow” *J. Chem. Eng. Japan*, *6*, (2), 147 – 152

Satterfield, C. N. (1975) “Trickle-Bed Reactors” *A.I.Ch.E. J., 21, (2),* 209-228.

Sederman, A. J. and Gladden, L. F. (2001) “Magnetic Resonance Imaging as a Quantitative Probe of Gas-Liquid Distribution and Wetting Efficiency in Trickle-Bed Reactors” *Chem. Eng. Sci., 56,* 2615-2628.

Sicardi, S., Baldi, G. and Specchia, V. (1980) “Hydrodynamic Models for the Interpretation of the Liquid Flow in Trickle-Bed Reactors” *Chem. Eng. Sci., 35,* 1775-1782

Specchia, V. and Baldi, G. (1977) “Pressure Drop and Liquid Holdup for Two Phase Concurrent Flow in Packed Beds” *Chem*. *Eng. Sci*., *32*, 515–523.

Stegeman, D., Van Rooijen, F. E., Kamperman, A. A., Weijer, S. and Westerterp, K. R. (1996) “Residence Time Distribution in the Liquid Phase in Cocurrent Gas-Liquid Trickle Bed Reactor” *Ind. Eng. Chem. Res., 35,* 378-385.

Tsochatzidis, N.A., Karabels, A.J., Giakoumakis, D. and Huff, G.A. (2002) “An Investigation of Liquid Maldistribution in Trickle Beds”, *Chem. Eng. Sci.*, 57, 3543 – 3555

Turek, F. and Lange, R. (1981) “Mass Transfer in Trickle-Bed Reactors at Low Reynolds Number” *Chem*. *Eng. Sci*., 36, 569 – 579

Van der Merwe, W. (2004) *The Morphology of Trickle Flow Liquid Holdup* Masters Dissertation, Department of Chemical Engineering, University of Pretoria, Pretoria, South Africa

Wammes, W. J. A., Middelkamp, J., Huisman, W. J., deBaas, C. M. and Westerterp, K.R. (1991) “Hydrodynamics in a Cocurrent Gas-Liquid Trickle Bed at Elevated Pressures” *A.I.Ch.E. J., 37,* 1849 - 1862.

Wang, R., Mao, Z. and Chen, J. (1995) “Experimental and Theoretical Studies of Pressure Drop Hysteresis in Trickle Bed Reactors” *Chem. Eng. Sci., 50, (14),* 2321-2328.

Westerterp, K.R. and Wammes, W.J.A (1992) “Three-phase Trickle-Bed Reactors”, in *Ullmann’s Encyclopedia of Industrial Chemisrty*, *B4: Principles of Chemical Reaction Engineering and Plant Design*, Elvers, B., Hawkins, S. and Shulz, G. (Eds.), VCH Publishers, Weinheim, 309 - 320.

Zimmerman, S. P. and Ng, K. M. (1986) “Liquid Distribution in Trickling Flow Trickle-Bed Reactors” *Chem. Eng. Sci., 41,* 861 - 866.

Appendix 1: Quantifying the Gas-Liquid Mass Transfer Coefficient (Goto and Smith, 1975)

To determine the volumetric gas-liquid mass transfer coefficient in the bed the mass transfer in the end regions need to be taken into account. The different concentrations and mass transfer coefficient, as defined by Goto and Smith (1975) are shown in figure A1.

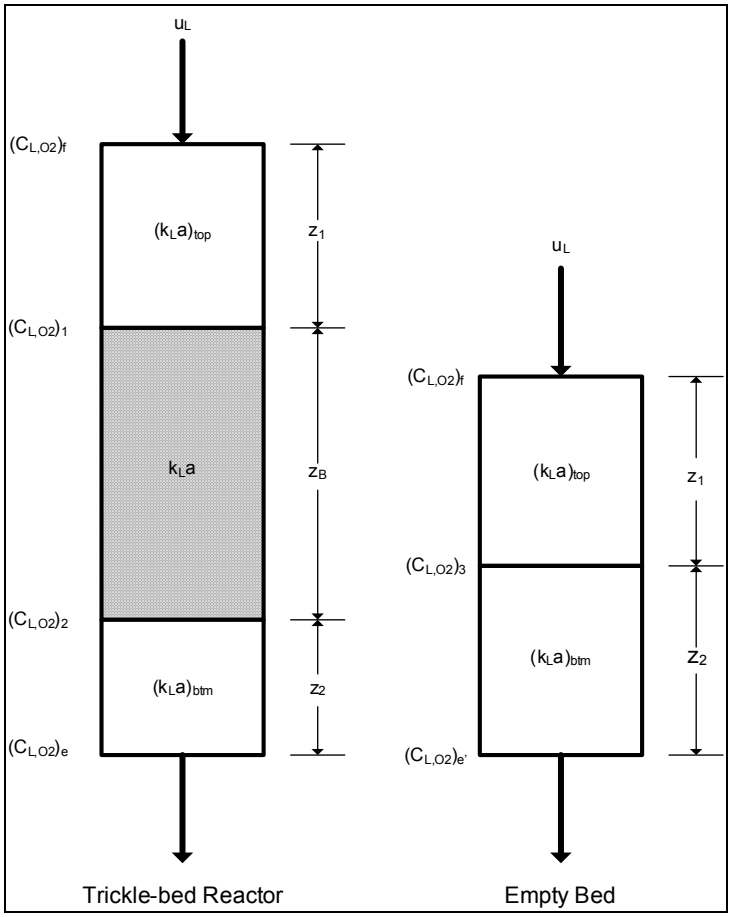

Figure A1: The modelling of end effects as shown by Goto and Smith (1975)

If axial dispersion is neglected, the mass balance for oxygen in the two end regions and the bed itself, for desorption is:

$$U_L dC_{L,O_2} = -(k_L a)_{top}\left(C_{L,O_2} - 0\right)dZ \qquad \text{(A1)}$$

$$U_L dC_{L,O_2} = -(k_L a)\left(C_{L,O_2} - 0\right)dZ \qquad \text{(A2)}$$

$$U_L dC_{L,O_2} = -(k_L a)_{btm}\left(C_{L,O_2} - 0\right)dZ \qquad \text{(A3)}$$

The resulting boundary conditions are:

At Z = 0

$$C_{L,O_2} = \left(C_{L,O_2}\right)_f \tag{A4}$$

At Z = Z_1

$$C_{L,O_2} = \left(C_{L,O_2}\right)_1 \tag{A5}$$

At Z = $Z_1 + Z_B$

$$C_{L,O_2} = \left(C_{L,O_2}\right)_2 \tag{A6}$$

At Z = $Z_1 + Z_B + Z_2$

$$C_{L,O_2} = \left(C_{L,O_2}\right)_e \tag{A7}$$

Solving equations (A1) to (A3) with the relevant boundary conditions leads to:

$$\int_{\left(C_{L,O_q}\right)_f}^{\left(C_{L,O_2}\right)_1} \frac{dC_{L,O_2}}{C_{L,O_2}} = \frac{-\left(k_L a\right)_{top}}{U_L} \int_0^{Z_1} dZ \tag{A8}$$

$$\ln\left(C_{L,O_2}\right)_1 - \ln\left(C_{L,O_2}\right)_f = -\left(k_L a\right)_{top} \frac{Z_1}{U_L} \tag{A9}$$

$$\ln\left[\frac{\left(C_{L,O_2}\right)_1}{\left(C_{L,O_2}\right)_f}\right] = -\left(k_L a\right)_{top} \frac{Z_1}{U_L} \tag{A10}$$

$$\left(C_{L,O_2}\right)_1 = \left(C_{L,O_2}\right)_f e^{-\left(k_L a\right)_{top} \cdot \frac{Z_1}{U_L}} \tag{A11}$$

Similarly,

$$\int_{\left(C_{L,O_q}\right)_1}^{\left(C_{L,O_2}\right)_2} \frac{dC_{L,O_2}}{C_{L,O_2}} = \frac{-\left(k_L a\right)}{U_L} \int_{Z_1}^{Z_1+Z_B} dZ \tag{A12}$$

leads to

$$\left(C_{L,O_2}\right)_2 = \left(C_{L,O_2}\right)_1 e^{-\left(k_L a\right) \cdot \frac{Z_B}{U_L}} \tag{A13}$$

and

$$\int_{\left(C_{L,O_q}\right)_2}^{\left(C_{L,O_2}\right)_e} \frac{dC_{L,O_2}}{C_{L,O_2}} = \frac{-\left(k_L a\right)_{btm}}{U_L} \int_{Z_1+Z_B}^{Z_1+Z_B+Z_2} dZ \tag{A14}$$

leads to

$$\left(C_{L,O_2}\right)_e = \left(C_{L,O_2}\right)_2 e^{-(k_L a)_{btm}.\frac{Z_2}{U_L}} \tag{A15}$$

Substituting equation (A13) into equation (A15) leads to:

$$\left(C_{L,O_2}\right)_e = \left(C_{L,O_2}\right)_1 e^{-\left[k_L a\frac{Z_B}{U_L}+(k_L a)_{btm}\frac{Z_2}{U_L}\right]} \tag{A16}$$

Substituting equation (A11) into equation (A16) leads to:

$$\left(C_{L,O_2}\right)_e = \left(C_{L,O_2}\right)_f e^{-\left[k_L a\frac{Z_B}{U_L}+(k_L a)_{btm}\frac{Z_2}{U_L}+(k_L a)_{top}\frac{Z_1}{U_L}\right]} \tag{A17}$$

$(k_La)_{btm}$ and $(k_La)_{top}$ can be solved by performing the experiments in an empty bed.

$$\int_{\left(C_{L,Oq}\right)_{f'}}^{\left(C_{L,O_2}\right)_3}\frac{dC_{L,O_2}}{C_{L,O_2}} = \frac{-(k_L a)_{top}}{U_L}\int_0^{Z_1} dZ \tag{A18}$$

$$\left(C_{L,O_2}\right)_3 = \left(C_{L,O_2}\right)_{f'} e^{-(k_L a)_{top}.\frac{Z_1}{U_L}} \tag{A19}$$

$$\int_{\left(C_{L,Oq}\right)_3}^{\left(C_{L,O_2}\right)_{e'}}\frac{dC_{L,O_2}}{C_{L,O_2}} = \frac{-(k_L a)_{btm}}{U_L}\int_{Z_1}^{Z_1+Z_2} dZ \tag{A20}$$

$$\left(C_{L,O_2}\right)_{e'} = \left(C_{L,O_2}\right)_3 e^{-(k_L a)_{btm}.\frac{Z_2}{U_L}} \tag{A21}$$

Substituting equation (A19) into equation (A21) leads to:

$$\left(C_{L,O_2}\right)_{e'} = \left(C_{L,O_2}\right)_{f'} e^{-\left[(k_L a)_{btm}\frac{Z_2}{U_L}+(k_L a)_{top}\frac{Z_1}{U_L}\right]} \tag{A22}$$

From equations (A17) and (A22):

$$\frac{(k_L a)_{btm}.Z_2}{U_L} = -\ln\left[\frac{\left(C_{L,O_2}\right)_e}{\left(C_{L,O_2}\right)_f}\right] - (k_L a)\frac{Z_B}{U_L} - (k_L a)_{top}\frac{Z_1}{U_L} \tag{A23}$$

$$\frac{(k_L a)_{btm}.Z_2}{U_L} = -\ln\left[\frac{\left(C_{L,O_2}\right)_{e'}}{\left(C_{L,O_2}\right)_{f'}}\right] - (k_L a)_{top}\frac{Z_1}{U_L} \tag{A24}$$

Substituting equation (A23) into (A24) leads to:

$$\ln\left[\frac{\left(C_{L,O_2}\right)_e}{\left(C_{L,O_2}\right)_f}\right] + (k_L a)\frac{Z_B}{U_L} + (k_L a)_{top}\frac{Z_1}{U_L} = \ln\left[\frac{\left(C_{L,O_2}\right)_{e'}}{\left(C_{L,O_2}\right)_{f'}}\right] + (k_L a)_{top}\frac{Z_1}{U_L} \tag{A25}$$

$$\ln\left(C_{L,O_2}\right)_{e'} - \ln\left(C_{L,O_2}\right)_{f'} + \ln\left(C_{L,O_2}\right)_{f} - \ln\left(C_{L,O_2}\right)_{e} = k_L a \frac{Z_B}{U_L} \quad \text{(A26)}$$

$$k_L a = \frac{U_L}{Z_B} \ln\left[\frac{\left(C_{L,O_2}\right)_{e'}\left(C_{L,O_2}\right)_{f}}{\left(C_{L,O_2}\right)_{e}\left(C_{L,O_2}\right)_{f'}}\right] \quad \text{(A27)}$$

Appendix 2: The Effect of Prewetting on the Pressure Drop

The effect of prewetting on the pressure drop at intermediate gas flow rates can be seen in figures A-2 and A-3.

From these figures it can be seen that the different prewetting modes result in two distinct regions and that the pressure drop increases with increasing liquid flow rate regardless of the prewetting procedure followed.

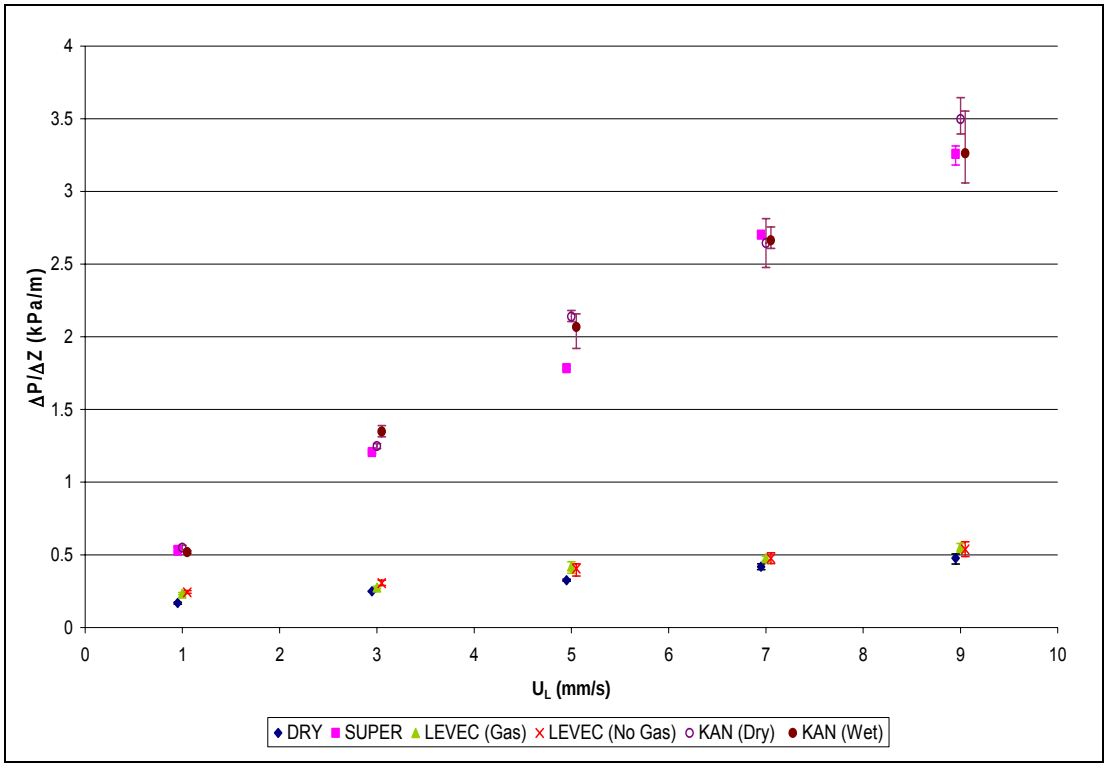

Figure A-2: The effect of prewetting on the pressure drop at U_G = 40mm/s

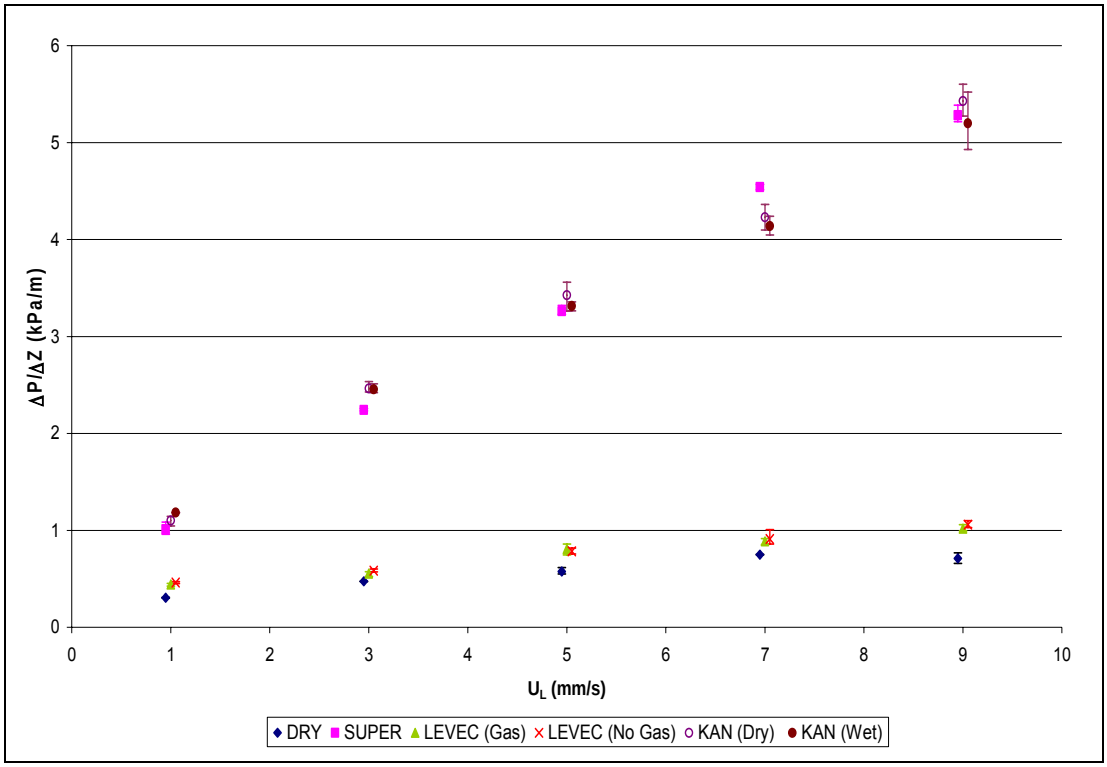

Figure A-3: The effect of prewetting on the pressure drop at U_G = 70mm/s

Appendix 3: The Effect of Prewetting on the Liquid Holdup

The effect of prewetting on the liquid holdup at intermediate gas flow rates can be seen in figures A-4 and A-5.

From the figures it can be seen that the different prewetting procedures result in four distinct regions and regardless of the prewetting procedure the liquid holdup is a function of the liquid flow rate and increases as the liquid flow rate increases.

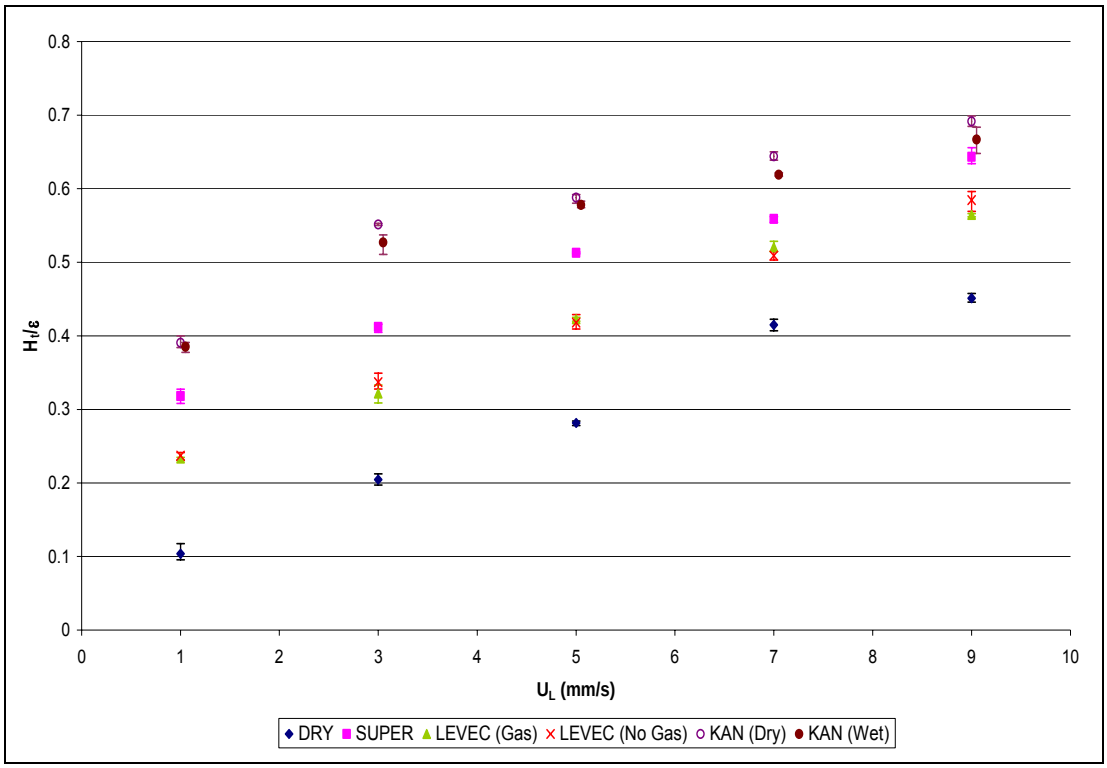

Figure A-4: The effect of prewetting on the total liquid holdup at U_G = 40mm/s

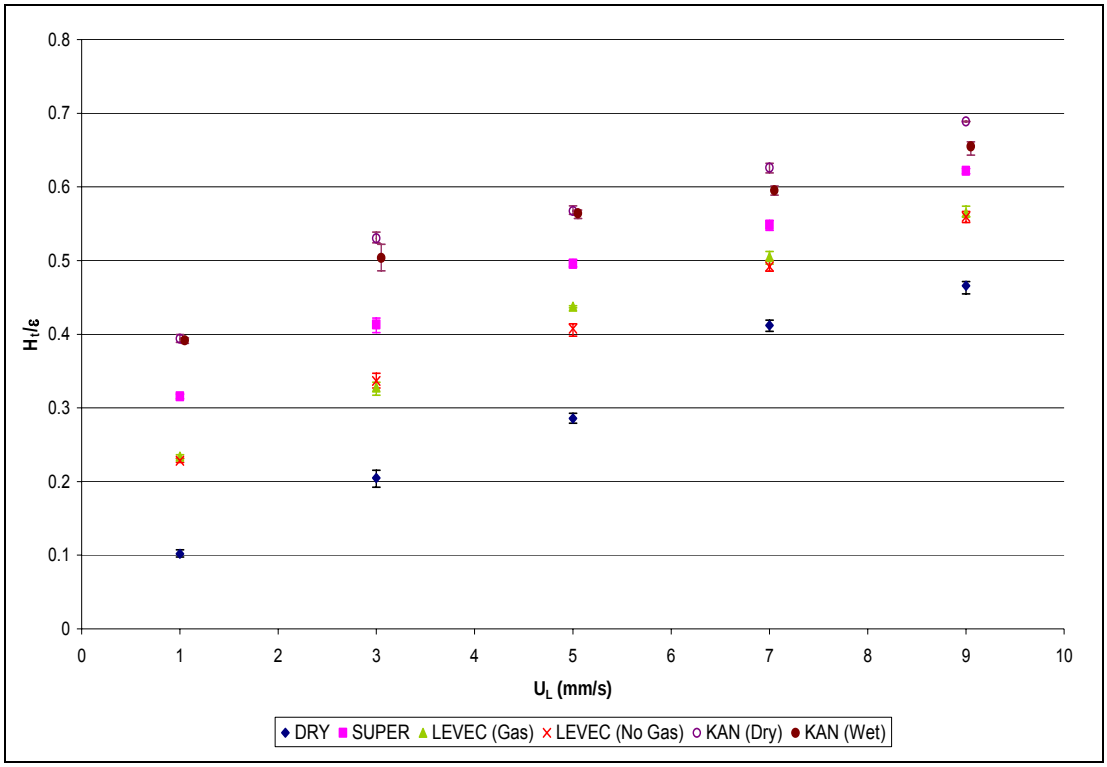

Figure A-5: The effect of prewetting on the total liquid holdup at U_G = 70mm/s

Appendix 4: The Effect of Gas Flow Rate on the Liquid Holdup

The effect of gas flow rate on the liquid holdup at intermediate liquid flow rates can be seen in figures A-6 to A-8.

From these figures it is clear that as the gas flow rate is increased, the liquid holdup decreases for the Kan, Super and Levec-prewetted beds. However, the dry bed does not appear to be affected by the gas flow rate at all.

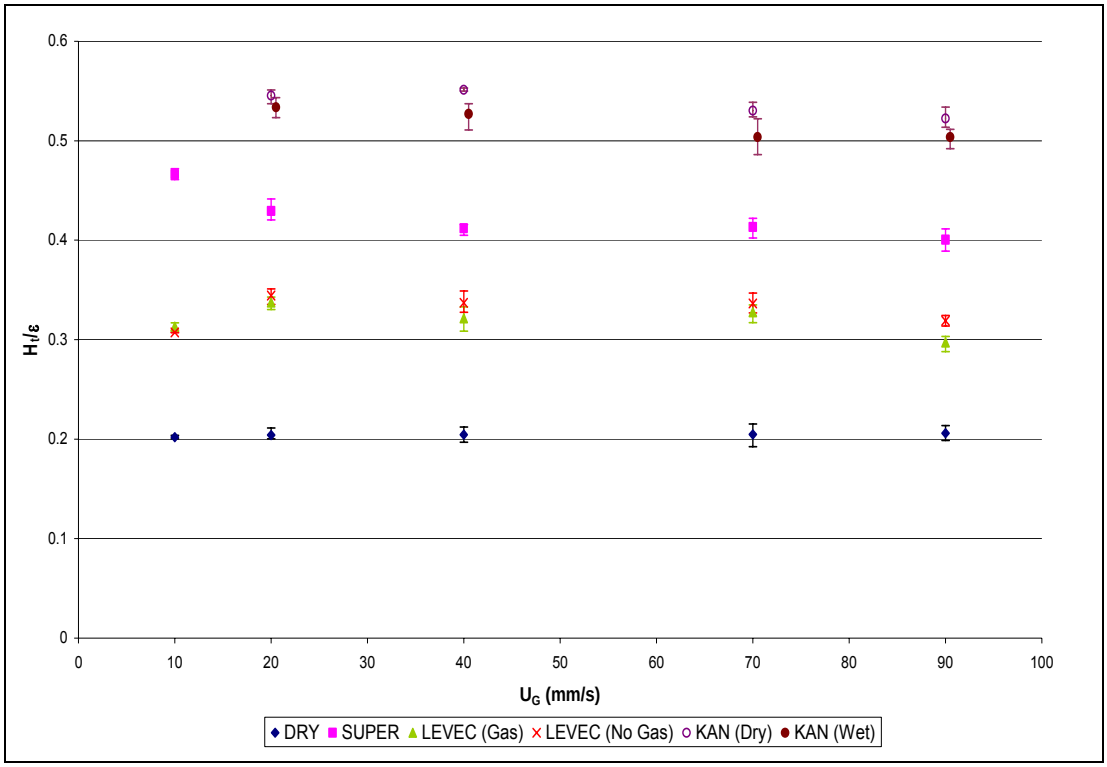

Figure A-6: The effect of the gas flow rate on the total liquid holdup for the different prewetting modes at U_L = 3mm/s

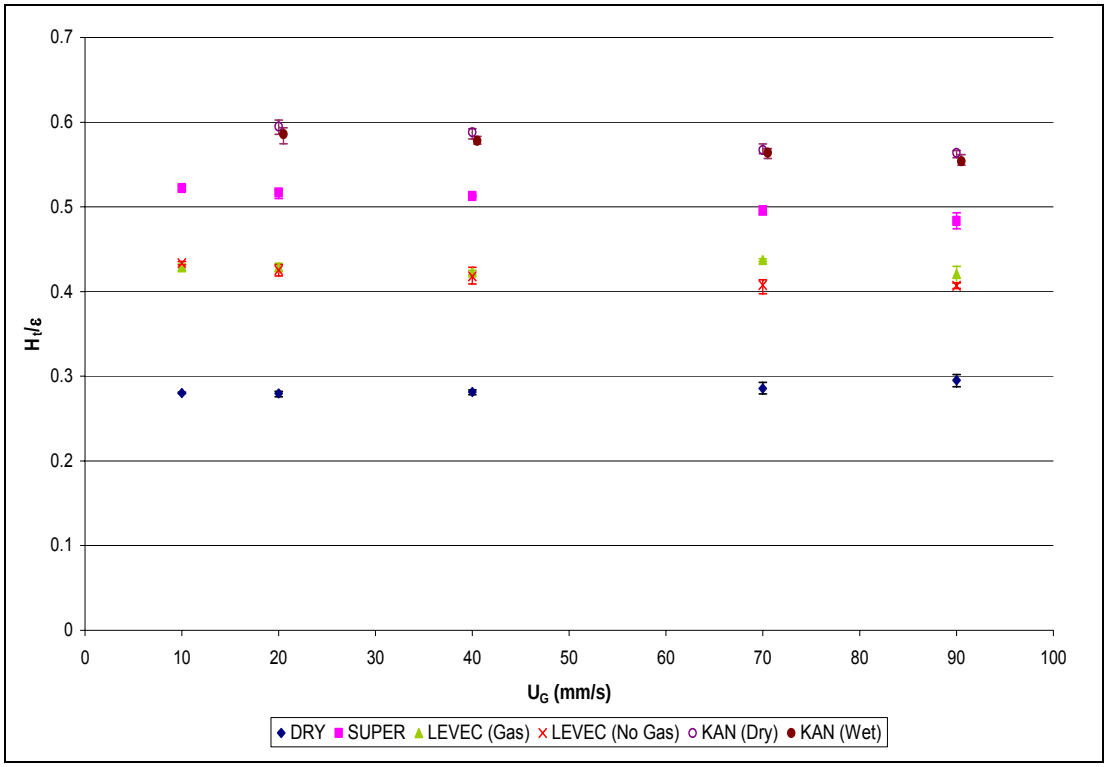

Figure A-7: The effect of the gas flow rate on the total liquid holdup for the different prewetting modes at U_L = 5mm/s

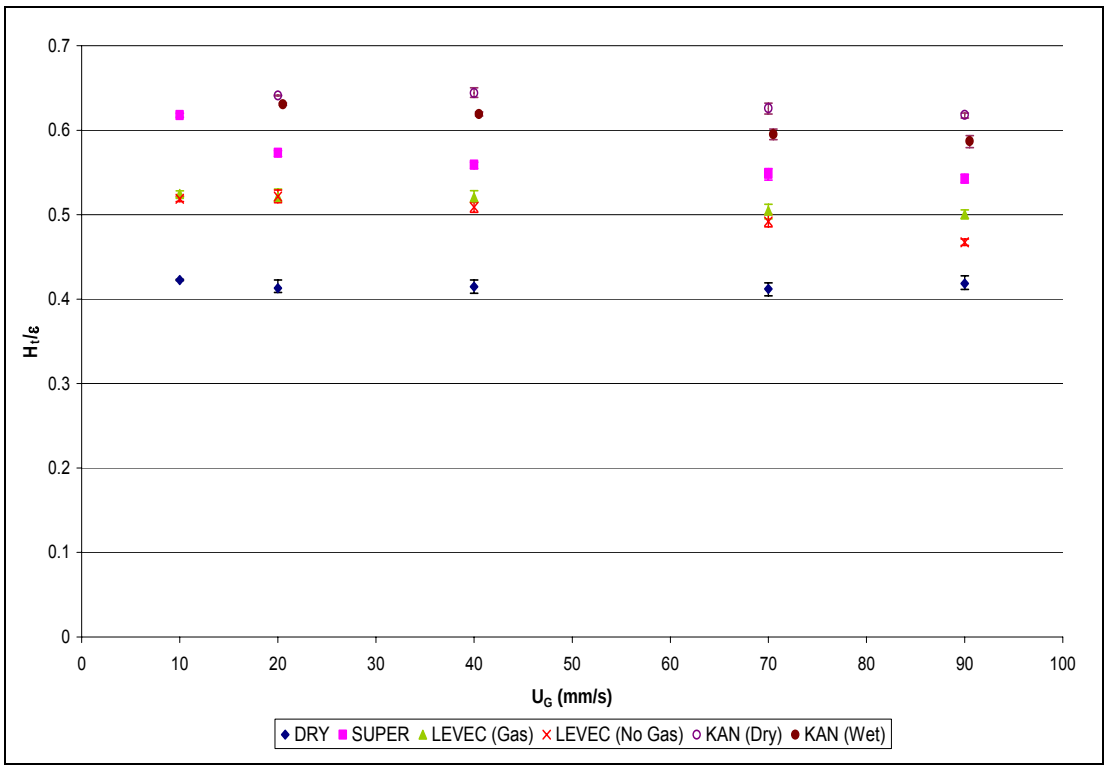

Figure A-8: The effect of the gas flow rate on the total liquid holdup for the different prewetting modes at U_L = 7mm/s

Appendix 5: The Effect of Prewetting on the Volumetric Gas-Liquid Mass Transfer

The effect of prewetting on the volumetric gas-liquid mass transfer coefficient at intermediate gas flow rates can be seen in figures A-9 and A-10.

From these figures it is clear that the different prewetting procedures result in three distinct regions and regardless of the prewetting procedure followed the mass transfer coefficient increases with liquid flow rate.

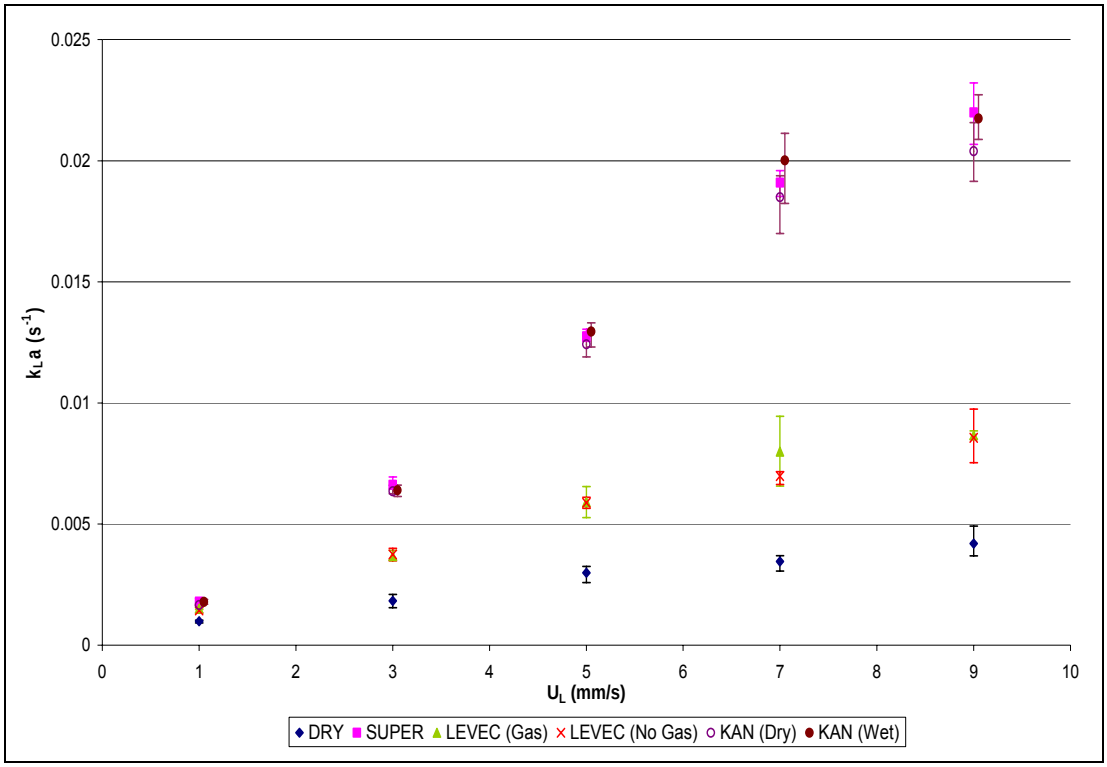

Figure A-9: The effect of prewetting on the volumetric gas-liquid mass transfer coefficient at U_G = 40mm/s

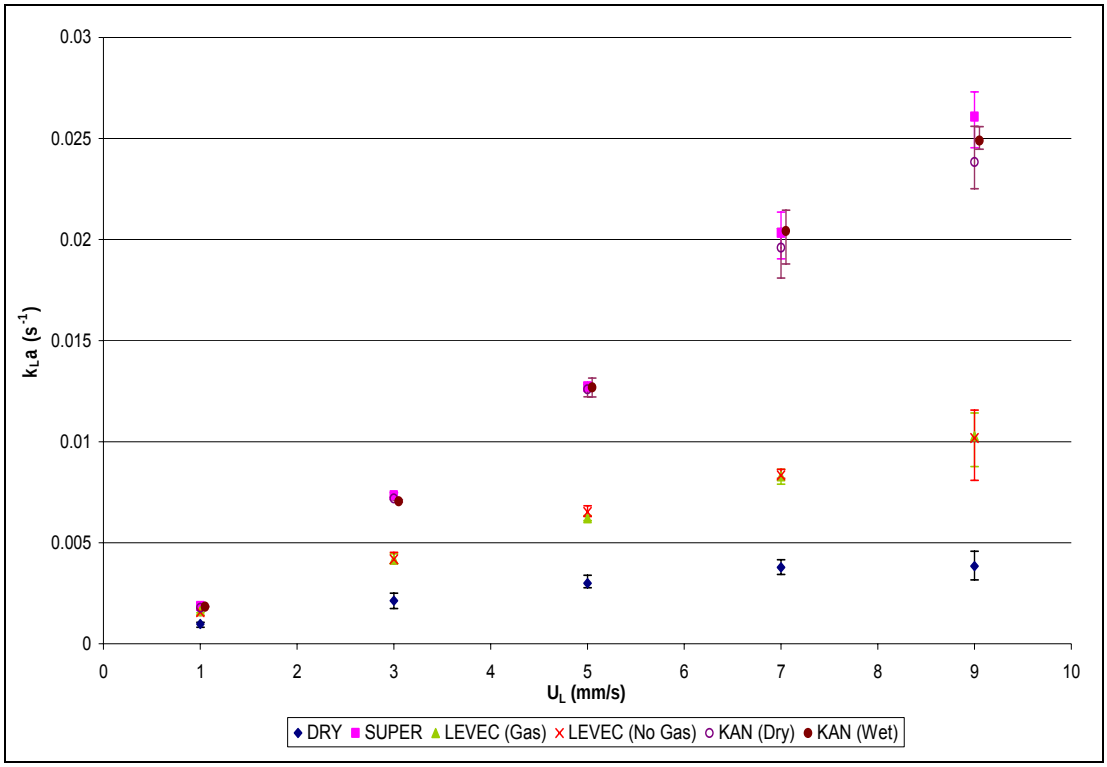

Figure A-10: The effect of prewetting on the volumetric gas-liquid mass transfer coefficient at U_G = 70mm/s

Appendix 6: The Effect of Gas Flow Rate on the Volumetric Gas-Liquid Mass Transfer Coefficient

The effect of gas flow rate on the volumetric gas-liquid mass transfer coefficient at intermediate liquid flow rates can be seen in figures A-11 to A-13.

In these figures it can be seen that, regardless of the prewetting procedure followed, the volumetric gas-liquid mass transfer coefficient increases with an increase in the gas flow rate

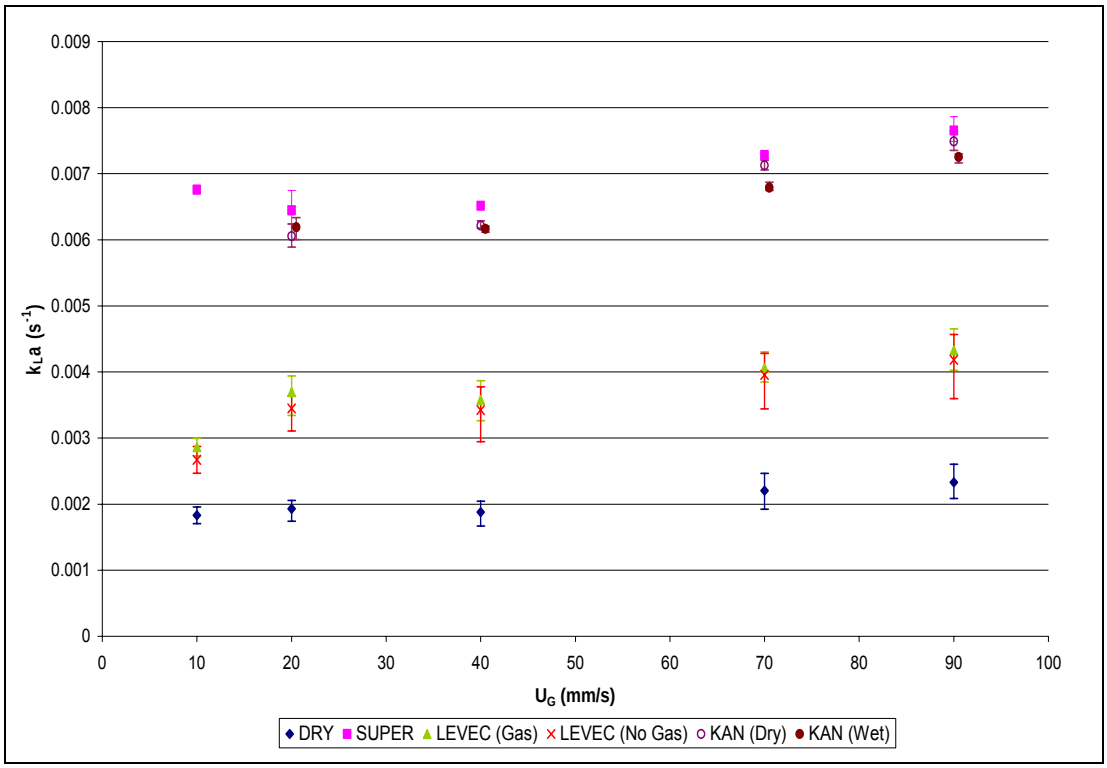

Figure A-11: The effect of the gas flow rate on the gas-liquid mass transfer coefficient for the different prewetting modes at U_L = 3mm/s

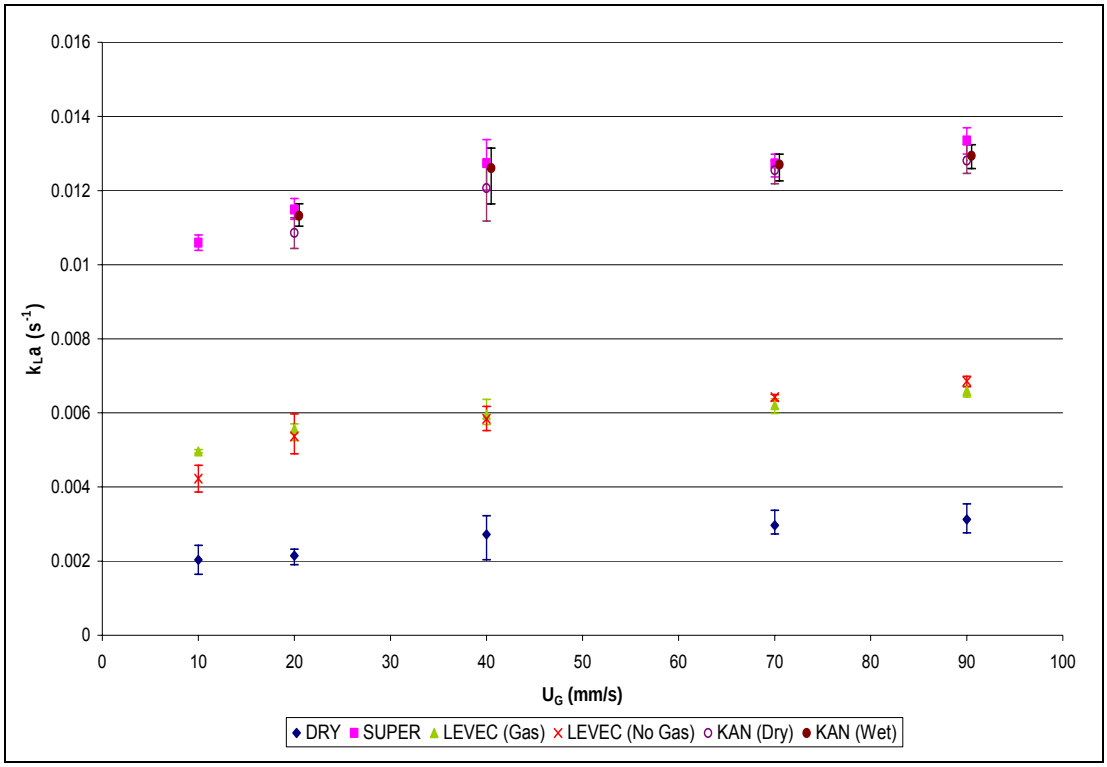

Figure A-12: The effect of the gas flow rate on the gas-liquid mass transfer coefficient for the different prewetting modes at U_L = 5mm/s

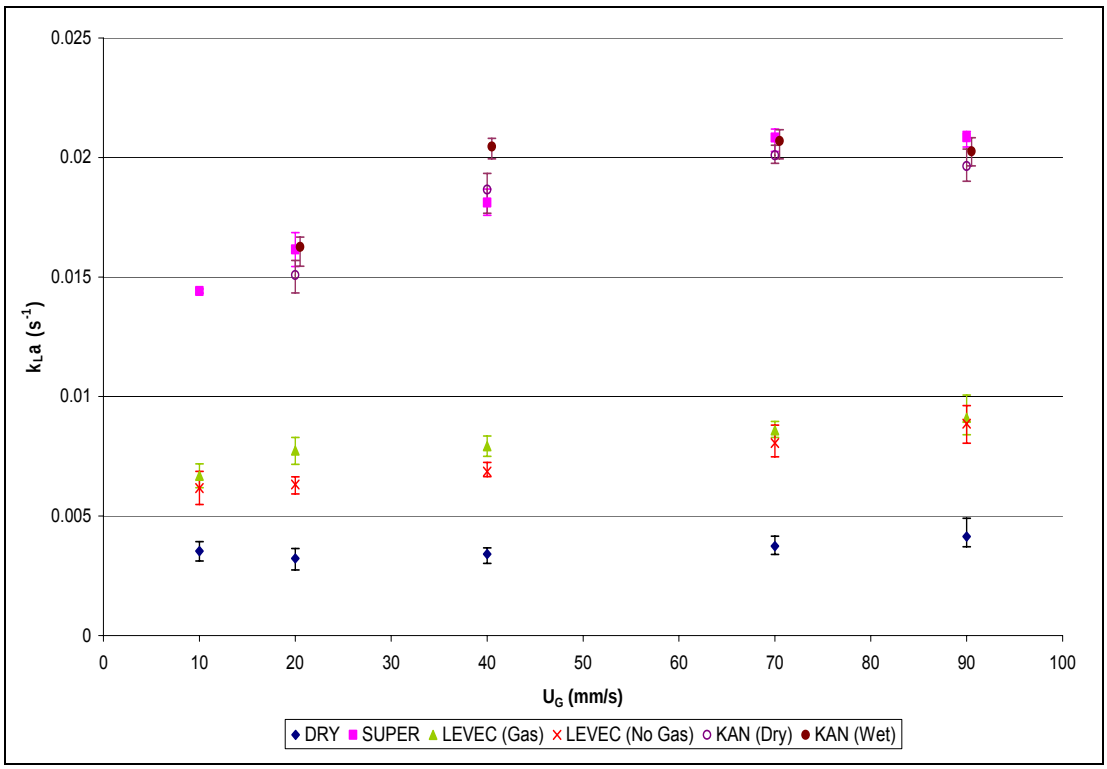

Figure A-13: The effect of the gas flow rate on the gas-liquid mass transfer coefficient for the different prewetting modes at U_L = 7mm/s

Appendix 7: Operating Between the Modes

Appendix 7.1: Pressure Drop

The results of the decreased draining time for the Levec wetted bed on the pressure drop for the intermediate gas flow rates are shown in figures A-14 and A-15.

From the figure it is clear that the decreased draining time for the Levec-wetted bed did not result in a pressure drop that was significantly higher than the ordinary Levec-wetted bed.

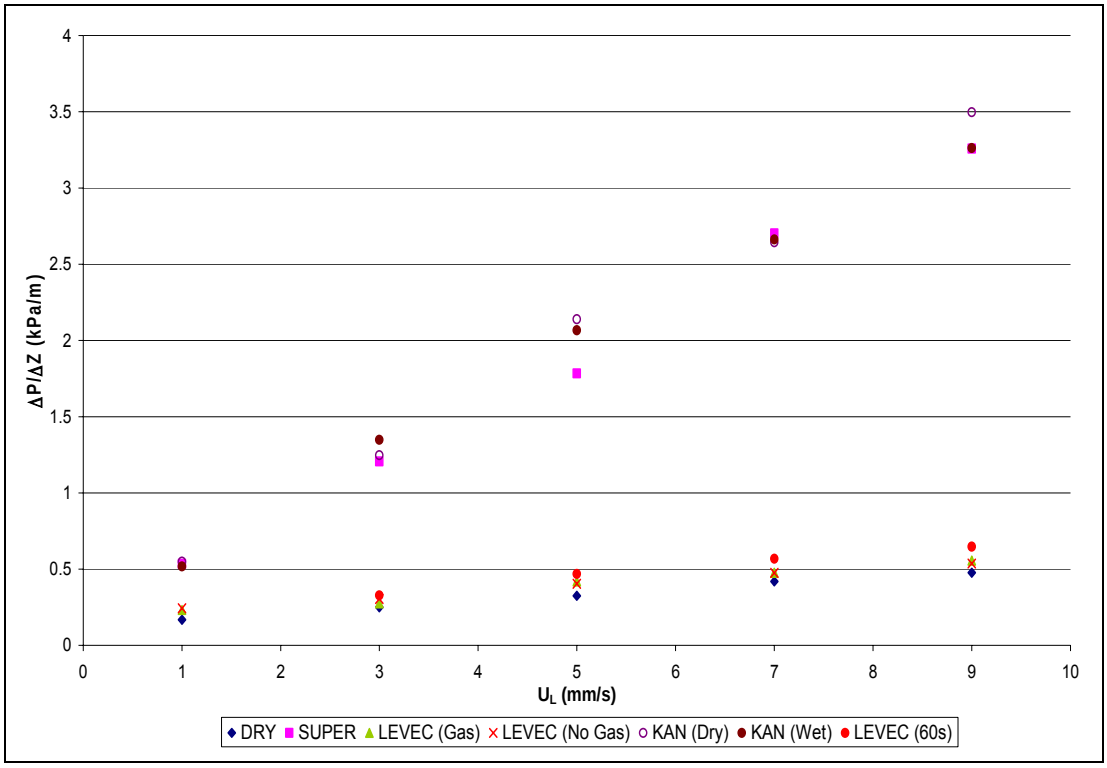

Figure A-14: The effects of the decreased draining time for a Levec-wetted bed on the pressure drop at U_G = 40mm/s

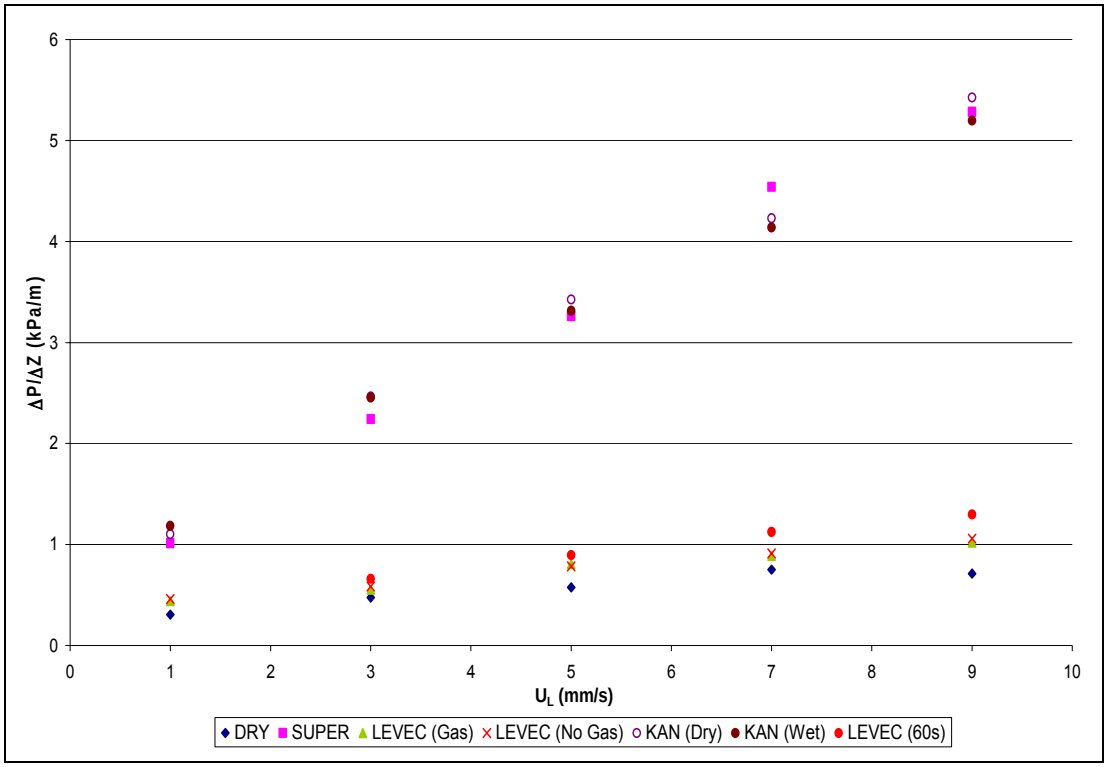

Figure A-15: The effects of the decreased draining time for a Levec-wetted bed on the pressure drop at U_G = 70mm/s

Appendix 7.2: Liquid Holdup

The results of the decreased draining time for the Levec wetted bed on the liquid holdup for the intermediate gas flow rates are shown in figures A-16 and A-17.

From the figures it can be seen that the decreased draining time for the Levec-wetted bed resulted in a liquid holdup that was between the holdup of the Super-wetted and the ordinary Levec-wetted bed at all of the liquid flow rates.

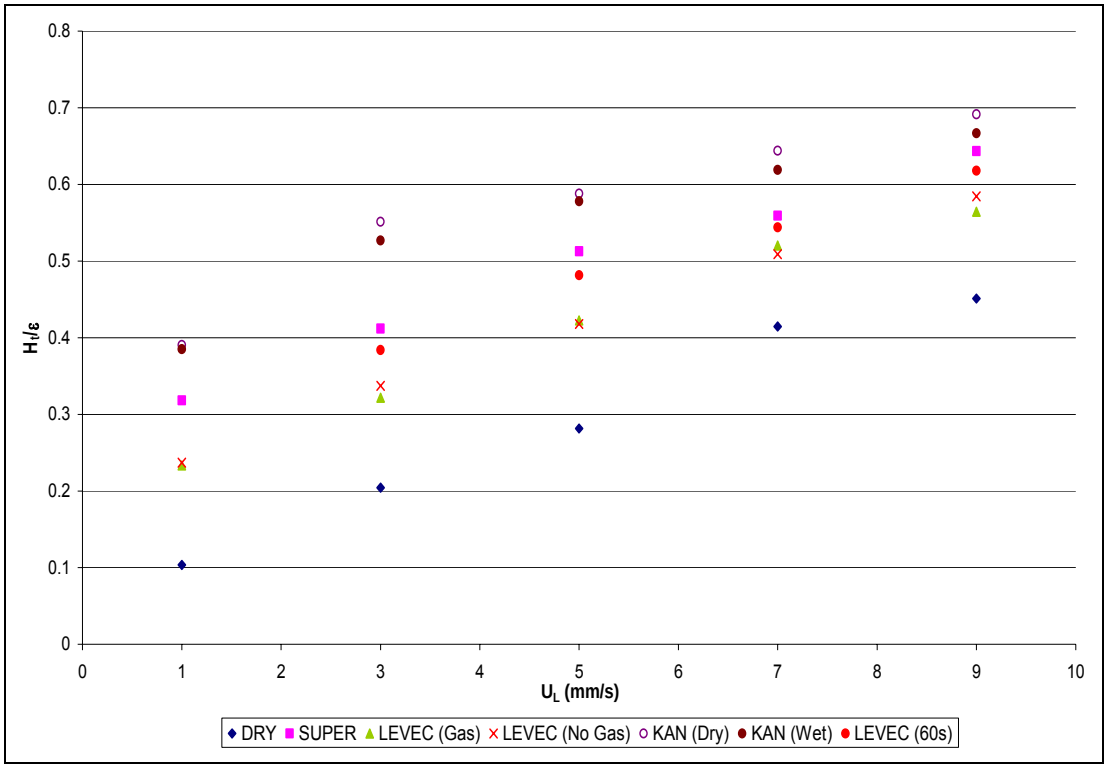

Figure A-16: The effects of the decreased draining time for a Levec-wetted bed on the total liquid holdup at U_G = 40mm/s

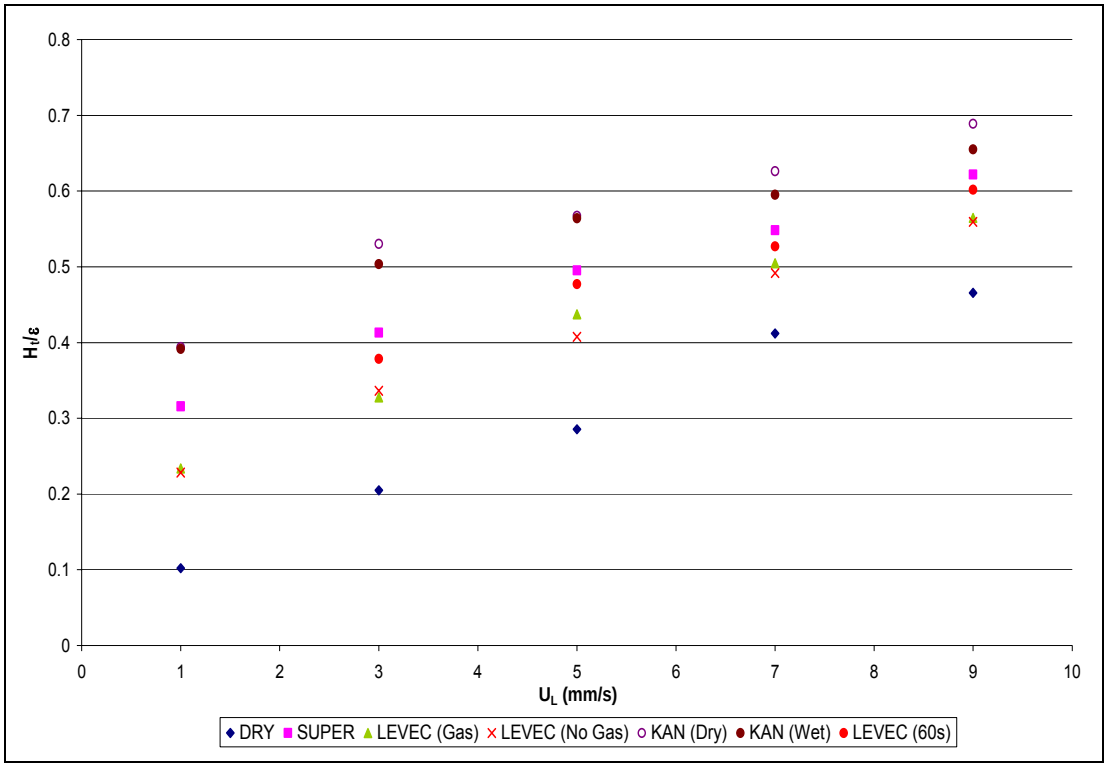

Figure A-17: The effects of the decreased draining time for a Levec-wetted bed on the total liquid holdup at U_G = 70mm/s

Appendix 7.3: Gas-Liquid Mass Transfer

The results of the decreased draining time for the Levec wetted bed on the volumetric gas-liquid mass transfer coefficient for the intermediate gas flow rates are shown in figures A-16 and A-17.

From the figures it can be seen that the decreased draining time for the Levec-wetted bed resulted in a mass transfer coefficient that was between the mass transfer coefficient of the Super-wetted and the ordinary Levec-wetted bed at all of the liquid flow rates.

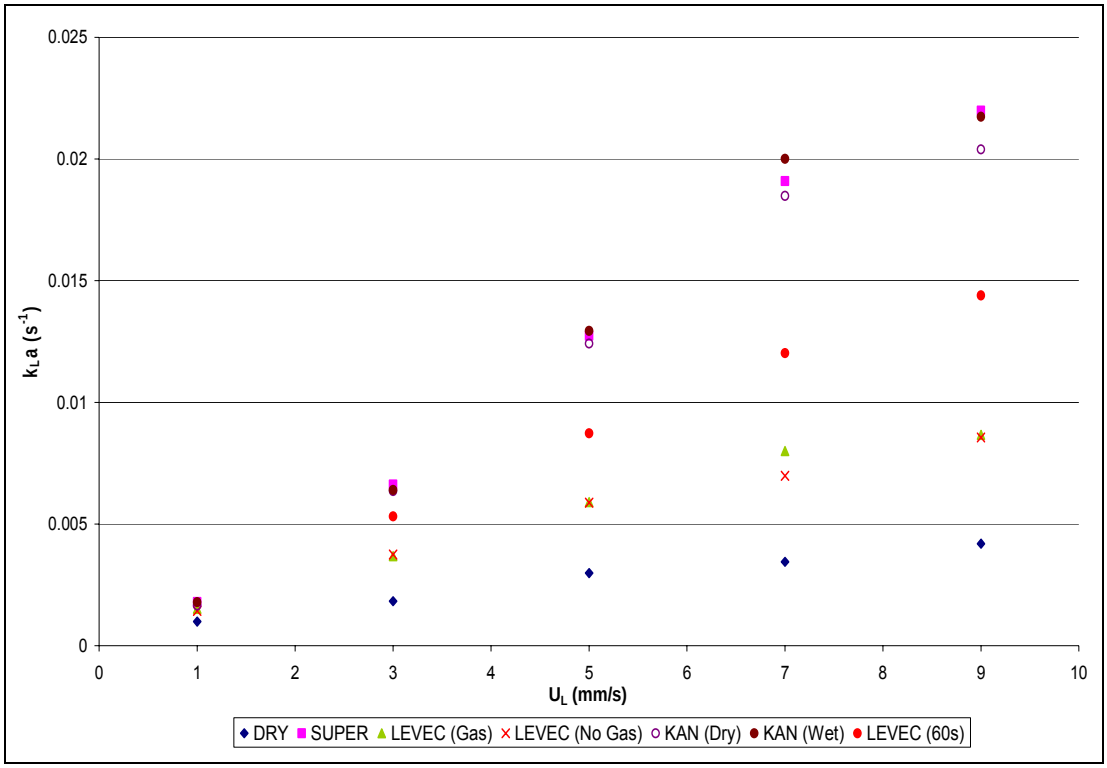

Figure A-18: The effects of the decreased draining time for a Levec-wetted bed on the gas-liquid mass transfer coefficient at U_G = 40mm/s

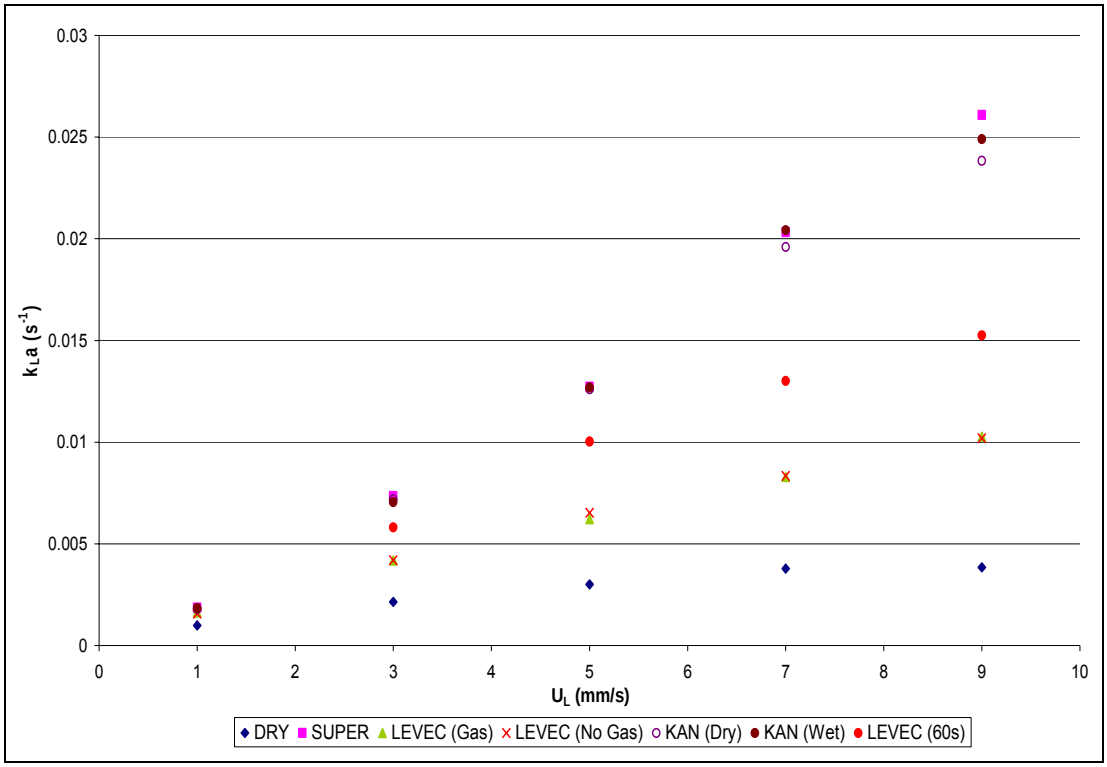

Figure A-19: The effects of the decreased draining time for a Levec-wetted bed on the gas-liquid mass transfer coefficient at U_G = 70mm/s

Appendix 8: Single Pressure Drop Correlations

The results of the single pressure drop correlations for the intermediate gas flow rates are shown in figures A-20 and A-21.

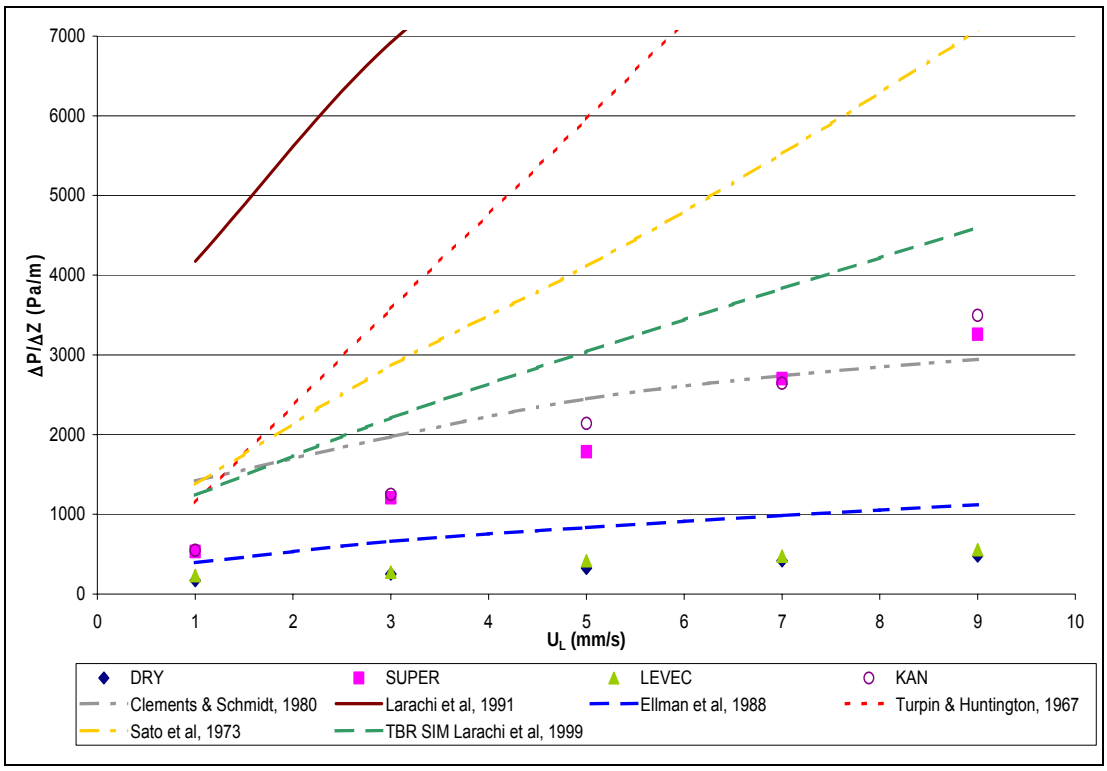

Figure A-20: The performance of the pressure drop correlations at U_G = 40mm/s

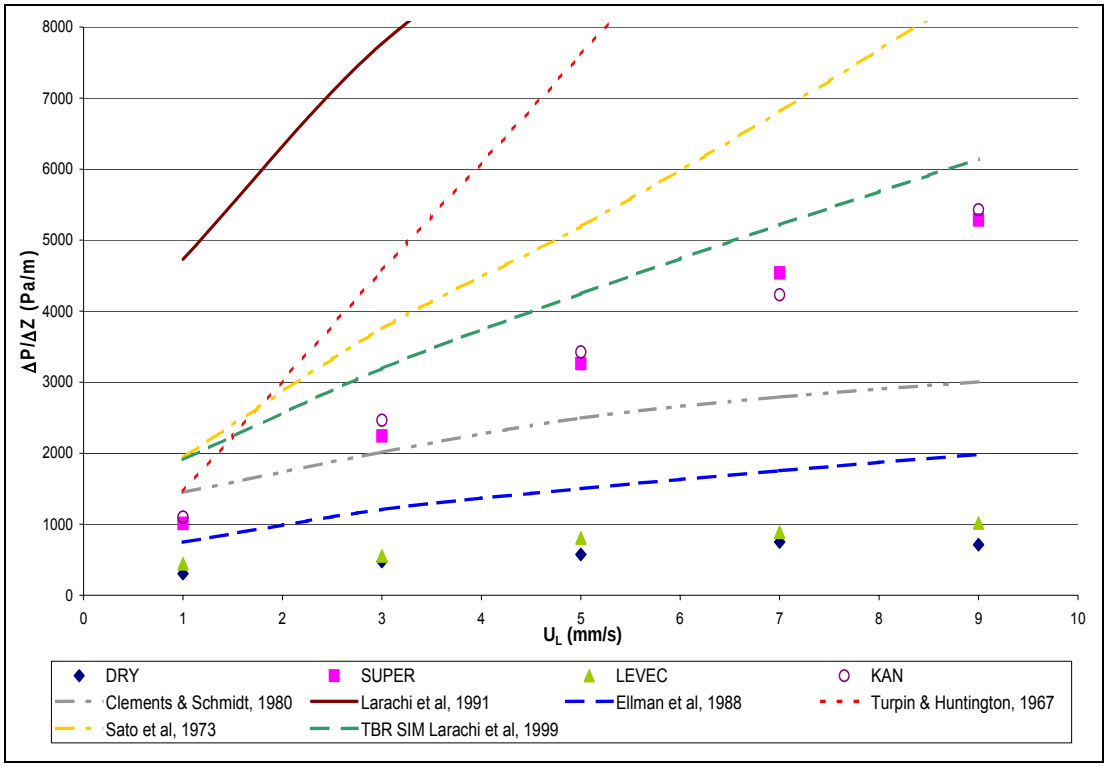

Figure A-21: The performance of the pressure drop correlations at U_G = 70mm/s

Appendix 9: Pressure Drop Correlation Holub *et al* (1992)

The results of the pressure drop predictions from the correlation proposed by Holub *et al* (1992) at the intermediate gas flow rates are shown in figures A-22 and A-23.

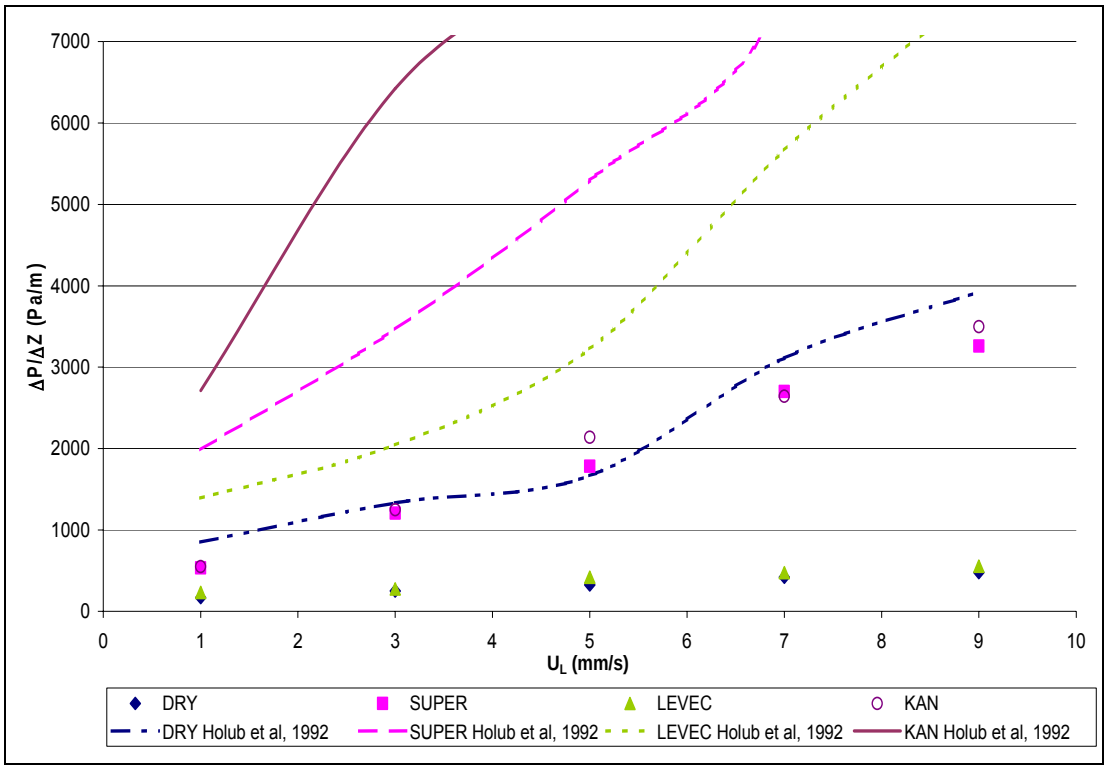

Figure A-22: The performance of the Holub et al (1992) pressure drop correlations at U_G = 40mm/s

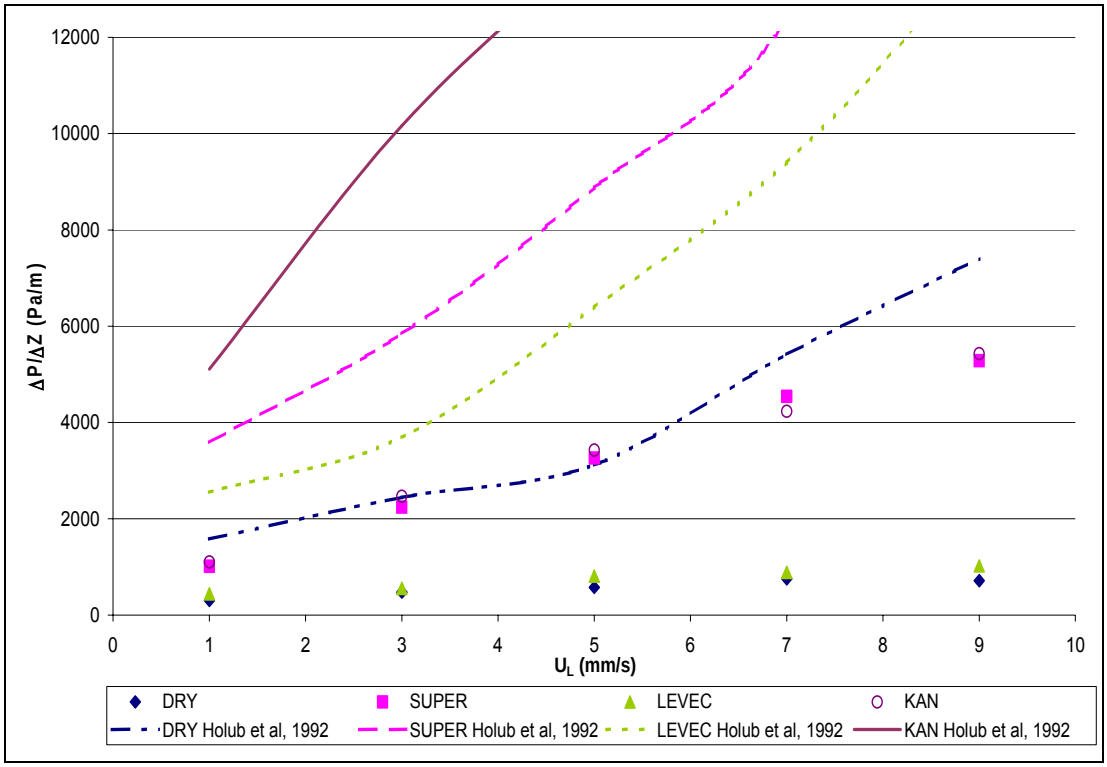

Figure A-23: The performance of the Holub et al (1992) pressure drop correlations at U_G = 70mm/s

Appendix 10: Pressure Drop Correlation Westerterp and Wammes (1992)

The results of the pressure drop predictions from the correlation proposed by Westerterp and Wammes (1992) for the lower gas flow rates are shown in figures A-24 to A-26.

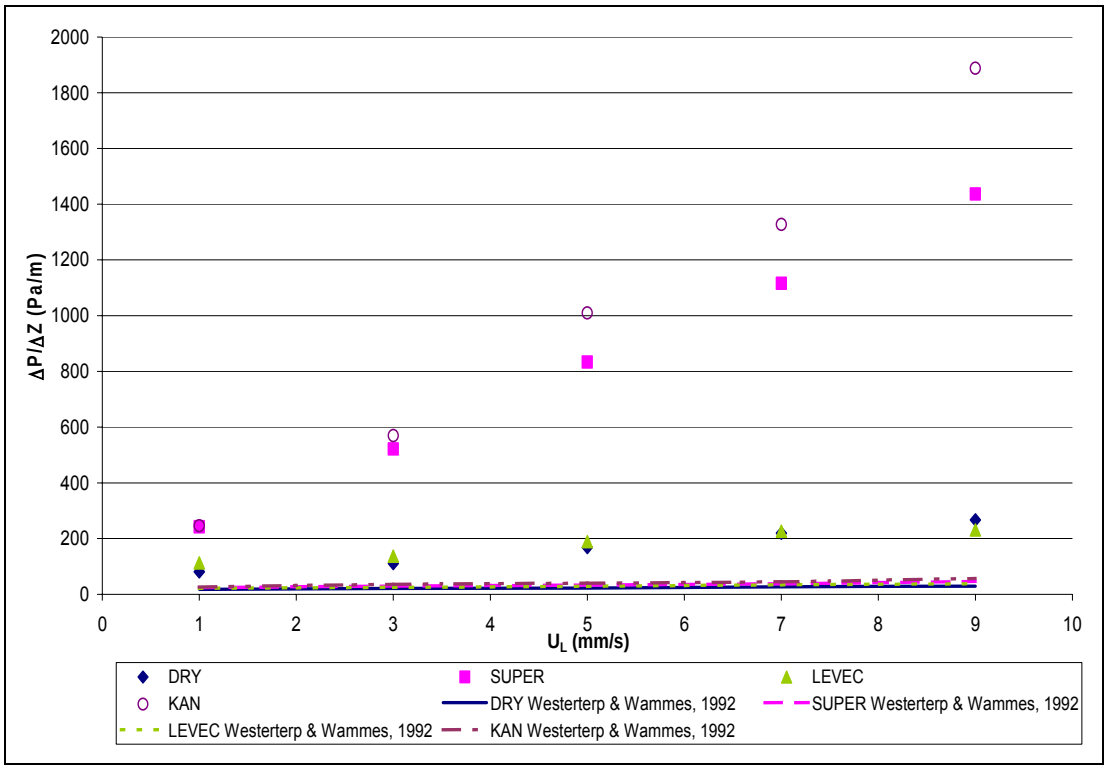

Figure A-24: The performance of the pressure drop correlation proposed by Westerterp and Wammes (1992) at U_G = 20mm/s

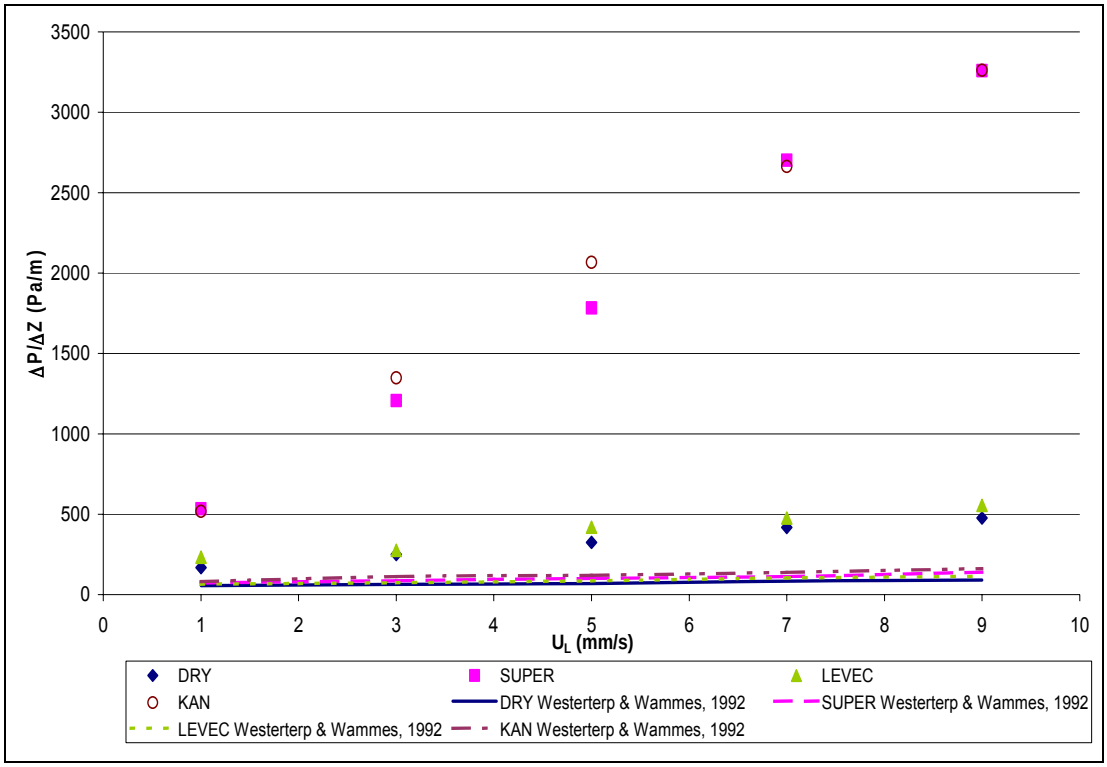

Figure A-25: The performance of the pressure drop correlation proposed by Westerterp and Wammes (1992) at U_G = 40mm/s

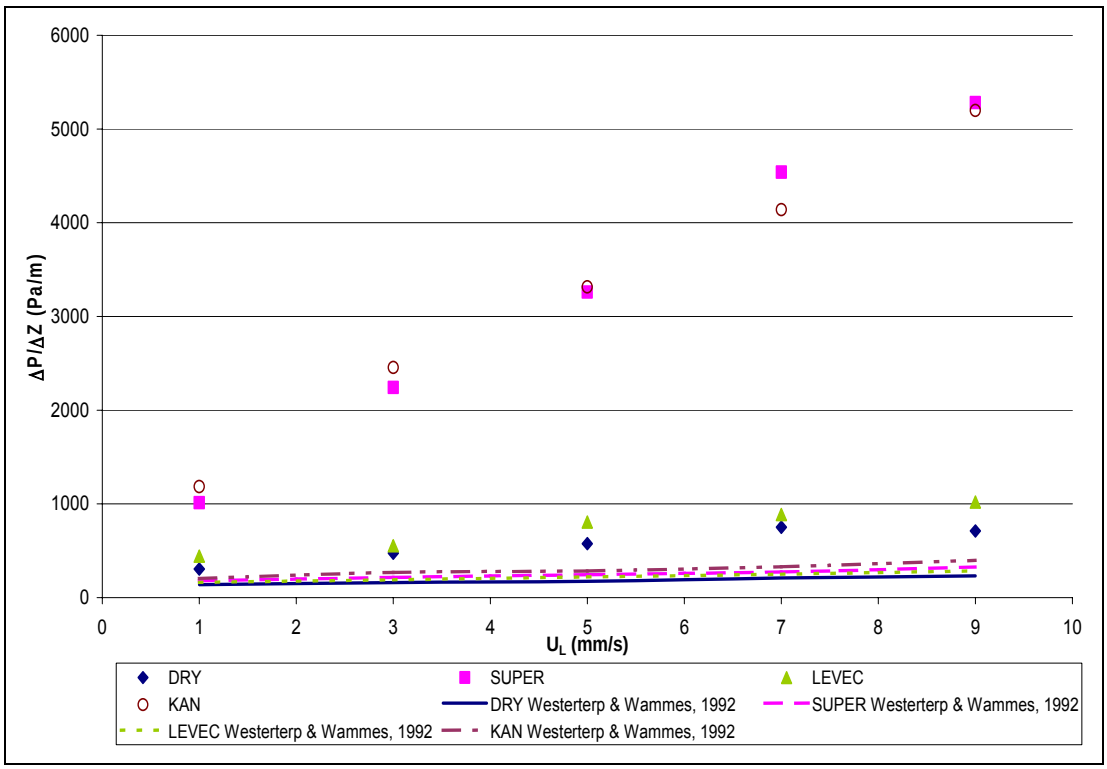

Figure A-26: The performance of the pressure drop correlation proposed by Westerterp and Wammes (1992) at U_G = 70mm/s

Appendix 11: Single Liquid Holdup Correlations

The results of the single liquid holdup correlations for the intermediate gas flow rates are shown in figures A-27 and A-28.

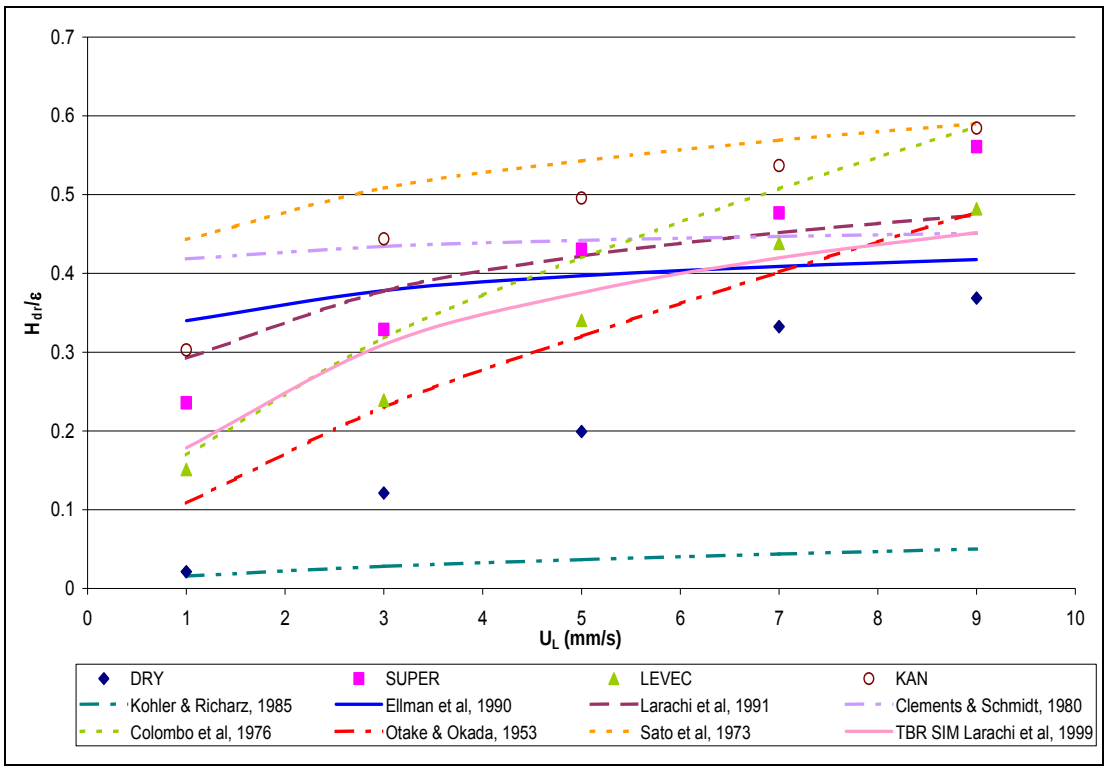

Figure A-27: The performance of the liquid holdup correlations at U_G = 40mm/s

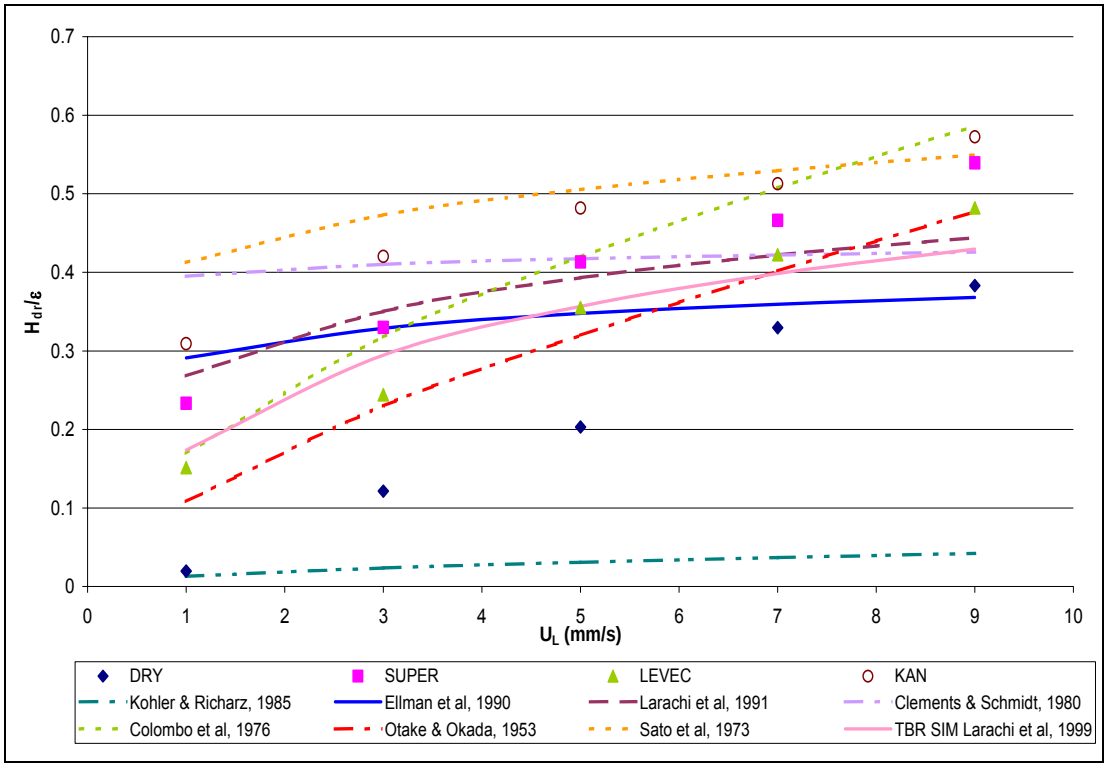

Figure A-28: The performance of the liquid holdup correlations at U_G = 70mm/s

Appendix 12: Liquid Holdup Correlation Holub *et al* (1992)

The results of the liquid holdup predictions from the correlation proposed by Holub *et al* (1992) at the intermediate gas flow rates are shown in figures A-29 and A-30.

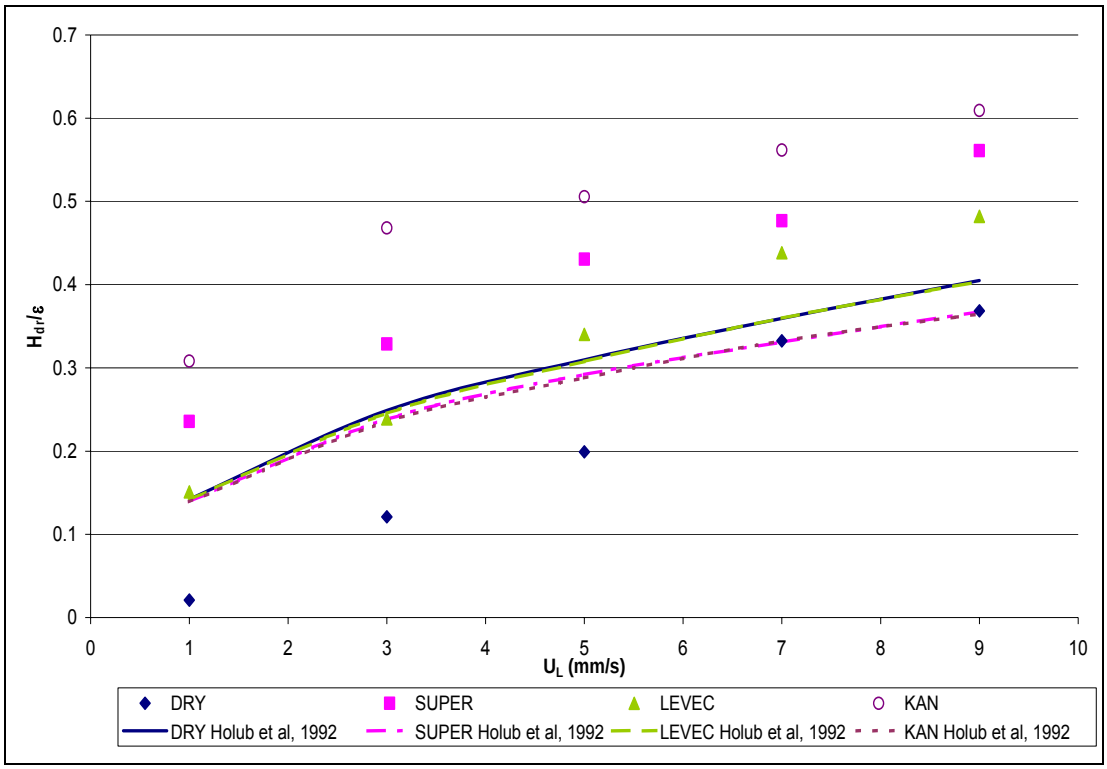

Figure A-29: The performance of the liquid holdup correlation proposed by Holub et al (1992) at U_G = 40mm/s

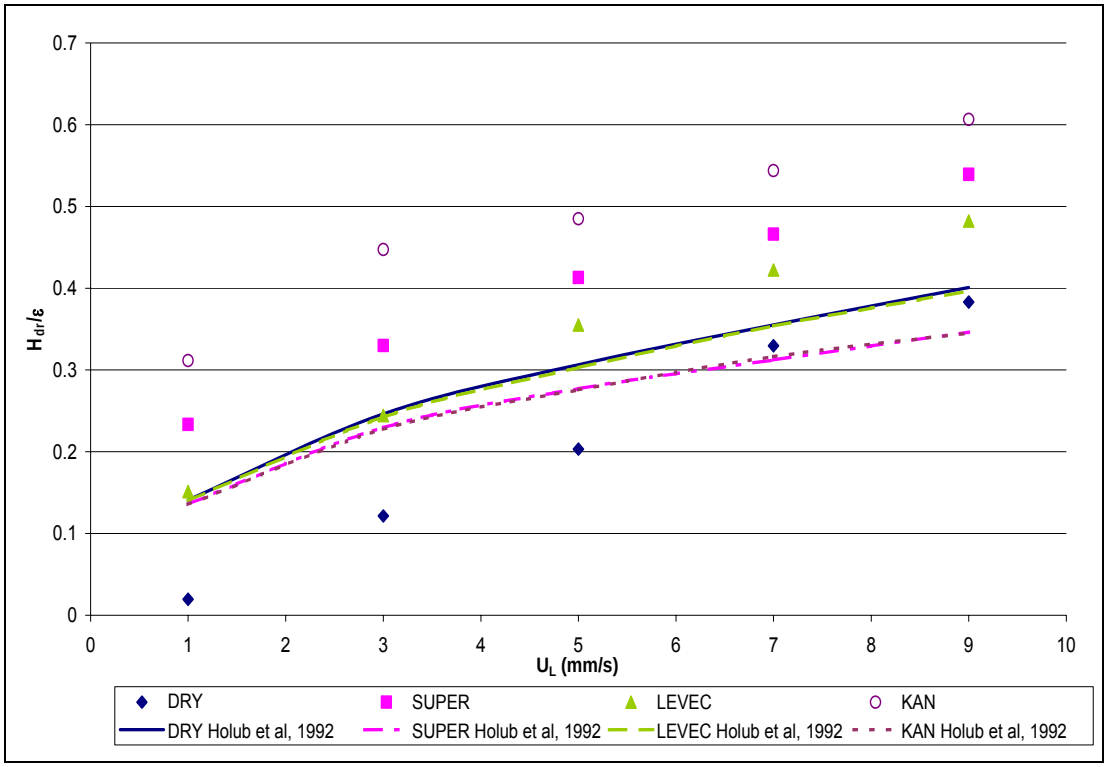

Figure A-30: The performance of the liquid holdup correlation proposed by Holub et al (1992) at U_G = 70mm/s

Appendix 13: Liquid Holdup Correlation Stegeman *et al* (1996)

The results of the liquid holdup predictions from the correlation proposed by Stegeman *et al* (1996) at the higher gas flow rates are shown in figures A-31 to A-33.

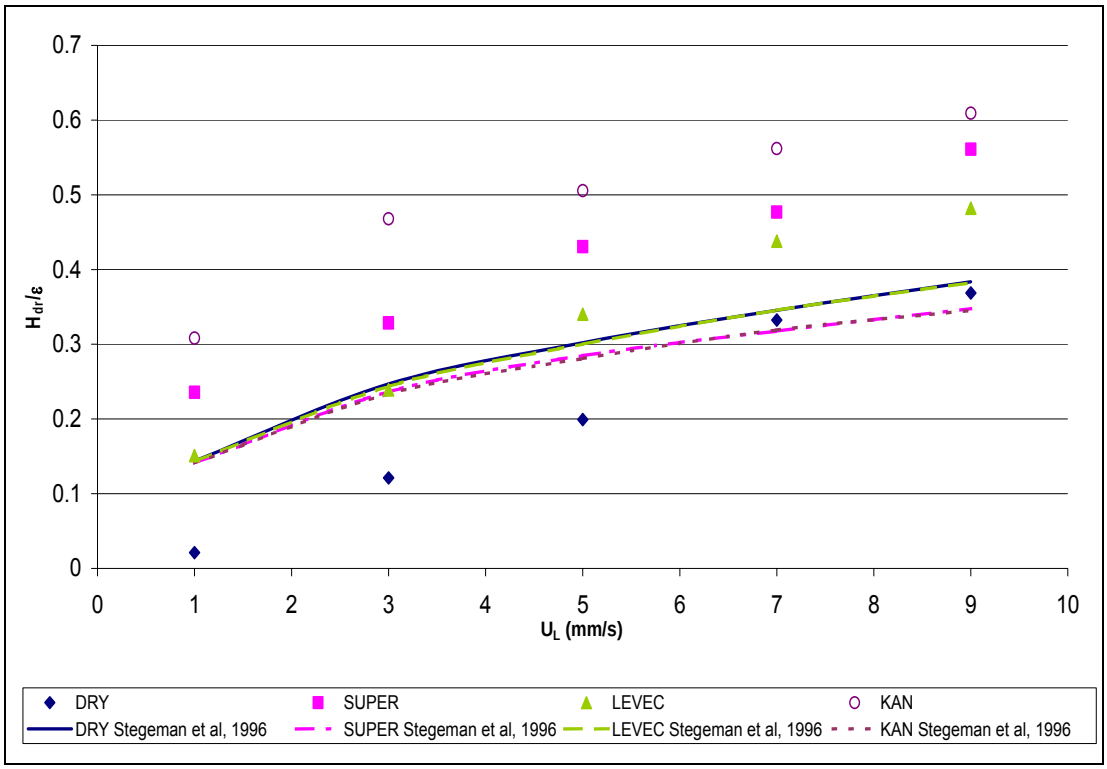

Figure A-31: The performance of the liquid holdup correlation proposed by Stegeman et al (1996) at U_G = 40mm/s

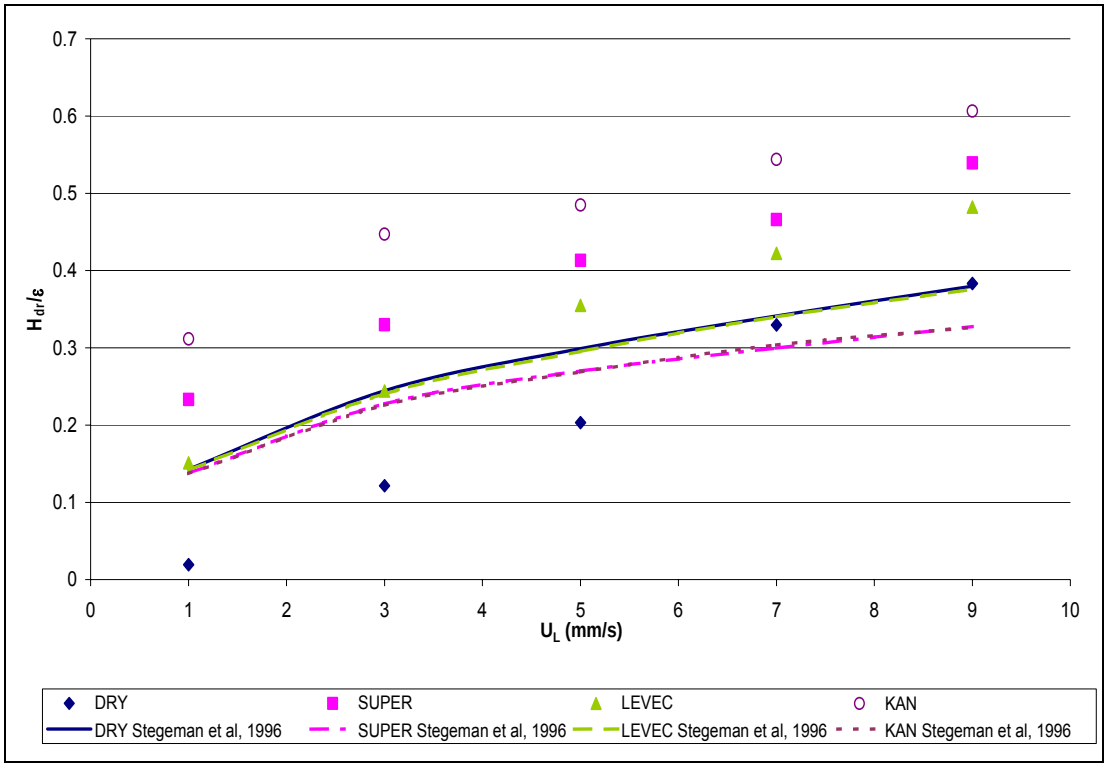

Figure A-32: The performance of the liquid holdup correlation proposed by Stegeman et al (1996) at U_G = 70mm/s

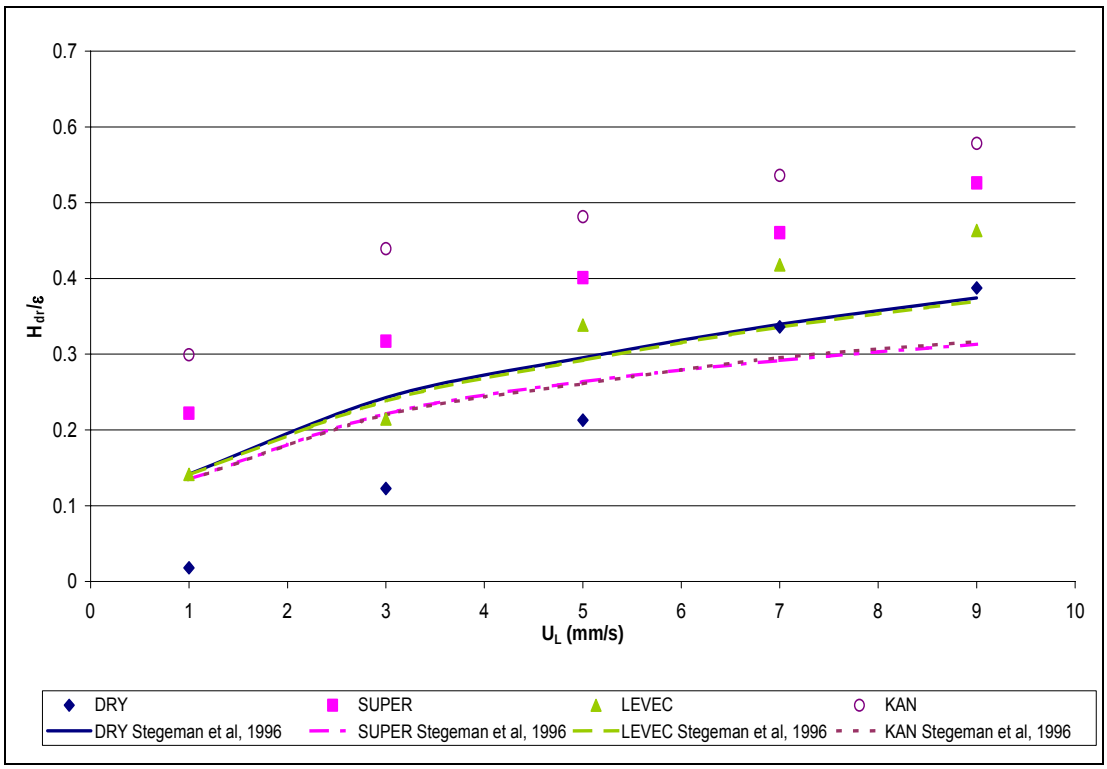

Figure A-33: The performance of the liquid holdup correlation proposed by Stegeman et al (1996) at U_G = 90mm/s

Appendix 14: Liquid Holdup Correlation Specchia and Baldi (1977)

The results of the liquid holdup predictions from the correlation proposed by Specchia and Baldi (1977) at the intermediate gas flow rates are shown in figures A-34 and A-35.

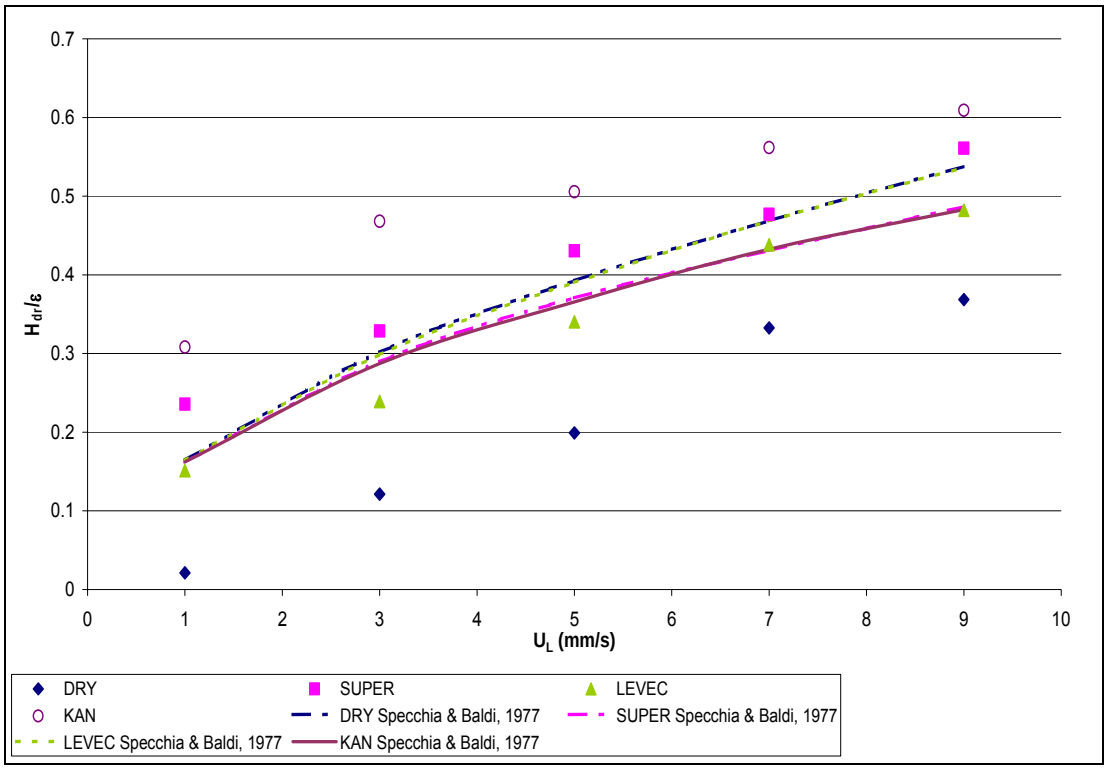

Figure A-34: The performance of the liquid holdup correlation proposed by Specchia and Baldi (1977) at U_G = 40mm/s

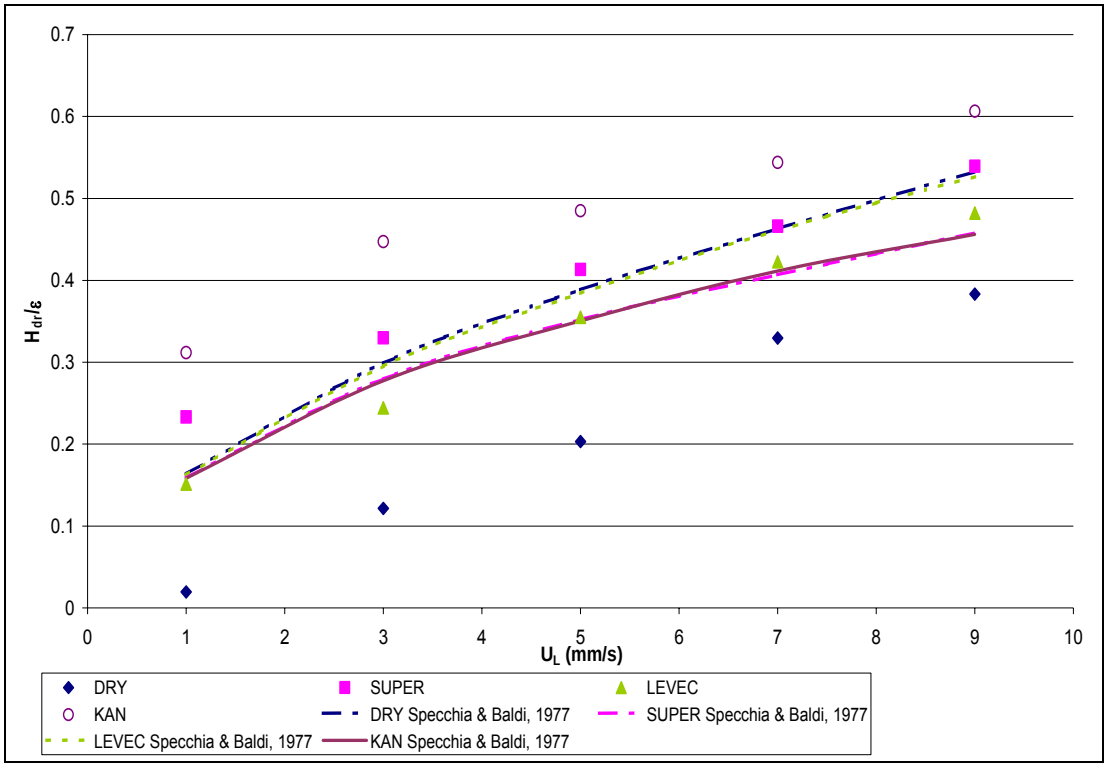

Figure A-35: The performance of the liquid holdup correlation proposed by Specchia and Baldi (1977) at U_G = 70mm/s

Appendix 15: Liquid Holdup Correlations based on the Relative Permeability Concept

The results of the liquid holdup predictions from the correlation based on the relative permeability concepts at the intermediate gas flow rates are shown in figures A-36 and A-37.

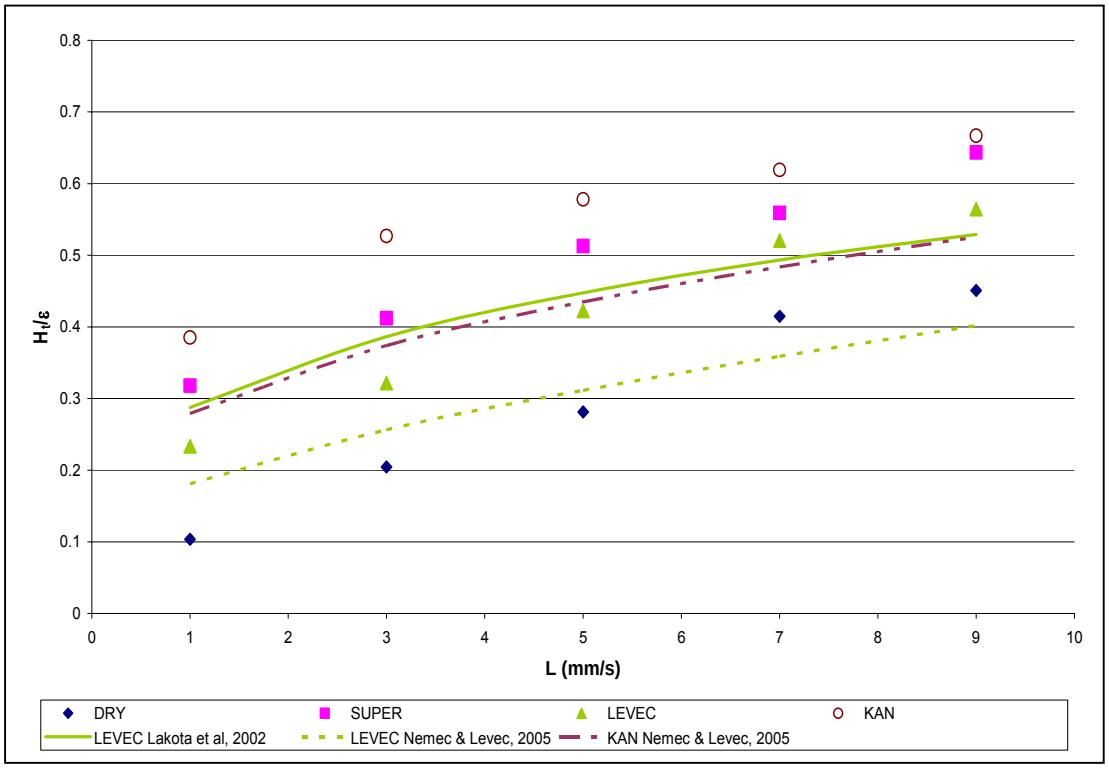

Figure A-36: The performance of the liquid holdup correlations based on the relative permeability concept at U_G = 40mm/s

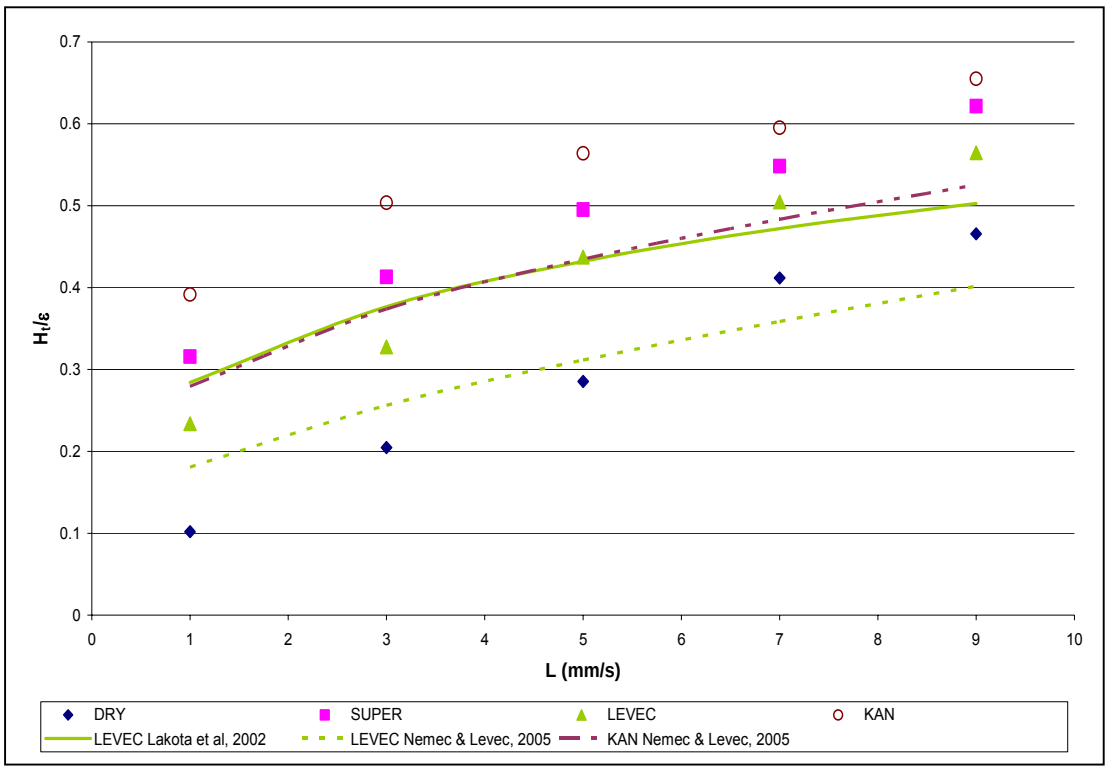

Figure A-37: The performance of the liquid holdup correlations based on the relative permeability concept at U_G = 70mm/s

Appendix 16: Single Gas-Liquid Mass Transfer Correlations

The results of the single gas-liquid mass transfer correlations for the intermediate gas flow rates are shown in figures A-38 and A-39.

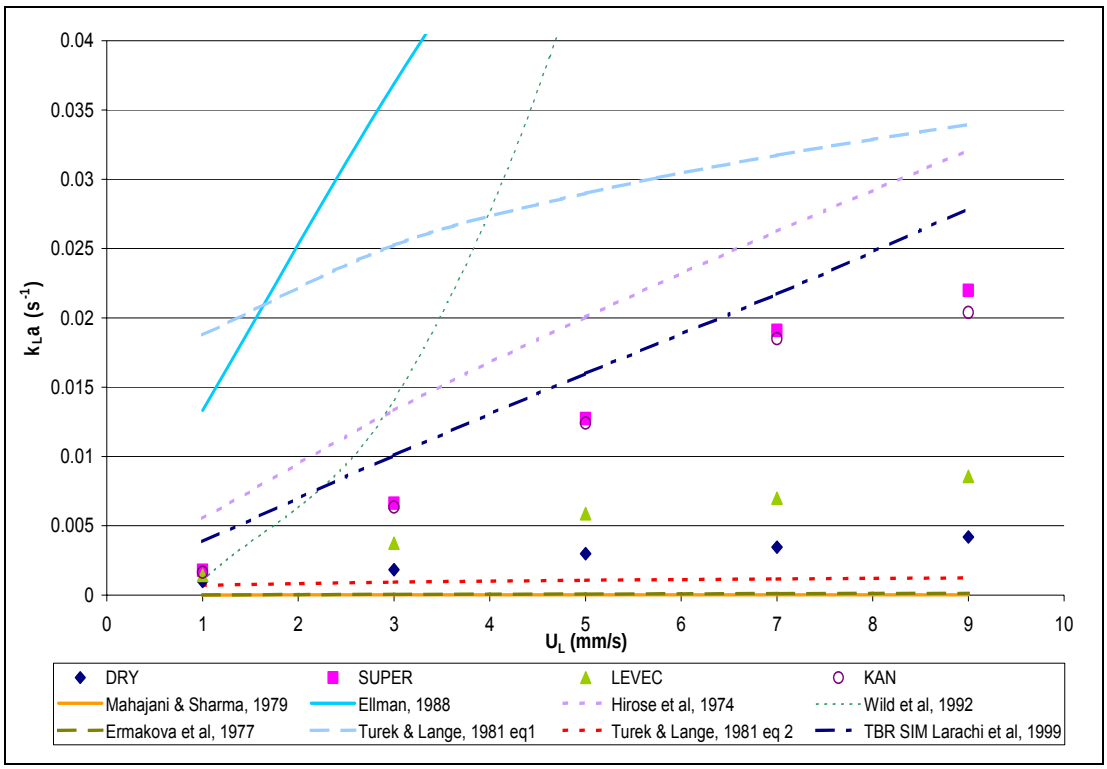

Figure A-38: The performance of the gas-liquid mass transfer correlations at U_G = 40mm/s

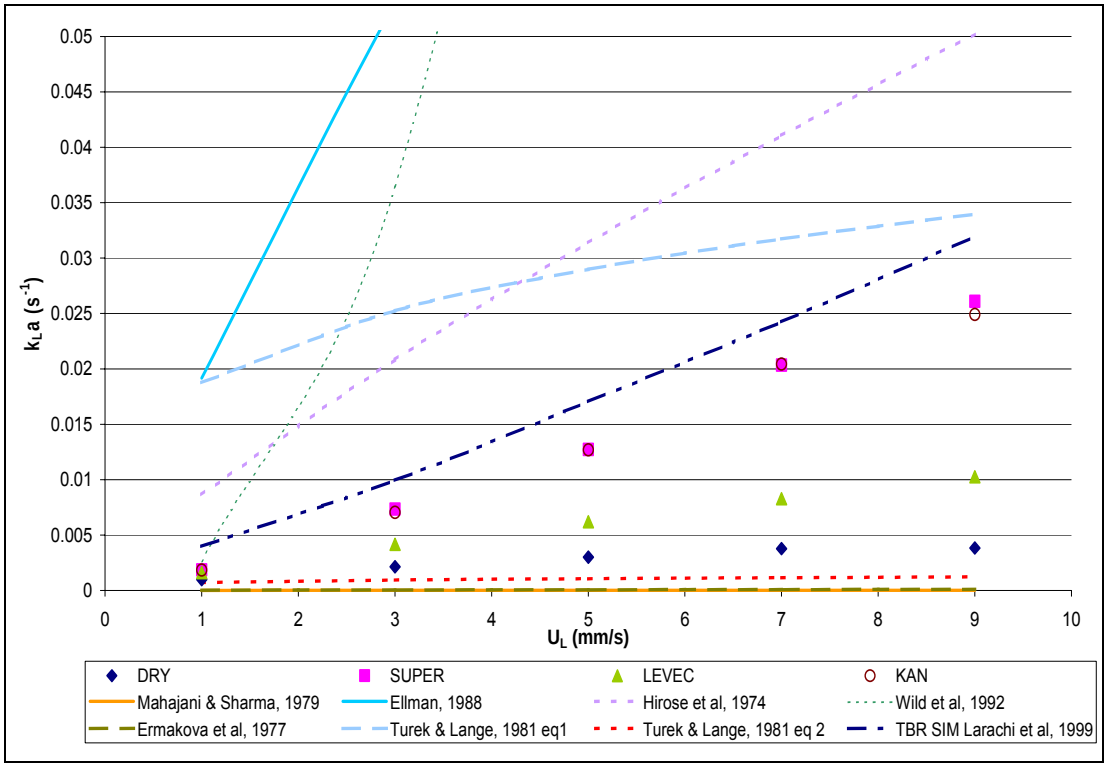

Figure A-39: The performance of the gas-liquid mass transfer correlations at U_G = 70mm/s

Appendix 17: Gas-Liquid Mass Transfer Correlation Reiss (1967)

The results of the gas-liquid mass transfer coefficient predictions from the correlation proposed by Reiss (1967) at the intermediate gas flow rates are shown in figures A-40 and A-41.

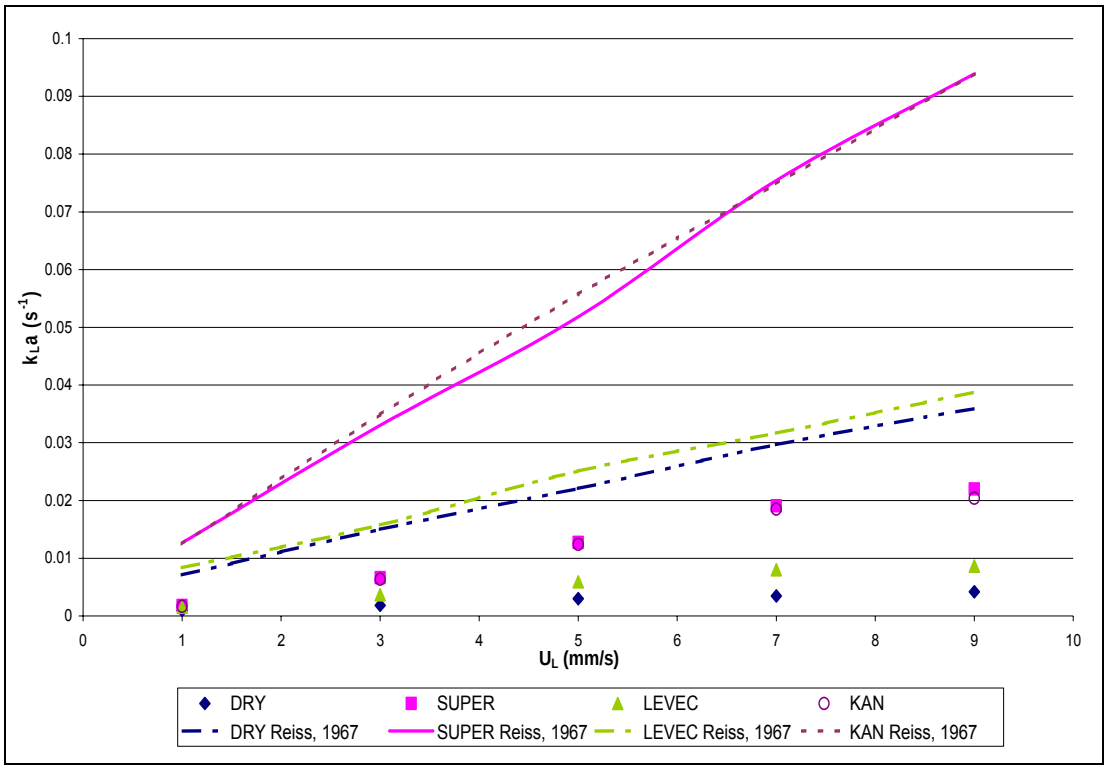

Figure A-40: The performance of the gas-liquid mass transfer correlation proposed by Reiss (1967) at U_G = 40mm/s

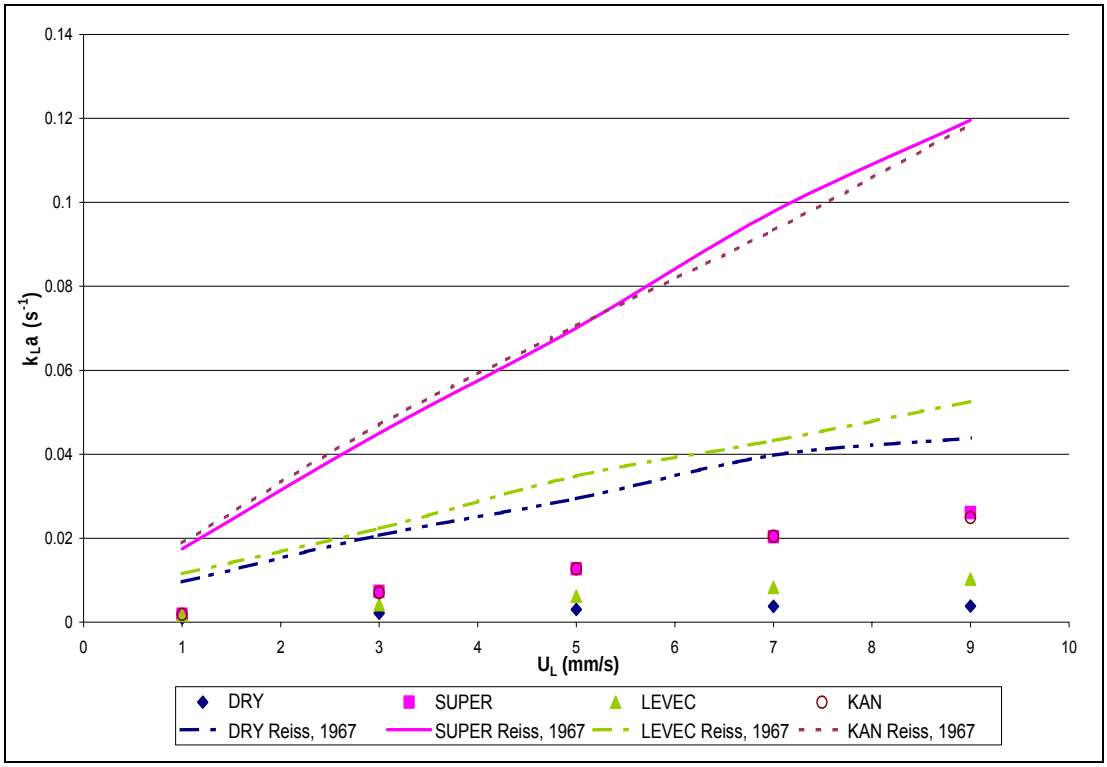

Figure A-41: The performance of the gas-liquid mass transfer correlation proposed by Reiss (1967) at U_G = 70mm/s

Appendix 18: Gas-Liquid Mass Transfer Correlation Fukushima and Kusaka (1977)

The results of the gas-liquid mass transfer coefficient predictions from the correlation proposed by Fukushima and Kusaka (1977) at the higher gas flow rates are shown in figures A-42 to A-44.

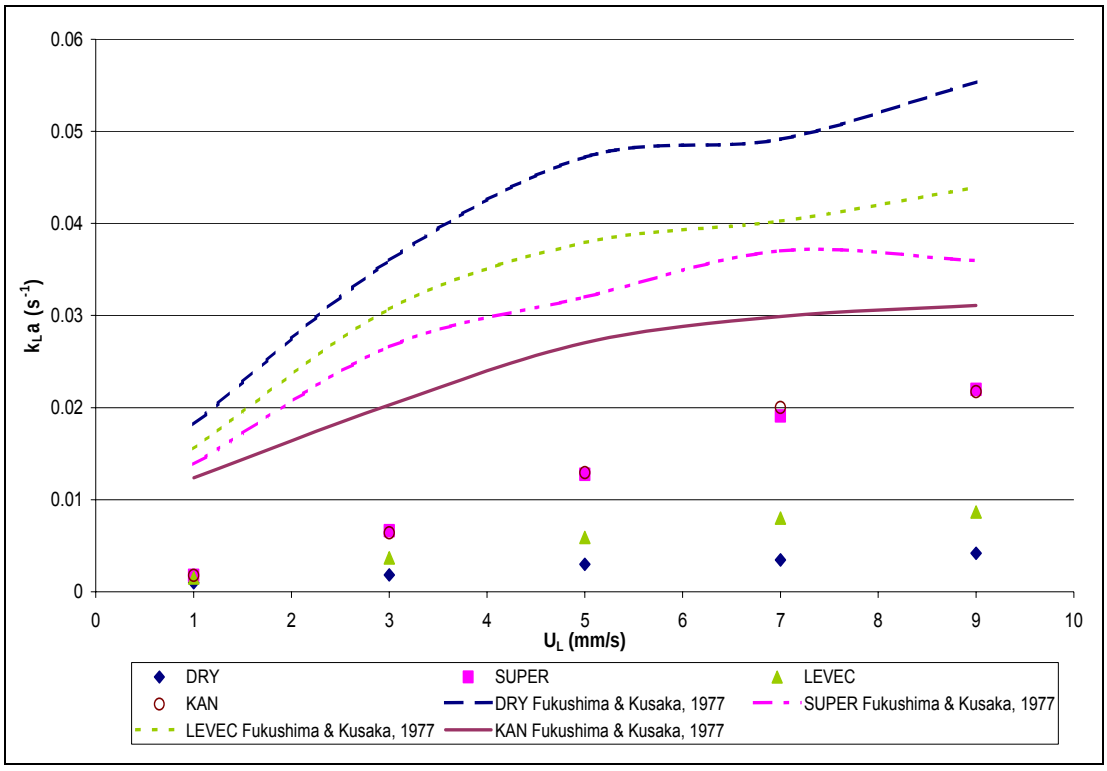

Figure A-42: The performance of the gas-liquid mass transfer correlation proposed by Fukushima and Kusaka (1977) at U_G = 40mm/s

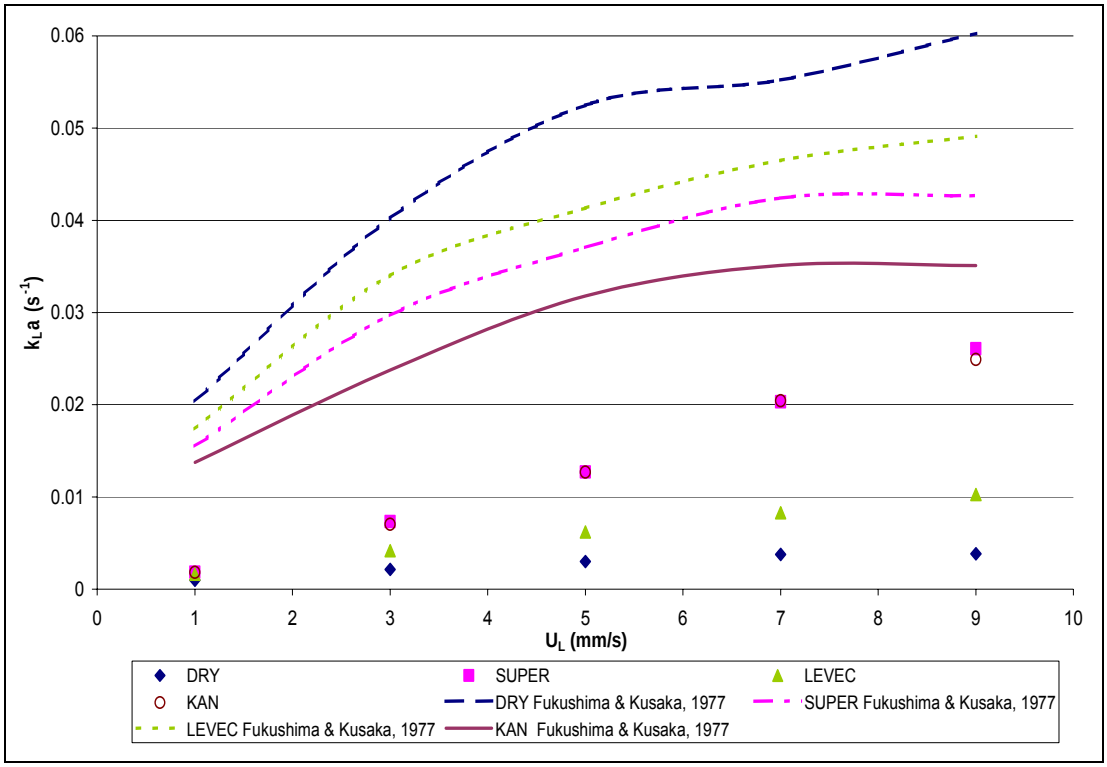

Figure A-43: The performance of the gas-liquid mass transfer correlation proposed by Fukushima and Kusaka (1977) at U_G = 70mm/s

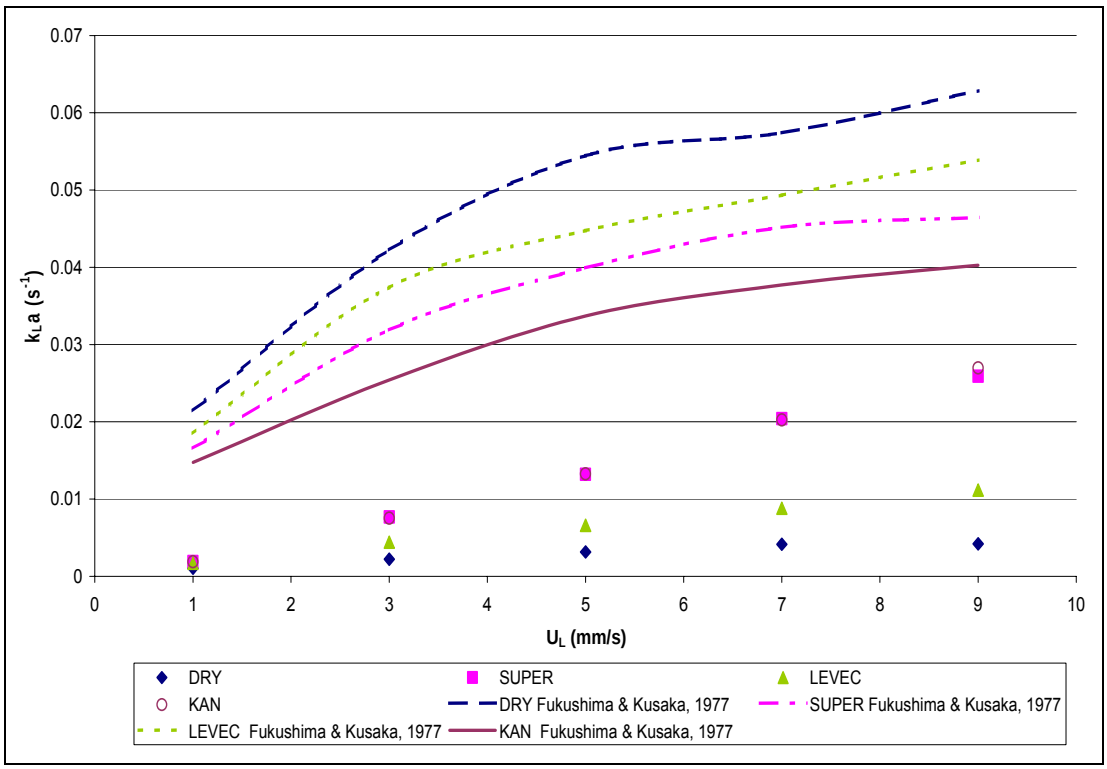

Figure A-44: The performance of the gas-liquid mass transfer correlation proposed by Fukushima and Kusaka (1977) at U_G = 90mm/s

Appendix 19: Gas-Liquid Mass Transfer Correlation Turek and Lange (1981)

The results of the gas-liquid mass transfer coefficient predictions from the correlation proposed by Turek and Lange (1981) at the higher gas flow rates are shown in figures A-45 to A-47.

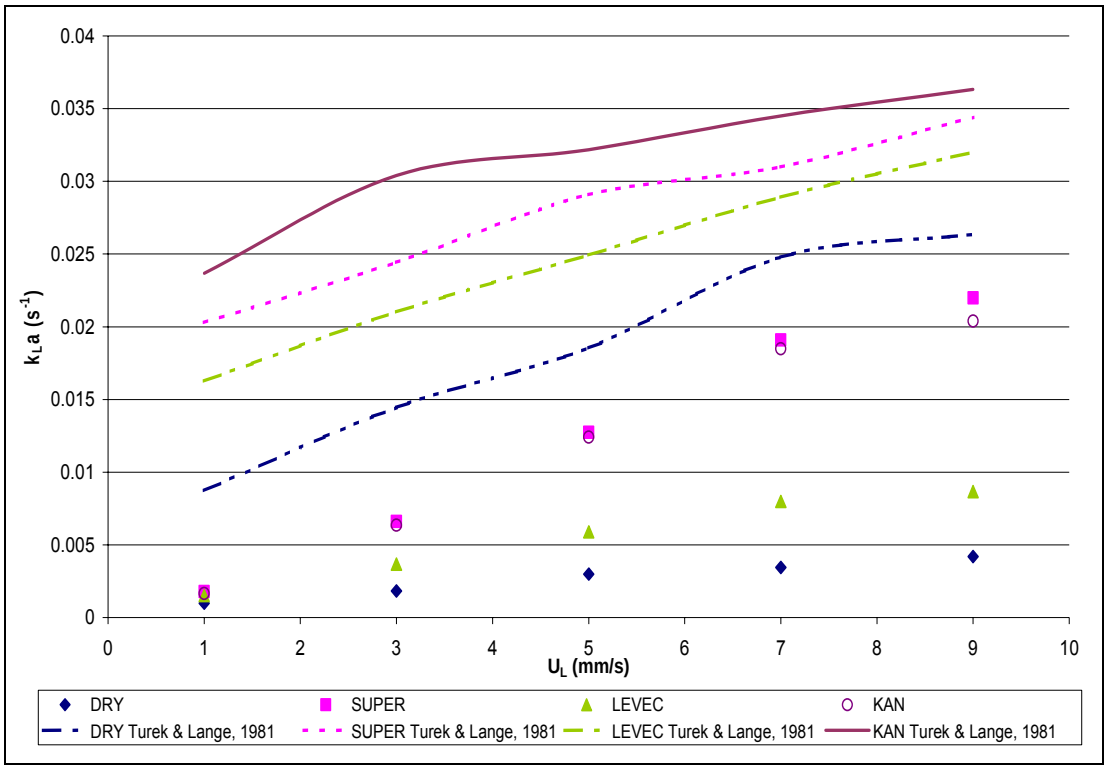

Figure A-45: The performance of the gas-liquid mass transfer correlation proposed by Turek and Lange (1981) at U_G = 40mm/s

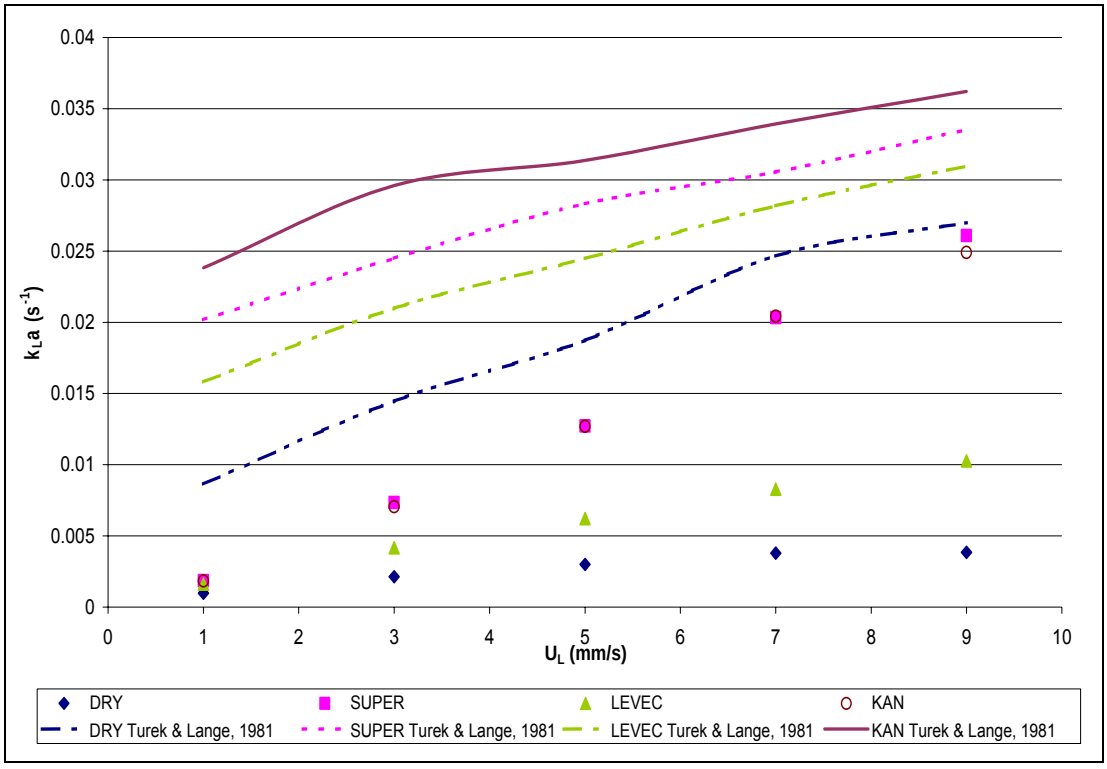

Figure A-46: The performance of the gas-liquid mass transfer correlation proposed by Turek and Lange (1981) at U_G = 70mm/s

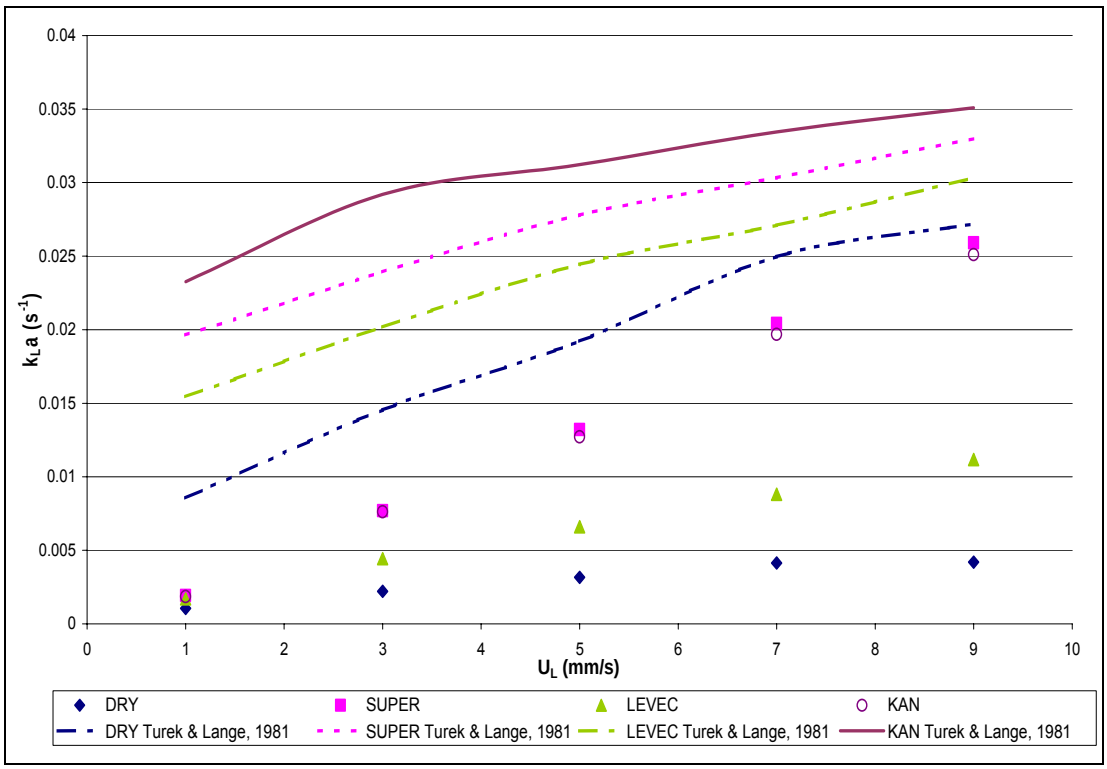

Figure A-47: The performance of the gas-liquid mass transfer correlation proposed by Turek and Lange (1981) at U_G = 90mm/s

Appendix 20: Gas-Liquid Mass Transfer Correlation Hirose *et al* (1974)

The results of the gas-liquid mass transfer coefficient predictions from the correlation proposed by Hirose *et al* (1974) at the higher gas flow rates are shown in figures A-48 to A-50.

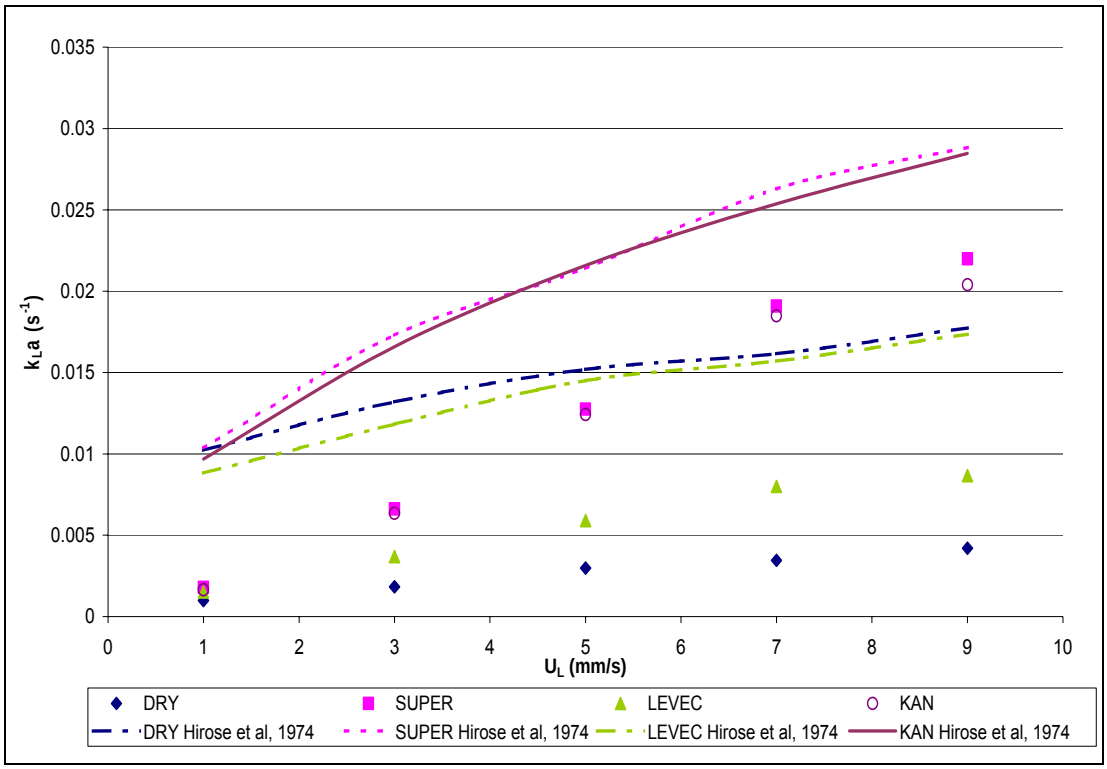

Figure A-48: The performance of the gas-liquid mass transfer correlation proposed by Hirose et al (1974) at U_G = 40mm/s

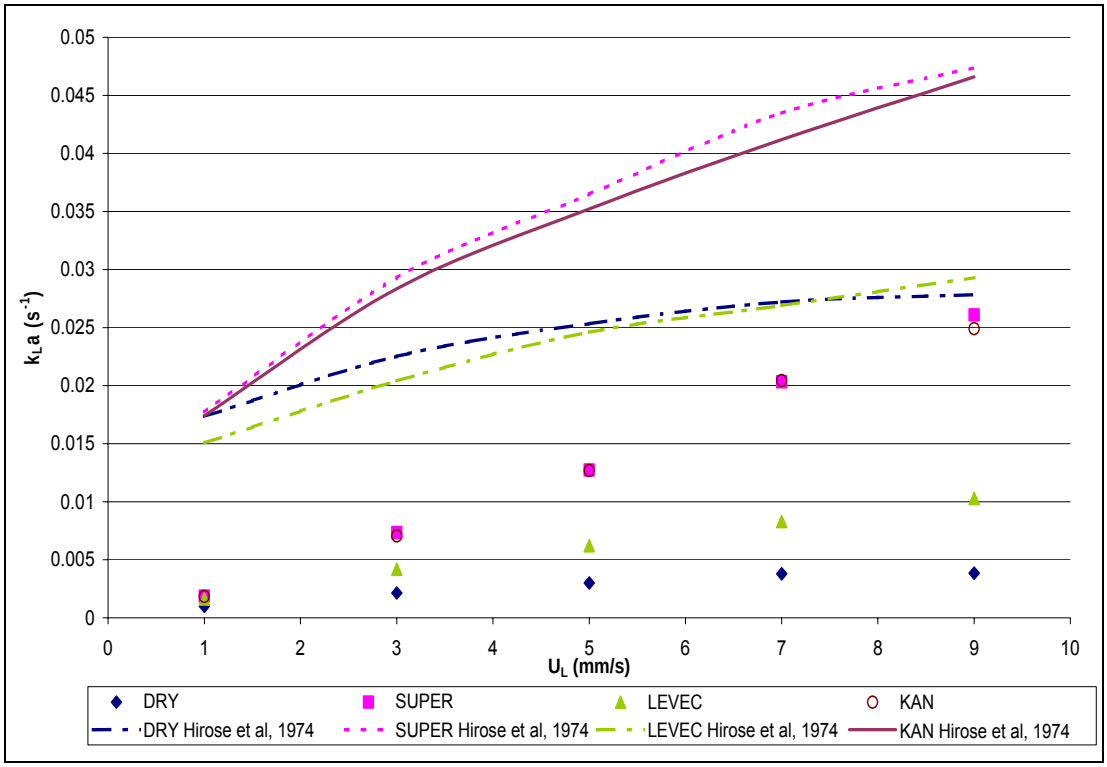

Figure A-49: The performance of the gas-liquid mass transfer correlation proposed by Hirose et al (1974) at U_G = 70mm/s

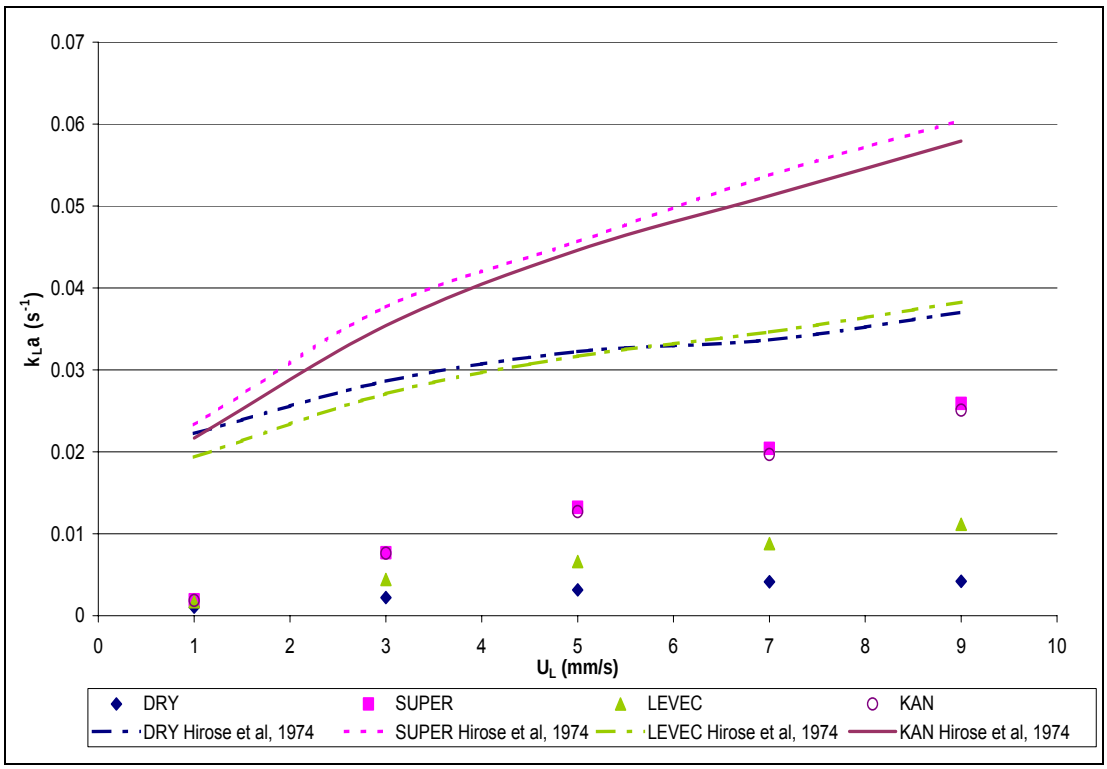

Figure A-50: The performance of the gas-liquid mass transfer correlation proposed by Hirose et al (1974) at U_G = 90mm/s